MORPHOLOGY AND RELATIONSHIPS OF *APTERNODUS* AND OTHER EXTINCT, ZALAMBDODONT, PLACENTAL MAMMALS

ROBERT J. ASHER
Frick Postdoctoral Fellow, Division of Paleontology
American Museum of Natural History
e-mail: asher@amnh.org

MALCOLM C. McKENNA
Frick Curator (Emeritus), Division of Paleontology
American Museum of Natural History;
Adjunct Professor of Geology and Geophysics
University of Wyoming, Laramie, WY 82071
e-mail: m4pmck@indra.com

ROBERT J. EMRY
Curator, Department of Paleobiology
National Museum of Natural History, Smithsonian Institution
Washington, DC 20560
e-mail: emry.robert@nmnh.si.edu

ALAN R. TABRUM
Scientific Preparator, Section of Vertebrate Paleontology
Carnegie Museum of Natural History
Pittsburgh, PA 15213
e-mail: tabrum@carnegiemuseums.org

DONALD G. KRON
(Deceased) Section of Geology, University of Colorado Museum
Boulder, CO 80309

BULLETIN OF THE AMERICAN MUSEUM OF NATURAL HISTORY
CENTRAL PARK WEST AT 79TH STREET, NEW YORK, NY 10024
Number 273, 117 pp., 60 figures, 7 tables
Issued November 27, 2002

 ISSN 0003-0090

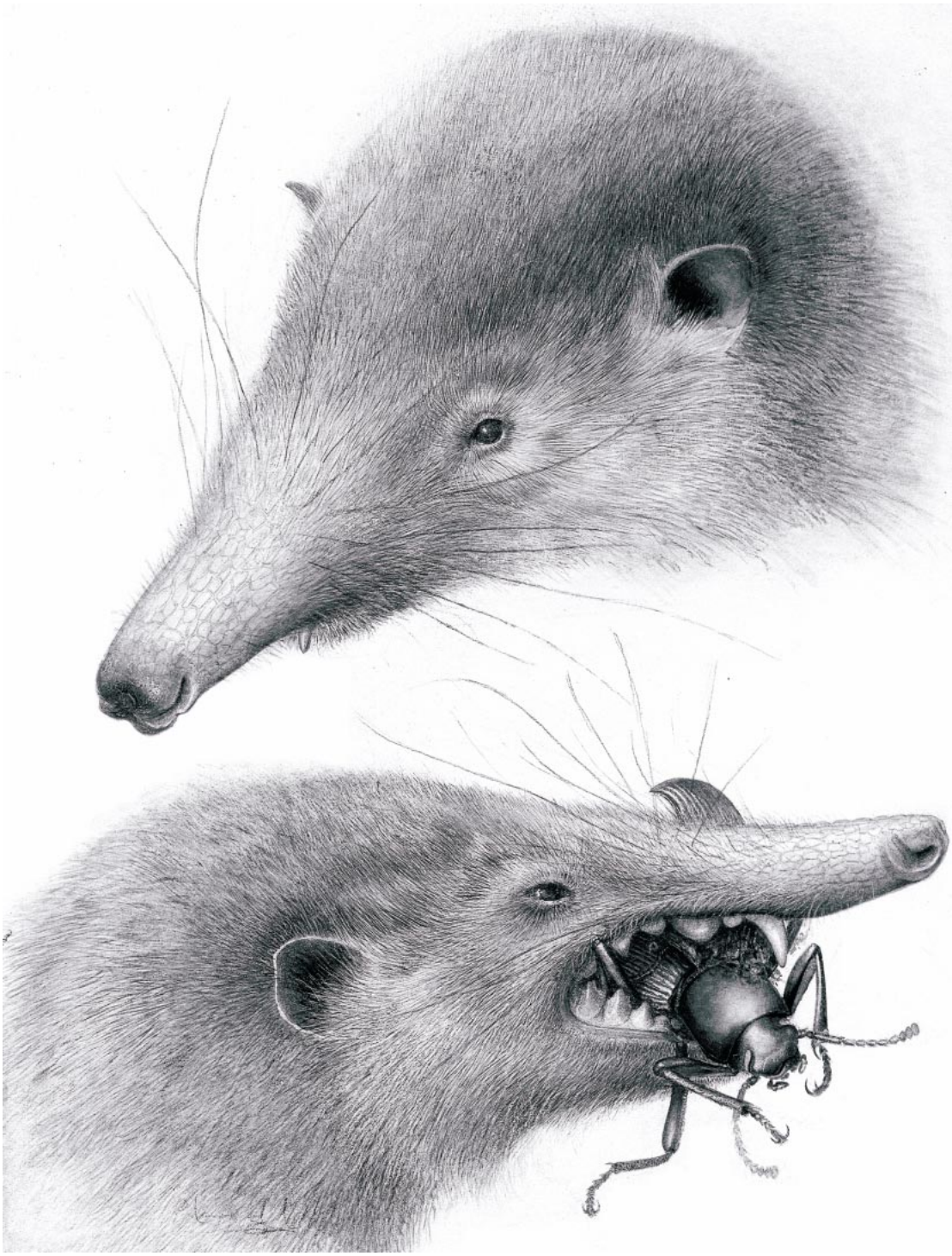

Frontispiece: Reconstruction of *Apternodus baladontus* sp. nov. based on the type specimen, FMNH PU1690. An elongate rod of cartilage is hypothesized to have been present anterior to the bony external nares based on the large size of the rostral muscle scars in this and other specimens. The enlarged, bulbous anterior dentition may have been used to crush chitinous insect exoskeletons in order to access the fleshy interior. Reconstruction drawn by Chester Tarka with the help of Malcolm McKenna.

CONTENTS

ABSTRACT

We describe and illustrate new, middle Cenozoic fossils of dentally zalambdodont, North American placentals, including six relatively complete crania of *Apternodus* and two of *Oligoryctes*, as well as many partial skulls, mandibles, and teeth of these and other taxa. Several of the new *Apternodus* specimens are also associated with postcrania. We recognize seven species of *Apternodus*, three of which are new, formally propose the combination *Oligoryctes altitalonidus*, and recognize two other genera of small, North American, anatomically zalambdodont placentals, *Parapternodus* and *Koniaryctes*. We regard two other taxa previously associated with North American fossil zalambdodonts, one Bridgerian and the other Tiffanian, as valid but do not name them in this paper. In addition, we argue that dental zalambdodonty entails a primary occlusal relationship between the paracone and the ectoflexid, and the reduction or absence of the metacone and talonid basin.

A phylogenetic analysis of cranial, dental, and postcranial characters of 30 fossil and Recent taxa leads us to conclude that (1) the Apternodontidae as defined in previous literature is not monophyletic and should be restricted to seven species of *Apternodus*, (2) the genus *Oligoryctes* contains at least two species and has a considerably longer geologic record than *Apternodus*, (3) neither *Micropternodus* nor currently known Paleocene taxa are closely related to *Apternodus* or *Oligoryctes*, and (4) a case can be made for a close relationship among modern soricids, *Parapternodus*, *Koniaryctes*, *Oligoryctes*, and *Apternodus* to the exclusion of other insectivoran-grade taxa. With the use of ordered, multistate character transformations, *Solenodon* comprises the sister taxon to a soricid-fossil zalambdodont clade.

INTRODUCTION

As defined by previous workers, the extinct mammalian family ''Apternodontidae'' is best known from two genera, *Apternodus* and *Oligoryctes*, which were most diverse in North America during the late Eocene. These genera are well represented by cranial and dental fossils and share a distinctive pattern of molar occlusion known as zalambdodonty (Butler, 1937; Patterson, 1956). The literature on these animals is based primarily on a few specimens from the latest Eocene and early Oligocene White River Group of the United States, but does not account for a great deal of new material.

The purpose of this revision is to assess this new material and provide anatomical and phylogenetic definitions of *Apternodus*, *Oligoryctes*, and other extinct taxa previously associated with the ''Apternodontidae'', documenting their temporal and geographic ranges. The phylogenetic questions of importance in this analysis concern the monophyly of each constituent ''apternodontid'' taxon as previously described in the literature. We are also interested in identifying their immediate sister taxa, living and extinct. Relationships among insectivoran-grade placental mammals have been the subject of considerable scrutiny in recent years, and it has become apparent that the ''Insectivora'' may not comprise a natural, monophyletic group (e.g., Stanhope et al., 1998; Murphy et al., 2001). Future analyses attempting to decipher relationships of constituent insectivoran groups must therefore be very broad in taxonomic scope. Such a large-scale phylogenetic analysis of the Insectivora is beyond the scope of this paper, but the data discussed here can be used toward that end.

INSTITUTIONAL ABBREVIATIONS

AMNH	American Museum of Natural History, New York, NY
BMNH	The Natural History Museum, London
CM	Carnegie Museum of Natural History, Pittsburgh, PA
DMNH	Denver Museum of Nature and Science, CO
FMNH	Field Museum of Natural History, Chicago, IL
KU	University of Kansas Museum of Natural History, Lawrence
MCZ	Museum of Comparative Zoology, Harvard University, Cambridge, MA
MPUM	Museum of Paleontology, University of Montana, Missoula
MV	Locality of the Museum of Paleontology, University of Montana, Missoula
RSM	Royal Saskatchewan Museum, Regina
SDSM	South Dakota School of Mines and Technology, Rapid City

UCM	University of Colorado Museum, Boulder
UCMP	University of California Museum of Paleontology, Berkeley
UMMP	University of Michigan Museum of Paleontology, Ann Arbor
USNM	United States National Museum (Smithsonian Institution), Washington, DC
UW	Collection of Fossil Vertebrates, Department of Geology and Geophysics, University of Wyoming, Laramie
TMM	Texas Memorial Museum, Austin
YPM	Yale Peabody Museum, New Haven, CT

ANATOMICAL ABBREVIATIONS

acf	anterior carotid foramen
ac	alisphenoid canal
ctpp	caudal tympanic process of the petrosal
ect	ectotympanic bone
ef	ethmoid foramen
en	entoglenoid process
eo	ear ossicle
ff	facial foramen
fis	foramen for inferior stapedial artery
fo	foramen ovale
fr	fenestra rotundum
fss	foramen for superior stapedial artery
fv	fenestra vestibulae
gp	greater palatine foramen
hy	hyoid bone
hf	hypoglossal foramen
if	incisive foramina
lf	lacrimal foramen
oc	occipital bone
of	optic foramen
pal	palatine foramina
pf	piriform fenestra
pgf	postglenoid foramen
pgp	postglenoid process
ph	pterygoid hamulus
plf	posterior lacerate foramen
pm	petromastoid bone
rtpp	rostral tympanic process of the petrosal
sf	sinus canal foramen
spf	sphenorbital fissure
sq	squamosal bone
stf	stapedius fossa
vf	vidian foramen
vo	vomer

TAXONOMIC HISTORY OF THE ''APTERNODONTIDAE''

Previous authors have proposed five genera in the ''Apternodontidae'' sensu lato: *Apternodus* Matthew, 1903; *Oligoryctes* Hough, 1956; *Parapternodus* Bown and Schankler, 1982; *Iconapternodus* Tong, 1997; and *Koniaryctes* Robinson and Kron, 1998. As described in the literature, each of the latter four genera contains one species: *O. cameronensis*, *P. antiquus*, *I. qii*, and *K. paulus*. Five species have been allocated to *Apternodus*: *A. mediaevus* Matthew, 1903; *A. gregoryi* Schlaikjer 1933; *A. brevirostris* Schlaikjer, 1934; ''*A.*'' *altitalonidus* Clark, 1937 (here recognized as a species of *Oligoryctes*); and *A. iliffensis* Galbreath, 1953. Below we summarize previous investigations of these taxa. Geographic data pertinent to this discussion are depicted in figure 1. Throughout this paper, quotation marks are used for taxa that are not demonstrably monophyletic, as when we refer to ''apternodontids'' as a group previously defined to include *Apternodus*, *Oligoryctes*, *Parapternodus*, *Koniaryctes*, plus unnamed Tiffanian and Bridgerian taxa.

In his study of fossil mammals collected by American Museum expeditions from exposures of the ''Titanotherium Beds'' near Pipestone Springs, Montana (fig. 1: locality 29), Matthew (1903) described two new genera of insectivoran-grade mammals, *Apternodus* and *Micropternodus*. *Apternodus mediaevus* was based on four unassociated mandibular fragments, the best of which (AMNH 9601; a left partial dentary with m2, m3, and partial m1; see fig. 2) was designated the type. A few years later, Matthew (1910) referred to *A. mediaevus* a fairly complete skull and mandibles from central Wyoming ''in the neighborhood of Bates's Hole, north of the Laramie Plains.'' Precise locality information for this specimen (AMNH 22466) is unknown; but it was almost certainly found in deposits of the White River Formation along the northern margin of the Shirley Basin, Wyoming (fig. 1: locality 3). This locality may have been in an area north of the northern intersection of Wyoming routes 77 and 487, east of Stinking Creek, and south of the Deer Creek Range, about 20 miles south of Casper, Wyoming (J. A. Lillegraven, personal commun.).

Matthew (1903, 1910) did not use the family name ''Apternodontidae'', and in fact did not specify the family(ies) to which he thought *Apternodus* and *Micropternodus* be-

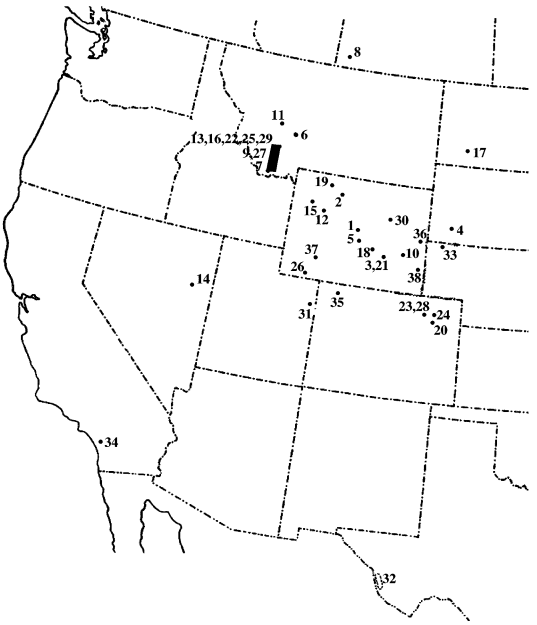

Fig. 1. Geographical distribution of ''apternodontids'' (sensu lato) in North America. Acronyms are given in parentheses for institutions that have made significant collections from each locality. Each number represents a locality, listed in alphabetical order, known to have produced ''apternodontid'' fossils, as follows: 1: Badwater (CM), 2: Banjo Quarry (YPM-PU), 3: Bates's Hole (AMNH, UW), 4: Big Badlands (USNM, YPM), 5: Cameron Spring, Beaver Divide (USNM), 6: Canyon Ferry (CM, USNM), 7: Cook Ranch (MPUM, CM), 8: Cypress Hills, Lac Pelletier (RSM), 9: Diamond O Ranch (MPUM, CM), 10: Dilts Ranch (UW), 11: Douglass Creek Basin (FMNH), 12: East Fork Basin (AMNH), 13: Easter Lily (MPUM, CM), 14: Elderberry Canyon (USNM), 15: Emerald Lake (AMNH), 16: Eureka Valley Road (MPUM, CM), 17: Fitterer Ranch (USNM), 18: Flagstaff Rim (USNM, AMNH), 19: Fort Union Fm., Clark's Fork Basin (UMMP), 20: Fremont Butte (DMNH), 21: Harshman Quarry (UW), 22: Highway 10N (MPUM, CM), 23: Horsetail Creek (DMNH), 24: Iliff (FMNH, KU), 25: Little Pipestone Creek (MPUM, CM, AMNH), 26: Lonetree, Wyoming (UCM), 27: McCarty's Mountain (FMNH, MPUM, CM), 28: Mellinger (UCM), 29: Pipestone Springs (MPUM, CM, AMNH), 30: Powder River Basin (UCM), 31: Powder Wash (CM), 32: Red Mound (TMM), 33: Raben Ranch (SDSM), 34: San Diego (UCMP), 35: Sand Wash Basin (DMNH), 36: Seamen Hills (AMNH), 37: Tabernacle Butte (CM, UMMP), 38: Torrington (MCZ).

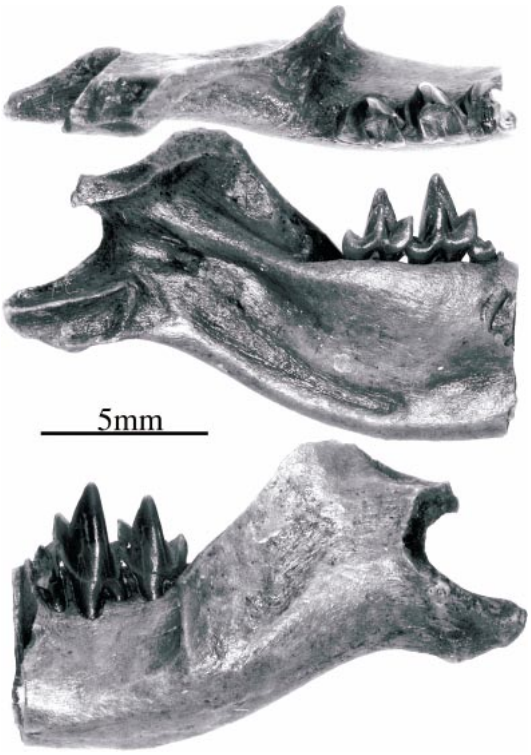

Fig. 2. AMNH 9601, *Apternodus mediaevus* type specimen from Pipestone Springs, Montana in lingual (top), lateral (middle), and occlusal (bottom) views.

longed. Gregory (1910: 258–259) suggested that both taxa were ''primitive member[s] of the Centetidae'' (i.e., Tenrecidae). Osborn (1910: 519), with input from Gregory, J. K. Mosenthal, and Matthew, assigned *Apternodus* to the ''Apternodontidae'' within the superfamily ''Centetoidea'', suborder Lipotyphla, order Insectivora. Osborn made no mention of *Micropternodus*. Simpson (1931) also gave *Apternodus* its own familial rank without explicit mention of *Micropternodus*.

Schlaikjer (1933) described a second skull and mandible of *Apternodus* from Orellan deposits of the Brule Formation southwest of Torrington, Wyoming (fig. 1: locality 38). He named this specimen (MCZ 17685) *A. gregoryi*, and placed both it and *A. mediaevus* in the subfamily ''Apternodontinae'', family Solenodontidae. The following year, Schlaikjer (1934) presented a reanalysis of the skull described by Matthew (1910), and argued that it did not belong to the same species as

the type specimen of *A. mediaevus*. Schlaikjer (1934) therefore reassigned AMNH 22466 (which at the time was housed in the University of Wyoming collections) to a new species, *A. brevirostris*.

In their review of the White River fauna, Scott and Jepsen (1936) illustrated the type specimen of *Apternodus gregoryi* (MCZ 17685) and briefly described ''*Apternodus*'' *altitalonidus* from the Chadron Formation of the Big Badlands area of southwestern South Dakota (fig. 1: locality 4), crediting it to John Clark (Scott and Jepsen, 1936: 12). Scott and Jepsen also named the genus ''*Clinodon*'' based on a lower jaw that resembles that of *Micropternodus*. Subsequently, Clark (1937: 306–307) expanded on the description of ''*A.*'' *altitalonidus* and noted that ''*Clinodon*'' was preoccupied; hence, Clark replaced it with *Clinopternodus*.

Simpson (1945) placed *Apternodus* in its own subfamily, the ''Apternodontinae'', within the Solenodontidae, and assigned both *Micropternodus* and *Clinopternodus* to the Solenodontinae. All three fossil genera along with the extant *Solenodon* were placed in the superfamily Tenrecoidea, order Insectivora.

Macdonald (1951) described what would have been the youngest ''apternodontid'' specimen from Whitneyan strata east of Rockyford, South Dakota. However, Gawne (1968) has since demonstrated that this partial skull, named *Apternodus bicuspis* by Macdonald, is actually referable to the erinaceid genus *Proterix*.

In 1953, Galbreath assigned an associated maxilla and mandible (KU 9112), collected from the Horsetail Creek Member of the White River Formation exposed north of Iliff, Colorado (fig. 1: locality 24) to his new species *Apternodus iliffensis*.

In a report on an area then scheduled to be flooded by a hydroelectric project, T. E. White (1954) mentioned two *Apternodus* specimens from Chadronian deposits in the vicinity of Canyon Ferry, Montana (fig. 1: locality 6). USNM 18914 is a fragmentary maxilla with M1, and CM 37455 (uncataloged at the time of White's paper and referred to using J. L. Kay's Carnegie Museum field number, ''38/40'') is a fragmentary skull and jaws associated with several postcranial elements. In the same paper, White (1954) named ''*Kentrogomphios strophensis*'' based on a partial skull also from the Chadronian part of the Canyon Ferry sequence; this taxon was subsequently synonymized with *Micropternodus* (see below).

The genus *Oligoryctes* was named by Hough (1956). The type species, *O. cameronensis*, was based on a partial skull and associated mandible (USNM 19909), collected from Chadronian deposits northeast of Cameron Spring, Wyoming (fig. 1: locality 5). This specimen was almost as small as Clark's ''*A.*'' *altitalonidus*, which, however, was not mentioned by Hough.

In his monograph on the Antillean insectivorans, McDowell (1958) included considerable detail on the anatomy of *Apternodus*, as well as his opinion of its phylogenetic affinities. The illustrations in that monograph continue to serve as an important reference for cranial and dental anatomy in insectivoran-grade mammals, although several errors have been noted by subsequent authors (see below and Patterson, 1962, unpublished MS; Butler, 1972; McKenna, 1975; Asher, 2001; Whidden and Asher, 2001). Specifically, McDowell argued for a novel scheme of dental cusp homologies in *Solenodon*, and inferred a pattern of arterial supply in *Apternodus* that, he believed, excluded it from close affinity to any insectivoran mammal. He suggested instead that *Apternodus* might be a creodont, a suggestion not accepted by subsequent authors (e.g., McKenna and Bell, 1997).

McDowell (1958: 175) made several accurate predictions concerning the lower molars of *Micropternodus* and *Clinopternodus*. He noted that ''. . . the hypoconid, although low in proportion to the trigonid, is quite distinct and salient, which suggests that it occluded between well-developed paracones and metacones (i.e., the upper dentition was dilambdodont).'' This suggestion, written in the absence of confirmed upper dentitions of either taxon, was substantiated by Russell (1960) when he associated White's (1954) ''*Kentrogomphios strophensis*'' with lower dental material then known for *Micropternodus borealis*. The latter name having priority, Russell synonymized ''*Kentrogomphios*'' with it, and noted that, as McDowell predicted, *Micropternodus* did indeed have a

prominent metacone on its upper cheek teeth (Russell, 1960: 941, 943). Accordingly, Russell removed *Micropternodus* from its previously vague association with ''apternodontids'', suggesting instead that it was related to geolabidine erinaceids (sensu McKenna, 1960). In their description of a partial skull and mandible of *Micropternodus morgani* from Oligocene strata of the John Day Formation of Oregon, Stirton and Rensberger (1964) echoed this possibility. Although the upper dentition of *Clinopternodus* remains unknown, we suspect that it also possesses upper molars with prominent metacones for the same reasons enumerated by McDowell (1958).

Konizeski (1961) assigned two partial mandibles from the Douglass Creek Basin, Montana (fig. 1: locality 11), about 80 miles northwest of Pipestone Springs, to *A. mediaevus*. He regarded the fauna from the Douglass Creek Basin as similar in composition to those from Pipestone Springs and the Chadronian part of the Canyon Ferry sequence.

McKenna et al. (1962) described two Bridgerian specimens from the Tabernacle Butte area north of Farson, Wyoming (fig. 1: locality 37) as ''Apternodontinae, undescribed genus and species''. One of these specimens (AMNH 55689) was a small, edentulous mandible tentatively considered by Simpson (in McGrew et al., 1959: 151–152) to be an indeterminate soricid. Both specimens were listed by West and Atkins (1970) as ''apternodontids'' from Tabernacle Butte. The presence of this species in the Bridgerian of Utah (fig. 1: locality 31) was also mentioned by McKenna et al. (1962: 21).

In a paper on comparative brain evolution, Edinger (1964: 8) noted that ''the oldest Neozoic mammalian endocranial cast I have seen is that of a tenrecoid insectivore, a lower Paleocene *Apternodus*.'' Other than noting some aspects of its morphology and institutional provenance (without a specimen number), Edinger made no further comment on this specimen. She was, nevertheless, referring to YPM PU16520, collected from the Tiffanian (late Paleocene) of the Fort Union Formation in northwestern Wyoming (fig. 1: locality 19). If it were actually an ''apternodontid'', this specimen would be the oldest occurrence of the family (as previously defined). Sloan (1969: fig. 8) figured the geological range of *Apternodus* as extending into the late Tiffanian based on this specimen and YPM PU16521. However, citing a personal communication from Donald Baird, Galbreath (1978) noted that YPM PU16520 ''is not *Apternodus* and its affinities are very dubious.''

Robinson et al. (1964) and Black and Dawson (1966a, 1966b), reported *Oligoryctes* and *Apternodus* from late Uintan to early Duchesnean age (Krishtalka et al., 1987) deposits in the Badwater Creek area of central Wyoming (fig. 1: locality 1). Krishtalka and Setoguchi (1977) included brief descriptions and photographs of *A.* cf. *A. iliffensis* and *Oligoryctes* sp. from this area.

Clark and Beerbower (in Clark et al., 1967) referred a skull with associated mandibles (CM 8669) from the Peanut Peak Member of the Chadron Formation in the Big Badlands of South Dakota to *Apternodus mediaevus* (fig. 1: locality 4). Unfortunately, they did not figure or provide details on the morphology of this specimen, which currently appears to be lost.

Emry (1973, 1992) reported the presence of both *Oligoryctes* and *Apternodus* from Chadronian deposits in the Flagstaff Rim area, southwest of Casper and north of Alcova, Wyoming (fig. 1: locality 18). On the specimen tags in the AMNH Frick Collection (Galusha, 1975), ''Flagstaff Rim'' is occasionally referred to as ''Bates Hole''. This should not be confused with the somewhat mysterious ''Bates's Hole'' of Matthew (1910), which was probably located some 20 miles to the southeast (see above). Discrepancies in the nomenclature of this region are due partly to the field notation made by collecting parties from the AMNH led by Charles Falkenbach in 1941 and 1954, who referred to the area ''6 miles NW of Alcova'' as the ''Bates Hole Area''. In fact, as determined in the late 1950s by M. Skinner, T. Galusha, and colleagues, Falkenbach's collecting area was located far to the northwest of Matthew's ''Bates's Hole''. Skinner therefore opted to coin a new locality name for the region northwest of Alcova, and asked local inhabitants for an appropriate choice.

The response was ''Flagstaff Rim'', based on the presence of a U.S. Coast and Geodesic Survey tower and flag pole (no longer standing) at the summit of this rim. Nevertheless, many AMNH specimens collected in the late 1950s under Skinner's direction (e.g., 74940–74942) from Flagstaff Rim have ''Bates Hole'' written on them. To our knowledge, the only AMNH specimen actually collected from the Bates's Hole of Matthew (1910) is the type of *A. brevirostris* (AMNH 22466). As reported by Matthew (1910), this specimen was originally housed at the University of Wyoming. Furthermore, it is probably associated with a mandible (UW 26) still part of the UW collections.

Love et al. (1976) listed ''*Apternodus* or *Micropternodus*'' from Chadronian deposits of the White River Formation in the Emerald Lake area, south of Yellowstone National Park in northwestern Wyoming (fig. 1: locality 15). This report was based on a partial mandible (AMNH 56374) containing a broken p4 and alveoli for p2–3, m1, and i1.

Novacek (1976a, 1976b) described and figured specimens representing the western and southernmost occurrences of ''apternodontids'' in North America. The western record is a minute, isolated upper molar (UCMP 96135), referred by Novacek (1976a) to ''?apternodontine, genus and species unnamed'' from Uintan deposits of San Diego County, California (fig. 1: locality 34). Walsh (1996) has also listed the occurrence of small, zalambdodont molars from the middle Eocene of San Diego County, which he has identified as representing two species of *Oligoryctes*. The southern record is based on a partial skull (TMM 40492-9) from the late Duchesnean Porvenir local fauna from Presidio County, Texas (fig. 1: locality 32), that Novacek (1976b) referred to *A.* cf. *A. brevirostris*.

In his unpublished master's thesis, Kron (1978) described several well-preserved *Apternodus* specimens from Chadronian deposits in the Dilts Ranch area near Orin, Wyoming (fig. 1: locality 10). These include a particularly large individual with several associated postcranial elements, formally assigned to a new species below.

Twenty-five years after naming *Apternodus iliffensis*, Galbreath (1978) described a fragmentary skull (FMNH PM34512) from a locality adjacent to that of the type specimen. Both sites are about 6 miles north of Iliff, Colorado (fig. 1: locality 24). He did not explicitly assign this specimen to any particular species, although his discussion indicates that it is very similar to *A. iliffensis*.

McKenna (1980) listed *Oligoryctes* sp. as part of an early Uintan fauna from the type section of the Tepee Trail Formation, near Dubois, Wyoming (fig. 1: locality 12). This record is based on AMNH 105310 (a right dentary with p4-m3) and comprises the oldest known occurrence of *O. altitalonidus*.

Bown and Schankler (1982) described another ''apternodontid'' taxon, *Parapternodus antiquus*, based on a fragmentary left dentary (YPM 31169) from the early Wasatchian of the lower Willwood Formation of north-central Wyoming (fig. 1: locality 2).

The northernmost occurrence of ''apternodontids'' in North America is in the Cypress Hills Formation of southwestern Saskatchewan (fig. 1: locality 8). *Oligoryctes* sp. is a member of the late Uintan Swift Current Creek local fauna (Storer, 1984), and both *Apternodus* and *Oligoryctes* occur in the Duchesnean Lac Pelletier Lower Fauna (Storer, 1995) and the Chadronian Calf Creek local fauna (Storer, 1996). Together with the material reported by Krishtalka and Setoguchi (1977) from Badwater locality 20 (fig. 1: locality 1), the Lac Pelletier fossils constitute the oldest record of the genus *Apternodus* in North America.

Ostrander (1987) included *Apternodus iliffensis* and *Oligoryctes cameronensis* in his faunal list from the middle Chadronian Raben Ranch local fauna of northwestern Nebraska (fig. 1: locality 33), about 2 miles southwest of Orella (Ostrander, 1983). He referred 23 specimens, including maxillary and mandibular fragments, to *O. cameronensis*, and six isolated teeth to *A. iliffensis*.

Emry (1990: 190) briefly mentioned a ''very small apternodontid'' from the Bridgerian Elderberry Canyon Quarry, south of Ely in eastern Nevada (fig. 1: locality 14). These specimens, consisting of a somewhat crushed lower left mandible with partial p3 through m3 (USNM 417464) and a maxillary fragment with M1-M3 (USNM 417465), are considerably smaller than other specimens

discussed here, except for the Bridgerian material mentioned above from Tabernacle Butte, Wyoming (McKenna et al., 1962).

Stucky et al. (1996) listed the presence of ''Apternodontidae sp.'' in the early Uintan from the Washakie Formation in the Sand Wash Basin of northwestern Colorado (fig. 1: locality 35).

In a summary of localities relevant to the Eocene-Oligocene transition in southwestern Montana, Tabrum et al. (1996) reported fossils of *Apternodus* and *Oligoryctes* from several localities of late Duchesnean through late Orellan age (fig. 1: localities 7, 9, 13, 25, 26, and 28). These include specimens from recent fieldwork conducted at Pipestone Springs, the type locality of *Apternodus mediaevus*. The late Orellan Cook Ranch locality near Lima, Montana (Tabrum et al., 1996) has yielded a specimen of *Oligoryctes* (MPUM 9560), one of the youngest such specimens yet known.

Tong (1997) described several middle Eocene, dentally zalambdodont specimens from Henan and Shangxi provinces in China, and named the taxon *Iconapternodus qii* based on upper and lower mandibular fragments from the Hetaoyuan Formation in Xichuan County, Henan Province. These fossils fall in the Irdinmanhanian Asian Land Mammal Age, which overlaps extensively with the Uintan Land Mammal Age in North America (Tong et al., 1995). Tong (1997) also described isolated teeth of *Iconapternodus* from the Rencun and Zhaili Members of the Hedi Formation, which correspond (respectively) to the Sharamurunian and Naduan Asian Land Mammal Ages (late Uintan or younger). Based on illustrations and measurements (Tong, 1997: fig. 12), *Iconapternodus* appears to be similar in size to *Oligoryctes cameronensis*. Tong (1997: fig. 11) also illustrated an isolated lower molar assigned to ''*Apternodus* sp.'' from the Rencun Member of the Hedi Formation in Mianchi County, Henan Province.

McKenna and Bell (1997) briefly referred to a middle Eocene ''apternodontid'' from Khaichin Ula, Mongolia, housed at the Paleontological Museum of the Russian Academy of Sciences, Moscow.

Robinson and Kron (1998) named *Koniaryctes paulus* based on a right lower dentary fragment from Wasatchian deposits exposed in the Powder River Basin of Johnson County, Wyoming (fig. 1: locality 30), about 6 miles north of Sussex (Robinson and Williams, 1997). Together with *Parapternodus*, *Koniaryctes* represents one of the oldest occurrences of the ''Apternodontidae'' as previously defined in the literature. Robinson and Kron (1998) also referred additional specimens to *Parapternodus*, including UMMP 81561, a mandibular fragment, and UMMP 81558, an isolated upper premolar, and noted that ''apternodontids'' constitute ''a rare but persistent element'' in Eocene faunae, referring specifically to the following localities: Willwood Formation, northwestern Wyoming (fig. 1: locality 2; Bown and Schankler, 1982); Bridgerian of Powder Wash, Utah (fig. 1: locality 31); Tabernacle Butte, Wyoming (fig. 1: locality 37; McKenna et al., 1962); Bridger Formation near Lonetree, Wyoming (fig. 1: locality 26); Uintan of Badwater Creek, Wyoming (fig. 1: locality 1; Krishtalka and Setogouchi, 1977); Swift Current Creek, Saskatchewan (fig. 1: locality 8; Storer, 1996); and the Orellan of north-central Colorado (fig. 1: locality 28) and northwest of Crawford, Nebraska (fig. 1: locality 33).

Like several other authors before them (e.g., Emry, 1979; Tabrum et al., 1996), Robinson and Kron (1998) referred to ''*Oligoryctes altitalonidus*'', a combination not formally defined in the literature. However, this usage was based on the commonly held view, articulated in previously circulated versions of this manuscript, that ''*A.*'' *altitalonidus* Clark (1937) is in fact better accommodated in *Oligoryctes* than in *Apternodus*.

Wood et al. (2000) tentatively suggested that an edentulous, fragmentary skull from the Paleocene of Park County, Wyoming (YPM PU16521), found roughly 12 miles to the west of the site that yielded the endocast (YPM PU16520; see fig. 1: locality 19) mentioned by Edinger (1964), could be related to *Apternodus*.

Hence, as currently recognized in the literature, the geographic range of the ''Apternodontidae'' spans western North America, from west Texas to Saskatchewan, and from South Dakota to southern California. ''Apternodontids'' appear also to have existed in

China and Mongolia. Temporally, they are known from the early Wasatchian (and by some accounts the Tiffanian) to the late Orellan—a timespan of nearly 25 million years.

NEW LOCALITIES

As indicated by the preceding review, additions to the ''apternodontid'' fossil record have been made with some regularity. However, the published record is actually quite sparse relative to the amount of currently undescribed material. To date, just two relatively complete *Apternodus* crania (AMNH 22466 and MCZ 17685) have been described (Matthew, 1910; Schlaikjer, 1933, 1934; McDowell, 1958), whereas there are no fewer than six undescribed crania (FMNH UM1690, DMNH 1747, UW 11046, UW 13508, UW 14072, USNM 455680) of similar or greater quality, three of which (UW specimens) are associated with postcrania. Well over a dozen less complete, undescribed cranial fragments of *Apternodus* and *Oligoryctes* are present in the collections of the American Museum, Carnegie Museum, Smithsonian Institution, University of Montana, and University of Wyoming. Similarly, just a single partial skull of *Oligoryctes* has been described (Hough, 1956), and only a single fragmentary mandible of ''*A.*'' *altitalonidus* has been treated in the literature (Clark, 1937).

We describe this well-preserved material in a later section on alpha taxonomy. Below, we briefly review several localities that have yielded unusually complete, undescribed fossil zalambdodonts. Each of these localities is listed alphabetically in figure 1. When available, relevant institutional locality numbers are also included. Other important localities known to have produced ''apternodontid'' fossils are summarized in the literature reviewed above.

Dilts Ranch, Wyoming (UW V76024, V76029; figure 1: locality 10)

Kron (1978) described the geology of several localities in the vicinity of Orin that have yielded some excellent specimens, such as UW 11046 and UW 13508, both of which are complete skulls with associated postcrania. Based on biostratigraphic data, Kron (1978) interpreted the age of these specimens as late Chadronian. Magnetostratigraphic data collected by Prothero (1985) are consistent with a middle or late Chadronian age for these localities. Unlike most other sites that have yielded specimens of *Apternodus*, no *Oligoryctes*-like taxa have been reported from this area.

Flagstaff Rim, Wyoming (figure 1: locality 18)

The area southwest of Casper and north of Alcova was described by Emry (1973) as Flagstaff Rim. Numerous field parties from the AMNH, DMNH, USNM, and UW have recovered material from this area, including two complete crania of *Oligoryctes* (USNM 516840 and USNM 516843). *Apternodus* and *Oligoryctes* from Flagstaff Rim have been recovered from the lower 420 feet of the measured section reported by Emry (1973), mainly between volcanic ashes B and G, radiometrically dated at approximately 35.9 and 35.6 Ma, respectively (Swisher and Prothero, 1990; Emry, 1992). Some specimens referred to ''*A.*'' *altitalonidus* have been collected from horizons stratigraphically below ash B (Emry, 1992).

Harshman Quarry, Wyoming (UW V68013; figure 1: locality 21)

Although the precise locality for the type skull of *Apternodus brevirostris* (AMNH 22466) probably will never be known, it is likely that it was near University of Wyoming locality V68013. This locality is on the northern margin of Carbon County, about 20 miles west-northwest of Marshall, in the northern part of the Shirley Basin. Harshman Quarry has yielded a flattened but nevertheless complete skull of *Apternodus* (UW 14072), associated with several distorted postcranial elements, including a partial vertebral column, scapula, proximal humerus, and tibia. The site represents Chadronian time.

West Canyon Creek, Wyoming (figure 1: locality 5)

A fairly complete skull of *Apternodus iliffensis* (USNM 455680) is known from de-

posits in the Beaver Divide area (Emry, 1975), approximately 10 miles southwest of the now abandoned town of Ervay. These deposits are older than those at Flagstaff Rim and represent either the early Chadronian or late Duchesnean. About 2 miles northwest of West Canyon Creek is Cameron Spring, the type locality of *Oligoryctes cameronensis*.

Northern Clark's Fork Basin, Wyoming (UMMP SC-210; figure 1: locality 19)

Winkler (1983) described an early Wasatchian locality north of Powell that has yielded several undescribed, fragmentary dentitions of *Parapternodus antiquus*, currently part of the University of Michigan collections (UMMP 81557–81563). Two of these (UMMP 81558 and 81561) were referred to *Parapternodus* by Robinson and Kron (1998).

Fitterer Ranch, North Dakota (figure 1: locality 17)

Isolated dentary and maxillary fragments referable to *Oligoryctes altitalonidus* have been collected by R. J. Emry from the lower part of the Brule Formation at Fitterer Ranch, about 15 miles west of Schefield. Hoganson et al. (1998) indicated that the lower part of the Brule Formation in North Dakota is Orellan in age. The channel deposit that yielded these fossils represents late Orellan time.

Fremont Butte, Colorado (DMNH 19; figure 1: locality 20)

This site consists of White River Group exposures just west of Elba, about 70 miles south and slightly west of the type locality of *A. iliffensis*. In addition to a somewhat crushed skull of *Apternodus* (DMNH 1747), it has yielded fossils of protoceratid (Artiodactyla) and cylindrodontid (Rodentia) mammals (R.K. Stucky, personal commun.). Such taxa are also found at Flagstaff Rim, Wyoming, but are widely dispersed throughout the measured section (Emry, 1992), as they are at several other late Eocene localities. Hence, although this site is probably Chadronian in age, it is not clear exactly what part of the Chadronian is represented.

McCarty's Mountain, Montana (figure 1: locality 27)

The McCarty's Mountain locality consists of a thick sequence of early Chadronian strata exposed over an area of approximately one quarter square mile north of the Big Hole River, about five miles south-southeast of McCarty's (now McCartney) Mountain. A detailed study of the McCarty's Mountain beds and fauna was conducted by Riel (1963). More recently, Tabrum et al. (1996) have discussed the locality at some length. Although local faulting within the McCarty's Mountain sequence complicates interpretation, a stratigraphic section totaling about 850 feet of continuously exposed beds was measured by D. R. Prothero in 1986 (Tabrum et al., 1996). *Apternodus* is represented at McCarty's Mountain by an undistorted skull and associated mandibles, the holotype of *A. baladontus*, described below. This specimen (FMNH UM1690) was collected from the upper part of the McCarty's Mountain sequence by James B. Orr in the summer of 1960, and was derived from beds that Tabrum et al. (1996: fig. 5) interpreted as representing Chron C16n1 (early Chadronian).

Little Pipestone Creek, Montana (MPUM MV 5905, 6001; figure 1: locality 25)

The Little Pipestone Creek localities consist of a series of sites exposed southeast of the junction of Montana highways 2 and 41 (''Cactus Junction''). The localities are about 3 miles south of the Pipestone Springs Main Pocket and Pipestone Springs Fence Pocket localities (see Kuenzi and Fields, 1971: fig. 3; Tabrum et al., 1996, 2001). The Little Pipestone Creek section is divisible (from oldest to youngest) into the University of Montana Cactus Junction (MV 6001), Honeymoon Quarry (included in MV 5905), and Little Pipestone Creek North Pocket (MV 8603) localities. The Cactus Junction locality is of middle Chadronian age, though somewhat younger than either the Pipestone Springs Main Pocket or Pipestone Springs Fence Pocket localities. The Honeymoon Quarry and Little Pipestone Creek North Pocket localities both appear to be of late Chadronian age. Most of the specimens of *Apternodus* from the Little Pipestone Creek

localities are referable to *A. mediaevus*, but one specimen (MPUM 0450) from the Cactus Junction locality is referable to the new species *A. baladontus* (described below).

Diamond O Ranch, Montana (MPUM MV 6726, 6727; figure 1: locality 9)

Specimens referred to the Diamond O Ranch local fauna were collected from several closely related localities in strata best referred to the Climbing Arrow Member of the Renova Formation exposed on the north side of the Beaverhead River about 2 miles west of Beaverhead Rock. The localities are approximately 7 miles southeast of the McCarty's Mountain locality. Tabrum et al. (1996) noted that Diamond O Ranch appeared to significantly predate the early Chadronian McCarty's Mountain fauna and assigned a late Duchesnean age to the assemblage. The Diamond O Ranch localities have yielded the majority of the known specimens of *Apternodus baladontus* sp. nov. (see below).

10N no. 2 (MPUM MV 8007; figure 1: locality 22)

The late Chadronian 10 N local fauna derives from several closely related localities in sediments of the Dunbar Creek Formation exposed on the east side of U.S. Highway 287 (formerly U.S. Highway 10N) about 3 miles north of its junction with Interstate Highway 90 (Tabrum, 1998; Tabrum et al. 2001). Locality 10N no. 2 (MV 8007) is the richest of the 10N localities and has yielded a well-preserved partial skull and associated mandible of *Apternodus mediaevus* (MPUM 6855; see below).

Eureka Valley Road, Montana (MPUM locality MV 6403; figure 1: locality 16)

The Eureka Valley Road locality (now largely destroyed) was a small exposure on the north side of a section-line road about 4 miles northwest of the town of Three Forks in sediments of Robinson's (1963) informal ''middle white unit'' of the Climbing Arrow Formation (United States Geological Survey locality f158; University of Montana locality MV6403). The fauna known from Eureka Valley Road and the nearby, closely related Rahn Farm locality is indicative of an early Chadronian age (Tabrum et al., 2001). In 1983, P. McKenna collected right and left maxillary fragments and an associated, partial petrosal of *Oligoryctes cameronensis* (MPUM 6859) from this locality.

ANATOMICAL ZALAMBDODONTY

With the notable exception of the edentulous Fort Union Formation cranial fragments (YPM PU16520 and YPM PU16521), fossils have usually been associated with *Apternodus* and/or *Oligoryctes* based on the possession of zalambdodont cheek teeth. For this reason, we describe in this section the precise, anatomical meaning of the term ''zalambdodont''. Throughout this paper we use this term descriptively, not taxonomically.

Cusp Homologies

Apternodus is dentally remarkable because its cheek-teeth possess a single, major V-shaped loph, the lingual apex of which is the paracone. A similar morphology is present in extant golden moles (Chrysochloridae), solenodons (Solenodontidae), and tenrecs (Tenrecidae). The main cusp of the zalambdodont upper molar has previously been identified as a ''zalambdocone'' (McDowell, 1958), an ''eocone'' (Vandebroek, 1961; Quinet and Misonne, 1965), a ''protocone'' (Leche, 1907; Gregory, 1910), an ''amphicone'' (Galbreath, 1953), and a ''paracone'' (Butler, 1937; Patterson, 1956, unpublished MS). Based on occlusal relationships with the lower dentition, we consider ''paracone'' to be correct.

McDowell (1958) argued that the main upper cusp of the anatomically zalambdodont *Solenodon* was not the paracone, but ironically provided in the same paper clear evidence to the contrary. His figure 22 (reproduced here as fig. 3) shows the upper and lower dentitions of *Solenodon* and the anatomically dilambdodont *Nesophontes* in occlusion, and demonstrates the close fit of the protocone into the talonid basin in both taxa, although the protocone is restricted to the cingulum and the talonid reduced in *Solenodon*. Similarly, this figure shows the paracone of each upper molar occluding with the

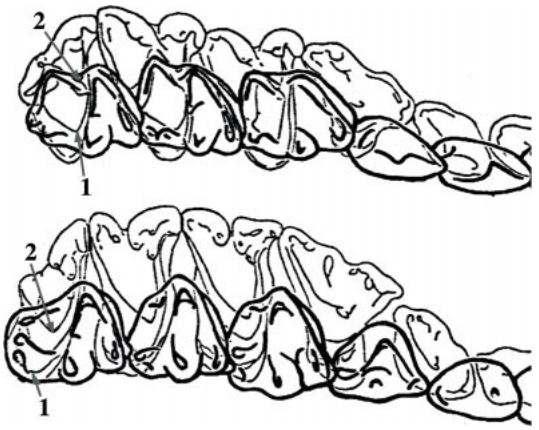

Fig. 3. P3-M3 occlusion in *Nesophontes* (top) and *Solenodon* (bottom). Upper teeth have light outline, lowers have dark outline. Note consistent relation of protocone with talonid basin (indicated with a ''1'') and paracone with hypoflexid (indicated with a ''2'') in both taxa. Adapted from McDowell (1958: fig. 22).

buccal hypoflexid of each lower molar, as well as varying degrees of shear between the preparacrista and protocristid (greater in *Solenodon*). These occlusal relationships, i.e., protocone-talonid, paracone-hypoflexid, and preparacrista-protocristid, are consistent throughout dentally tribosphenic mammals, and have been consistently recognized since the 1960s (e.g., Van Valen, 1966; Szalay, 1969; Bown and Kraus, 1979), and often before (e.g., Butler, 1937; Patterson, 1956). Occlusion between the protocone and talonid is usually much more conspicuous than that between the paracone and hypoflexid (e.g., *Didelphis*); however, the reverse is true among zalambdodont mammals.

Hence, anatomical zalambdodonty may be defined when the primary occlusal relationship between upper and lower cheek teeth occurs between the paracone and hypoflexid, primary shearing occurs between the preparacrista and protocristid, and the metacone and talonid basin are reduced or absent. A small metacone is present in the anatomically zalambdodont tenrecs *Potamogale* and *Protenrec* (Butler, 1985), and a small talonid basin is present in *Potamogale* and *Solenodon*. However, the metacone is difficult to detect in worn specimens, and the presence of a metacone and small talonid basin does not change the fact that the primary occlusion between upper and lower teeth in these taxa occurs between the paracone and hypoflexid, and shearing between the preparacrista and protocristid.

Together with the complementary term ''Dilambdodonta'', the term ''Zalambdodonta'' was coined by Gill (1883: 119) in reference specifically to extant golden moles, solenodons, and tenrecs. Gill used ''zalambdodont'' in both a taxonomic and descriptive sense. Taxonomically, the definition was at the rank of an infraorder, containing the Chrysochloridae, Solenodontidae, and Tenrecidae. Gill's ''Dilambdodonta'' contained the Tupaiidae, Macroscelididae, Erinaceidae, Soricidae, and Talpidae. Anatomically, Gill (1883: 119) defined zalambdodont mammals as ''Bestiae with narrow molar teeth having V-shaped ridges'' and dilambdodont mammals as ''Bestiae with broad molar teeth surmounted by W-shaped ridges''. These anatomical definitions of di- and zalambdodonty were expanded slightly in Gill (1884: 135–136):

> All the Insectivora of the northern hemisphere, or rather the temperate portions, have oblong molars with two V-shaped (W) ridges, while certain tropical forms have transverse molars (that is, they are very short in the line of the jaws), surmounted with but one V-shaped ridge. Those with two V-shaped ridges are called Dilambdodonta (from the Greek dis, double, the letter Λ, lambda, and odous, odonta, teeth), and the others, with one V-shaped ridge are conversely named Zalambdodonta (from the Greek za, signifying emphatically, the letter Λ, and odous, odonta).

When Gill published this definition, consensus did not exist regarding cusp homologies in therian molars; hence, he did not call the primary cusp of the zalambdodont upper molar the ''paracone''. Nevertheless, the animals upon which Gill based his definition of zalambdodonty are currently recognized as having a common pattern of cusps and dental occlusion (Patterson, 1956, unpublished MS), and should therefore form the anatomical reference point for the meaning of the dental term ''zalambdodont''.

WHICH MAMMALS ARE ZALAMBDODONT?

In the years following Gill (1883), ''zalambdodont'' has come to be used loosely as

a descriptive term for a variety of mammals with generally triangular, transversely elongate upper cheek teeth, usually associated with a relatively small talonid of the lowers. Such animals often referred to as ''zalambdodont'' include deltatheridiids (Schlaikjer, 1933), micropternodontids (Matthew, 1903), palaeoryctids (Matthew, 1913; Thewissen and Gingerich, 1989), and most notably, zalambdalestids (Gregory and Simpson, 1926). In fact, none of these taxa is anatomically zalambdodont in the same sense as golden moles, *Solenodon*, or tenrecs.

Gregory and Simpson (1926) did not provide an etymological definition of the family Zalambdalestidae or genus *Zalambdalestes*. However, previous use of the root of this name by Gill and others suggests that Gregory and Simpson (1926) chose their generic and familial names based on the perceived shape of the cheek teeth. The type specimen of *Zalambdalestes lechei* (AMNH 21708) has heavily worn teeth, showing transversely elongate upper molars and lowers with a tall trigonid. Material recovered since Gregory and Simpson's description (e.g., Kielan-Jaworowska, 1968) demonstrates that in contrast to the golden moles, solenodons, and tenrecs to which Gill was referring, zalambdalestids possess prominent metacones on their upper molars, broad talonid basins on their lowers, and have a primary occlusal relationship between protocone and talonid basin (Kielan-Jaworowska, 1968: 187). Although not as well developed as those of *Zalambdalestes* and *Deltatheridium*, the metacones and talonid basins of *Micropternodus* and palaeoryctids are prominent; consequently, none of these taxa is anatomically zalambdodont.

Patterson (1956: 53–56) noted the close correspondence between the cheek teeth of Gill's zalambdodonts and those of certain late Jurassic, ''pantothere''-grade mammals such as *Dryolestes*, noting that (p. 54) ''the resemblance between the molars of pantotheres and of specialized zalambdodonts is extraordinarily close, amounting nearly to identity in almost all features of the crown.'' Hence, ''zalambdodont'', as an adjective defined above, applies to most dryolestoids (*sensu* McKenna and Bell, 1997), the marsupials *Notoryctes*, *Necrolestes*, and *Yalkaparidon*, in addition to placental golden moles, *Solenodon*, tenrecs, *Apternodus*, *Oligoryctes*, and parapternodontids (see below). Interestingly, the vespertilionid bat *Harpiocephalus* also appears to be zalambdodont, with no metacone and a diminutive talonid (Miller, 1907), in contrast to the dentition of other bats. If the relationship hypothesized below between ''apternodontids'' and shrews is valid, the dentition in *Harpiocephalus* would provide a similar case of zalambdodonty occurring within a group of otherwise dilambdodont mammals. In any event, as an anatomical condition, zalambdodonty has occurred several times independently within Mammalia (Asher and Sánchez-Villagra, 2000).

SPECIES RECOGNITION

Recognition of a ''phylogenetic species'' (Rosen, 1978; Cracraft, 1983; Nixon and Wheeler, 1992; McKenna and Bell, 1997: 5) should depend on the recognition of ''the smallest diagnosable autapomorphic units amenable to cladistic analysis'' (Nixon and Wheeler, 1992: 127). An emphasis on apomorphy in recognizing species is useful because of the difficulty of consistently recognizing reproductive barriers (particularly ''potential'' ones) among groups of organisms (particularly extinct ones). In practice, the process of paleontological species recognition amounts to grouping sets of monomorphic specimens into terminal taxa. Understanding supraspecific relationships may then proceed by analyzing such taxa cladistically and applying names to the resulting monophyletic sets of terminal taxa.

Alpha Taxonomy

Previous authors have identified many autapomorphies among existing ''apternodontid'' species, although type specimens vary considerably in quality. In this paper, we recognize all of the previously defined species as terminal taxa, and add to this number more terminals based on unique character combinations that, for reasons defined below, do not fit into existing species-level diagnoses.

In this section we are concerned with defining the terminal taxa, i.e., species, that will form the basis of our phylogenetic analysis. Supraspecific units discussed in this section are consistent with the phylogenetic conclusions detailed in the next section, unless enclosed between quotation marks.

Species of *Apternodus* recognized here include *A. mediaevus* Matthew, 1903; *A. gregoryi* Schlaikjer, 1933; *A. brevirostris* Schlaikjer, 1934; *A. iliffensis* Galbreath, 1953; *A. baladontus* (sp. nov.), *A. major* (sp. nov.), and *A. dasophylakas* (sp. nov.). ''*Apternodus*'' *altitalonidus* Clark, 1937 is also a valid terminal taxon, but does not belong in the genus *Apternodus*. Instead, following previous, informal usage (e.g., Emry, 1979), we propose the combination *Oligoryctes altitalonidus*. *Oligoryctes cameronensis* Hough, 1956; *Parapternodus antiquus* Bown and Schankler, 1982; and *Koniaryctes paulus* Robinson and Kron, 1998 are all valid taxa, as are the unnamed Bridgerian taxon from Tabernacle Butte, Wyoming (McKenna et al., 1962) and the Paleocene Silver Coulee taxon from Park County, Wyoming (Wood et al., 2000). The preceding taxa have all been referred to the ''Apternodontidae'' in the literature, but do not exclusively share a single common ancestor with *Apternodus*. Hence, the Apternodontidae as defined here is restricted to the seven species of *Apternodus* listed above. Five taxa previously assigned to the ''Apternodontidae'' sensu lato are here placed in two new families within Eutheria, *incertae sedis*: Oligoryctidae (*O. cameronensis*, *O. altitalonidus*, and the Tabernacle Butte taxon) and Parapternodontidae (*Koniaryctes* and *Parapternodus*).

Diagnoses of these taxa, including five new species (three of which are named here), are given below. Numbers following localities listed under the ''temporal and geographic distribution'' subsection for each species correspond to numbered localities shown in figure 1. A key summarizing differences among extinct, North American zalambdodont taxa is provided in table 1.

CLASS MAMMALIA LINNAEUS, 1758

COHORT EUTHERIA HUXLEY, 1880

ORDER UNDETERMINED

FAMILY APTERNODONTIDAE MATTHEW, 1910[1]

INCLUDED GENERA: *Apternodus* Matthew, 1903.

DISTRIBUTION AND DIAGNOSIS: As for *Apternodus*.

Apternodus Matthew, 1903

TYPE SPECIES: *Apternodus mediaevus* Matthew, 1903

INCLUDED SPECIES: *Apternodus gregoryi* Schlaikjer, 1933; *A. brevirostris* Schlaikjer, 1934; *A. iliffensis* Galbreath, 1953; *A. major* sp. nov.; *A. baladontus* sp. nov.; *A. dasophylakas* sp. nov.

TEMPORAL AND GEOGRAPHIC DISTRIBUTION: Duchesnean (late middle Eocene) through early Orellan (early Oligocene) throughout western North America.

DIAGNOSIS: These insectivoran-grade mammals range in size from a large shrew (cf. *Crocidura*) to *Erinaceus*. Metacones are absent; talonids are reduced to a single cusp without a basin; and P4/p4 are molariform. The dental formula is 2.1.3.3/3.1.3.3, showing enlarged and procumbent upper and lower anterior incisors. The anterior margin of the coronoid process extends anteriorly to occlude part of m3 from lateral view. The lacrimal foramen is enlarged and faces laterally. The anterior margin of the infraorbital canal is concave, providing attachment space for sizable muscles of the anterior rostrum. A sagittal crest is present, continuous posteriorly with the prominent nuchal crest and forking anteriorly into anterolaterally running crests flanking the posterior margin of the nasal bone. The ethmoid foramen and sinus canal open into the orbitotemporal region via the roof of the sphenorbital fissure. The posterolateral braincase is expanded into lambdoid plates comprised of the squamosal,

[1] Under the currently accepted International Code of Zoological Nomenclature, art. 36 (International Commission on Zoological Nomenclature, 1999: 45), all family-group names are coordinate and date from the first published, in this case Apternodontinae Matthew, 1910. Therefore, if we are to follow the Code, Apternodontidae Matthew, 1910, dates from Matthew's use of the subfamily name Apternodontinae (Matthew, 1910: 35, published March 22, 1910) rather than from Matthew, Gregory, and Mosenthal's (in Osborn, 1910: 519) family name Apternodontidae coined in October of the same year.

TABLE 1
Key to North American Fossil Zalambdont Species[a]

A) Talonid basin and metacones absent
1) yes: go to B
2) no: find some other key

B) Lambdoid plates
1) present: go to C
2) absent: go to J

C) Entoglenoid mediolaterally elongate, provides posterior support for condyle of dentary medial to postglenoid foramen and anterior to middle ear promontory
1) yes: *Apternodus*, go to D
2) no: Silver Coulee taxon, (dentition unknown)

D) Anterior dentition large and bulbous, reduced p3 cingulid, lower molars gracile relative to anterior dentition
1) yes: *A. mediaevus* or *baladontus*, go to E
2) no: other *Apternodus*, go to F

E) Ventral lambdoid plate extends well ventral to jaw joint and external auditory meatus (EAM), elongate I2 and P2, posterior cusp on p3, well-defined m2 cingulid
1) yes: *A. mediaevus*
2) no: *A. baladontus* (spherical I2 and P2, simple p3 without distal cusp, ventral lambdoid plate extends only slightly below entoglenoid process)

F) Lacrimal foramen set off from anterior orbit by distinct crest
1) yes: *A. brevirostris, iliffensis*, or *dasophylakas*—see G (lacrimal region unknown in *dasophylakas*)
2) no: *A. gregoryi* or *major*, see I

G) Upper molar protocones present, antemolar diastemata absent
1) yes: *A. brevirostris*
2) no: *A. iliffensis* or *dasophylakas*—go to H

H) Antemolar diastemata present, M3 similar in buccolingual width as M2
1) yes: *A. dasophylakas*
2) no: *A. iliffensis*

I) EAM shows prominent torus, anterior lambdoid plate sharply curved laterally, medial ridge on petrosal, small/absent antemolar diastemata
1) yes: *A. major*
2) no: *A. gregoryi* (narrow, sharply angled EAM; ventrally sharp, projecting lambdoid plate)

J) Talonid cusp on m3, buccal cingulid on molars, anterior incisors gracile
1) yes: *O. cameronensis*, *O. altitalonidus*, or Tabernacle Butte taxon, see K
2) no: *Parapternodus* or *Koniaryctes*, see M

K) Internal coronoid process pocketed
1) yes: *O. altitalonidus* or *O. cameronensis*, see L (three cusps on i2-3, foramen ovale enlarged)
2) no: Tabernacle Butte taxon (incisors and cranium unknown, smallest animal in this study)

L) Four lower premolars, maxillary zygoma lateral to M2
1) yes: *O. altitalonidus* (smaller than *O. cameronensis*)
2) no: *O. cameronensis* (three lower premolars, maxillary zygoma lateral to posterior M1)

M) Paraconid notch present
1) yes: *Parapternodus antiquus* (premolariform p4)
2) no: *Koniaryctes paulus* (known only from mandibular fragments and molars)

[a] Tooth notation: capital letters indicate upper and lower case indicates lower teeth.

petromastoid, and occipital bones, all of which are exposed laterally. The mandibular condyle is supported posteriorly by an enlarged entoglenoid process, medial to the postglenoid foramen and anterior to the middle ear. A postglenoid process is absent and the zygomatic arch is incomplete. An ossified auditory bulla is absent; and a piriform fenestra is usually present. The epitympanic recess extends anteriorly into a space bounded ventrally by the entoglenoid process, making the anterior wall of the tympanic cavity concave.

Apternodus mediaevus Matthew, 1903

TYPE SPECIMEN: AMNH 9601 (left dentary with m1-m2; see fig. 2).

REFERRED SPECIMENS: AMNH 9607, left dentary with p3 (see Schlaikjer, 1933: 6, footnote 2); AMNH 76745, posterior braincase with most of left lambdoid plate and petrosal, associated right partial maxilla with I2, C, P2, broken I1, left dentary fragment with p2–3, broken p4, isolated right and left canines, left i3, several other isolated tooth fragments, isolated ?lumbar and caudal vertebrae, right and left proximal humeri with partial right shaft, right distal humerus (fig. 4), metapodial fragments; AMNH 97255, left dentary with p2-m3 (fig. 5); AMNH 97256, right dentary with m1-m3; AMNH 97258, left dentary with p3-m2; USNM, 18966, right dentary with p3-m3; MPUM 0576, right dentary with p4-m2, roots of m3; MPUM 3799, palate with left I1-P3, right C-M1 and alveoli for I1–2, associated with left lambdoid plate (fig. 6); MPUM 6767, left dentary with p3-m3; MPUM 6768, right dentary with p3-m1; MPUM 6855, skull missing anterior rostrum (fig. 7), associated right dentary with p4-m3 (fig. 8); MPUM 6856, left maxillary fragment with canine; MPUM 7820, right dentary with p3-m3; CM 13676, rostrum with left I1-M3, left I2-P2 (original lost, known only from photographs; see fig. 9); CM 31323, right maxilla with C and P2; CM 37455, fragmentary rostrum with right I1-C, left I1, P2, maxillary fragments with partial right M1–2, left P4-M1, associated right and left dentaries with fragmentary right m1-m3, left i1, and roots for p4-m2, isolated lower right i1, c, p2, p3, lower left i3, c, and other fragmentary upper and lower teeth, many disarticulated, fragmentary bits from right and left maxillae and dentaries, isolated cervical and lumbar vertebrae, distal tibia and ulna, partial calcaneus, and phalanx (fig. 10); CM 71569, right maxilla with P2-M2; and CM 71570, right dentary with p3-m2.

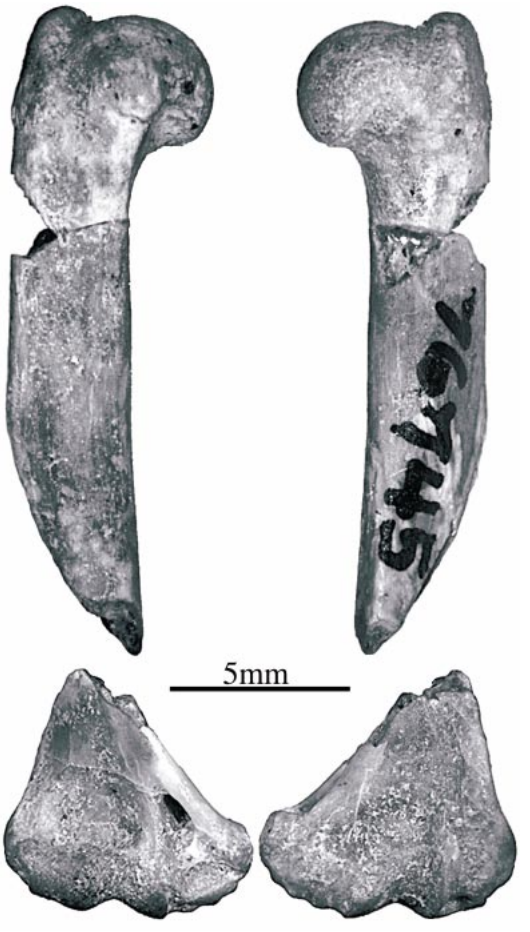

Fig. 4. AMNH 76745, *Apternodus mediaevus* proximal and distal fragments of right humerus (associated partial skull and dentition not figured).

TEMPORAL AND GEOGRAPHIC DISTRIBUTION: Middle to late Chadronian (Late Eocene) of southwestern Montana (Pipestone Springs 29, Canyon Ferry 6, West Easter Lily 13, Highway 10N 22, and Little Pipestone Creek 25). In this section and those that follow, numbers given after localities correspond to those depicted on the map shown in figure 1.

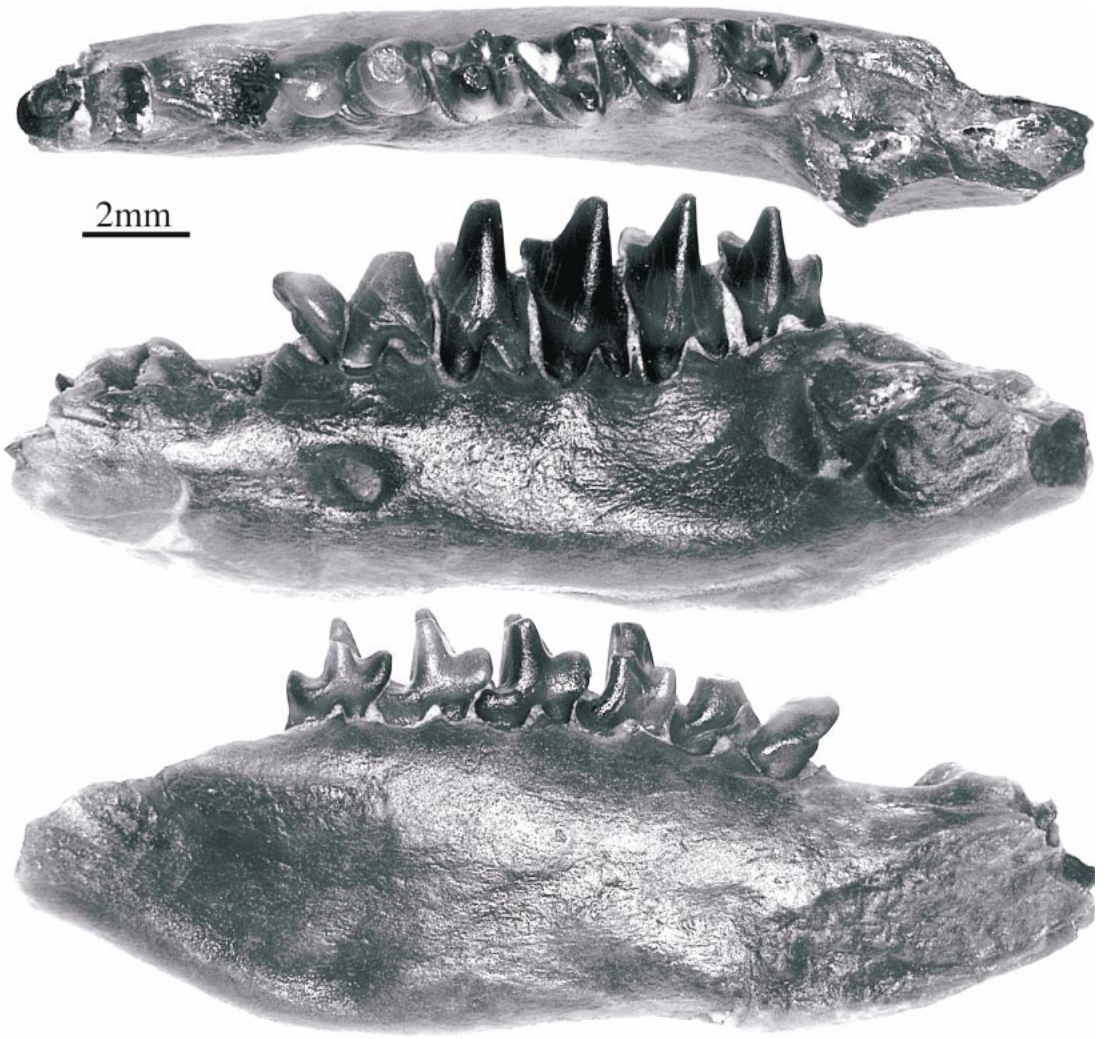

Fig. 5. AMNH 97255, *Apternodus mediaevus* mandible from Pipestone Springs, Montana in occlusal (top), lateral (middle), and lingual (bottom) views.

DIAGNOSIS: The upper and lower canines have elongate, bulbous crowns. The upper canine has two broad roots, anterior and posterior; some specimens (e.g., MPUM 3799; fig. 6) show a small, lingually situated third root. The P2 is slightly enlarged and elongate, with a distinct crest running distally from the main cusp and a slender, lingual, third root extending from the midpoint of the tooth. The i2 is diminutive with a small, poorly defined alveolus that abuts against the much larger i1. The i3, canine, p2, and p3 are also enlarged and bulbous. The p3 shows a distinct posterior cusp and a slight buccal cingulum. The upper molars have distinct protocones. Buccal cingulids are present on the lower molars. Basicranially, the rostral tympanic process of the petrosal exhibits a medial ridge. The posttympanic process extends well ventral to the external auditory meatus.

REMARKS: Particularly noteworthy among the *Apternodus mediaevus* specimens not previously discussed in the literature are MPUM 3799, an associated rostrum and partial posterior braincase (fig. 6); AMNH 76745, a fragmentary skull with associated postcranial fragments (fig. 4); MPUM 6855,

Fig. 6. MPUM 3799, *Apternodus mediaevus* partial skull from Little Pipestone Creek, Montana. Lateral (top left) and occlusal (top right) views of rostrum, lateral view of associated lambdoid place (bottom).

Fig. 7. MPUM 6855, *Apternodus mediaevus* partial skull from 10N no. 2 in stereo ventral (top), lateral (middle), and dorsal (bottom) views.

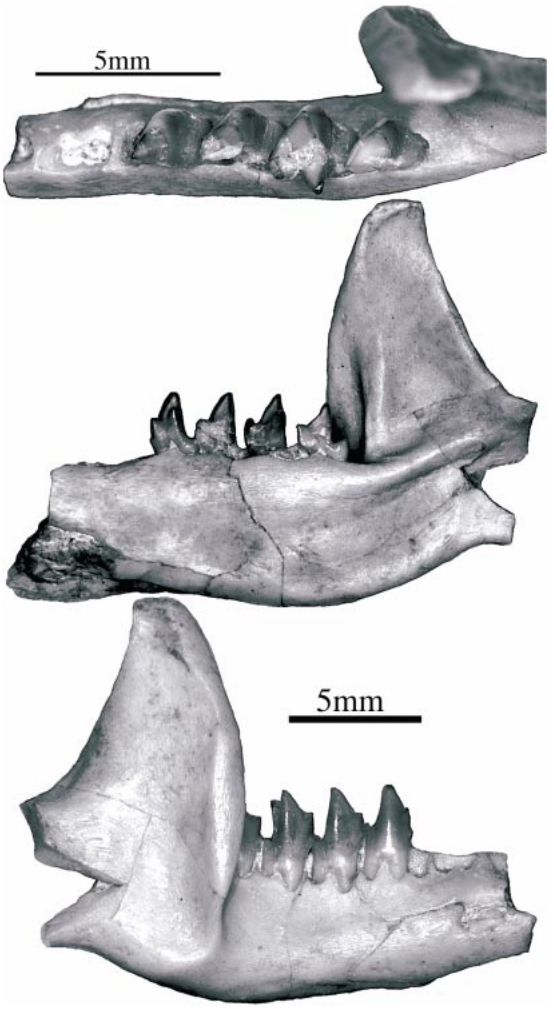

Fig. 8. MPUM 6855, *Apternodus mediaevus* mandible from 10N no. 2 in lingual (top), lateral (middle), and occlusal (bottom) views.

a partial skull (fig. 7) and associated mandible (fig. 8); CM 13676, a rostrum and complete upper dentition (fig. 9; original lost); CM 37455, a fragmentary skull and mandibles associated with several broken postcranial elements (fig. 10); and AMNH 97255, a well-preserved dentary (fig. 5). These specimens provide a fairly complete picture of the skull of *A. mediaevus*, as well as some information about its skeleton. With the exception of the more gracile upper P2 and I2, the more ventrally pronounced lambdoid plate, the diminutive i2, and the posterior cusp and cingulid on p3, *A. mediaevus* resembles *A. baladontus* sp. nov., described below.

The Canyon Ferry specimen preserving associated cranial and postcranial fragments (CM 37455; White, 1954) is included in *Apternodus mediaevus* based on the morphology of its I2, P2, p3, and enlarged, bulbous upper and lower canines. However, this specimen is larger than others in *A. mediaevus*; its inclusion increases the size range in this species (see later section on metric variation). The only other *Apternodus* specimen known from Canyon Ferry (USNM 18914, a maxillary fragment with M1 and alveoli for P3-P4, M2-M3) is smaller and well within the range of variation for *A. mediaevus*. Nevertheless, considerable variation in size does occur in some modern taxa (see below); more importantly, CM 37455 is anatomically cohesive with specimens in the *A. mediaevus* hypodigm, and for the present is retained in this species.

One mandible in the AMNH collection from Pipestone Springs (AMNH 76747, a left dentary with an erupting p3 and broken m1-m3) does not fit into existing specific diagnoses, and may represent yet another species from Montana. This specimen differs from *A. mediaevus* in showing a very gracile coronoid process and dentary. The coronoid does not anteriorly overlap with m3, and the mandibular corpus is thinner and more gracile than those of any other Pipestone Springs specimen, including one with erupting permanent premolars (CM 71570). Some breakage and postmortem damage has made the mandibular condyle of AMNH 76747 shorter mediolaterally than it was in life. Although the trigonids of all three molars of AMNH 76747 are severely damaged and the intact p3 is not yet fully erupted, remnants of its teeth closely resemble those of other *Apternodus* specimens from Pipestone Springs. In particular, the p3 is bulbous, with a distinct posterior cusp and weak buccal cingulum. Because of these similarities and because AMNH 76747 represents a juvenile and possibly pathologic individual, we refrain from recognizing it as a new species.

Apternodus baladontus, new species

TYPE SPECIMEN: FMNH UM1690, complete skull (fig. 11) with both mandibles (fig.

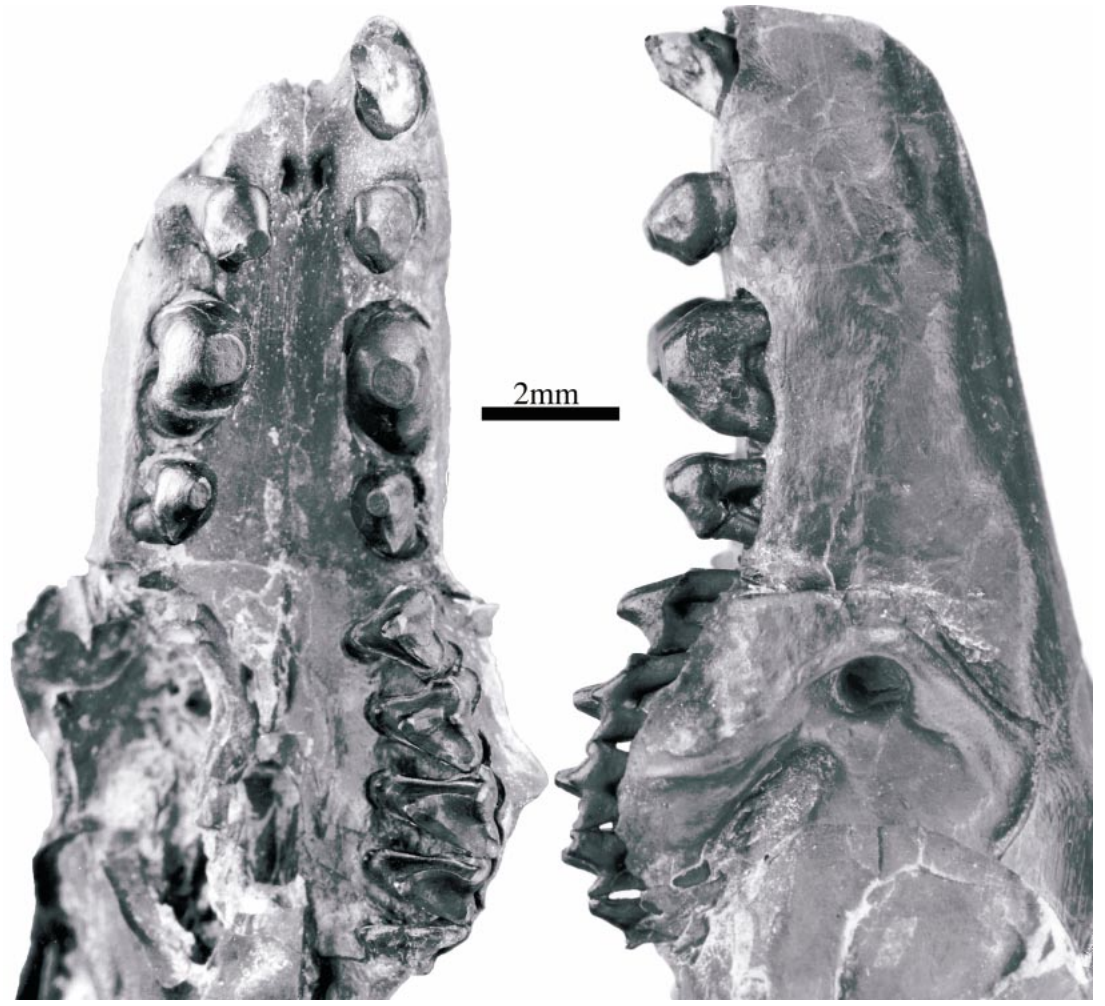

Fig. 9. CM 13676, *Apternodus mediaevus* rostrum from Pipestone Springs, Montana in ventral (left) and lateral (right) views. Photos by Chester Tarka.

12). Damage to FMNH UM1690 is confined mainly to the occiput, the anterior upper incisors, and the coronoid process of the left mandible. Part of the cerebellar cast is exposed by damage to the posterior parts of the parietals. Otherwise, the specimen is very well preserved. The frontispiece of this monograph shows a reconstruction of *Apternodus baladontus* as it may have appeared in life, based on this specimen.

REFERRED SPECIMENS: MPUM 0450, left dentary with broken p3-m2; MPUM 2620, rostrum with left I2-P3, right C-P2; MPUM 2634, rostrum (fig. 13) and mandibles (fig. 14) with nearly complete upper and lower dentition, missing anterior incisors and crown of left m1; MPUM 2645, right maxilla with canine; CM 9552, right dentary with p4-m2, erupting p3; CM 71563, right dentary with p3-m3.

TEMPORAL AND GEOGRAPHIC DISTRIBUTION: Late Duchesnean (late middle Eocene) to middle Chadronian (late Eocene) of southwestern Montana (McCarty's Mountain 27, Diamond O Ranch 9, and Little Pipestone Creek 25).

ETYMOLOGY: Named for the sphere-shaped anterior dentition, based on the Greek words for ''ball'' and ''tooth''.

DIAGNOSIS: In addition to large, bulbous up-

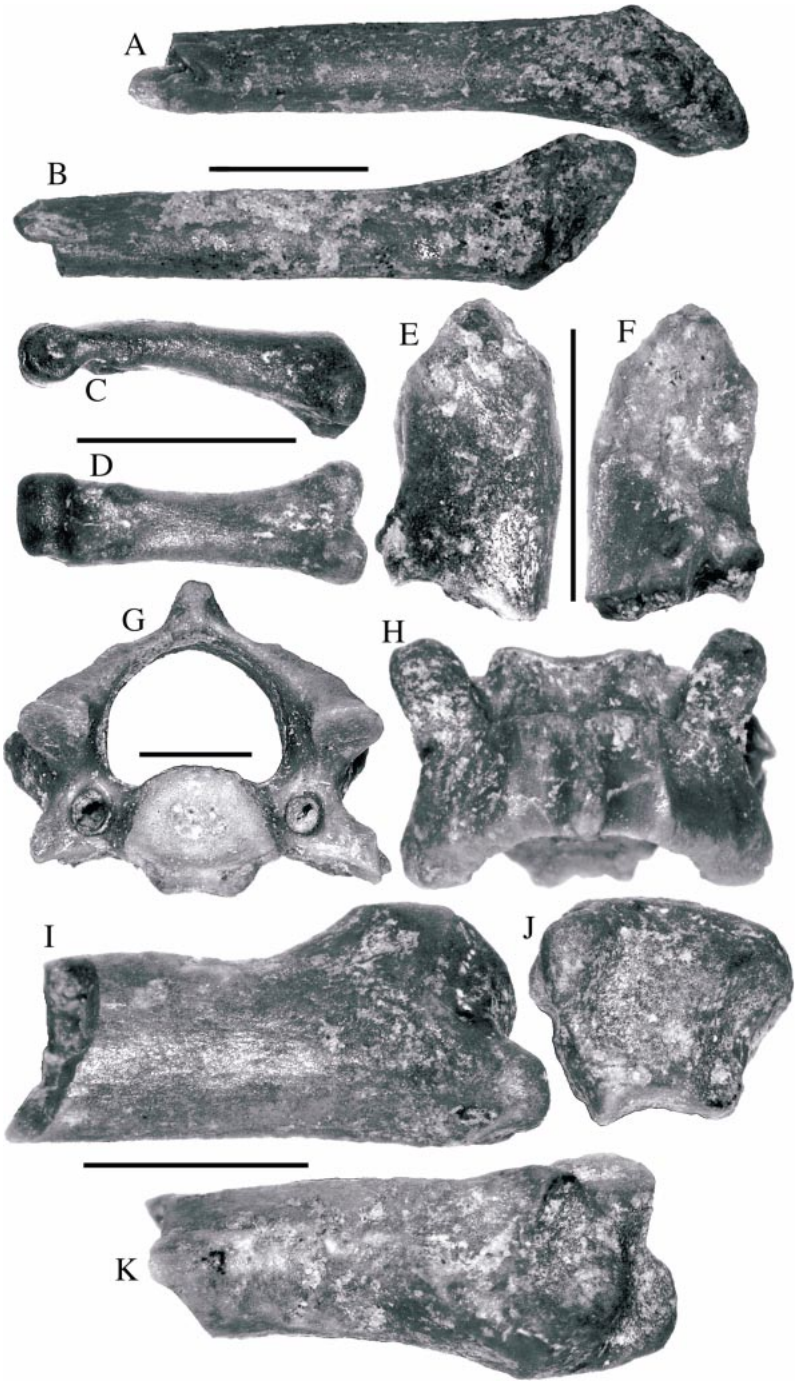

Fig. 10. CM 37455, *Apternodus mediaevus* postcrania from Canyon Ferry, Montana, as follows: lateral (A) and medial (B) views of distal ulna with partial shaft; lateral (C) and ventral (D) views of phalanx; lateral (E) and medial (F) views of proximal calcaneus; posterior (G) and dorsal (H) views of cervical vertebra; anterior (I), ventral (J), and posterior (K) views of distal tibia. Scale bars represent 3mm; note that elements are not illustrated to the same scale.

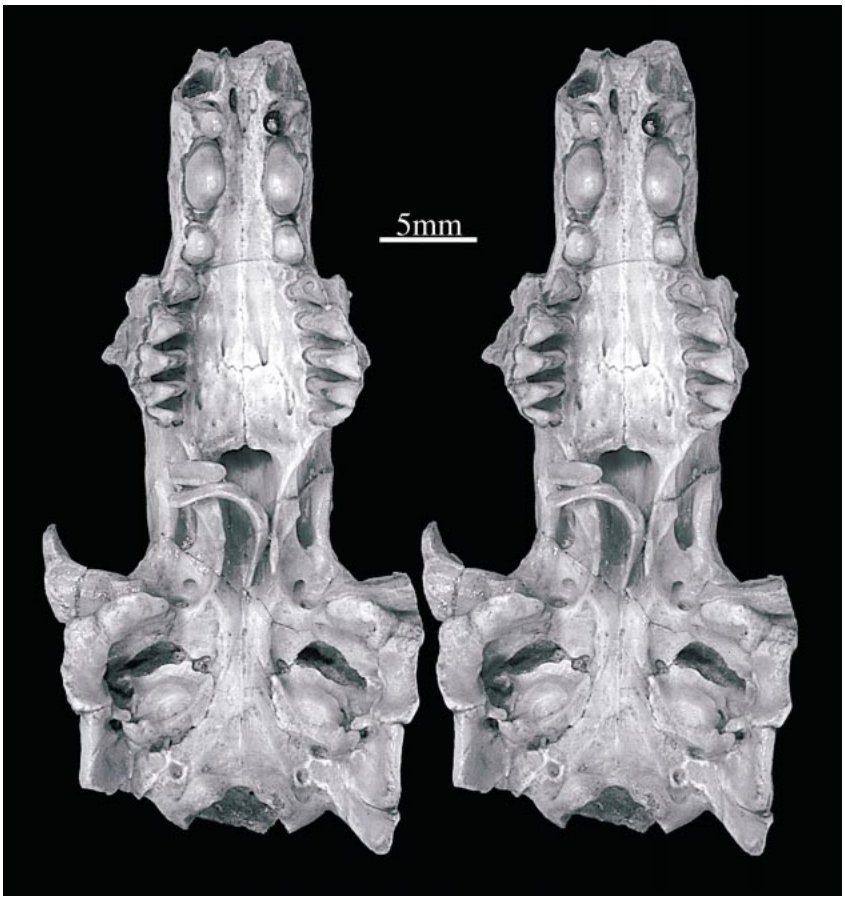

Fig. 11. FMNH UM1690, *Apternodus baladontus* sp. nov. type specimen from McCarty's Mountain, Montana. Stereo view of ventral skull, (p. 27) anatomical guide to ventral view (see text for abbreviations), (p. 28) dorsal (top) and lateral (middle and bottom) views of skull, (p. 29) detail of left ear region. See text for abbreviations. Dorsal and lateral photos of skull by Chester Tarka.

per canines, bulbous i3-p3, and prominent molar protocones, *A. baladontus* shows a large, spherical upper P2 and I2, with P2 showing at least three and sometimes four roots (e.g., MPUM 2645). The upper canine has a prominent, buccally situated third root. The p3 lacks a prominent posterior cusp. *A. baladontus* is further distinguished from *A. mediaevus* by the small but distinct i2 which has an alveolus separate from that of i1, small cheek teeth with molars that show weak or absent buccal cingulids, the presence of a bony torus defining the ventrolateral margin of the external auditory meatus, and the ventrally short posttympanic process (fig. 11).

REMARKS: In addition to the type, the other exceptional element of the *A. baladontus* hypodigm is MPUM 2634, a rostrum (fig. 13) with complete mandibles (fig. 14). This specimen is unusual in that it preserves a suture between the maxilla, palatine, and frontal in the orbital mosaic, and demonstrates that *Apternodus* possessed a maxilla that extended far into the orbit. Remnants of the orbital sutures of the maxilla are also evident in a specimen of *A. mediaevus* (MPUM 6855; fig. 7). In other specimens (e.g., AMNH 22466 and MCZ 17685) these sutures are fused, and do not permit estimates of the maxillary contribution to the orbital mosaic (contra McDowell, 1958). Although many of its cranial sutures are untraceable, the *A. baladontus*

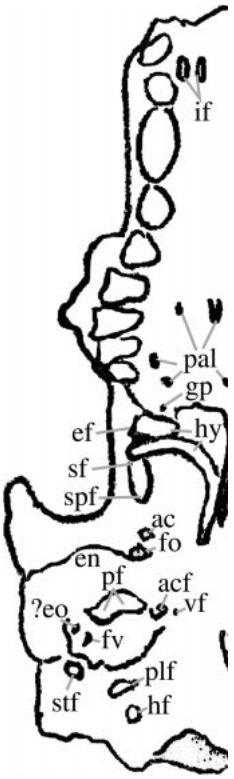

Fig. 11. Continued.

type (FMNH UM1690) is otherwise complete enough to warrant particular attention, as follows.

ROSTRUM: The nasals, maxillaries, and premaxillaries have completely fused. Above the enlarged upper incisors, a shallow pit can be seen on each premaxillary, just posterior to the anterior end of the bony snout. The dorsomedial boundary of a large muscle scar extends from the medial edge of these pits back to a point above the lacrimal foramen. This scar covers most of the side of the snout and evidently supported powerful musculature for the movement of some sort of proboscis. Similarity to the snouts of *Solenodon*, *Nesophontes*, and *Centetodon* (Lillegraven et al., 1981) is marked. The anterior rim of the orbit is likewise similar to that of *Nesophontes*, *Solenodon*, and *Centetodon*. There is a large lacrimal foramen, from which the nasolacrimal canal runs anteromedially across the roof of the infraorbital canal. The latter is relatively short. A short nubbin over M1 is all that remains of the zygomatic wing of the maxillary bone. In other insectivorans (e.g., most tenrecs and *Solenodon*), this structure is usually larger and more posteriorly located. Several nutritive foramina open into the infraorbital canal. The sphenopalatine and greater palatine foramina open separately into the lower part of the orbit and are even with the posterior end of the palate.

The palatines extend forward to a point opposite the posterior half of M1. Their combined anterior border takes a straight course across more than half of the palate, although the squamous nature of the contact results in an irregular series of about eight forward-projecting lobes of bone. The posterior border of the palate terminates relatively farther behind the level of M3 than in *A. brevirostris*, in agreement with the condition in *A. gregoryi*. The border is swollen at the internal nares and projects somewhat ventrally, but a true torus is not present, nor is there any posterodorsal shelf behind the swelling. The border is instead notched at the midline in this specimen. There are no palatal fenestrae.

At least seven pairs of palatal foramina are present posterior to the level of P2. The most posterior pair is the largest, situated posteromedial to M3, and presumably carried the greater palatine artery. Dorsally, the opening of the greater palatine foramen is ventrolateral to that of the sphenopalatine foramen; the two are not coincident. The greater palatine artery apparently divided into a number of branches that emerged onto the palate at intervals. A small, paired foramen can be seen anteromedial to the opening for the minor palatine artery at the level of M3. Anterolabial to this foramen lies another paired foramen in the maxillopalatine suture opposite the interdental embrasure between M2 and M3; this gives rise to a faint groove that runs forward on the surface of the maxillary close to the lingual roots of the molars. This may be related to a feature called the third supply tract of the palate in *Centetodon* (McKenna 1960: 139). The next pair of foramina is located at the anterior limits of the palatine bones. Approximately 1 mm from each side of the midline, a large vascular foramen is present. The maxillary is grooved from there to a point opposite P3. The groove from each

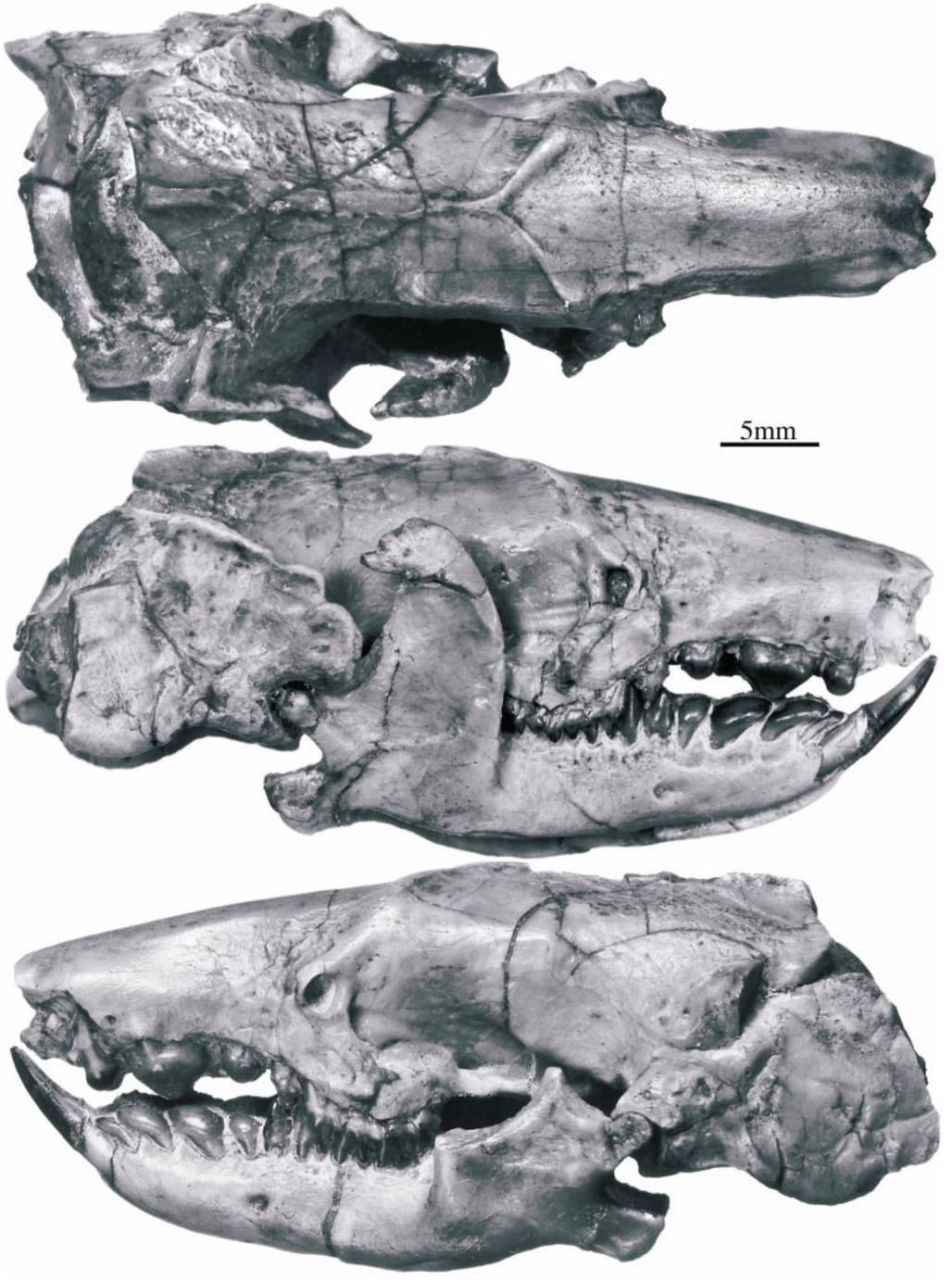

Fig. 11. Continued.

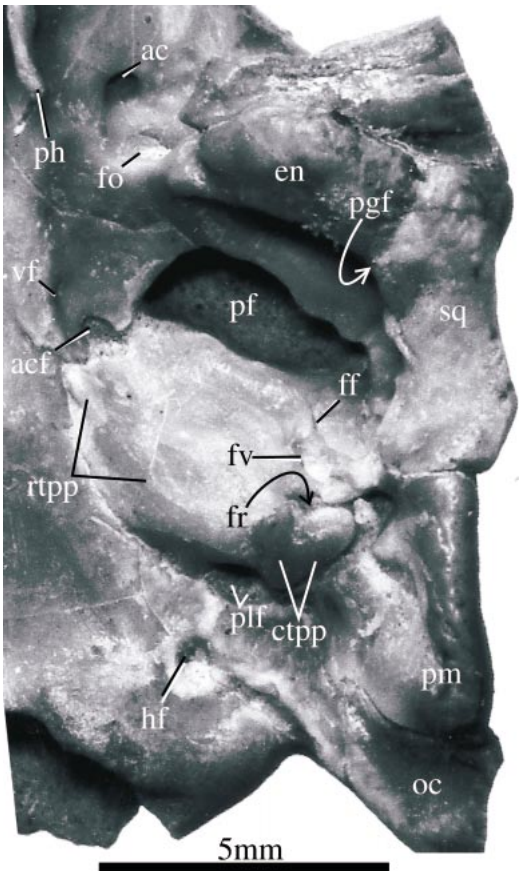

Fig. 11. Continued.

foramen of the pair divides into two slightly divergent grooves. Between the lingual roots of P2 and P3 are two small foramina on each side. Anteriorly, no additional paired foramina are present except for the large incisive foramina between the incisors.

ORBITOTEMPORAL REGION AND BASICRANIUM: The ventrally projecting pterygoids are similar to those of several insectivorans, including *Microgale* and *Solenodon*. Only a single pair of ventral projections is present; each of these hooks posteriorly opposite the posterior opening of the alisphenoid canal as in *Microgale cowani* and probably supported a membrane separating the trachea from the rear of the oral cavity, in addition to musculature of the soft palate and auditory tube. Lateral to the ventral border of the pterygoid is a flat surface for attachment of the internal pterygoid muscle.

The sphenorbital fissure and associated foramina in FMNH UM1690 are quite distinctive and well preserved. A massive overhanging wall of bone extends forward as a continuation of the lateral wall of the sphenorbital fissure, terminating at a point approximately even with the posterior border of the palate. In the roof of the resulting vault are several foramina, all of which are hidden from lateral view. The most anterior of these is the ethmoidal foramen, which leads into the anterior cranial fossa and posterior ethmoidal region. Immediately posterior to the ethmoidal foramen are two tiny foramina of uncertain significance. Posterior to these is the large anterior opening of the sinus canal, which in life transmitted the superior ramus of the stapedial artery along the interior of the braincase. Medial to this is a small optic foramen. Immediately posterior to the optic and sinus canal foramina is the much larger opening for the ophthalmic and maxillary divisions of the trigeminal nerve. No separate foramen rotundum is present. Other specimens that preserve the sphenorbital fissure in good condition include some with breakage that permits examination of these foramina from both dorsal and ventral perspectives (e.g., *A. brevirostris* AMNH 74951). These specimens share the morphology exhibited by FMNH UM1690.

Behind the posterior base of the sphenorbital fissure, just anterior to foramen ovale, is the small posterior opening of the alisphenoid canal. It is about 0.5 mm in diameter and opens directly into the floor of the sphenorbital fissure. The foramen ovale is about 0.7 mm in diameter and faces anteroventrally, medial to the glenoid fossa.

Apternodus baladontus possesses a piriform fenestra, as the squamosal and alisphenoid bones fail to contact the anterolateral edge of the petrosal. The rostral tympanic process of the petrosal (MacPhee, 1981) projects ventrally along the area postulated (erroneously) by McDowell (1958: 169) to contain a shallow groove for the internal carotid artery in *A. brevirostris*.

The anterior carotid foramen, through which the internal carotid artery presumably entered the braincase, lies in the petrosal-sphenoid suture at the anteromedial corner of the tympanic roof, just medial to the point at

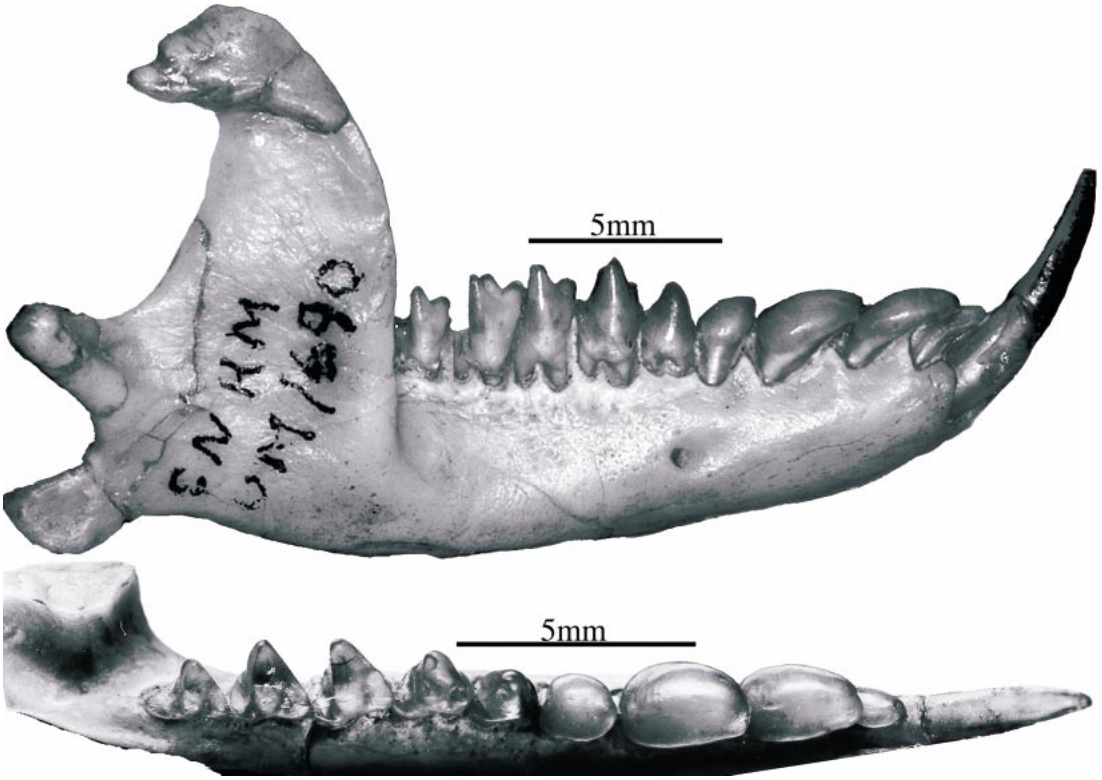

Fig. 12. FMNH UM1690, mandibles of *Apternodus baladontus* sp. nov. type specimen from McCarty's Mountain, Montana in lateral (top, right mandible) and occlusal (bottom, left mandible) views.

which the suture separates to produce the piriform fenestra. Further expansion of the piriform fenestra would engulf the anterior carotid foramen, resulting in passage of the internal carotid artery through the enlarged fenestra, much as in soricids. Slightly anteromedial to the anterior carotid foramen, a small opening in the alisphenoid is evident; this presumably transmitted a vidian branch of the internal carotid artery.

JAW JOINT: Figure 25 of McDowell (1958: 170) is an excellent illustration of the differences between the entoglenoid and postglenoid processes. McDowell recognized that for posterior support of the mandibular condyle, *Solenodon* and *Nesophontes* (along with soricids, moles, and tenrecs) possess a modified entoglenoid process located medial to the postglenoid foramen and anterior to the promontory of the petrosal. These taxa lack a true postglenoid process (see also MacPhee, 1981: 220). Strangely, McDowell did not recognize that this was also the case for *Apternodus*. As exemplified by the type of *A. baladontus*, and similar to the condition in *Tenrec* figured by McDowell (1958: fig. 25C), the mandibular condyle of *Apternodus* is supported posteriorly by a flange of squamosal that is coincident with the anterior border of the middle ear, grooved by the chorda tympani, and located anteromedial to the postglenoid foramen. Some variation exists in the contribution of the alisphenoid to the entoglenoid process; in *Tenrec* it is considerable, while in *Solenodon* and *Apternodus* it is small.

This contrasts with a true postglenoid process (as illustrated in *Leptictis* by McDowell 1958: fig. 25A), which is located anterolateral to the postglenoid foramen, and well lateral to the promontory of the petrosal and path of the chorda tympani. McDowell's figure 24 (p. 169) accurately shows the morphology of the entoglenoid process in *Apternodus*, which can be seen to differ as noted

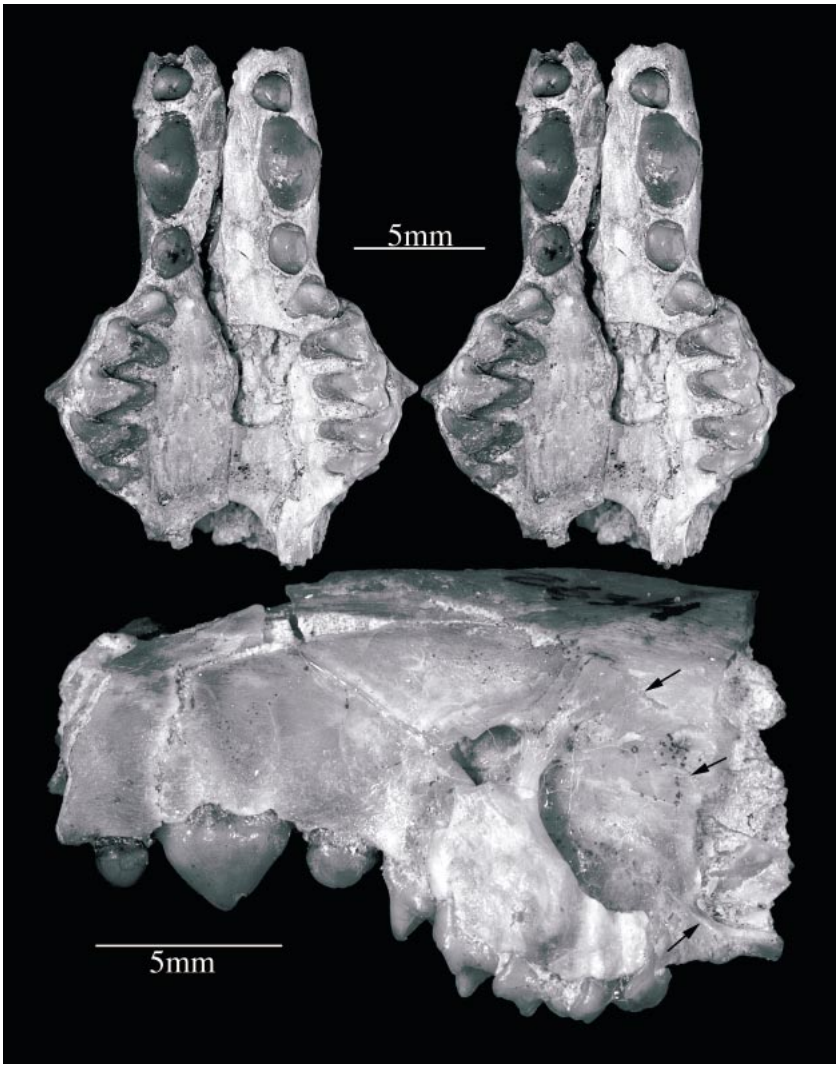

Fig. 13. MPUM 2634, *Apternodus baladontus* rostrum from Diamond O Ranch, Montana. Stereo ventral (top) and lateral (bottom) views. Arrows in lateral view indicate posterior extent of maxilla into orbital mosaic.

above from the postglenoid process of *Leptictis*.

BRAINCASE: The parietals of FMNH UM1690 are quite rugose, a feature in keeping with powerful temporal muscles. The ventral margin of the lambdoid plate does not reach as far ventrally as that of other members of the genus *Apternodus*. In contrast, other species show a ventral mastoid rim of the lambdoid plate well below the level of the jaw joint.

HYOID APPARATUS: In the course of preparation of the skull, two hyoid elements were found. These appear to be (1) an ankylosed complex made up of the basihyal and both thyrohyals and (2) either a right ceratohyal (of Sprague, 1944, or epihyal of Allen, 1910) or a right hypohyal (also of Sprague, 1944, or ceratohyal of Allen). If the latter really is a ceratohyal, as seems probable because of its large size relative to the basihyal-thyrohyal complex, then the hypohyal must have been very small, a special similarity to *Solenodon* among insectivorans in which the

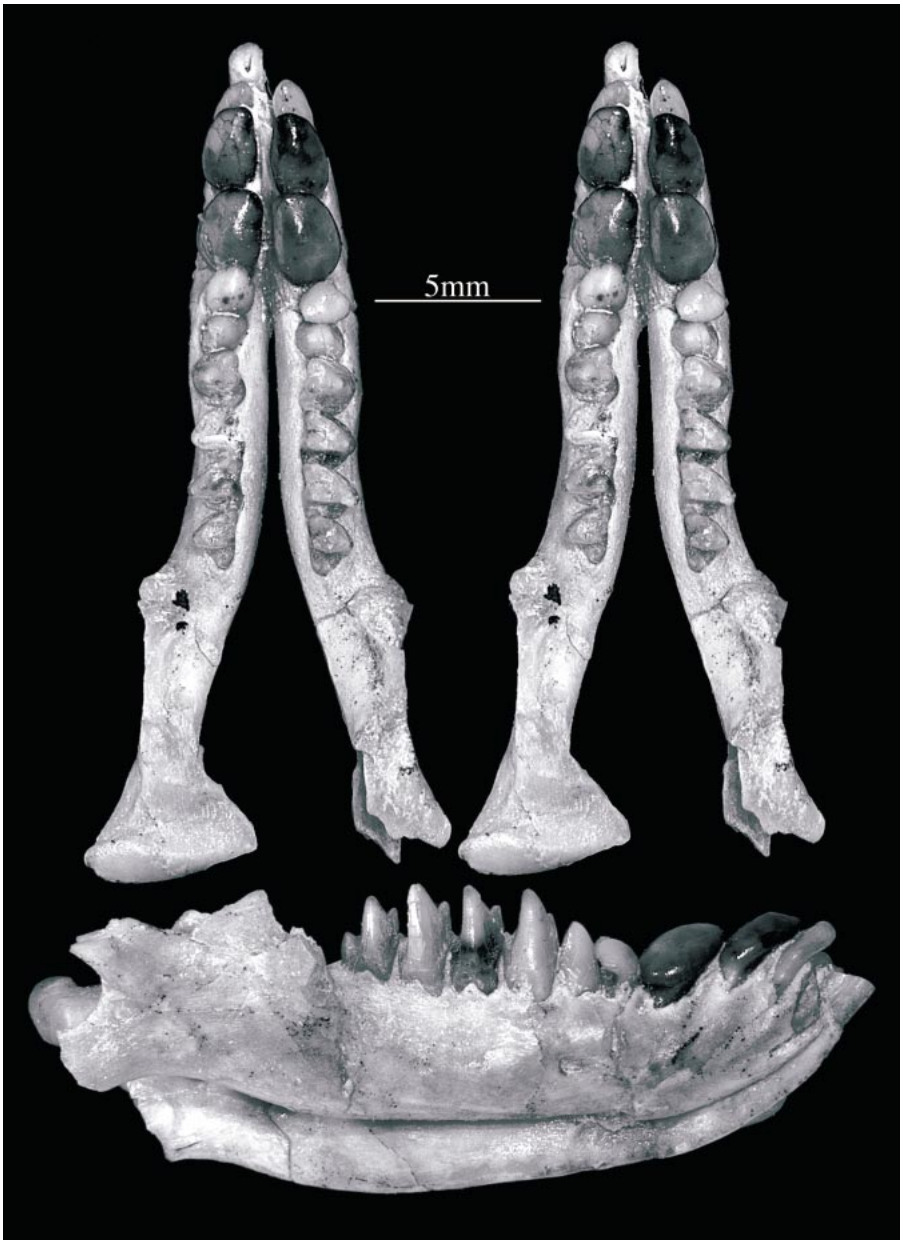

Fig. 14. MPUM 2634, *Apternodus baladontus* mandibles from Diamond O Ranch, Montana in stereo occlusal (top) and lateral (bottom) views. Note that the right p2 has been incorrectly repaired so that the anterior tip of the tooth faces posterolingually.

hyoid region is known (Sprague, 1944: table l). If the bone is a large hypohyal, then there is little similarity to that of any other insectivoran.

DENTITION: The dental formula of *A. baladontus* is the same as that of other *Apternodus* species: 2.1.3.3/3.1.3.3. The few *Apternodus* specimens that preserve erupting teeth (e.g., AMNH 76747, CM 9552, CM 71570) have three fully erupted molars posteriorly, and are thus consistent with the replacement pattern observed in most other

placental mammals. Based on this pattern, we assume that the premaxillary teeth of taxa discussed here are incisors, the anteriormost maxillary tooth is a canine, and the anterior three lower teeth are incisors, followed by a canine.

Accepting these assumptions, there are only two upper incisors in FMNH UM1690, identified here as I1 and I2 based on the observation that in some other insectivorangrade placentals, I3 is small or absent (e.g., *Solenodon* and *Tenrec*). The crown of I1 is not preserved on either side of the skull. The root of the left I1 is 2.0 mm in anteroposterior diameter just within its alveolus. The right and left I1 pitch toward each other and may have met medially, depending on the length of the crown. The tips of the enlarged anterior lower incisors pass forward between the right and left I1 and are accommodated by a gutter in the bone below the nares when the mouth is closed. Lateral motion of the anterior end of the occluded mandible is thereby restricted. I2 has a bulbous crown, and is smaller and more spherical than the elongate, semipremolariform I2 of *A. mediaevus*. The root is straighter than in CM 13676 or *A. brevirostris*, but the tooth is tilted medially in the same manner. Wear is confined to a flat facet at the apex of the tooth.

The upper canine is a massive crushing tooth with a bulbous conical crown, supported by three roots. The anterior and posterior roots are massive and diverge slightly when seen from the side. The third, medial root supports the anterolabial corner of the tooth and projects anterodorsally in the wall of the snout, approximately parallel with the anterior root. The crown overhangs the root medially. Wear is confined to a flat surface at the apex. The wear surface tilts slightly medial from the horizontal.

As in most other placentals with three premolars, we consider P1/p1 (or dP1/dp1) of *Apternodus* to be absent. P2 possesses two main roots and has a third, posterolingual root that is also present in *A. mediaevus*. The crown is circular and bulbous, larger than P2 of *A. brevirostris*, but less elongate than P2 of *A. mediaevus*. Wear is confined to a flat surface at the apex of the crown. P3 is small and triangular, with a weak posterolabial shearing crest. The cingula meet lingually, but a protocone is only faintly indicated. The molars are more gracile, but are otherwise similar to those of *A. mediaevus* from Pipestone Springs.

The anteriormost lower incisor (i1) is greatly enlarged and procumbent, and contacts the opposite anterior incisor for about half the length of its crown. The root is oval in cross section and, in contrast to *Solenodon*, is not hollowed out medially. No serrations are present along the upper edge of the labial enamel surface. The second lower incisor is small, but not as diminutive in FMNH UM1690 as it is in *A. brevirostris*; unlike the latter, the i2 of *A. baladontus* has a distinct alveolus. As in the upper dentition, i3 to p2 present a series of bulbous, procumbent crowns, presumably adapted for crushing. This curious morphology somewhat resembles an overlapping series of inverted spoons. All are single-rooted.

The lower canine and p2 are similar in appearance and possess bulbous crowns. This contrasts with species of *Apternodus* common outside of Montana, in which both teeth are premolariform. The ventral side of the anterior part of the canine crown of FMNH UM1690 is hollowed to fit the rear of the crown of i3. No trace of a central high cusp or ridge remains. The second lower premolar of *A. brevirostris* possesses a crested crown, whereas p2 of *A. baladontus* does not. The third lower premolar is the first double-rooted lower cheek tooth, and is more premolariform than anterior teeth. Its crown forms a low cone with a very weak posterior crest that runs from the apex to a tiny ridge that lies directly ventral to the paraconid of p4. The first and second lower molars are approximately equal in size; m3 is slightly smaller. Buccal cingulids on the molars of the type (fig. 12) and most referred specimens (e.g., fig. 14) are very slight.

The teeth of FMNH UM1690 seem to retain traces of pigment once present in life. Pigment is present in various soricid teeth as far back as the Oligocene (Patterson and McGrew, 1937: 247) and can also be seen in *Solenodon* (especially under ultraviolet illumination). The pigment is visible as an opacity blocking the normal yellow or orange radiation emanating from the enamel near the apices of cusps. In the preserved upper den-

tition of FMNH UM1690, only the left I2 is fully pigmented, but traces of pigment can be seen within the enamel of all teeth, especially M2, distributed near cusp apices. The lower anterior incisors are heavily pigmented on the labial and medial faces, but not on the preserved upper face. Similar pigmentation is present in the type specimen of *A. brevirostris*, in the upper dentition of the type specimen of *A. iliffensis*, and in some specimens from Pipestone Springs (e.g., AMNH 97255). It is of course possible that in some cases ''pigment'' may be an artifact of fossilization, and is in any event obscured in specimens (e.g., MPUM 3799, AMNH 76745, USNM 18966, CM 71569) with jet-black teeth. Although the distribution of pigment in *Apternodus* teeth resembles that of soricids and probably had a biological cause, we note that many vagaries of preservation and wear heavily influence whether or not pigmentation is observable in any given specimen. We therefore refrain at present from attributing much systematic importance to this character.

Apternodus brevirostris Schlaikjer, 1934

TYPE SPECIMEN: AMNH 22466, slightly damaged complete skull (fig. 15) with associated lower left dentary, complete except for the crown of i1 and coronoid process (fig. 16). This specimen was originally accessioned into the UW collections (Schlaikjer, 1933: 15) and is probably associated with UW 26, a right dentary with p4-m3.

REFERRED SPECIMENS: AMNH 74941, broken skull with left P2-M2; AMNH 74942, broken skull, missing anterior rostrum, associated with left dentary with m2-m3 and unprepared right dentary with p4-m3; AMNH 74946, rostrum with left P3-P4 and broken M1; AMNH 74948, rostrum with right P2-M2, broken M3, left C, P3-M3; AMNH 74949, rostrum with right P2-M1, broken M2, left P2-M2; AMNH 74950, half rostrum with left P3-M3; AMNH 74951, broken skull preserving orbitotemporal regions, left petrosal, fragments of left and right lambdoid plates, and rostrum with left P2, broken P4-M3, right canine, broken P3-M1, M3, associated left dentary with p4-m3 and right dentary with m1-m3, also associated with fragmentary left distal humerus; AMNH 76692, left maxillary fragment with P2-M3; USNM 437460, rostrum (fig. 17) with right and left C-M3, left I2, alveoli and roots for both I1s and right I2, missing buccal margins of right P3-M3; associated with left (fig. 18) and right dentaries with i2-m3 and broken i1s. (For purposes of exhibition, and long before this writing, USNM 437460 was attached to the basicranium of another individual from a different part of the Flagstaff Rim section.)

TEMPORAL AND GEOGRAPHIC DISTRIBUTION: Chadronian (late Eocene) of central Wyoming (Flagstaff Rim 18, Bates's Hole 3).

DIAGNOSIS: As the name implies, the rostrum is short, holding a closely packed dentition anterior to P4, usually with overlap between the posterior root of P2 and the anterior root of P3 and without diastemata on either side of the upper canine. The anterior dentition is gracile, with premolariform upper and lower I2-P3. The upper molars have lingually situated protocones that are similar in size to the molar parastyles. The i2 is very small (Schlaikjer, 1934), with an alveolus continuous with that of the larger i1. Both the upper and lower second premolars are much smaller than adjacent teeth; and the p3 shows a prominent buccal cingulum and posterior cusp. The rostral tympanic process of the petrosal is medially flat. The external auditory meatus is ventrally concave. The lacrimal foramen is offset posteriorly from the orbit by the superior margin of the infraorbital canal.

REMARKS: Several rostra with complete or nearly complete dentitions are now known for *A. brevirostris* (AMNH 74941, 76692, 74950, 74948, 74949, and USNM 437460), most of which were collected by Morris Skinner and colleagues from the Flagstaff Rim area, Wyoming during the 1950s. The type (AMNH 22466) remains the most complete specimen known. Surprisingly, very few specimens have been recovered with associated mandibles. One of these is AMNH 74951, which preserves not only a rostrum and posterior mandibles, but is also associated with a distal humerus, petrosal, and fragmentary lambdoid plate. Several braincases and basicrania are known from Flagstaff Rim, including AMNH 74940, one the

few specimens known to preserve an ectotympanic (fig. 19). These are presumably referable to *A. brevirostris*, but without the dentition it is impossible to be certain. Frustratingly, no specimen unambiguously referable to *A. brevirostris* preserves the ventral margins of the lambdoid plates. These can nevertheless be inferred to have extended well below the level of the glenoid fossa, based on the size of their breakage scars, which are quite large posterior to the external auditory meatus and presumably extended for several millimeters farther ventrally (as reconstructed by Schlaikjer, 1934).

Although a closely packed I2-P4 toothrow characterizes this species, some variation is present in the size of the P2-P3 diastema. For example, in AMNH 74948 (identifiable as *A. brevirostris* by virtue of its upper molar protocones, gracile anterior dentition, small canine diastemata, and ridge separating the lacrimal foramen from the orbit) the space between P2 and P3 is small, but the roots of the two teeth do not overlap. The ratio of palate length to width in *A. brevirostris* is smaller than that of other *Apternodus* species, but not always with decisive statistical significance (fig. 20). Within the *A. brevirostris* hypodigm, the rostrum of the type specimen (AMNH 22466) is one of the shortest.

McDowell (1958) published a discussion and four illustrations of *Apternodus* that contained several mistakes. He based these illustrations primarily on the type of *A. brevirostris* (AMNH 22466), with missing parts restored from the type of *A. gregoryi* (MCZ 17685) and with the inferred morphology of one side reconstructed from a mirror image of the other. Both skulls are imperfectly preserved and do not show a number of characters depicted in McDowell's reconstruction.

First, McDowell (1958: fig. 23A) repeated Schlaikjer's error (1933: fig. 3, top; see also section below on *A. gregoryi*) of running a suture between the parietal and occipital (Schlaikjer's mastoid) bones diagonally across the posterolateral corner of the skull roof. There is no evidence for a suture at this site.

Similarly, there is no evidence to support McDowell's (1958: fig. 23) placement of the squamosal-parietal, fronto-parietal, and fronto-nasal sutures. The dorsal exposures of most dermal braincase elements are completely fused, and leave no indication of any sutures.

McDowell (1958: 170) argued that ''from the American Museum skull (AMNH 22476 [sic, actually 22466]), it can be determined that the maxilla forms little of the orbital wall, an important contrast to the Lipotyphla.'' In fact, the sutures of the maxilla in the orbital mosaic are completely fused in both AMNH 22466 (fig. 15) and MCZ 17685 (fig. 21), as they are in the majority of other *Apternodus* skulls, with the two exceptions mentioned above: MPUM 2634 (*A. baladontus*) and MPUM 6855 (*A. mediaevus*). In the former, a suture is clearly visible on both sides curving around the anterior border of the sphenopalatine foramen and posterior to the lacrimal region (fig. 13). Similarly, both sides of the skull in MPUM 6855 (fig. 7) show distinct, wavy lines representing the maxillary-frontal suture and indicating that the maxillary incursion into the orbital mosaic of *Apternodus* is considerable, similar to that of *Erinaceus* (MacPhee and Novacek, 1993: fig. 3.5).

McDowell's reconstructed cribriform plate (1958: fig. 23) is located too far posteriorly, and is oriented too vertically. A partial, broken skull of *A. brevirostris* (AMNH 74951) exposes most of the cribriform plate intact, and shows its posteriormost point just anterior to the sella turcica, as in most other mammals. Externally, this corresponds with a point just anterior to the glenoid fossa of the mandible, close to the posteriormost external opening of the sphenorbital fissure. Relative to this point, the cribriform plate in *Apternodus* extends both anteriorly and dorsally toward the anterior end of the sagittal crest, to a point coincident with a coronal plane shared with the posterior margin of the hard palate.

McDowell's figure 23C incorrectly shows a completely solid tympanic roof, with no piriform fenestra on either side. In fact, the region immediately anterior to both petrosals in AMNH 22466 is perforate, although the large size of these ''fenestrae'', particularly on the left side, is due to postmortem damage. Nevertheless, most specimens of *Apternodus* that preserve the relevant anatomy

Fig. 15. AMNH 22466, cranium of *Apternodus brevirostris* type specimen from Bates's Hole, Wyoming. Stereo ventral (top), dorsal (middle), and lateral (bottom) views of skull, (opposite page) anatomical guide to ventral view. See text for abbreviations.

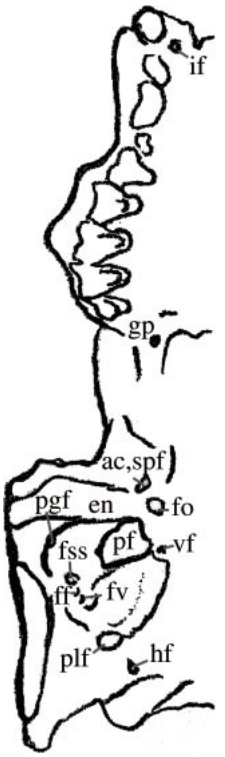

Fig. 15. Continued.

(e.g., FMNH UM1690, AMNH 74941, USNM 455680, UW 11046) clearly show prominent piriform fenestrae anterior to the petrosal. This was shown in AMNH 22466 by Matthew (1910), who included photographs in his original description of the specimen. The type of *A. gregoryi* (MCZ 17685; see below) was also incorrectly reconstructed as lacking piriform fenestrae by Schlaikjer (1933: fig. 3) and Scott and Jepsen (1936: plate 1). In some individuals (MPUM 6855 and AMNH 74940) the fenestrae are indeed small or absent; AMNH 74942 appears to show a piriform fenestra on the left side but not on the right, although this is undoubtedly the result of postmortem damage. In general, the tympanic roof anterior to the petrosal is naturally perforate in most specimens of *Apternodus*, including the type of *A. brevirostris*.

McDowell (1958: figs. 23C, 24, and p. 168) argued that the internal carotid artery of *A. brevirostris* runs medial to the middle ear after giving off a stapedial branch that occupies a groove on the promontorium ventral to the vestibular foramen. This pattern, he wrote, was ''very different . . . from that of the Lipotyphla, [and is] more like that of creodonts . . . '' (p. 168). In fact, as discussed elsewhere (Asher, 2000, 2001; Whidden and Asher, 2001) McDowell overestimated the conservatism of cranial blood supply among insectivoran mammals, and drew a misleading contrast between an alleged ''lipotyphlan pattern'' and a speculative model of arterial circulation presented for *Apternodus* based on AMNH 22466 and MCZ 17685. In short, although there is a faint arterial groove associated with the proximal stapedial artery in the immediate vicinity of the vestibular foramen in the petrosal of AMNH 22466, there is no indication of a groove for the internal carotid artery. Neither the medial aspect of the petrosal of AMNH 22466, nor its ventral apex, is marked by subtle depressions that in other specimens define the course of the internal carotid artery along the ventrum of the tympanic roof. As noted elsewhere (Whidden and Asher, 2001), other specimens of *Apternodus* (e.g., AMNH 74942, 76745; USNM 455680) do preserve shallow grooves running between the anterior carotid foramen and ventral apex of the petrosal in a position well lateral to the petrosal-basisphenoid suture. These specimens indicate either that arterial circulation in *Apternodus* was polymorphic, or more likely, that McDowell's vascular reconstruction (1958: fig. 24) was incorrect. In sum, it is doubtful that the course of the internal carotid artery in *Apternodus* was located farther medially than that of many insectivorans, such as *Microgale* (MacPhee, 1981; Asher, 2001).

Apternodus gregoryi Schlaikjer, 1933

TYPE SPECIMEN: MCZ 17685, complete skull (fig. 21) with left C, P3-M2, right C, P2-M2, broken M3, missing premaxillae and anterior dentition, associated mandibles with left p3-m3, right i1, and p3-m3.

REFERRED SPECIMEN: UW 13508, skull (fig. 22) with intact but distorted basicranium, palate with left I1 root, C-M3, roots for right I1–2, plus right C-M3, associated with mandibles (fig. 23) including broken left i1, i3-c, p3-m3, and broken right i1, i3-m3. Also

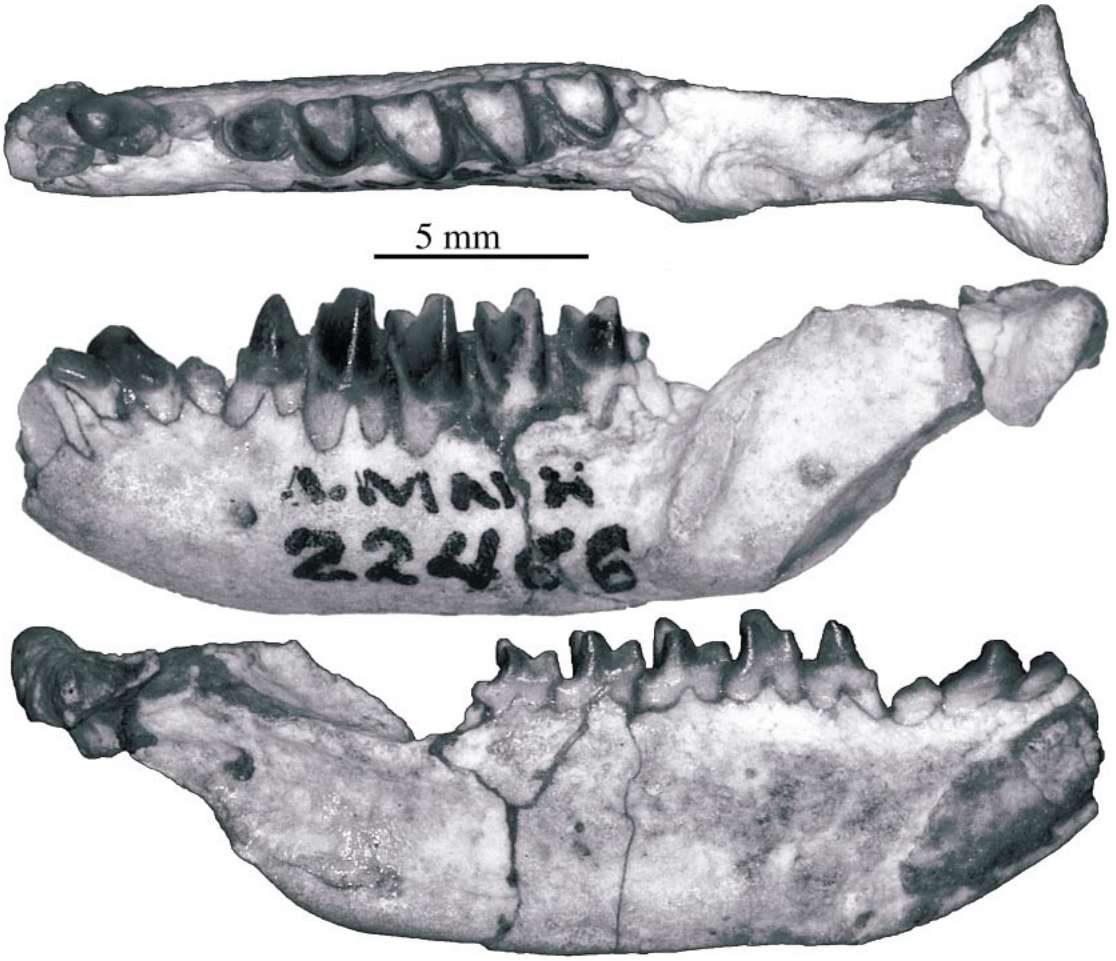

Fig. 16. AMNH 22466, type mandible of *Apternodus brevirostris* from Bates's Hole, Wyoming in occlusal (top), lateral (middle), and lingual (bottom) views.

associated with proximal and distal fragments of the femur and os coxae (fig. 24), a fragment of the proximal ulna, five fragmentary caudal vertebrae, and several indeterminate fragments of ribs and/or longbones.

TEMPORAL AND GEOGRAPHIC DISTRIBUTION: Chadronian (late Eocene) to Orellan (early Oligocene) of eastern Wyoming (Dilts Ranch 10; Torrington 38).

DIAGNOSIS: The rostrum of *Apternodus gregoryi* shows small diastemata between P2 and P3 and on either side of the canine. The external auditory meatus is very narrow and defined posteriorly by a ventrally projecting posttympanic process. Anteriorly, this notch is defined by a ventrally elongate lower lip of the entoglenoid process. The rostral tympanic process of the petrosal is flat. The lacrimal foramen of *A. gregoryi* is posteriorly continuous with the anterior orbit. That is, unlike *A. brevirostris*, *iliffensis*, *mediaevus*, and *baladontus* (but similar to *A. major*), the superior margin of the infraorbital canal is set apart from the lacrimal foramen posteriorly, leaving this region without a ridge of bone defining the posterior aspect of the foramen (figs. 21, 22). Protocones on the upper molars are reduced, smaller than their corresponding parastyles. The cingulid and posterior cusp of p3 are reduced.

REMARKS: The only specimen known of *A. gregoryi* besides the type is UW 13508. This

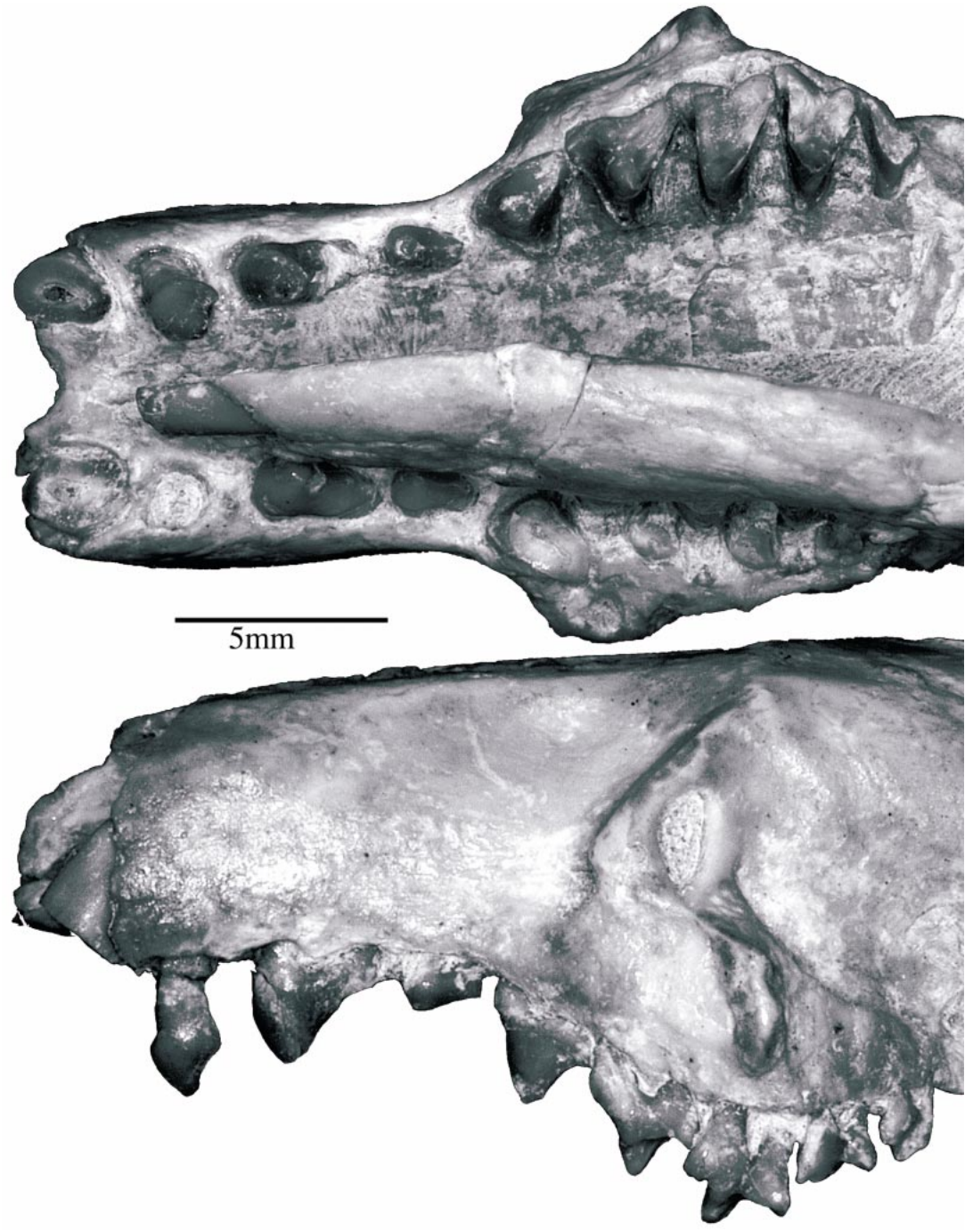

Fig. 17. USNM 437460, *Apternodus brevirostris* rostrum from Flagstaff Rim, Wyoming in occlusal (top) and lateral (bottom) views.

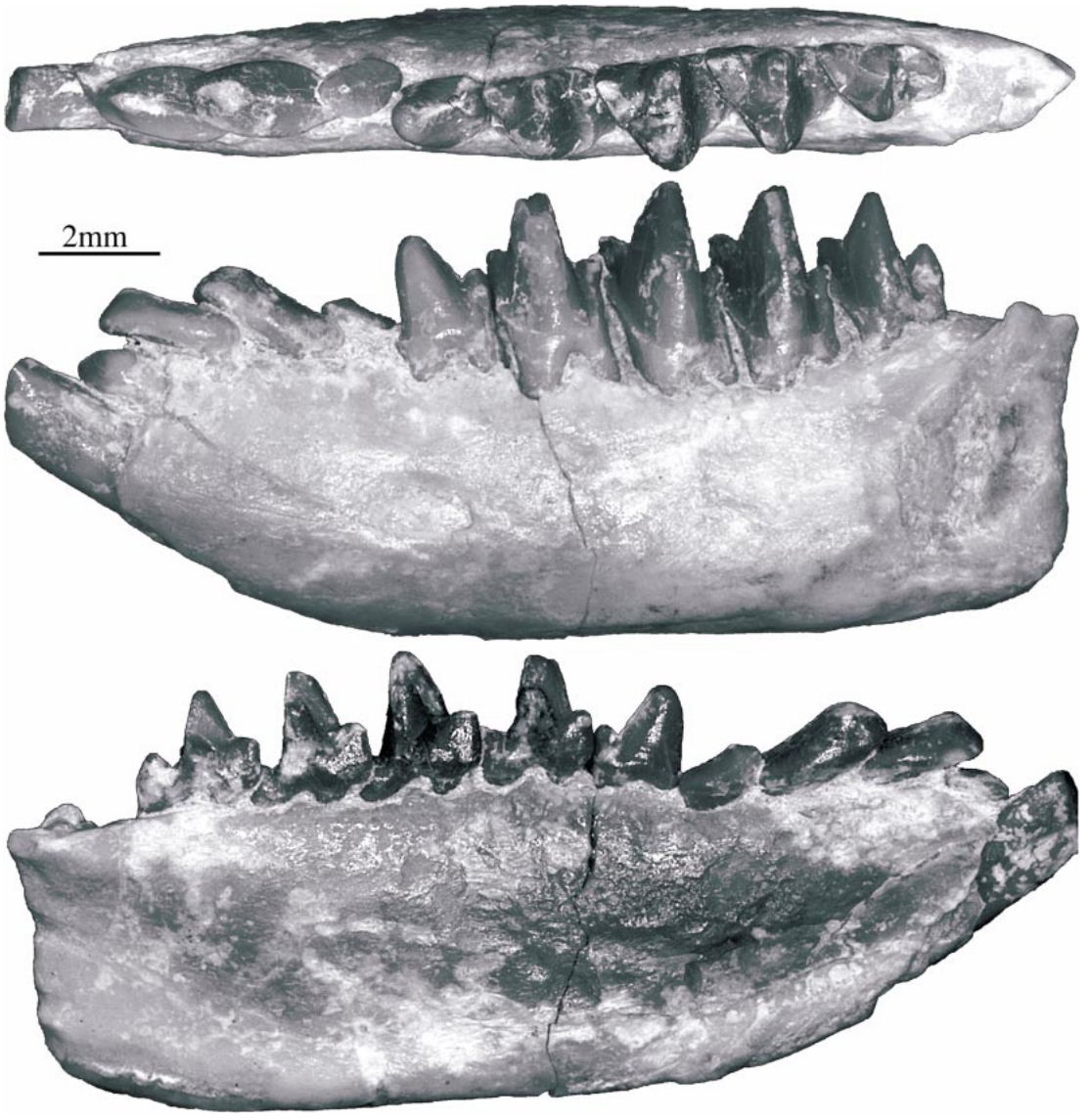

Fig. 18. USNM 437460, *Apternodus brevirostris* mandible from Flagstaff Rim, Wyoming in occlusal (top), lateral (middle), and lingual (bottom) views.

specimen consists of a nearly complete skull (fig. 22) and lower dentition (fig. 23) from both sides, as well some postcranial elements (fig. 24). The skull is quite similar to MCZ 17685, although the ventral lambdoid plates of UW 13508 are broken. The large size of their breakage scars indicates that the lambdoid plates were ventrally extensive. What remains of the external auditory meatus is sharply concave, as in the *A. gregoryi* type specimen (fig. 21).

Postcranially, the femur and partial os coxae of UW 13508 appear small for an animal with a skull of this size. However, the ratio of anteroposterior skull length to indices of proximal femur and acetabular size (fig. 25) is similar to that of extant groups such as talpids and soricids; hence, we assume that

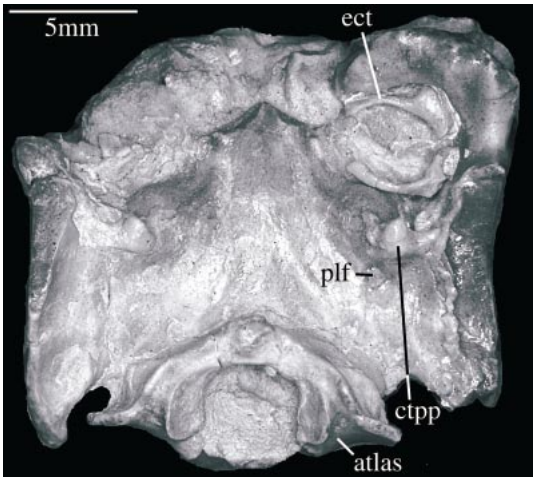

Fig. 19. AMNH 74940, basicranium of *Apternodus* sp. from Flagstaff Rim, Wyoming preserving ectotympanic bone. See text for abbreviations.

the partial femur, os coxae, and skull represent the same individual. In fact, prior to preparation, the distal femur of UW 13508 was embedded in matrix adjacent to the basicranium, making clear at least that the two specimens were deposited in close proximity, although in an anatomically unexpected position. The dentition of the associated skull is fully erupted, but shows minimal wear. Furthermore, the sphenoccipital synchondrosis of the skull is not completely fused (fig. 22), consistent with its association with the juvenile represented by the partial femur.

The distal femur preserves only the epiphysis. Proximally, the femur also appears to be detached from the epiphysis, although in this case the epiphysis is missing. Perhaps as a consequence, the femoral head lacks any sign of a fovea capitis. If what remains of the proximal femur (missing the epiphysis) accurately reflects the shape of the femoral head, then it is dorsally flattened and not separated from the greater trochanter by a deep dorsal concavity, in contrast to the morphology seen in most other insectivoran-grade taxa (e.g., *Echinosorex*; see MacPhee, 1994: 131). Extant animals with a similar femoral morphology include *Didelphis*, *Orycteropus*, *Tenrec* (MacPhee, 1994: 130–131), and soricids. To varying degrees, these taxa show arboreal, fossorial, and terrestrial locomotor patterns and do not present a simple locomotor analogue to *Apternodus*.

Schlaikjer's (1933) study of *Apternodus gregoryi* was considerably more detailed than that of Matthew (1910), but contained the following points that we cannot confirm.

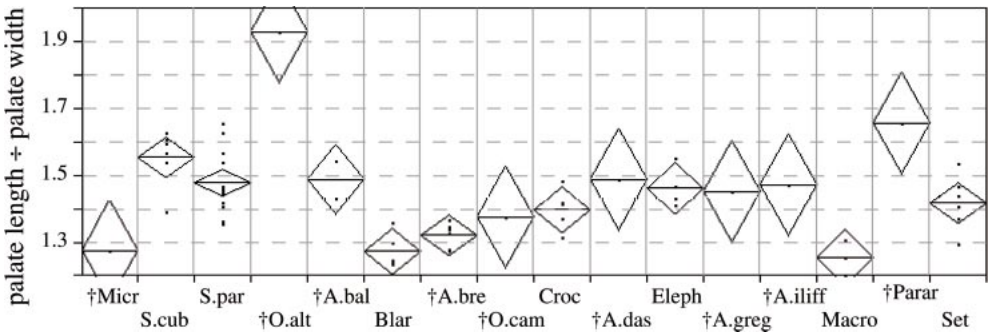

Fig. 20. Ratio of palatal length to width across selected taxa. See figure 52 for measurements taken. Dots indicate individual specimens measured. Diamonds indicate 95% confidence intervals of the mean; non-overlapping diamonds indicate a significant difference at alpha = 0.05, assuming normality. Crosses denote extinct taxa. Taxonomic abbreviations are as follows: A.bal = *Apternodus baladontus*; A.bre = *Apternodus brevirostris*; A.das = *Apternodus dasophylakas*; A.greg = *Apternodus gregoryi*; A.iliff = *Apternodus iliffensis*; A.maj = *Apternodus major*; A.med = *Apternodus mediaevus*; Blar = *Blarina* sp.; Croc = *Crocidura* sp.; Eleph = *Elephantulus brachyrhynchus*; Kon = *Koniaryctes paulus*; Macro = *Macroscelides proboscidiens*; Micr = *Micropternodus morgani*; O.alt = *Oligoryctes altitalonidus*; O.cam = *Oligoryctes cameronensis*; Parap = *Paratpernodus antiquus*; Parar = *Pararyctes pattersoni*; S.cub = *Solenodon cubanus*; S.par = *Solenodon paradoxus*; Set = *Setifer setosus*; TabB = Tabernacle Butte taxon.

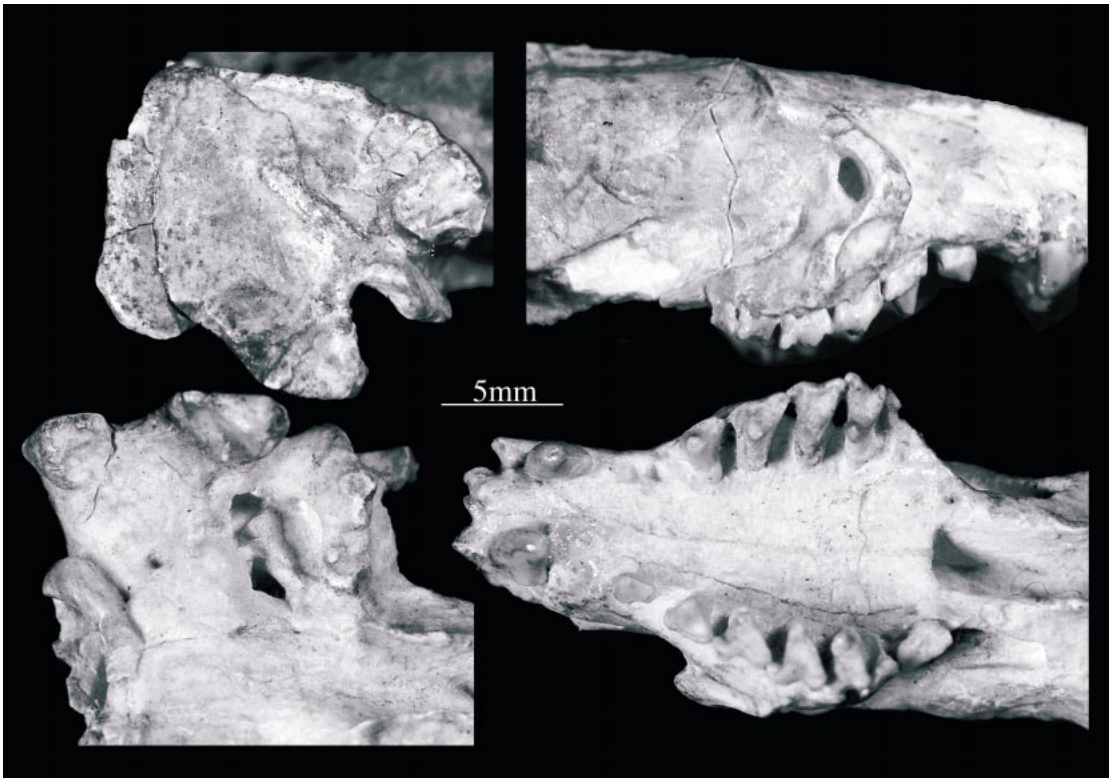

Fig. 21. MCZ 17685, skull of *Apternodus gregoryi* type specimen from the Brule Formation near Torrington, Wyoming. Lateral view of lambdoid plate (top left), lateral view of right orbitotemporal region (top right), ventral view of right auditory region (bottom left), ventral view of palate (bottom right).

First, Schlaikjer (1933: 10 and fig. 4) thought that there was some evidence that the mastoid extended onto the occiput to contact the exoccipital and supraoccipital. However, the mastoid-occipital suture actually lies on the lateral-facing lambdoid plate, as noted by Matthew and later by Schlaikjer himself (1934: 6). There is no visible exoccipital-supraoccipital suture on skulls of *A. brevirostris* or *A. gregoryi*. The entire occiput is composed of fused parts of the occipital bone.

The squamosal was believed to extend back on the lambdoid plate to what in reality is the mastoid-occipital suture. Schlaikjer's (1933: fig. 3) figure of the lateral view of the skull omitted the squamosal-mastoid suture. The latter was corrected by Schlaikjer (1934) and McDowell (1958: 165, fig. 23).

On the lambdoid plate, Schlaikjer's (1933: fig. 3, top) identification of the lateral exposure of the occipital as a part of the mastoid bone led him to depict a faint ''mastoid-parietal'' suture on the dorsal view of the skull. A suture between the occipital and the parietals was assumed to run along the lambdoid crests. A similar interpretation was given by McDowell (1958: fig. 23A). However, in available material of *A. gregoryi*, dorsal exposures of dermal cranial bones are fused and sutures cannot be accurately distinguished.

As noted above, piriform fenestrae were incorrectly shown as absent by Schlaikjer (1933, 1934) in both *A. gregoryi* and *A. brevirostris*. The type of *A. gregoryi* shows a relatively undistorted piriform fenestra (fig. 21). This region is less well-preserved in UW 13508 (fig. 22), but also appears to exhibit an incompletely ossified tympanic roof.

Apternodus iliffensis Galbreath, 1953

TYPE SPECIMEN: KU 9112, left maxillary fragment with P3-M3, associated left dentary with p4-m3 (fig. 26).

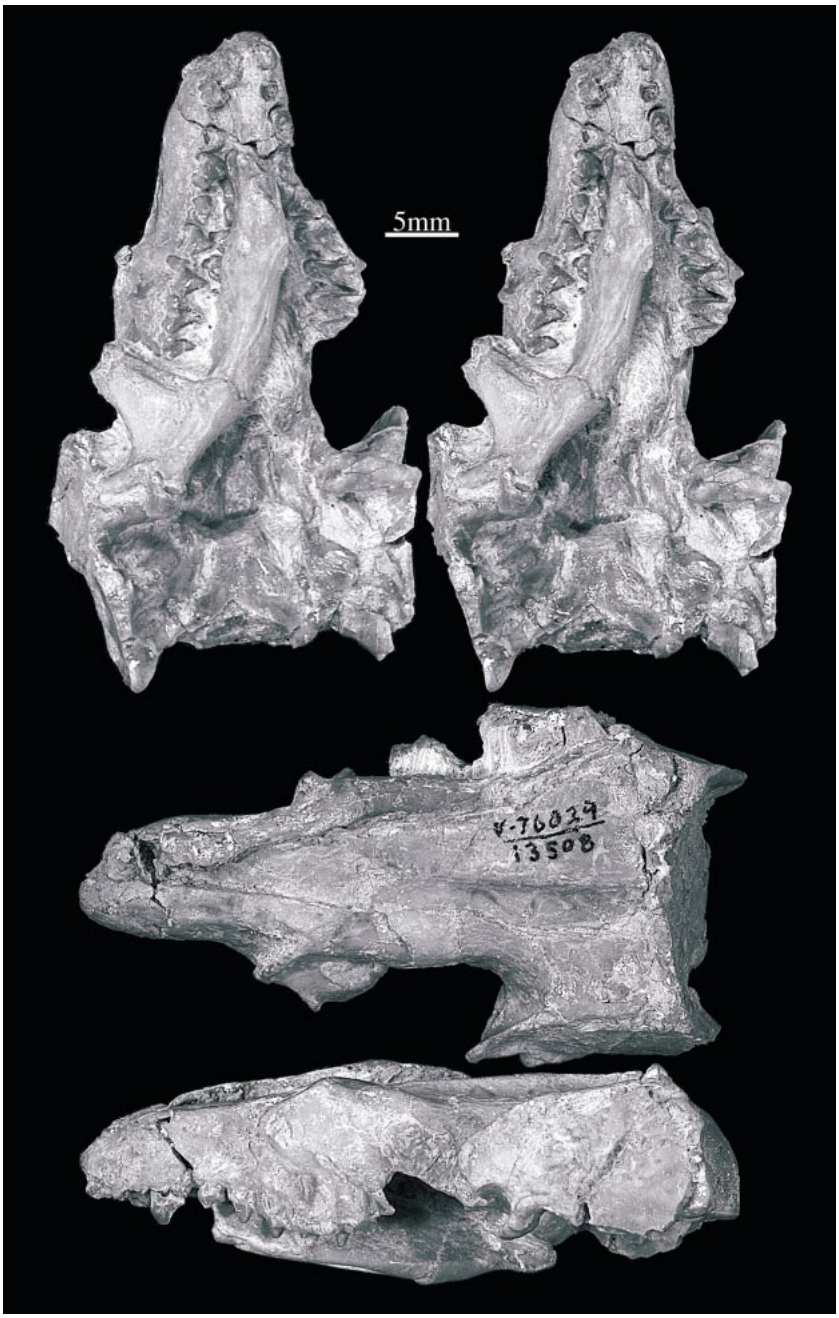

Fig. 22. UW 13508, *Apternodus gregoryi* skull from Dilts Ranch, near Orin, Wyoming in stereo ventral (top), dorsal (middle), and lateral (bottom) views.

REFERRED SPECIMENS: USNM 455680, skull (fig. 27) with left P3-M3, fragmentary right I2 and canine root, associated left (fig. 28) and still articulated right posterior mandibles with m1-m3 and m2-m3, respectively; DMNH 1747, skull (fig. 29) with left C-M2 and right canine; FMNH PM34512, rostrum with right and left P2, left P3 and partial P4,

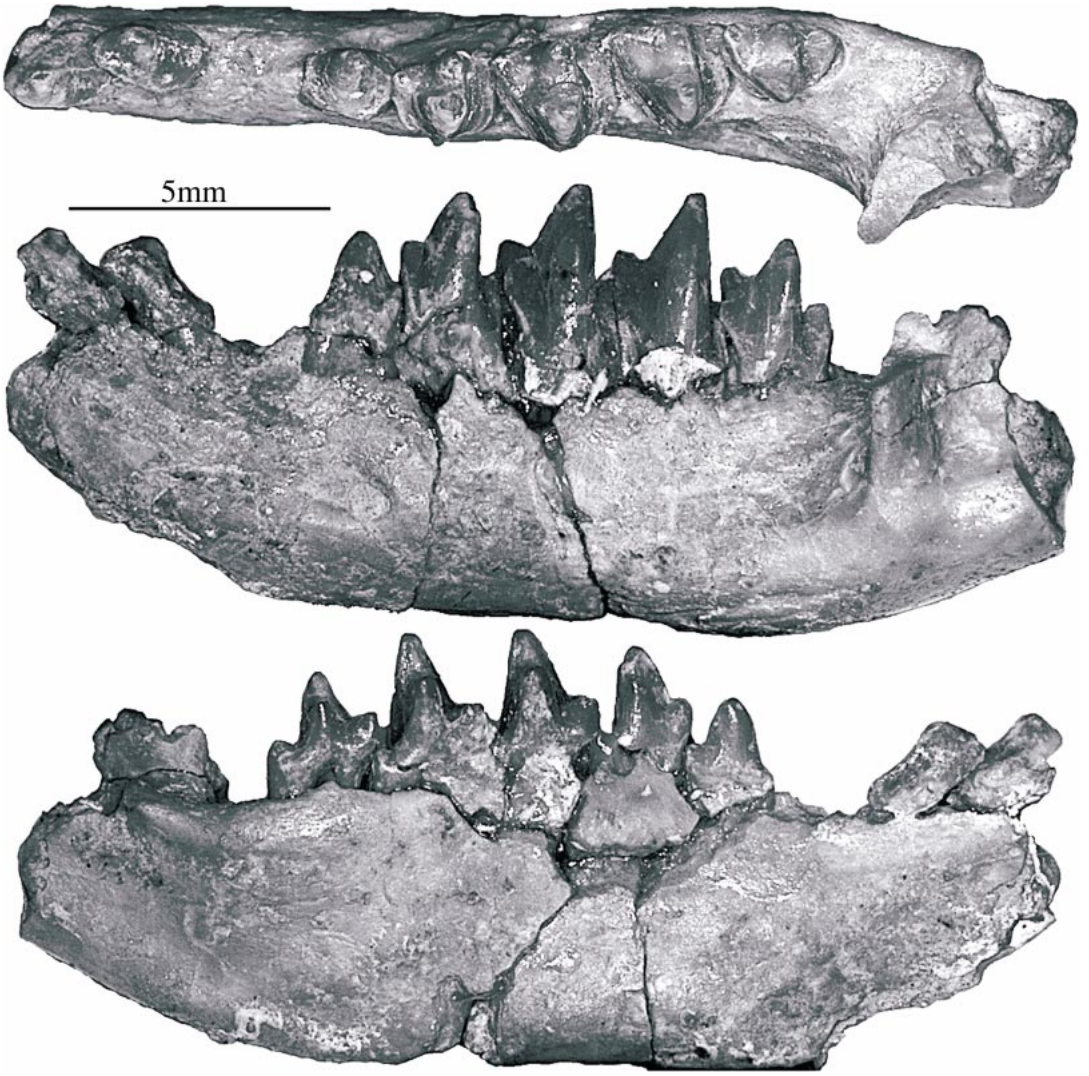

Fig. 23. UW 13508, *Apternodus gregoryi* mandible from Dilts Ranch, near Orin, Wyoming in occlusal (top), lateral (middle), and lingual (bottom) views.

lingual roots of M1-M2, alveoli for right and left canines, associated with brain endocast, right lambdoid plate, and petrosal; and TMM 40492-9, rostrum with left P4-M2, right P4-M1, M3, partial P3, preserving pterygoid and orbitotemporal regions (fig. 30).

TEMPORAL AND GEOGRAPHIC DISTRIBUTION: Chadronian (late Eocene) of northeastern Colorado (Iliff 24, Fremont Butte 20) and central Wyoming (Beaver Divide 5); and late Duchesnean (late middle Eocene) of west Texas (Red Mound 32).

DIAGNOSIS: The type and referred specimens of *Apternodus iliffensis* are smaller than other species of *Apternodus*. They have reduced upper molar protocones that are continuous with the molar lingual cingula and a small M3. The anterior dentition of USNM 455680 and DMNH 1747 is premolariform, not bulbous; a diastema is absent between P2 and P3; and minute diastemata are present on either side of the canine. The lacrimal foramen is set off from the orbit by a prominent crest, formed by the proximity of the infra-

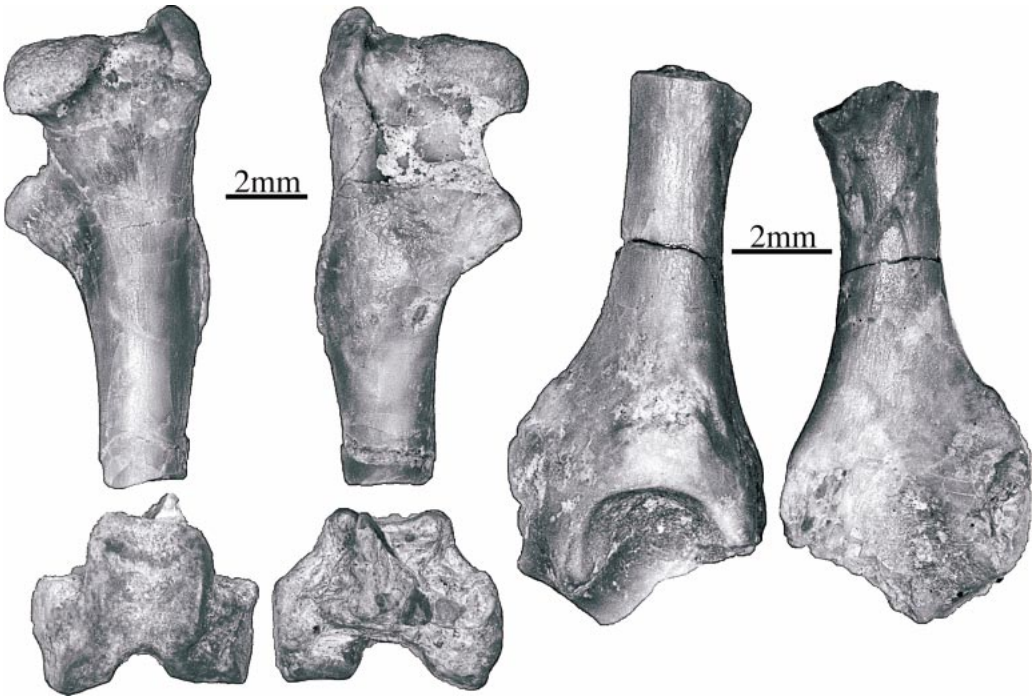

Fig. 24. UW 13508, *Apternodus gregoryi* proximal and distal fragments of left femur (left) and left os coxae (right).

orbital canal. Medial to the promontory, the rostral tympanic process of the petrosal is flat. The external auditory meatus is weakly concave ventrally, and the ventral margin of the lambdoid plate does not extend far below the glenoid region, similar to the condition in *A. baladontus*.

REMARKS: Cranially, this species is the smallest within *Apternodus*, even though its cheek teeth are relatively larger than those of *A. mediaevus* and *A. baladontus*. Two nearly complete skulls are now known for *A. iliffensis*: USNM 455680 (figs. 27, 28) and DMNH 1747 (fig. 29). The lower dentition anterior to p4 remains unknown.

As indicated by DMNH 1747 and USNM 455680, the upper anterior dentition of *A. iliffensis* closely resembles that of *A. brevirostris* and *A. gregoryi*. That is, the P2, canine, and I2 are small, premolariform, non-bulbous teeth. I2 has one root, P2 and canine two. I2 has a small but distinct posterior cusp, connected to the apex of the tooth by a crest.

The basicranium is mediolaterally narrower than that of other species. However, structures of the posterior braincase (i.e., the lambdoid plate, temporal fossa, and sagittal and nuchal crests) are at least as robust as those of other taxa.

USNM 455680 displays a large, undistorted piriform fenestra anterior to the petrosal, bounded medially by a strut of alisphenoid, which defines the lateral border of the anterior carotid foramen. The smaller vidian foramen is present anteromedial to the anterior carotid foramen. The petrosal retains a subtle but distinct groove extending from the apex of the promontory, medial to the vestibular foramen, anteromedially toward the anterior carotid foramen. In life this groove was associated with the internal carotid artery and contradicts McDowell's (1958: 168) interpretation that the internal carotid artery of *Apternodus* had a medial course adjacent to the petrosal-basisphenoid suture.

Referring the west Texas specimen (TMM 40492-9; fig. 30) to *A. iliffensis* makes this species the most geographically widespread within *Apternodus*. Novacek (1976b) tentatively referred this specimen to "*A.* cf. *bre-*

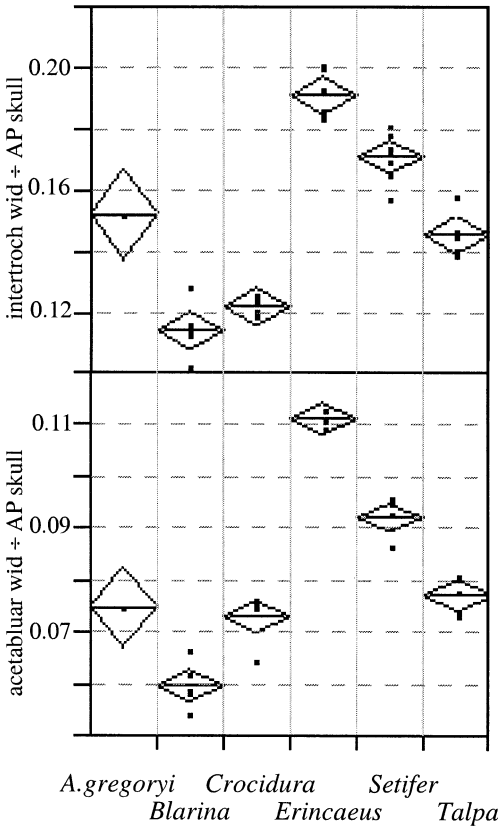

Fig. 25. Intertrochanter width (top) and acetabular width (bottom) divided by anteroposterior skull length in selected taxa (in millimeters). See figure 52 for measurements taken. Dots indicate individual specimens measured. Diamonds indicate 95% confidence intervals of the mean; nonoverlapping diamonds indicate a significant difference at alpha = 0.05, assuming normality.

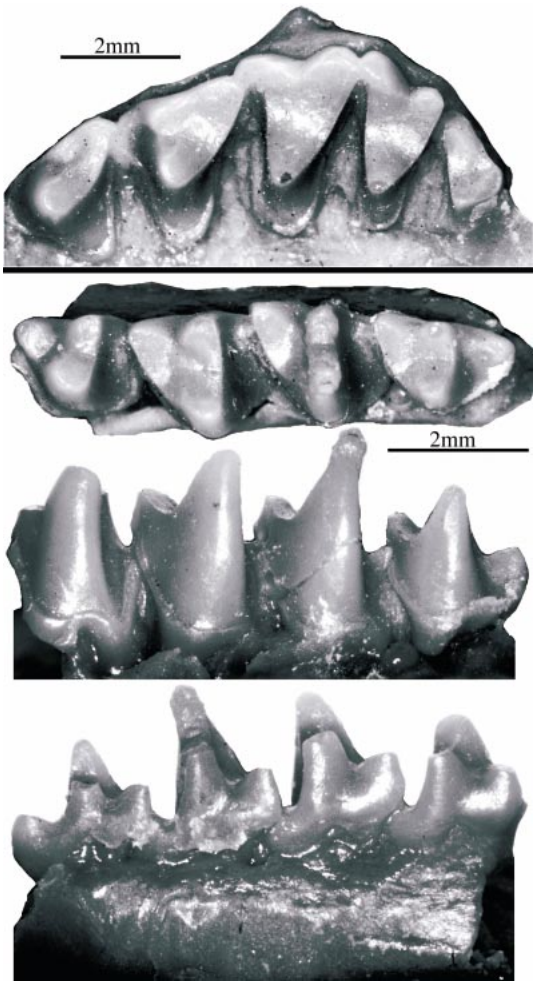

Fig. 26. Cast of KU 9112, *Apternodus iliffensis* type specimen from the White River Formation north of Iliff, Colorado, maxillary (top) and associated mandibular (bottom) fragments.

virostris''. However, TMM 40492-9 contrasts with *A. brevirostris*, and is similar to the *iliffensis* type specimen, in having reduced molar protocones, a mesiodistally elongate P3, and a small M3. In fact, the M3 of TMM 40492-9 is considerably smaller than that of any other *Apternodus* specimen. It further differs from most other *Apternodus* individuals in showing a particularly elongate P3. Hence, at present we regard this specimen as a member of *A. iliffensis;* however, recovery of additional material from west Texas may justify the recognition of a new species.

In his 1978 paper describing a second apternodontid specimen (FMNH PM34512) from White River Formation exposures north of Iliff, Colorado, Galbreath made several confusing statements. First, Galbreath (1978: 302) stated that ''there should not be any doubt that the new specimen [i.e., FMNH PM34512] is an apternodontid but not an apternotid.'' However, Galbreath's intended meaning for the term ''apternotid'' is unclear. He may have been of the opinion that his new specimen should not be included in the genus *Apternodus*, in which case we would disagree for reasons given below.

Galbreath (1978: 301) indicated that ''oth-

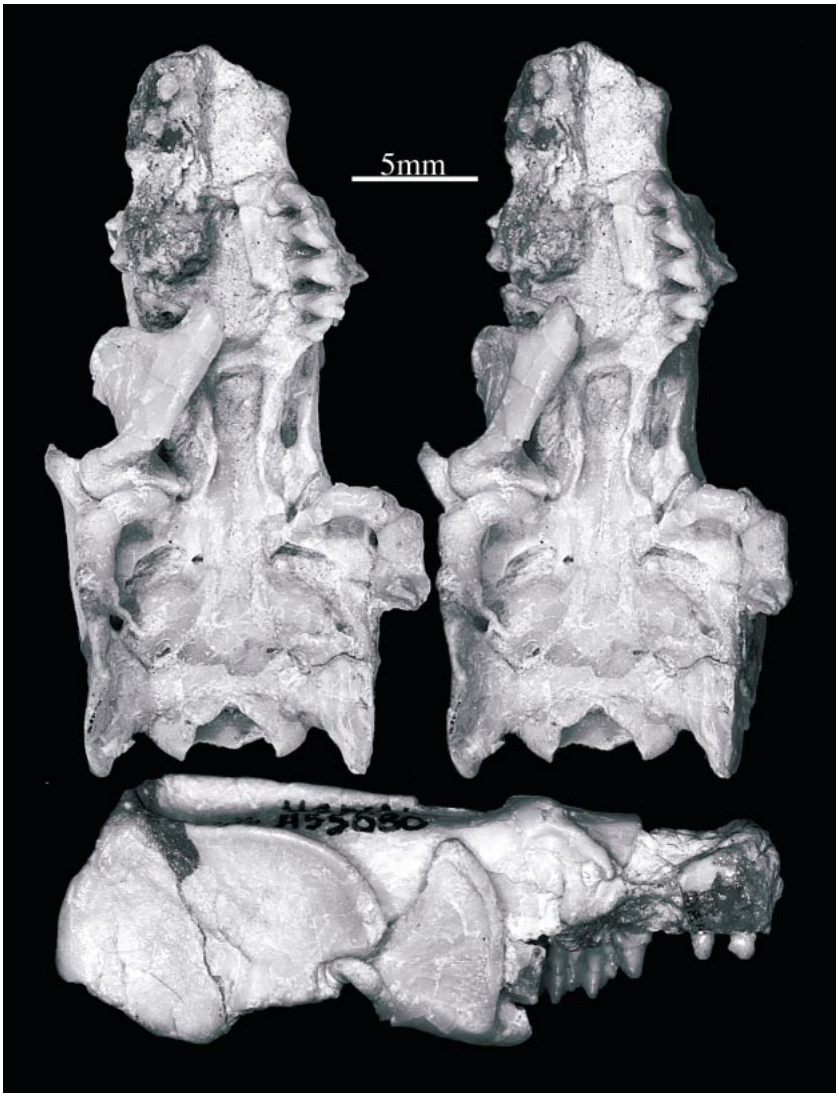

Fig. 27. USNM 455680, *Apternodus iliffensis* skull from West Canyon Creek, Beaver Divide, Wyoming in stereo ventral (top) and lateral (bottom) views.

er details not mentioned in the original description of *A. iliffensis* acquire significance now with the discovery of a second apternodontid from the same locality'', and described some aspects of the *A. iliffensis* infraorbital canal, presumably based on FMNH PM34512. However, on the next page he argued that ''the dissimilar details of the infraorbital canal suggests that the two [i.e., KU 9112 and FMNH PM34512] would not be in the same specific taxon'', in contrast to his previous implication that both specimens illuminate the anatomy of *A. iliffensis*.

Galbreath (1978: 299) stated that the ''preorbital ridge so characteristic on the maxillaries of *A. brevirostris* and *A. gregoryi*'' is missing on FMNH PM34512. However, a ''preorbital ridge'' has not been explicitly mentioned by other authors, and Galbreath does not illustrate or further elaborate on the identity of this character. There is some variation in the distance between the superior

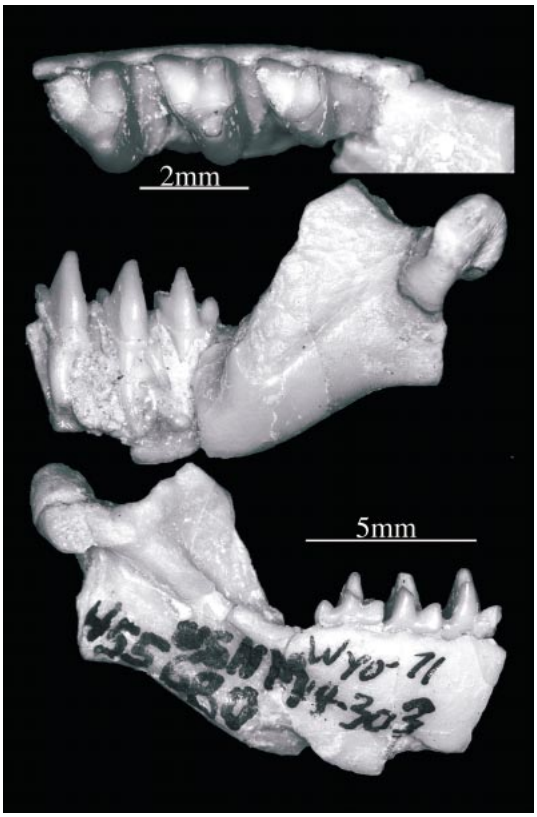

Fig. 28. USNM 455680, *Apternodus iliffensis* partial dentary from West Canyon Creek, Beaver Divide, Wyoming in occlusal (top), lateral (middle), and lingual (bottom) views.

margin of the infraorbital canal to the lacrimal foramen; in *A. brevirostris* this distance is shorter than that in *A. gregoryi* and defines the border between the lacrimal foramen and orbit with a ridge. However, this feature serves to distinguish the two species, not characterize them. Furthermore, a ridge posterior to the lacrimal foramen is present in FMNH PM34512. Hence, we regard this character as a misinterpretation by Galbreath of breakage along the lateral margin of the maxilla in FMNH PM34512.

The fragmentary teeth of FMNH PM34512, consisting of an intact P2, P3, partial P4, and the lingual remnants of M1-M2, are identical in size and appearance to the corresponding parts of P3-M2 in KU 9112. Most importantly, both specimens lack protocones and are from temporally and geographically adjacent localities, and can easily be accommodated in the single species, *Apternodus iliffensis*.

Krishtalka and Setoguchi (1977) described upper and lower dental remains of ''*Apternodus* sp. cf. *A. iliffensis*'' from Badwater locality 20, now considered to be early Duchesnean in age. One of these specimens. CM 29012 (fig. 31), is a right maxillary fragment with P4-M1, not M1–2 as stated by Krishtalka and Setoguchi (1977), with weak protocones that presumably led these authors to associate the Badwater specimens with *A. iliffensis*. However, the protocones of CM 29012 are actually larger than those of the *A. iliffensis* type. Other potentially useful anatomical regions (e.g., P3 and M3) are missing. Hence, this specimen and others from Badwater locality 20 are not sufficiently diagnostic for identification at the species level. Nevertheless, the Badwater locality 20 *Apternodus* specimens, and similar material described by Storer (1995) from the approximately contemporaneous Lac Pelletier Lower Fauna of Saskatchewan, document the first occurrence of this genus in the middle Eocene of North America. The small ''*Apternodus* sp.'' described by Tong (1997) from China may be similar or even older in age.

Ostrander (1987) referred several isolated upper and lower teeth from the middle Chadronian Raben Ranch Local Fauna of Nebraska to *A. iliffensis*. However, Ostrander did not provide illustrations of these specimens, and the mesiodistal and buccolingual dimensions he reports are broadly consistent with those of several *Apternodus* species. In our experience, isolated upper or lower molars cannot be assigned with confidence to a single species of *Apternodus*.

Apternodus major, new species

TYPE SPECIMEN: UW 11046, nearly complete skull (fig. 32) preserving base of left I1, C, P3-M3, right I1, C-M3, missing posterior palate and pterygoid region, articulated right dentary with broken i1, c, broken p3, p4-m3, and associated left dentary (fig. 33) with p4-m3; associated ulna, proximal and distal fragments of right humerus (fig. 34), fragments of scapulae, cervical vertebrae, and ribs.

Fig. 29. DMNH 1747, *Apternodus iliffensis* skull from Fremont Butte, Colorado in stereo ventral (top), dorsal (middle), and lateral (bottom) views.

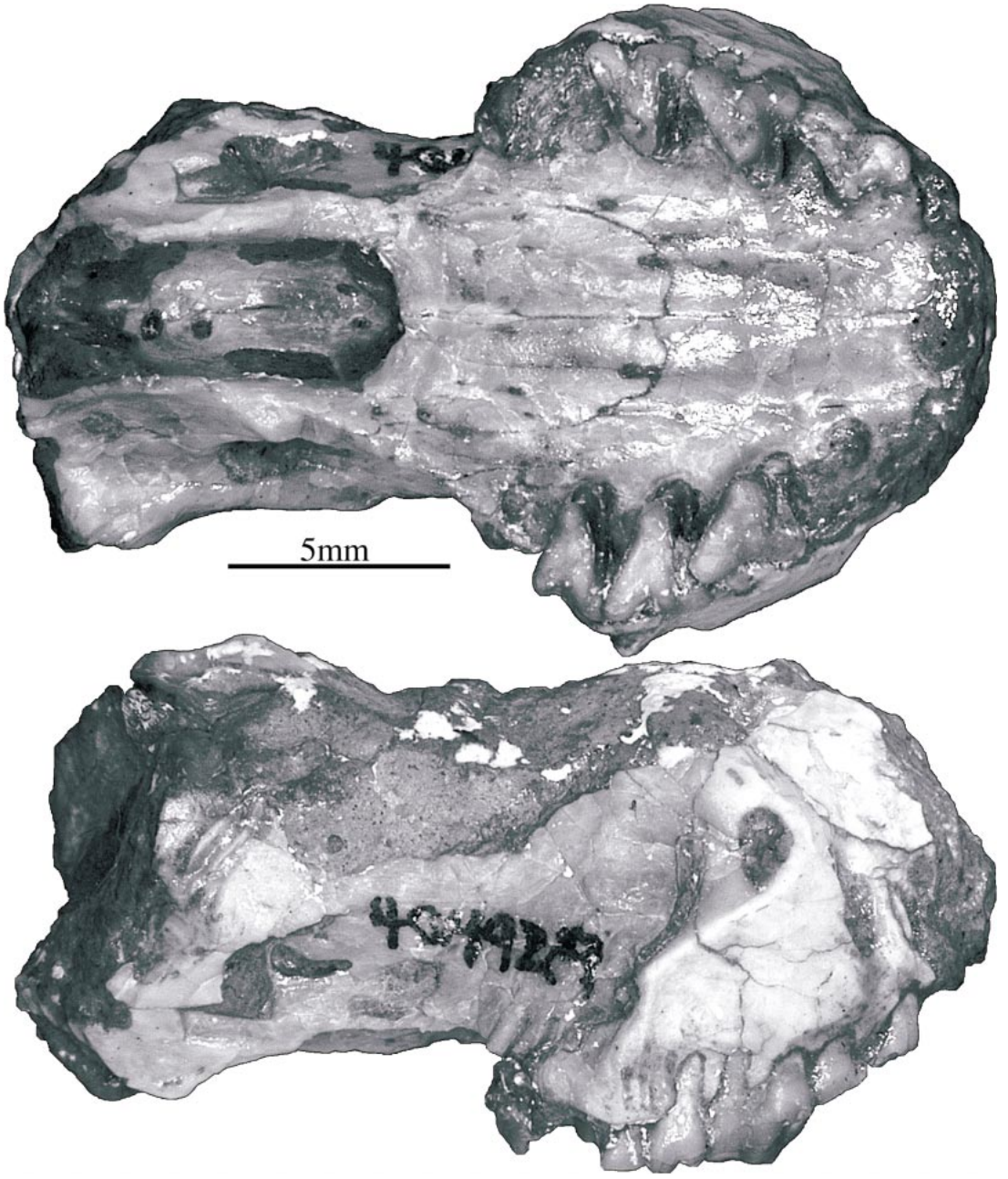

Fig. 30. TMM 40492–9, *Apternodus iliffensis* rostrum from Red Mound, Texas in ventral (top) and lateral (bottom) views.

REFERRED SPECIMENS: UW 10981, rostrum associated with partial right dentary with p3-m3, broken i1, i3, c; UW 10984, fragmentary skull with left M1-M3, right M1-M2; UW 11291, partial rostrum with left P2-P4, broken M1-M2; UW 11292, fragmentary skull with right M1-M3, associated left maxilla with P3-M2; UW 11295, fragmentary rostrum with left P3-P4, articulated posterior left dentary, associated with anterior left den-

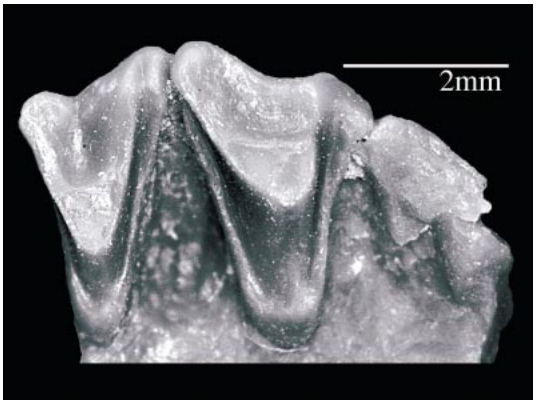

Fig. 31. Cast of CM 29012, *Apternodus* sp. maxillary fragment from Badwater 20, Wyoming in occlusal view.

tary containing p4-m1; and UW 11296, rostrum with articulated left and right dentaries, with complete dentition except for I/i1 and P/p2.

ETYMOLOGY: The name ''*major*'' was coined originally by Kron (1978) and refers to the large size of this species.

TEMPORAL AND GEOGRAPHIC DISTRIBUTION: Chadronian (late Eocene) of eastern Wyoming (Dilts Ranch 10).

DIAGNOSIS: This species is the largest yet known in the genus *Apternodus*. It is anatomically distinctive by virtue of the laterally flared anterior lambdoid plates and the enlarged, bony torus present along the ventral margin of the external auditory meatus. Unlike *A. iliffensis*, the external auditory meatus is ventrally concave, but not to the extent seen in *A. gregoryi* (fig. 21). *A. major* also has a prominent, anteromedially running rostral tympanic process of the petrosal, a laterally prominent maxillary rudiment of the zygoma, and a lacrimal foramen continuous with the anterior orbit. Diastemata between the upper incisors and adjacent to P3 are lacking. The anterior dentition of *A. major* is large, but premolariform, resembling that of *A. gregoryi*. The large, two-rooted, premolariform P2 of *A. major* is similar in size to P3 and much larger than the P2 of *A. brevirostris*. Protocones on the upper molars are reduced and barely distinguishable from the lingual cingulum.

REMARKS: Several specimens collected and first described by Kron (1978) are well-preserved, but none is as complete as the type. This specimen (UW 11046) is a particularly large and robust individual, showing extreme development of the anteriorly flared lambdoid plates, a laterally expansive maxillary zygoma, and distinct fossae in the maxillae above each canine. *A. major* is found nowhere else except at the Dilts Ranch area examined by Kron (1978), which has also yielded other species of *Apternodus* (UW 13508 *A. gregoryi* and AMNH 74952 possibly *A. brevirostris*) but none of *Oligoryctes*. In addition to the details summarized in the diagnosis, the morphology of the type skull is as follows.

The maxilla adjacent to the anterior infraorbital canal is damaged on both sides. However, it can be seen on the left side to project far anterolaterally (fig. 32), providing extensive surface area for the attachment of anterior facial muscles. Following Butler (1956), the muscles that originate from this area include levator labii superioris, levator alae nasi, and zygomaticus. Whidden (MS in progress) has recently confirmed Butler's assessment for the origin of these muscles in insectivoran-grade taxa such as *Solenodon*. *A. major* possesses a relatively huge area for the attachment of anterior snout-muscles, somewhat more elaborate than that of *Solenodon*, which supports an elongate rod of cartilage that stretches anteriorly from the external nares. Hence, the rostral morphology of *A. major*, and that of *Apternodus* generally, appears compatible with an anteriorly elongate, cartilaginous extension of the proboscis (as reconstructed anterior to the elongate upper incisor in the frontispiece of this monograph).

The dorsal braincase of *A. major* is rugose (fig. 32). Due in part to its laterally extensive anterior lambdoid plate, *A. major* has more surface area for the attachment of the temporalis muscle than other species of *Apternodus*. The robust temporalis musculature of *A. major* is also reflected in the pronounced muscle scar on the lateral aspect of the mandibular coronoid process (fig. 33).

As in other species of *Apternodus*, *A. major* shows prominent piriform fenestrae in the tympanic roof anterior to the pars cochlearis of the petrosal. Anteromedial to the prom-

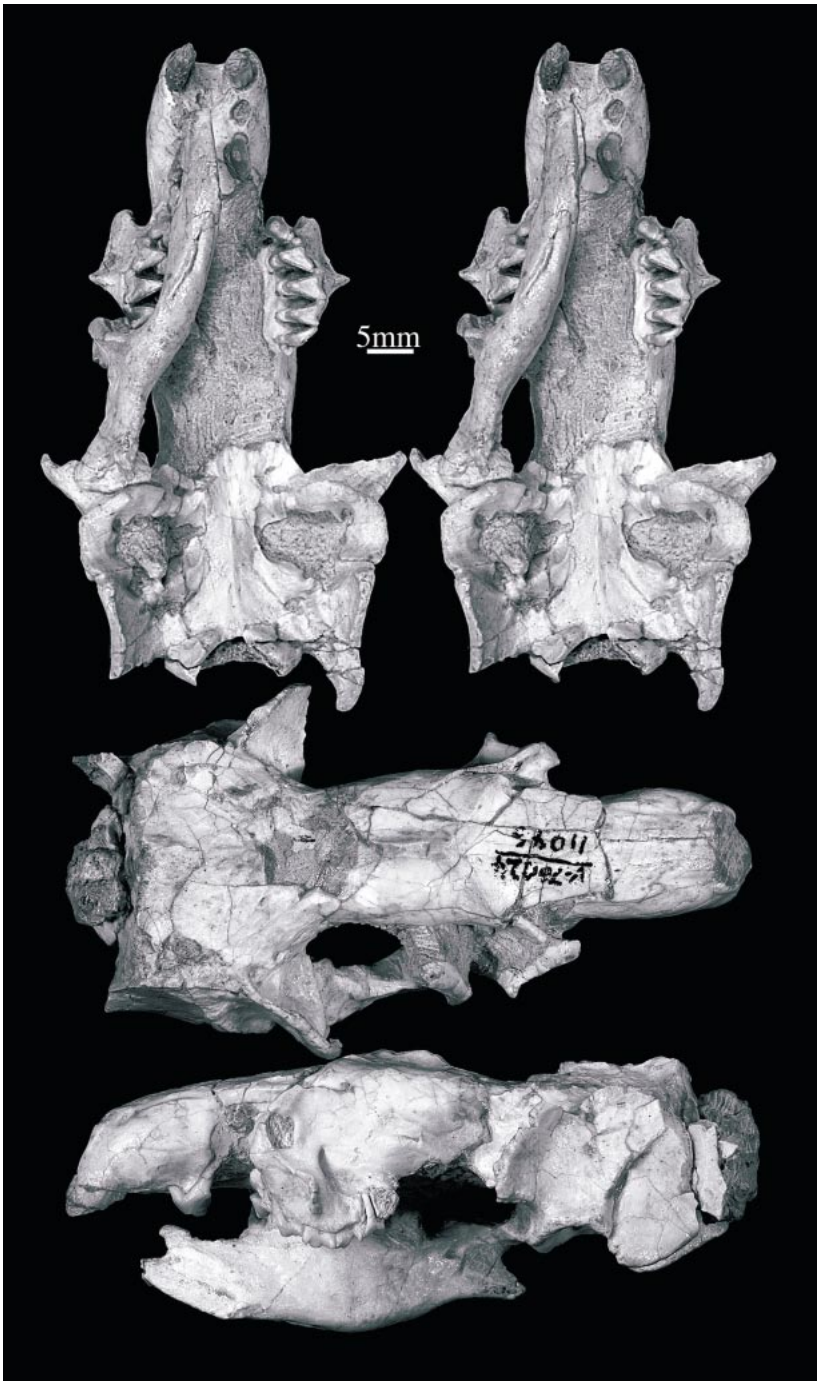

Fig. 32. UW 11046, skull of *Apternodus major* type specimen from Dilts Ranch, Wyoming in stereo ventral (top), dorsal (middle), and lateral (bottom) views.

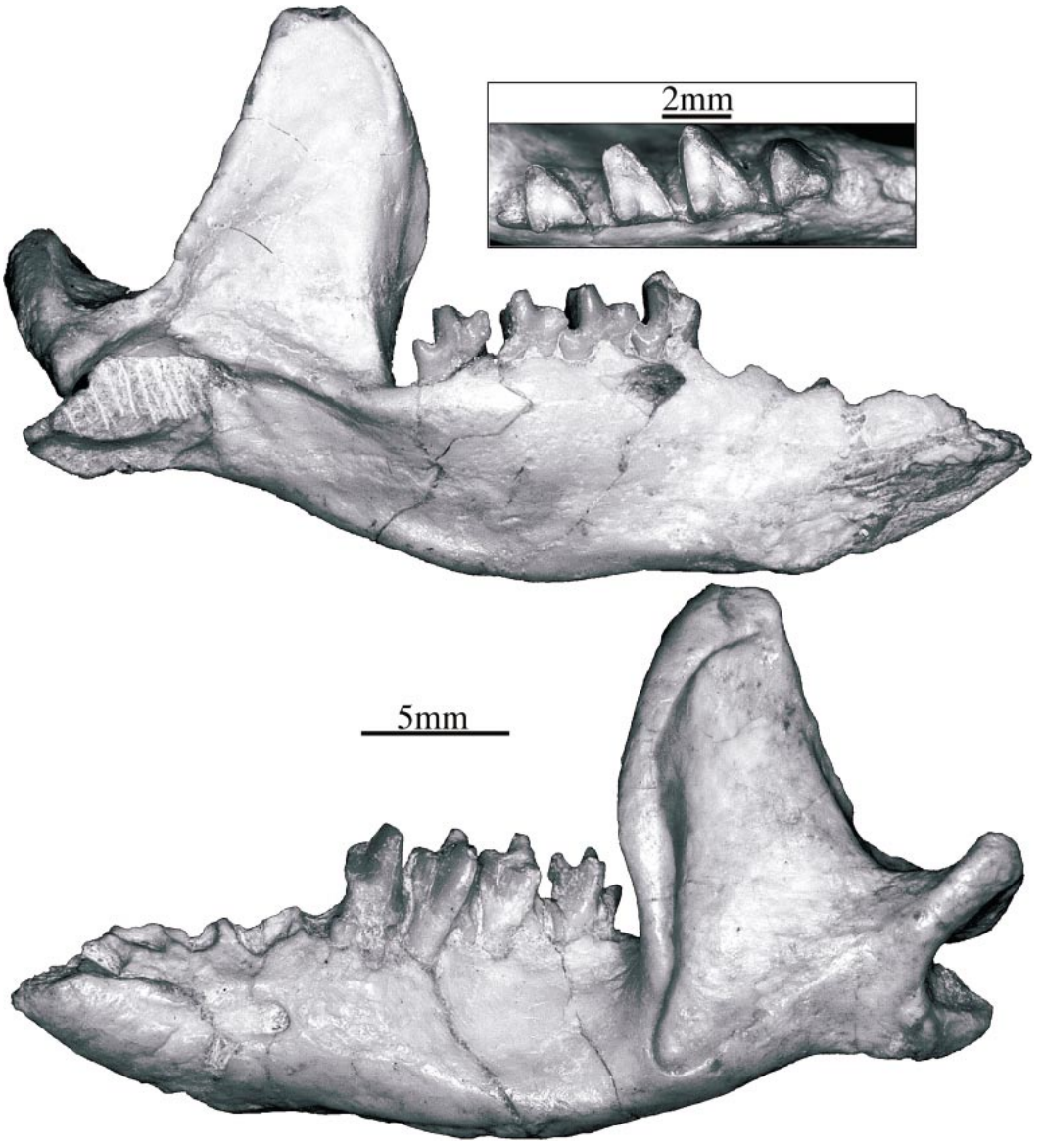

Fig. 33. UW 11046, mandible of *Apternodus major* type specimen from Dilts Ranch, Wyoming in occlusal (inset), lingual (top), and lateral (bottom) views.

ontory, on the lateral margin of the basisphenoid, a distinct vidian foramen is evident. The anterior carotid foramen appears to be confluent with the piriform fenestra (fig. 32). Anterior and slightly ventral to the caudal tympanic process of the right petrosal, UW 11046 preserves fragments of what might be a broken ectotympanic or tympanohyal (fig. 32).

The posterior palate and pterygoid region are not preserved in UW 11046, but from other, more fragmentary specimens (e.g., UW 10981, UW 10984, UW 11292) they can be inferred to be similar to those of other species of *Apternodus*. The jaw joint, well preserved in the type, also resembles that of other *Apternodus*, as described above for *A. baladontus*.

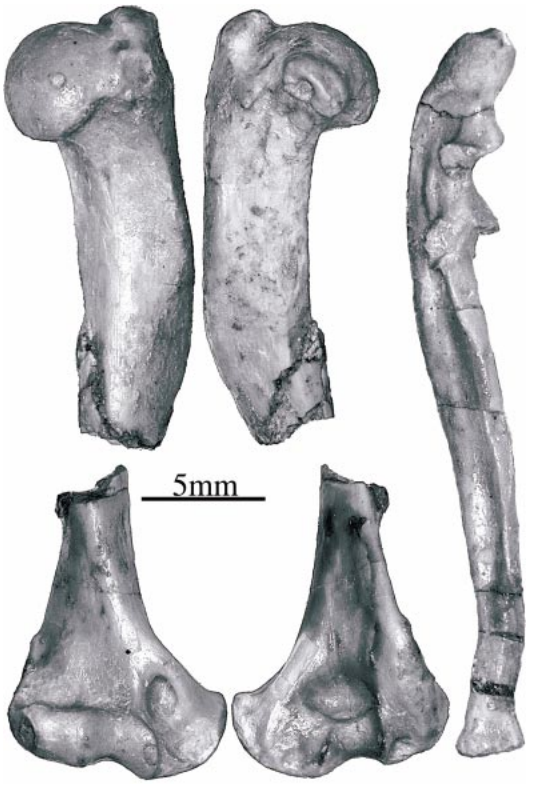

Fig. 34. UW 11046, humerus of *Apternodus major* type specimen from Dilts Ranch, Wyoming in anterior (left) and posterior (middle) views, with ulna (right).

UW 11046 is one of the few *Apternodus* specimens with associated postcrania. These include a left ulna and both proximal and distal left humeral fragments (fig. 34). Both elements resemble those of *Solenodon*, but are smaller. The proximal humerus shows a broad greater tuberosity and well-defined fossa for the biceps tendon. The distal humerus shows an entepicondylar foramen, prominent medial epicondyle, well-defined trochlea and capitulum, and a small fossa posterior to the capitulum that is continuous with the supinator crest. The proximal ulna differs from that of *Solenodon* in having a smaller, more gracile olecranon process.

Distal fragments of both scapulae, a clavicle, vertebrae, and ribs are also preserved together in an associated block of matrix. The right scapula appears to be articulated with the proximal end of the right clavicle. On both sides, the scapulae are unremarkable, with concave glenoid fossae for articulation with the proximal humeri. The neural arches of several vertebrae, probably thoracic, are partially exposed. Spinous processes of these vertebrae were either very small or not preserved in this specimen.

Apternodus dasophylakas, new species

TYPE AND ONLY SPECIMEN: UW 14072, crushed but otherwise complete skull (fig. 35) preserving left I1, C-M3, right I1, broken C, P2, broken P3, P4-M3, articulated left dentary with complete dentition, associated right dentary with i1-i2, c-m3 (fig. 36), associated tibia, atlas, axis, partial scapula, proximal humerus, distal ulna, ribs, and other fragmentary postcranial fragments (fig. 37). All elements are slightly distorted due to postmortem deformation.

ETYMOLOGY: This species is named in honor of the faculty, students, and staff of the Department of Geology and Geophysics, University of Wyoming, under whose auspices the type and only specimen was collected and is now curated. The Greek word transliterated as ''*dasophylakas*'' is an interpretation of the English word ''cowboy'', the UW mascot. Literally, the trivial name means ''ranger'' or ''guardian of wild land and forest'' (N. Soulunias and I. Trivilas, personal commun.).

TEMPORAL AND GEOGRAPHIC DISTRIBUTION: Chadronian (late Eocene) of southeastern Wyoming (Harshman Quarry 21).

DIAGNOSIS: Protocones on the upper molars are absent, a condition somewhat exacerbated by wear. The anterior dentition is premolariform, not bulbous. P3 has an elongate stylar margin, and diastemata are evident on either side of the upper canine, between I1 and I2, and probably also between P2 and P3; some distortion in the maxilla between P2-P3 on both sides precludes certainty as to the size of the P2-P3 diastema. Both P2 and p2 are smaller than adjacent teeth and are similar in proportion to those of *A. brevirostris*. The mental foramen on the dentary is located just below p2, a position slightly anterior to that of other *Apternodus* species. The p3 shows a slight buccal cingulid and a distinct posterior cusp. The ex-

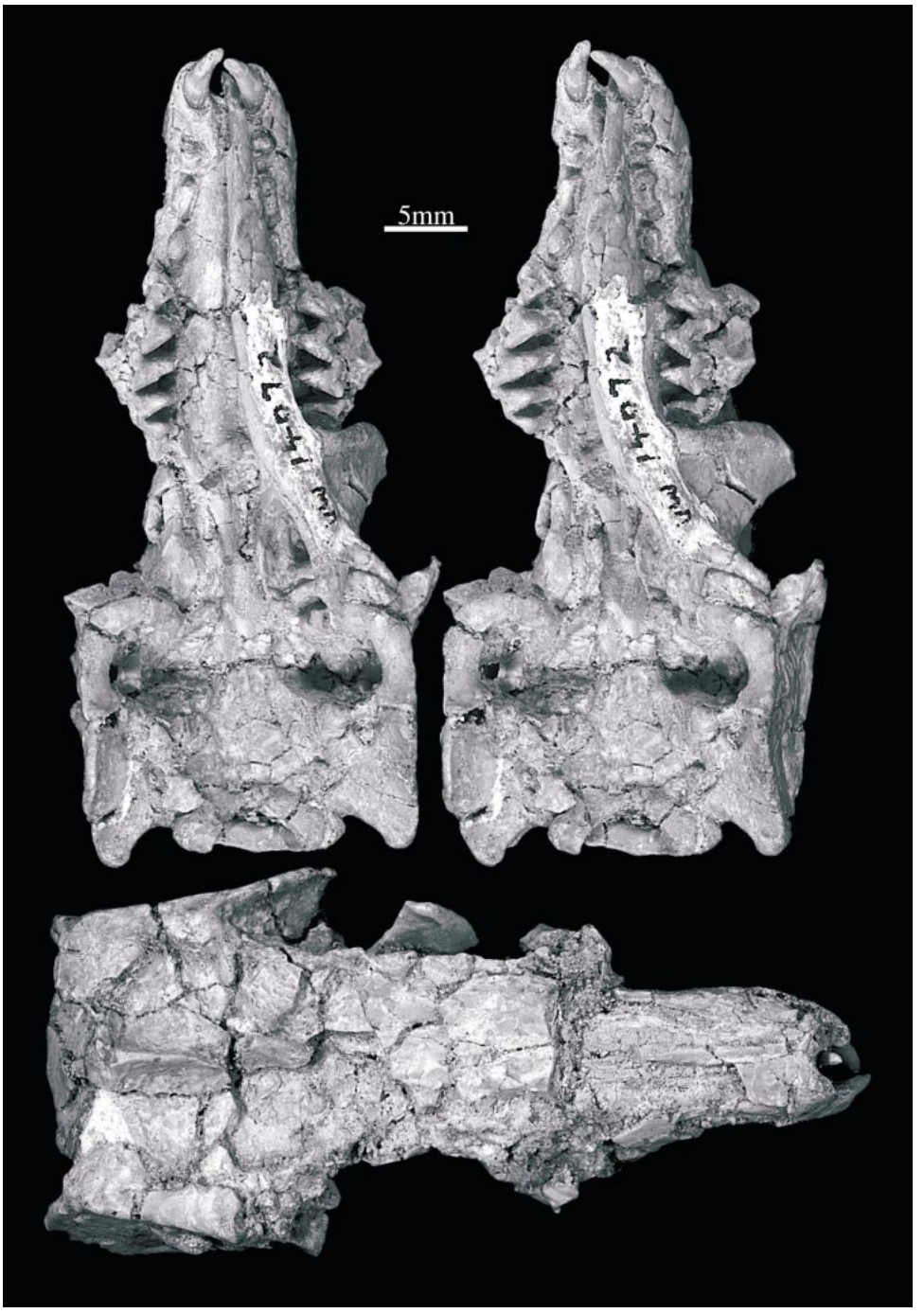

Fig. 35. UW 14072, skull of *Apternodus dasophylakas* type specimen from Harshman Quarry, Wyoming in stereo ventral (top) and dorsal (bottom) views.

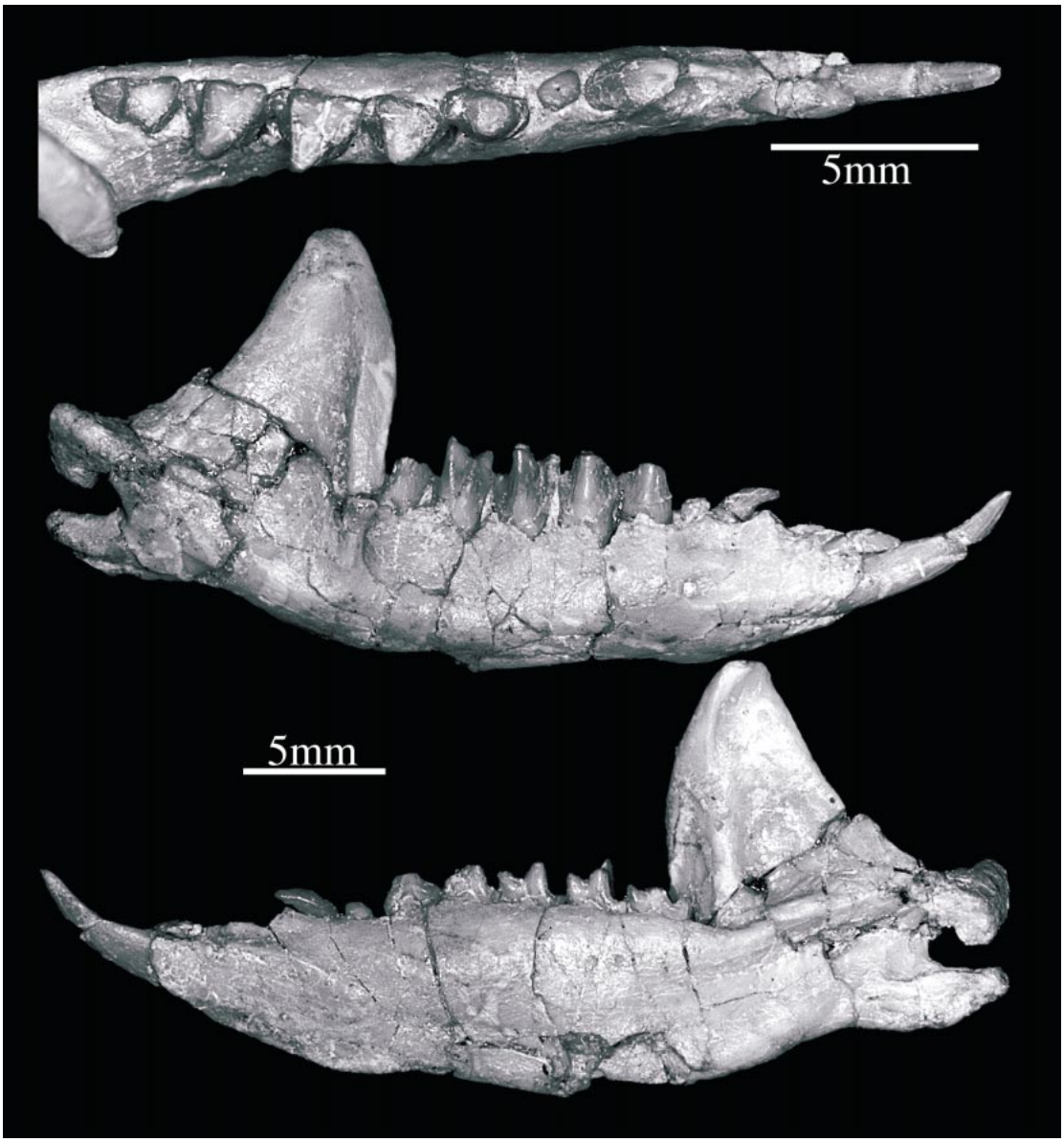

Fig. 36. UW 14072, mandible of *Apternodus dasophylakas* type specimen from Harshman Quarry, Wyoming in occlusal (top), lateral (middle), and lingual (bottom) views.

ternal auditory meatus of UW 14072 is not marked by a torus, in contrast to that of *A. major*, but is flat as in *A. iliffensis*. Another similarity to *A. iliffensis* is the ventral margin of the lambdoid plate, which reaches just slightly ventral to the level of the jaw joint. The rostral tympanic process of the petrosal is flat. A piriform fenestra is evident, lateral to a small anterior carotid foramen.

REMARKS: UW 14072 is a large version of *A. iliffensis*, sharing with it aspects of the ear and lambdoid region as well as reduced upper molar protocones and an elongate P3 (polymorphic in *A. iliffensis*). UW 14072 differs qualitatively from individuals of *A. iliffensis* in having an M3 similar in buccolingual width to the M2, an elongate rostrum with diastemata on either side of the canine,

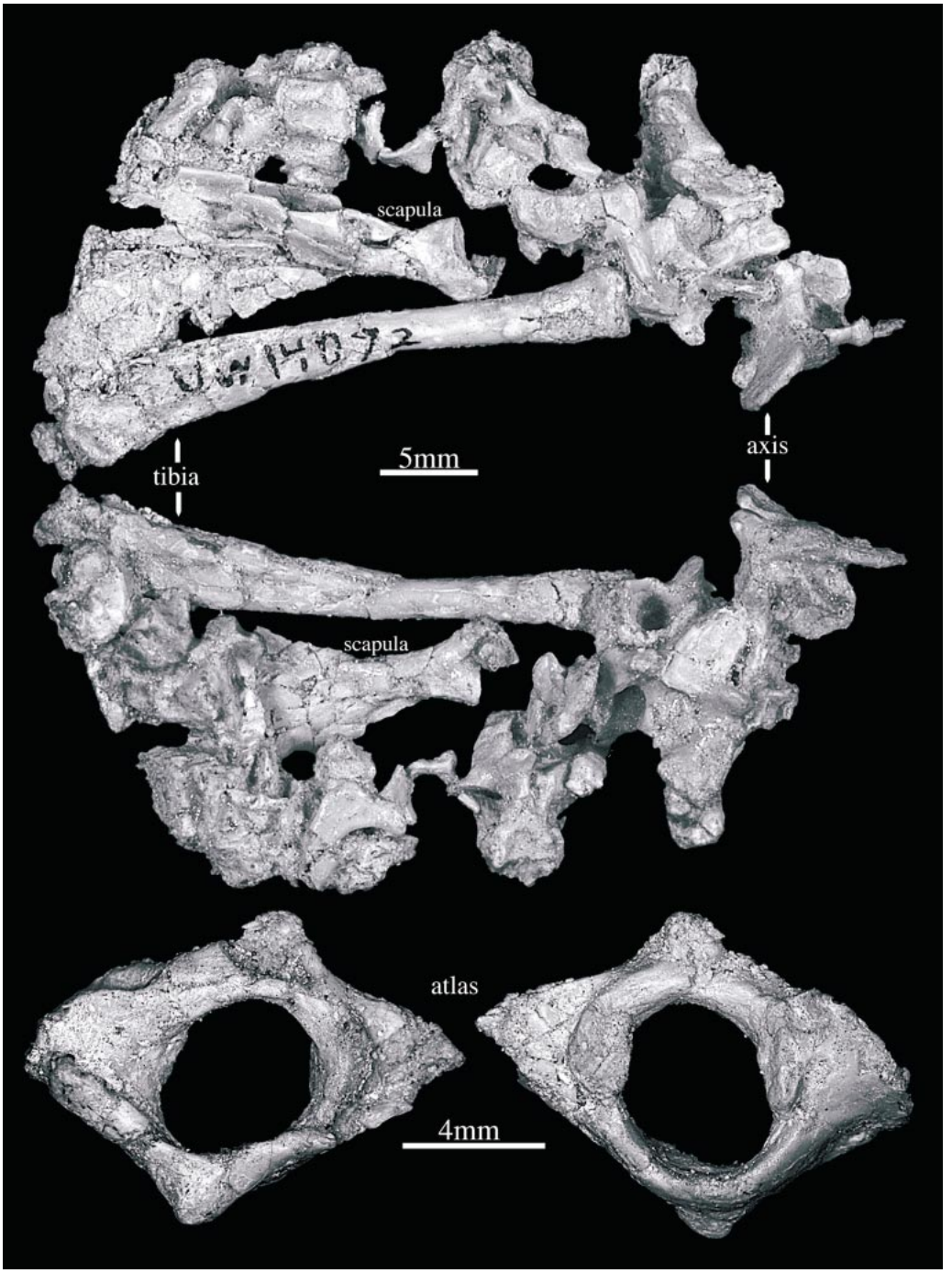

Fig. 37. UW 14072, scapula, tibia, fragmentary vertebral column including the axis (top and middle) and atlas (bottom) of *Apternodus dasophylakas* type specimen from Harshman Quarry, Wyoming.

and a transversely wide basicranium. It differs from other *Apternodus* species in having a mental foramen ventral to p2; the position of the mental foramen(ina) is unknown in *A. iliffensis*. Cranial proportions are similar to those of *A. gregoryi*, with the exception that *A. dasophylakas* has a very shallow external auditory meatus and a lambdoid plate that does not extend far ventral to the jaw joint. The orbitotemporal region of UW 14072 is crushed, leaving a very distorted lacrimal foramen on the left side, and none on the right. It is therefore difficult to tell if the posterior border of the lacrimal foramen is flush with the anterior orbit as in *Apternodus gregoryi* (figs. 21, 22) and *A. major* (fig. 32). The left craniomandibular joint, with the jaw still in articulation, preserves what might be part of an ossified articular disk separating the condyle from the glenoid fossa (fig. 35). However, due to the postmortem distortion of the specimen, it is difficult to discount the possibility that this region contains multiple fragments of the mandibular condyle itself.

Postcranially, what little is known of *A. dasophylakas* (fig. 37) does not appear to be specialized for a nonterrestrial locomotor repertoire. The only exception to this observation in any *Apternodus* specimen may be the structure of the proximal femur in *A. gregoryi* (UW 13508; see above). The distal tibia of *A. dasophylakas* is not fused with the fibula. The scapula has a triangular shape, narrow laterally at the glenoid fossa and broadening dorsomedially toward the vertebral column. The second cervical vertebra shows a ventrally projecting keel on the posteroventral aspect of its centrum (similar to the axis of shrews and *Echinosorex*); and the first cervical vertebra shows two widely separated facets for the occipital condyles of the skull.

FAMILY **OLIGORYCTIDAE,** NEW FAMILY

INCLUDED GENERA: *Oligoryctes* Hough, 1956

DISTRIBUTION AND DIAGNOSIS: As for *Oligoryctes*.

Oligoryctes Hough, 1956

TYPE SPECIES: *Oligoryctes cameronensis* Hough, 1956

INCLUDED SPECIES: *O. altitalonidus* Clark, 1937 (new combination) and the Tabernacle Butte taxon (unnamed in this paper; see below).

TEMPORAL AND GEOGRAPHIC DISTRIBUTION: Bridgerian (late early Eocene) through Orellan (early Oligocene) throughout the North American western interior, including Wyoming, Montana, Colorado, North Dakota, South Dakota, Saskatchewan, California, Nevada, Utah, Texas, and Nebraska, possibly including Asia if material described by Tong (1997) is included.

DIAGNOSIS: *Oligoryctes* is a shrew-sized animal with zalambdodont molars, lacking metacones and with reduced talonid basins. The m3 talonid cusp is slightly taller than the m3 paraconid. The upper molars have distinct protocones and anterior cingula, and the posterior two lower incisors are tricuspid. The medial aspect of the coronoid process is deep or pocketed. *Oligoryctes* has a relatively unspecialized posterior braincase without the elaborate lateral extensions of the squamosal, petromastoid, and occipital that form the lambdoid plates in *Apternodus*. Instead, *Oligoryctes* has a laterally rounded squamosal and petromastoid. It shows a prominent entoglenoid process for posterior support of the jaw joint, medial to the postglenoid foramen and anterior to the promontory of the middle ear. The basicranium shows an enlarged foramen ovale and lacks an alisphenoid canal. The squamosal extends posteriorly along the ventrolateral margin of the braincase, lateral to the large piriform fenestra. The anterior exit of the sinus canal and ethmoid foramen are located well anterior to the sphenorbital fissure and are not incorporated into its superior margin. As in *Apternodus*, the lacrimal foramen is large and laterally oriented.

Oligoryctes cameronensis Hough, 1956

TYPE SPECIMEN: USNM 19909, rostrum (38) with right P2-P4, broken M1, M2-M3, left P3-M3, preserving pterygoid region, associated left dentary with p3-m3 (fig. 39); original lost, known only from illustrations.

REFERRED MATERIAL: USNM 516840, undistorted cranium (fig. 40), missing premaxillae and mandibles, preserving left ?C, P2,

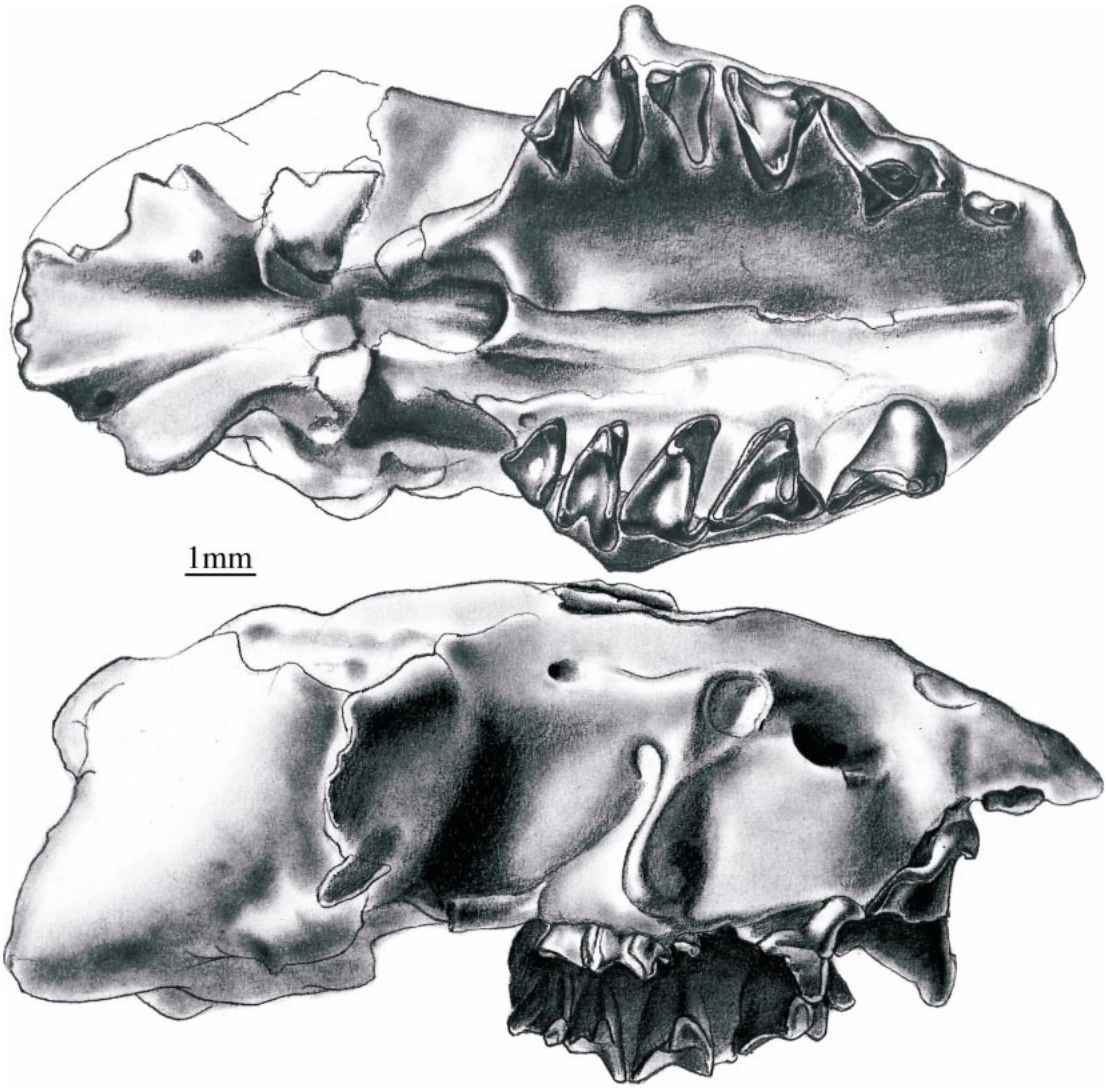

Fig. 38. USNM 19909, type rostrum of *Oligoryctes cameronensis* from Cameron Spring, Wyoming in ventral (top) and lateral (bottom) views. Illustrations by Lawrence Isham.

dP3, erupting P3, P4-M3, right P2, dP3, erupting P3, P4-M3; USNM 516846, left dentary with p3-m3; UCM 52446, rostrum (fig. 41) with left broken I2, I3-M3, right I2, P2-M3, orbitotemporal region, articulated left dentary with complete dentition except for missing crown of i3, associated right dentary with p3-m3 (fig. 42); MPUM 6677, left dentary with heavily worn i1-m3; MPUM 6859, right ?M1, left maxillary fragments with P3-M3, associated left petromastoid fragment preserving superior semicircular canal and stapedius fossa, missing bulk of pars cochlearis; CM 17193, rostrum with right and left P3-M3 plus anterior alveoli (fig. 43; original lost, known only from photos); CM 73977, associated right and left dentaries, each with p4-m3.

TEMPORAL AND GEOGRAPHIC DISTRIBUTION: Chadronian (late Eocene) of central Wyoming (Cameron Spring 5, Flagstaff Rim 18) and western Montana (Pipestone Springs 29, Eureka Valley Rd. 16), probably also northwestern Nebraska (33; see Ostrander, 1987).

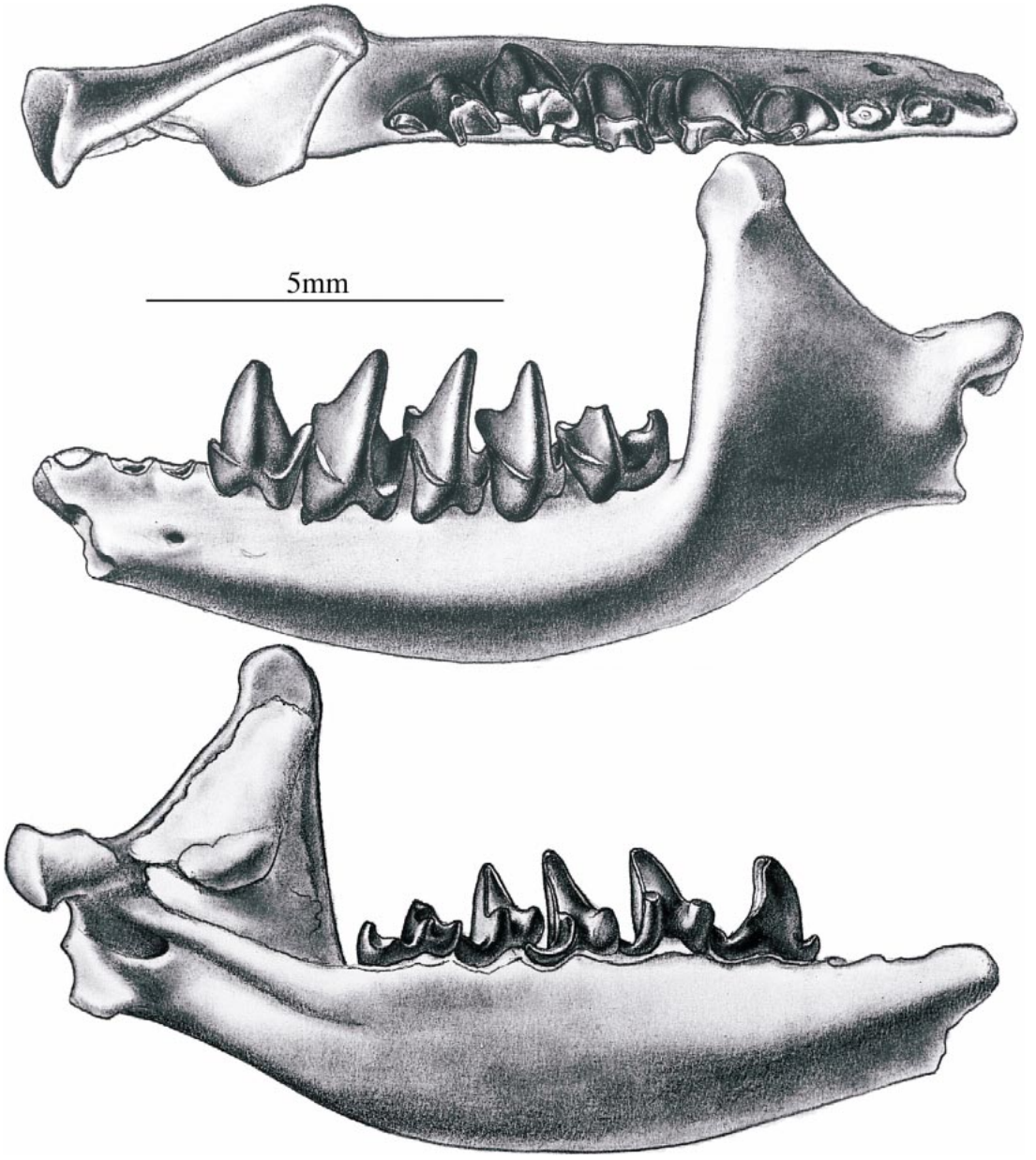

Fig. 39. USNM 19909, type mandible of *Oligoryctes cameronensis* from Cameron Spring, Wyoming in occlusal (top), lateral (middle), and lingual (bottom) views. Illustrations by Lawrence Isham.

DIAGNOSIS: The small maxillary rudiment of the zygoma is located lateral to the posterior edge of M1. The type skull shows a foramen in the alisphenoid posterior to the enlarged foramen ovale, similar in position to the alisphenoid foramen transmitting the inferior stapedial ramus in some tenrecs (Asher, 2001). A small foramen is evident on the rostrum near the nasal-frontal suture, as are foramina laterally along the path of the sinus canal, above the external auditory meatus and jaw joint. The dental formula is 3.1.3.3/3.1.3.3, differing from that of *Apternodus* in having one more upper incisor. The

crown of P3 is longer than that of P4; both show a prominent, anteriorly projecting parastyle. The trigonids of the lower molars decrease progressively in width, with that of m1 the largest and m3 the smallest. The talonid of the m3 is elongate, making this tooth the longest in the molar series. As in *O. altitalonidus*, the m3 talonid cusp is slightly greater in height than the m3 paraconid; the medial aspect of the coronoid process is pocketed; and the coronoid process is externally convex.

REMARKS: USNM 516840, collected by one of us (RJE) from Flagstaff Rim, is by far the best specimen yet known of this taxon (fig. 40). It is one of the few small ''apternodontid'' specimens known that preserves petrosals and elements of the deciduous dentition; and its pristine state of preservation is also quite remarkable. The undistorted rostrum shows sutures between the nasals and maxilla; the nasal-frontal suture is faint, but appears to delimit a posteriorly narrow nasal. A small foramen is present in the rostrum at the posterior margin of the nasal. Premaxillae are missing. The lacrimal foramen is large, laterally directed, and situated on the anterior aspect of the infraorbital canal. The frontal-maxillary suture is also visible and appears to extend well into the orbit, accompanied by the roots of the maxillary teeth (fig. 40). The maxilla anterior to the infraorbital canal is also perforate and shows roots of the erupting permanent P3. The posterior ethmoid region is broad and contributes to a slight postorbital constriction.

The braincase is well preserved and shows no sign of sutures within the frontal or between the frontal, parietal, and occipital, although numerous hairline cracks, some bilateral, may represent such sutures. In contrast, the petromastoid shows well-defined sutures with the occipital, parietal, and squamosal, and is well-exposed laterally. The petromastoid-squamosal suture extends ventrally onto the basicranium and defines the lateral boundary of the tympanic cavity. The squamosal also shows fairly well-defined sutures with the parietal and alisphenoid. On the squamosal side of the squamosal-parietal suture are three foramina, two located adjacent to the petromastoid, and one dorsal to the jaw joint.

USNM 516840 shows four foramina anterior to the sphenorbital fissure. The anteriormost is a large ethmoid foramen, providing a conduit into the anterior cranial fossa and posterior ethmoid region. Immediately posterior and ventral is a much smaller foramen which may also connect the orbit with the anterior cranial fossa. Continuing posteriorly, the next large foramen is the anterior exit point of the sinus canal; slightly medial to that is a small optic foramen. Both the sinus canal and the optic foramen are located immediately anterior to the large sphenorbital fissure, the ventral boundary of which is continuous with the pterygoid. Posterior to the palate, sutures are evident between the V-shaped vomer and pterygoids.

The most conspicuous openings on the basicranium of USNM 516840 are the large piriform fenestra and foramen ovale. The latter is slightly larger than the sphenorbital fissure, and the piriform fenestra is as large as the bony promontory itself. Posterior to foramen ovale, and within the base of the entoglenoid process, is a foramen that served as a conduit for the inferior ramus of the stapedial artery (mentioned above as similar in position to that of tenrecs such as *Geogale*; see Asher, 2001). Subtle grooves on the promontory bone indicate that the internal carotid artery entered the tympanic cavity at the ventral apex of the pars cochlearis, just medial to the prominent caudal tympanic process of the promontory. It immediately bifurcated into a proximal stapedial ramus, which traversed laterally toward the fenestra vestibuli, and a transpromontorial internal carotid (sensu Wible, 1986), which ran anteromedially, entering the braincase via the piriform fenestra. A foramen in the basisphenoid at the dorsomedial margin of the tympanic cavity is smaller in caliber than the groove for the internal carotid on the pars cochlearis. Hence, we believe this foramen provided a conduit for a small vidian artery, branching from the internal carotid immediately proximal to the latter's path through the piriform fenestra.

Zygomatic arches are completely lacking, and both maxillary and squamosal rudiments of the zygoma are reduced. As in *Apternodus*, the jaw joint is defined posteriorly by the entoglenoid, not postglenoid, process.

Fig. 40. USNM 516840, *Oligoryctes cameronensis* skull from Flagstaff Rim, Wyoming. Stereo ventral (top), lateral (middle), and dorsal (bottom) views; (opposite page) anatomical guide to ventral view. See text for abbreviations.

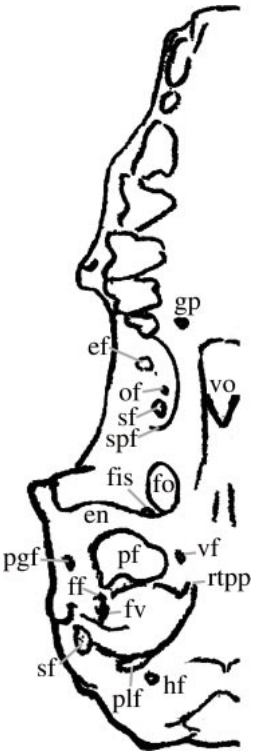

Fig. 40. Continued.

This is located medial to the postglenoid foramen and anterior to the middle ear.

The upper molars of USNM 516840 are fully erupted and show minimal wear. P4 is almost fully erupted; P3 is still in its crypt, but some cusps are evident dorsal to dP3. P2 is fully erupted and minute in size. The right upper canine is missing; on the left side it is intact but not yet fully erupted and is displaced posteriorly.

Also noteworthy among the new specimens of *O. cameronensis* is UCM 52446, a well-preserved rostrum (fig. 41) and associated, largely complete mandible (fig. 42). Its dentition is fully erupted and shows a permanent P3 that is larger than the dP3 of USNM 516480, particularly the paracrista running posterior to the paracone. The dentary shows trigonids of m1-m3 becoming progressively smaller posteriorly, as well as multicuspid incisors. Otherwise, UCM 52446 conforms with the morphology evident in USNM 516840.

Some of Hough's (1956) original description of *Oligoryctes* does not accord with the material that we now have available. Unfortunately, the type specimen designated by her (USNM 19909) now appears to be lost; however, one of us (MCM) previously had an opportunity to examine it. Her diagnosis stated (1956: 538) that the basicranial region differs from that of *Apternodus* ''in having lateral descending processes of the basisphenoid, which embrace medially the small anterior bullae.'' The features in question are actually the medial walls of the sphenorbital fissures; and the contents of the ''anterior bullae'' consist principally of matrix fillings of the trigeminal nerve tracts. If the lower teeth are placed in occlusion with the uppers, this area may be seen to lie well in front of the jaw suspensorium. The medially excavated coronoid process of the mandible was not seen by Hough because the specimen was incompletely prepared at the time it was described.

McDowell (1958: 171, 172) also mistakenly regarded *Oligoryctes* as possessing an ossified auditory bulla, going even farther than Hough by arguing (p. 171) that *Apternodus* also possessed an ossified bulla, based on a presumed close relationship between the two genera. However, elsewhere in his paper (McDowell, 1958: 167–168), he seems to have recognized Hough's mistake: ''Hough (1956) claims that the basisphenoid tympanic wing is present in *Oligoryctes*, a genus probably closely related to *Apternodus*. However, this is not clear from the specimen and appears rather to be but a slight selvage of basisphenoid against the ear chamber and does not have the characteristic position of the lipotyphlan basisphenoid, abutting against the Eustacian cartilage.'' In any event, new material described here of both *Apternodus* and *Oligoryctes* clearly demonstrates that the middle ear of both taxa is similar to that of soricids and *Solenodon*, with neither taxon showing an ossified auditory bulla, and both showing a piriform fenestra (polymorphic within *A. brevirostris* and *A. mediaevus*).

Oligoryctes altitalonidus Clark, 1937
(new combination, formerly ''*Apternodus*'' *altitalonidus*)

TYPE SPECIMEN: YPM PU13774, left dentary with p4-m3; original lost but casts remain (fig. 44).

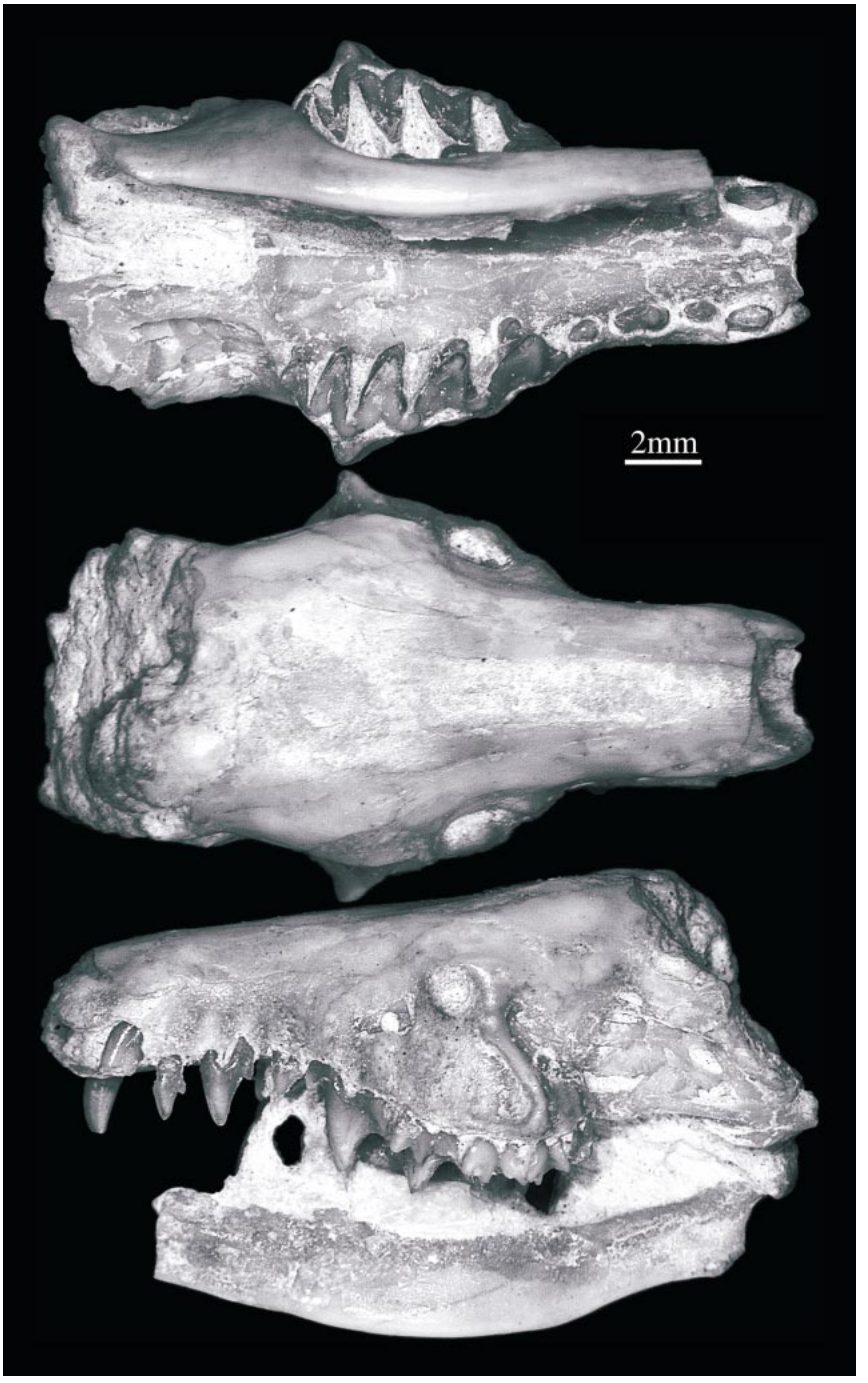

Fig. 41. UCM 52446, *Oligoryctes cameronensis* rostrum from Cameron Spring, Wyoming in ventral (top), dorsal (middle), and lateral (bottom) views.

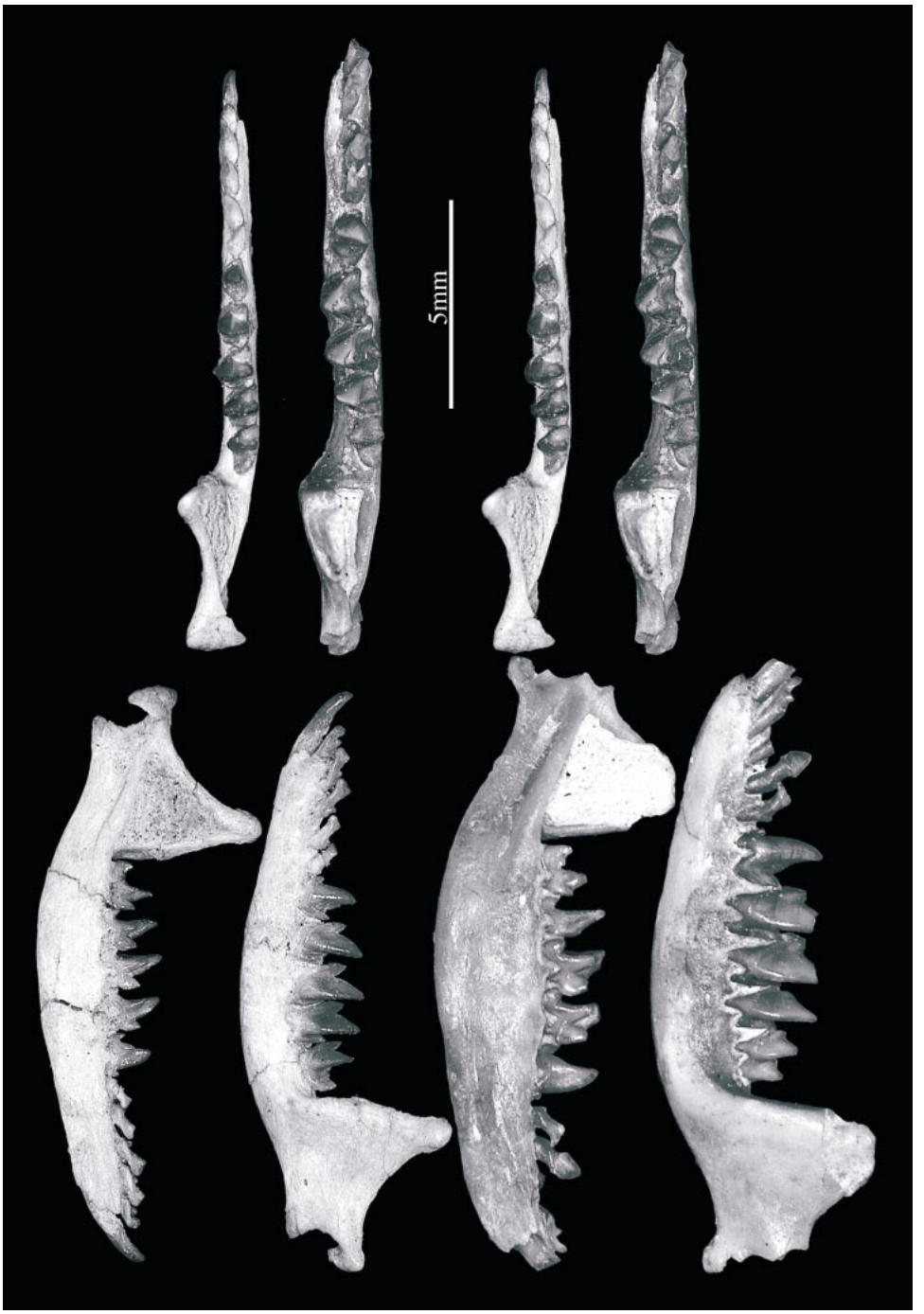

Fig. 42. Mandibles of *Oligoryctes cameronensis* (UCM 52446, stereo right, bottom right) and *Oligoryctes altitalonidus* (USNM 516843, stereo left, bottom left).

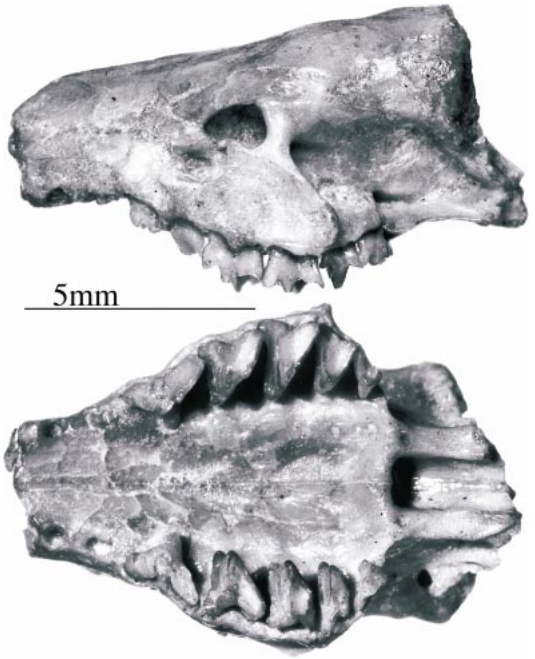

Fig. 43. CM 17193, *Oligoryctes cameronensis* rostrum from Cameron Spring, Wyoming in lateral (top) and ventral (bottom) views. Photos by Chester Tarka

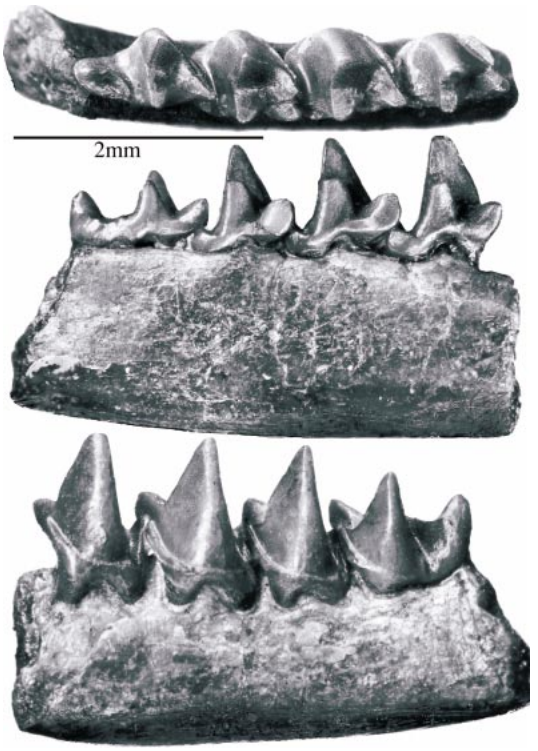

Fig. 44. YPM-PU 13774, type mandibular fragment of *Oligoryctes altiatalonidus* from the Big Badlands of South Dakota in occlusal (top), lingual (middle), and lateral (bottom) views. Photos by Chester Tarka.

REFERRED MATERIAL: USNM 516843, nearly complete skull (fig. 45), slightly compressed dorsoventrally, missing petrosals, with associated mandibles with left i1-m3 and right p3-m3 (fig. 42); USNM 22816, associated right maxillary fragments with P2-M3 (fig. 46); USNM 516841, left dentary with m1-m3; USNM 516842, rostrum with nearly complete dentition including dP3 and dP4 and erupting left P3-P4 in crypts, plus associated mandibles with complete dentition; USNM 516847, left dentary with p3-m3; USNM 516848, left dentary with p4-m3; USNM 516849, left dentary with p4-m3; USNM 516850, right dentary with p3-m3; USNM 516851, right dentary with p4-m3; USNM 516852 left dentary with m1; USNM 516853, left dentary with p3-m3; USNM 516854, rostrum with right and left P3-M3; USNM 516855, rostrum with heavily worn left C-M3 and right P3-M3; USNM 516856, rostrum with right C-M3 and left C-P4; USNM 516857, rostrum with right P3-M3 and left P3-P4; USNM 516858, right dentary with m2-m3; USNM 516862, left maxilla with P3-M2; USNM 516863, right maxilla with P3, M1-M3; USNM 516864, right maxilla with M1-M3; USNM 516865, left dentary with m1-m3; USNM 516866 left maxilla with M1-M2; USNM 516867, anterior braincase and rostrum with right P3-M3 and left P4-M3; USNM 516868, left dentary with m1-m3; USNM 516869, left dentary with p3-m3; USNM 516870, left dentary with m2; AMNH 105310, right dentary with p4-m3; MPUM 0414, left dentary with p3-m3; MPUM 2592, left dentary with m2-m3; MPUM 6797, left dentary with p4-m2; MPUM 6857, left dentary with p4-m3; MPUM 6858, rostrum with right and left P3s; CM 9260, right dentary with p3–4, m2–3; CM 71571, left dentary with p4-m2; CM 71572, left dentary with m1-m2; CM 71573, left dentary with m2–3; and CM 73976, right maxilla with P4-M2.

TEMPORAL AND GEOGRAPHIC DISTRIBUTION:

Uintan (middle Eocene) through Orellan (early Oligocene) of Wyoming (Flagstaff Rim 18, East Fork Basin 12), Montana (Pipestone Springs 29, Diamond O Ranch 9, Little Pipestone Creek 25, Cook Ranch 7), South Dakota (Big Badlands 4), and North Dakota (Fitterer Ranch 17). Geographic distribution probably also includes Saskatchewan (8; see Storer, 1996) and California (34; see Walsh, 1996).

DIAGNOSIS: Unlike *Apternodus*, and like most other mammals including *Oligoryctes cameronensis*, *O. altitalonidus* lacks the extensive, box-shaped structures of the posterior braincase. Instead, its braincase is rounded and gracile, as in *Microgale*. *O. altitalonidus* possesses a maxillary rudiment of the zygoma lateral to M2, slightly posterior to that of *O. cameronensis*. *O. altitalonidus* is smaller than all other Tertiary zalambdodonts except for the unnamed Tabernacle Butte taxon (McKenna et al., 1962; Bloch et al. in prep.). Perhaps the most conspicuous similarity with *O. cameronensis* is the large size of foramen ovale, which is greater in diameter than the jugular foramen (fig. 45). The squamosal is posteriorly elongate, forming the lateral border of the large piriform fenestra. The stylar crests of P3 are elongate, as in *O. cameronensis*. In contrast to *Apternodus* and *O. cameronensis*, this species possesses a p1, one of eight teeth anterior to the three lower molars; hence, its dental formula is 3.1.3.3/3.1.4.3. The p3 shows a cingulid buccally. As in *O. cameronensis*, the m3 is longer than more anterior cheek teeth, and the posterior two incisors are tricuspid. The tall trigonid cusp on m3, for which this species was named, is also present in the larger *O. cameronensis* and the Tabernacle Butte taxon. Unlike *O. cameronensis*, the molar trigonids of *O. altitalonidus* are similar in size and do not decrease markedly from m1 to m3. The medial side of the coronoid process is pocketed, as in modern soricids. Unlike soricids, the coronoid process is bowed in shape, or externally convex.

REMARKS: USNM 516843 (figs. 42, 45) is the best specimen of *O. altitalonidus* yet known. Several additional specimens from Pipestone Springs (USNM 22816; fig. 46) and Flagstaff Rim (e.g., USNM 516842, 516854, and 516857) confirm details of cranial anatomy of this genus evident from USNM 516843. USNM specimens from Fitterer Ranch (516868–516870) document the previously unknown presence of this species in the Orellan of North Dakota. In addition to fully erupted M1-M3, USNM 516842 shows an erupting P3 and P4 in the process of replacing their deciduous precursors, demonstrating that unlike shrews, *O. altitalonidus* had functional deciduous teeth. As in *O. cameronensis*, P4 erupts prior to P3.

Oligoryctes altitalonidus resembles *O. cameronensis* more than it does any species of *Apternodus*. It shares a zalambdodont dentition with both *Apternodus* and *O. cameronensis*, but lacks the derived shape of the *Apternodus* posterior braincase. *O. altitalonidus* shares with *O. cameronensis* an enlarged foramen ovale, an elongate P3, and multicuspid lower incisors. For these reasons, many previous authors (e.g.,. Emry, 1979; Tabrum et al., 1996; Robinson and Kron, 1998) have referred to this species using the name *Oligoryctes altitalonidus*, a combination that we support.

UNNAMED TAXON FROM TABERNACLE BUTTE AND ELSEWHERE (formerly ''*Eoryctes*'' Romer, 1966 nomen nudum)

TYPE SPECIMEN: To be determined by Bloch et al. (manuscript in progress).

REFERRED MATERIAL: USNM 417465, left maxillary fragment with M1-M3; USNM 417464, distorted left dentary with p3-m3; CM 13627, left dentary with m1-m3, original lost but casts remain (see fig. 47); CM 13859, left dentary with m2; DMNH 8776, right dentary fragment with broken m1, talonid of m2, and partial alveolus for m3; probably also AMNH 55689, edentulous mandibular fragment mentioned by Simpson in McGrew et al. (1959).

TEMPORAL AND GEOGRAPHIC DISTRIBUTION: Bridgerian (early middle Eocene) of eastern Nevada (Elderberry Canyon 14), southwestern Wyoming (Tabernacle Butte 37), northeastern Utah (Powder Wash 31), and Uintan (middle Eocene) of northwestern Colorado (Sand Wash 35).

REMARKS: Among taxa that lack a talonid basin and metacone, the Tabernacle Butte

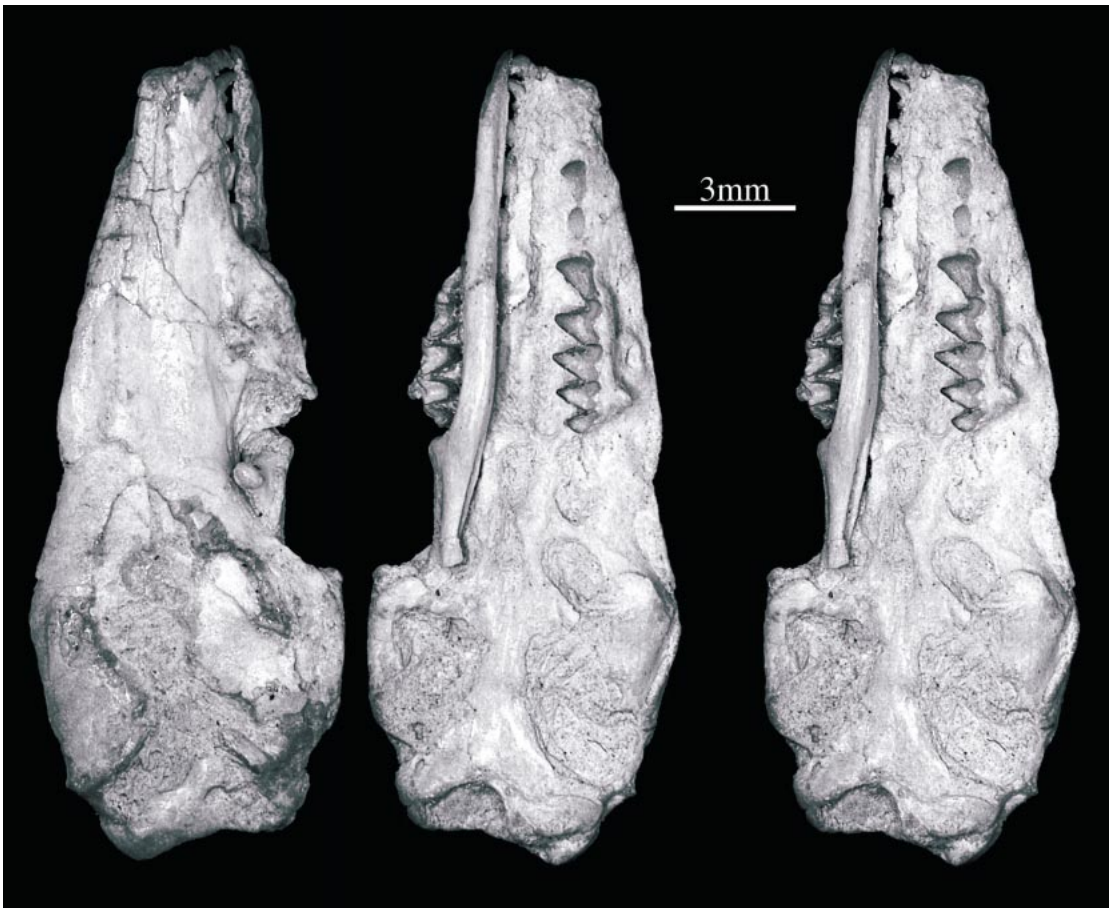

Fig. 45. USNM 516843, *Oligoryctes altitalonidus* skull from Flagstaff Rim, Wyoming. Stereo ventral (right) and dorsal (left) views, (opposite page) anatomical guide to ventral view. See text for abbreviations.

species is unique by virtue of its deep anterior cingulum and large protocones of the upper molars, medially deep but not fully pocketed coronoid process, and extreme small size.

Several authors, including McKenna et al. (1962) and Emry (1990), have acknowledged the presence of this as yet unnamed, diminutive, early-middle Eocene ''apternodontid''. In fact, based on previously circulated, unpublished versions of this paper, Romer (1966) prematurely called this taxon ''*Eoryctes*'', a name now unavailable as it was used by Thewissen and Gingerich (1989) for a genus of palaeoryctid. As of early 2002, J. Bloch et al. have a manuscript in progress that will name this taxon, including additional material from southwestern Wyoming in the University of Michigan collections. We defer to them for nomenclature, but will use available material of this species as an informally named terminal taxon (i.e., ''Tabernacle Butte taxon'') in our phylogenetic analyses.

PARAPTERNODONTIDAE, NEW FAMILY

INCLUDED GENERA: *Parapternodus* Bown and Schankler, 1982; *Koniaryctes* Robinson and Kron, 1998.

TEMPORAL AND GEOGRAPHIC DISTRIBUTION: Wasatchian (early Eocene) of northern Wy-

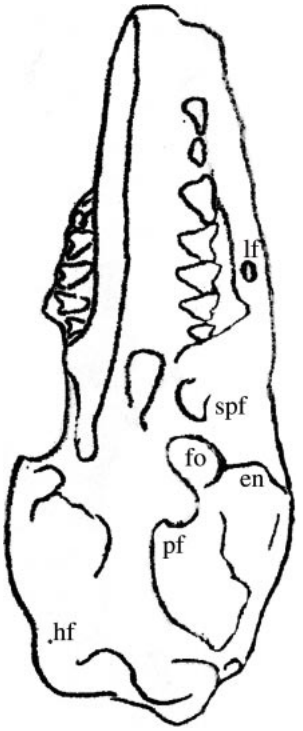

Fig. 45. Continued.

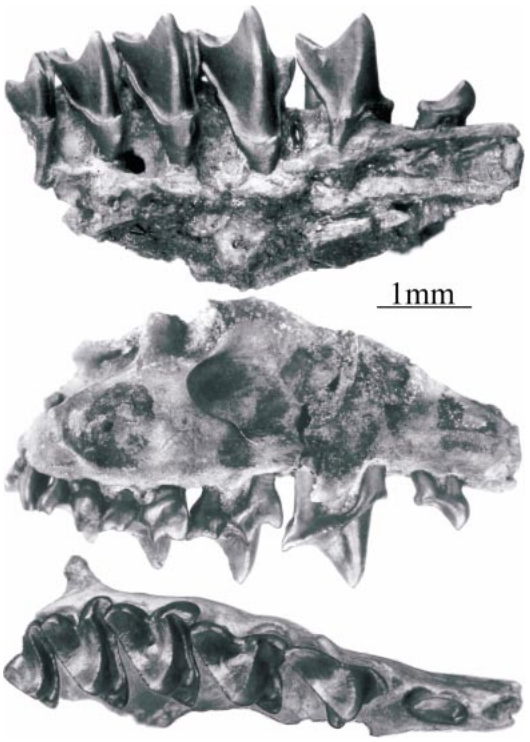

Fig. 46. USNM 22816, *Oligoryctes altitalonidus* maxillary fragment from Pipestone Springs, Montana in lingual (top), lateral (middle), and occlusal (bottom) views. Photos by Chester Tarka.

oming (Clark's Fork, Bighorn, and Powder River basins).

DIAGNOSIS: Known only from fragmentary teeth and jaws, the members of this small, shrew-sized family have zalambdodont molars with a reduced, unbasined talonid and lack buccal cingulids and an m3 posterior cusp. The m3 is anteroposteriorly shorter than m1 or m2. The anterior incisor is enlarged, leaving a large alveolus that extends posteriorly along the base of the jaw at least as far posteriorly as p3 (figs. 48, 49).

Parapternodus Bown and Schankler, 1982

TYPE AND ONLY SPECIES: *P. antiquus*.

DISTRIBUTION AND DIAGNOSIS: As for *P. antiquus*.

Parapternodus antiquus Bown and Schankler, 1982

TYPE SPECIMEN: YPM 31169, left dentary with m2–3.

REFERRED MATERIAL: UMMP 81557, right dentary with p4-m2, m2 trigonid broken; UMMP 81560, right dentary with m2-m3 and base of coronoid process (fig. 48); UMMP 81561, left dentary with a fragmentary incisor root and p4-m3 (fig. 49); UMMP 81558, maxillary fragment with left ?P3; UMMP 81559, left dentary fragment with lower molar; UMMP 81562, maxillary fragment with right upper molar; UMMP 81563, maxillary fragment with left P4 or M1.

TEMPORAL AND GEOGRAPHIC DISTRIBUTION: Wasatchian (early Eocene) of northern Wyoming (Clark's Fork Basin 19).

DIAGNOSIS: The talonids of *Parapternodus* are exceedingly small and form no basin. Anterior to m3, the talonids consist only of a ridge capped by a weak cusp. *Parapternodus* is slightly smaller than *O. cameronensis* (contra Bown and Schankler, 1982) and is similar in size to *O. altitalonidus*. It differs from the latter in having a premolariform p4, an anteroposteriorly short m3 talonid, and mental foramina adjacent to each p4 root. It

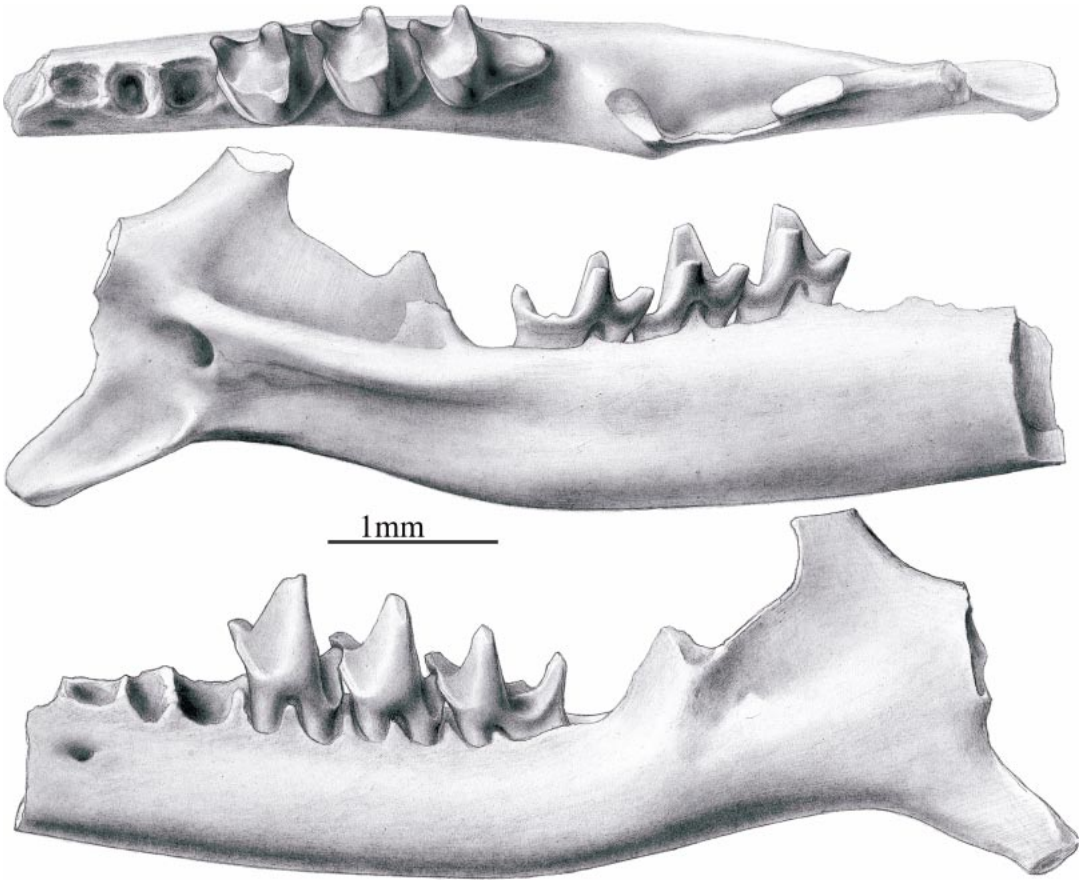

Fig. 47. CM 13627, mandible of the Tabernacle Butte taxon from locality 5 of McGrew et al. (1959) in occlusal (top), lingual (middle), and lateral (bottom) views. Illustrations by Chester Tarka.

also lacks buccal cingulids on its lower molars. UMMP 81561 preserves a fragmentary, enlarged root of an anterior incisor that extends posteriorly at least as far as the region below p3. Although no specimen retains an intact coronoid process, the region immediately posterior to m3 on UMMP 81560 and 81561 is not expanded transversely, indicating that the coronoid process is more gracile than that of *Apternodus*. The base of the coronoid process in UMMP 81650 is excavated deep to the alveolar plane of the dentary, suggesting that like soricids and the larger two species of *Oligoryctes*, *Parapternodus* also possessed a coronoid process that was pocketed medially. Alternatively, this excavation could be a dorsally broken entrance for the inferior alveolar nerve and artery; however, we consider this explanation unlikely because of the considerable dorsoventral size of this space and its anterodorsal proximity to the toothrow (fig. 48).

REMARKS: Perhaps due to the fragmentary type material, Bown and Schankler (1982: 67) used some continuous, unquantified comparisons to define *Parapternodus*, such as ''m2 paracristid and postvallid relatively narrower transversely than in *Oligoryctes* or *Apternodus* . . . '' and ''trigonid less compressed anteroposteriorly than *Oligoryctes*''. These statements cannot be verified based on presently available material. Nevertheless, Bown and Schankler (1982) accurately identified a valid species based on an extremely limited sample, which has improved only slightly since 1982.

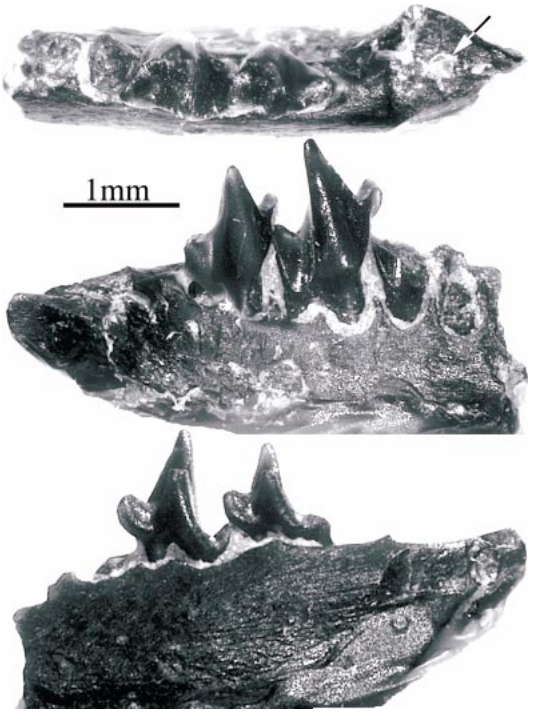

Fig. 48. UM 81560, *Parapternodus antiquus* right mandibular fragment with m2-m3 from the Clark's Fork Basin, Wyoming in occlusal (top), lateral (middle), and lingual (bottom) views. Arrow in dorsal view points into remnant of pocketed coronoid process.

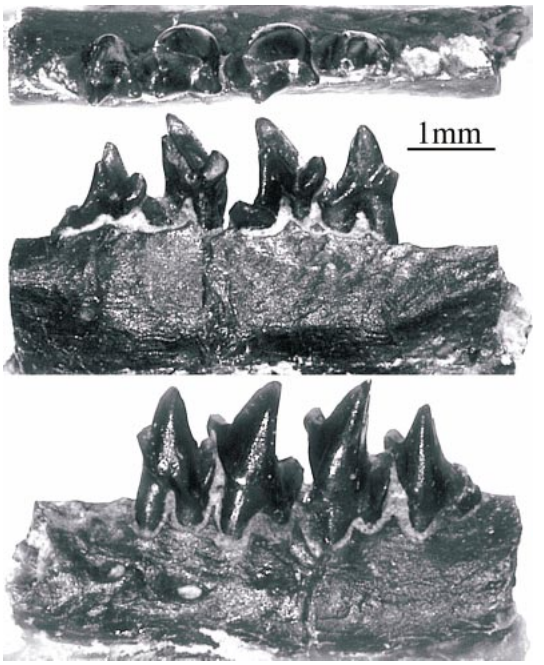

Fig. 49. UM 81561, *Parapternodus antiquus* left mandibular fragment with p4-m3 from the Clark's Fork Basin, Wyoming in occlusal (top), lingual (middle), and lateral (bottom) views.

Koniaryctes Robinson and Kron, 1998

TYPE AND ONLY SPECIES: *Koniaryctes paulus* Robinson and Kron, 1998

DISTRIBUTION AND DIAGNOSIS: As for *K. paulus*.

Koniaryctes paulus Robinson and Kron, 1998

TYPE SPECIMEN: UCM 58291, right dentary fragment with m1-m2.

REFERRED MATERIAL: UCM 59843, right dentary fragment with broken m2, preserving talonid (fig. 50).

TEMPORAL AND GEOGRAPHIC DISTRIBUTION: Wasatchian (early Eocene) of northeastern Wyoming (Powder River Basin 30).

DIAGNOSIS: *Koniaryctes* is slightly larger than *Parapternodus*. As in other zalambdodonts, the talonid is reduced to a crest and has no basin. *K. paulus* lacks buccal cingu-

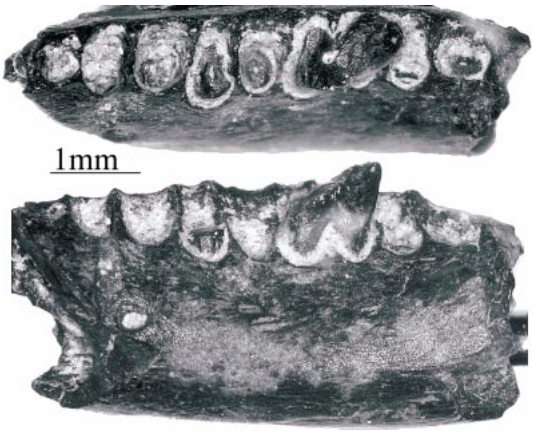

Fig. 50. UCM 59843, *Koniaryctes paulus* left mandibular fragment with broken m2 from the Powder River Basin, Wyoming in lingual (top) and lateral (bottom) views. Note alveolus for enlarged anterior incisor at left and mental foramen inferior to p4 alveolus.

lids and has an anteroposteriorly short m3. In contrast to *Parapternodus*, there is no evidence of a notch below the paraconid into which the talonid rudiment of the anterior tooth would fit. This is consistent with Robinson and Kron's (1998) observation that the talonid cusp is absent throughout the molar toothrow. A second specimen (UCM 59843) preserves an unbasined m2 talonid which lacks a cusp, and is therefore referable to *Koniaryctes*. The rudiment of an enlarged alveolus for an anterior incisor is evident below the p4 alveoli; this specimen also preserves alveoli for m1, m3, the posterior root of p3, and a mental foramen below p4. The dentary lateral to m3 shows a breakage scar that was probably connected to the base of a robust, anteriorly placed coronoid process (fig. 50).

REMARKS: The position of the mental foramen below p4 in UCM 59843 supports the identification of the type specimen (UCM 59821) as m1-m2; the dentary of the latter specimen shows no mental foramina. Without this association, the possibility that the type specimen represents p4-m1, and not m1-m2 as stated by Robinson and Kron (1998), would be difficult to reject. The absence of a talonid cusp and paraconid notch support the status of *Koniaryctes paulus* as a real species, distinct from *Parapternodus antiquus*. Moreover, if UCM 59843 is correctly attributed to it, *Koniaryctes* is further distinguishable from *Parapternodus* (and is similar to *Apternodus*) by virtue of a robust, anteriorly extensive coronoid process. Nevertheless, this sample is even smaller than that of *Parapternodus*, and a definitive evaluation of its validity must await the discovery of better material.

FAMILY UNDETERMINED

Unnamed Paleocene "Silver Coulee apternodontid"

TYPE SPECIMEN: To be determined by C. B. Wood (manuscript in progress).

REFERRED SPECIMENS: YPM PU16520, endocast with partial edentulous skull; YPM PU16521, edentulous skull missing rostrum, basicranium intact (fig. 51).

TEMPORAL AND GEOGRAPHIC DISTRIBUTION: Puercan (early Paleocene) and Tiffanian (late Paleocene) of Park County, northwestern Wyoming (Ft. Union Formation 19).

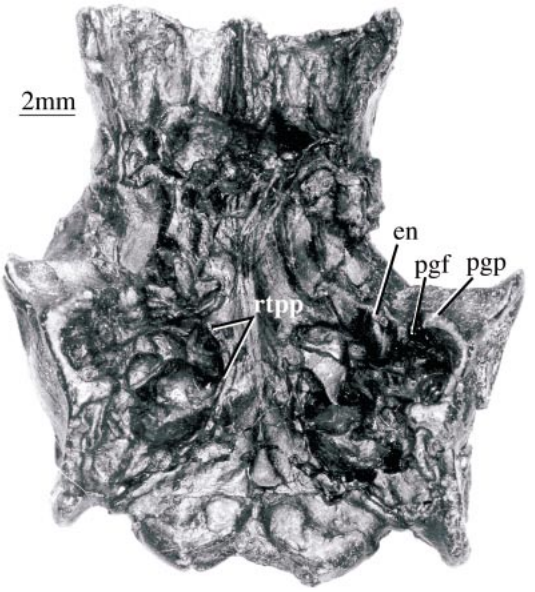

Fig. 51. YPM-PU 16521, ventral view of Silver Coulee skull from Park County, Wyoming. Photo by Chester Tarka.

REMARKS: YPM PU16521 has laterally expansive, boxlike muscle attachments on its posterior braincase, reminiscent of those in *Apternodus*. The same is presumably true for YPM PU16520, although we have not been able to observe this specimen directly. Based on the appearance of the posterior braincase in these specimens, Edinger (1964) and Sloan (1969) suggested that *Apternodus* was present in the Paleocene. Unlike *Apternodus* and *Oligoryctes*, YPM PU16521 has a true postglenoid process supporting the jaw joint posteriorly (fig. 51). As in many placental mammals (e.g., *Leptictis*; see McDowell, 1958: fig. 25), but not most insectivorans, this process is located lateral to the postglenoid foramen and middle ear. An entoglenoid process is present, but does not support the mandibular condyle posteriorly. YPM PU16521 also shows remnants of an ossified auditory bulla, comprised at least in part by the rostral tympanic process of the petrosal and basisphenoid, and possibly also by an entotympanic.

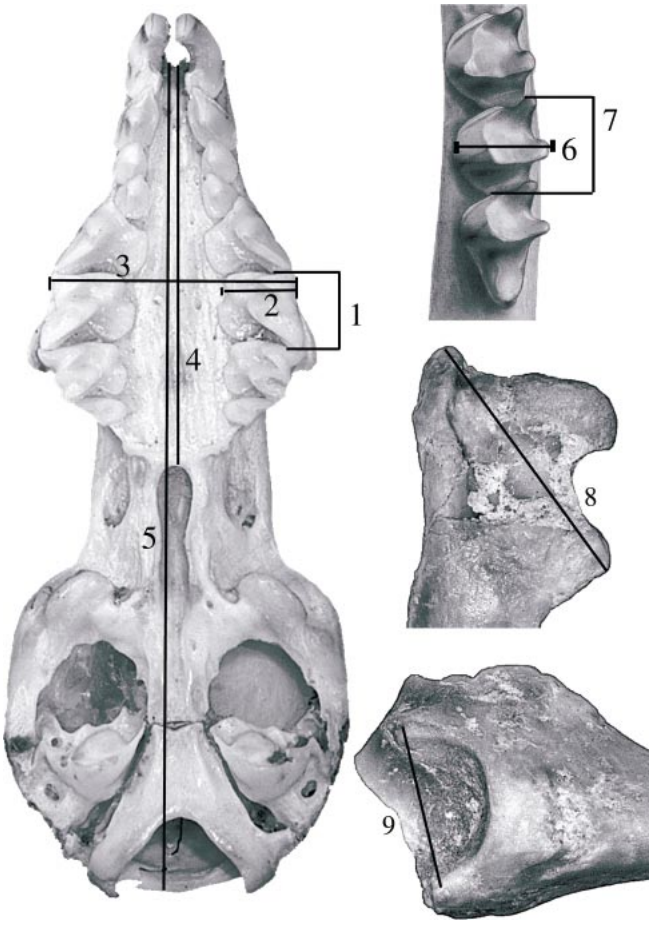

Fig. 52. Illustration of measurements taken in this study, using ventral view of *Crocidura olivieri* skull (left), occlusal view of Tabernacle Butte taxon mandible (top right), posterior view of *Apternodus gregoryi* proximal femur (middle right), and lateral view of *Apternodus gregoryi* os coxae (bottom right). Measurements are as follows: 1 = M1 length, 2 = M1 width, 3 = palatal width, 4 = palate length, 5 = skull length, 6 = m2 width, 7 = m2 length, 8 = intertrochanteric width, 9 = acetabular width.

''Apternodontid'' Material Not Directly Examined in This Study

The descriptions above account for the vast majority of ''apternodontid'' fossils currently known. However, there are several specimens we have not examined, including material reported from California (Novacek, 1976a; Walsh, 1996), Saskatchewan (Storer, 1996), Nebraska (Ostrander, 1987), Mongolia (McKenna and Bell, 1997), and China (Tong, 1997). The fossil ''shrew'' *Cretasorex* (Nessov and Gureyev, 1981) may also be relevant to the fossil history of one or more of the dentally zalambdodont taxa discussed in these pages, but has not been examined during the course of this study. Nor have we been able to directly examine the Paleocene endocast of an ''apternodontid'' (YPM PU16520) referred to by Edinger (1964).

We can only comment on the material of *Iconapternodus* and ?*Apternodus* sp. described by Tong (1997) based on published figures. *Iconapternodus* shows a better defined talonid basin than *Oligoryctes* on at least some of its lower molars, similar in appearance to the small m3 talonid basin in *Solenodon*. The isolated tooth assigned to ?*Ap-*

TABLE 2
Measurements[a]

		Palate		M1		m2				
Taxon	Museum no.	length	width	length	width	length	width	acetab	Skull length	intertr
Blarina	AMNH 135691	7.9	6.4	2.1	2.0	1.7	1.1	1.2	22.1	2.5
Blarina	AMNH 207020	8.3	6.4	1.9	2.0	1.6	1.1	1.3	22	2.5
Blarina	AMNH 207018	8.3	6.1	2.0	1.8	1.6	1.1	1.4	22.5	2.3
Blarina	AMNH 207017	8.2	6.6	2.0	2.1	1.6	1.1	1.3	22.3	2.6
Blarina	AMNH 207019	8.6	6.9	2.1	2.2	1.7	1.2	1.5	22.5	2.9
Crocidura	AMNH 48491	11.9	8.4	2.7	3.0	2.5	1.5	2.2	29.5	3.7
Crocidura	AMNH 48490	11.5	8.4	2.5	2.8	2.1	1.5	2.2	29.5	3.5
Crocidura	AMNH 236229	10.9	8.3	2.5	2.7	2.0	1.4	2.1	27.5	3.4
Crocidura	AMNH 161792	11.2	7.9	2.4	2.4	2.1	1.4			
Crocidura	AMNH 161791	12.0	8.1	2.4	2.6	2.2	1.3			
Crocidura	AMNH 239321							2.2	34.1	4.1
Crocidura	AMNH 239302							2.1	27.8	3.5
Erinaceus	AMNH 42563							6.3	57.7	11.6
Erinaceus	AMNH 3770							6.2	56	10.4
Erinaceus	AMNH 69553								61.5	11.9
Erinaceus	AMNH 41296							6.6	59.4	10.9
Erinaceus	AMNH 10737							6.4	56.9	10.6
Erinaceus	AMNH 200221							6.1	54.8	11
Setifer	AMNH 170547							4.2	46.5	7.7
Setifer	AMNH 170537							3.9	45.2	7.1
Setifer	AMNH 207076							4.3	44.9	8
Setifer	AMNH 170581							4.4	47.4	8.2
Setifer	AMNH 170548							4.5	49.8	9
Setifer	AMNH 207005							4.3	45.3	7.7
Setifer	AMNH 170532							4.2	44.2	7.7
Talpa	AMNH 244225							2.8	36	5.3
Talpa	AMNH 244226							2.5	34.1	4.8
Talpa	AMNH 119495							2.9	35.9	5
Talpa	AMNH 244223							3.1	38.6	6.1
Talpa	AMNH 70784							2.5	33.8	4.9
A. gregoryi	MCZ 17685	19.0	13.1	2.5	3.8	2.2	2.4			
A. gregoryi	UW 13508		12.6	2.8	3.9	2.3	2.2	3.3	44	6.7
A. brevirostris	AMNH 74949	16.7	12.4	2.4	4.5					
A. brevirostris	AMNH 74950		12.2	2.2	3.6					
A. brevirostris	AMNH 74951	17.1	13.4	2.4	4.0	2.1	2.1			
A. brevirostris	AMNH 76692			2.3	3.8					
A. brevirostris	AMNH 74942					2.0	2.1			
A. brevirostris	AMNH 74941	15.6	11.4	2.3	3.7					
A. brevirostris	AMNH 74948	17.1	12.9	2.3	4.2					
A. brevirostris	USNM 437460	17.0	12.7[b]	2.4	3.8	2.1	1.9			
A. mediaevus	AMNH 9601					1.9	2.0			
A. mediaevus	AMNH 97255					1.9	1.8			
A. mediaevus	AMNH 97256					1.7	1.7			
A. mediaevus	AMNH 97258					2.0	1.8			
A. mediaevus	CM 37455					2.6	2.3			
A. mediaevus	CM 71569			2.2	3.4					
A. mediaevus	CM 71570					2.1	2.1			
A. mediaevus[c]	CM 13676		10.0[b]	2.0	2.7					
A. mediaevus	MPUM 0576					2.1	1.9			
A. mediaevus	MPUM 3799		12.1[b]	2.2	3.3					
A. mediaevus	MPUM 6767					1.7	1.9			
A. mediaevus	MPUM 6855			2.3	3.5					

TABLE 2
(Continued)

Taxon	Museum no.	Palate		M1		m2	
		length	width	length	width	length	width
A. mediaevus	MPUM 7820					2.0	2.0
A. mediaevus	USNM 18966					2.0	2.1
A. baladontus	MPUM 2634	16.3	11.4	2.2	3.2	1.7	1.8
A. baladontus	FMNH 1690	17.9	11.6	2.0	3.2	1.8	1.6
A. baladontus	CM 9552					1.9	1.8
A. baladontus	CM 71563					1.8	1.8
A. iliffensis	KU 9112			2.4	3.7	2.1	1.9
A. iliffensis	USNM 455680		10.6[b]	2.2	3.3	2.0	1.8
A. iliffensis	DMNH 1747	15.3	10.4	2.2	3.6		
A. iliffensis	TMM 40492-9		12.2	2.3	3.6		
A. dasophyl	UW 14072	19.8	13.3	2.5	3.4	2.3	2.0
A. major	UW 11046		16.9	2.8	4.6	2.5	2.8
A. major	UW 10981					2.4	2.8
A. major	UW 10984			2.4	3.6		
A. major	UW 11292			3.0	4.4		
A. major	UW 11295						
O. altitalonidus	CM 71571					0.8	0.9
O. altitalonidus	CM 71572					1.0	0.8
O. altitalonidus	CM 71573					0.9	1.0
O. altitalonidus	CM 73976			1.1	1.6		
O. altitalonidus	CM 9620					0.8	0.9
O. altitalonidus	MPUM 0414					1.0	0.9
O. altitalonidus	MPUM 2592					0.9	1.0
O. altitalonidus	MPUM 6797					1.0	0.8
O. altitalonidus	MPUM 6857					1.0	1.0
O. altitalonidus	USNM 22816			1.1	1.8		
O. altitalonidus	USNM 516841					1.0	0.8
O. altitalonidus	USNM 516843	8.3	4.3	1.0	1.4	1.0	1.1
O. altitalonidus	USNM 516847					1.1	0.9
O. altitalonidus	USNM 516848					0.9	0.9
O. altitalonidus	USNM 516850					0.9	0.9
O. altitalonidus	USNM 516854		3.8	0.9	1.3		
O. altitalonidus	USNM 516855		5.1				
O. altitalonidus	USNM 516862			1.1	1.7		
O. altitalonidus	USNM 516863			1.0	1.3		
O. altitalonidus	USNM 516867			1.0	1.4		
O. altitalonidus	USNM 516868					0.9	0.7
O. altitalonidus	USNM 516869					0.9	0.9
O. altitalonidus	YPM PU13774					0.8	0.9
O. cameronensis	MPUM 6677					1.1	1.2
O. cameronensis	MPUM 6859			1.3	1.8		
O. cameronensis	UCM 52446	9.9	7.2	1.4	2.0	1.0	1.1
O. cameronensis	USNM 516840		6.4	1.4	2.0		
O. cameronensis	USNM 516846					1.1	1.2
O. cameronensis	CM 73977					1.2	0.8
O. cameronensis[d]	USNM 19909		6.9	1.3	1.9	1.2	1.2
O. cameronensis[c]	CM17193			6.8	1.4	1.8	
Koniaryctes	UCM 58291					1.2	0.9
Parapternodus	YPM 31169					1.1	0.9
Parapternodus	UM 81561					0.9	0.8
Parapternodus	UM 81560					1.0	0.8
Parapternodus	UM 81557						

TABLE 2
(Continued)

Taxon	Museum number	Palate length	Palate width	M1 length	M1 width	m2 length	m2 width
Taber. Butte	CM 13627					0.7	0.7
Taber. Butte	CM 13859					0.8	0.6
Taber. Butte	USNM 417465			0.9	1.1		
Micropternodus	AMNH 9602					2.0	1.8
Micropternodus	UCMP 60801	13.4	10.5	2.2	2.5	2.3	1.9
Pararyctes	UM 80855	11.6	7.0	1.9	2.1	1.8	1.6
S. paradoxus	MCZ 34825	33.6	23.0	4.1	7.8		
S. paradoxus	MCZ 34833	35.6	24.6	4.7	7.4		
S. paradoxus	MCZ 34832	33.4	21.7	4.8	7.6		
S. paradoxus	MCZ 34836	37.3	23.8	4.3	7.4		
S. paradoxus	MCZ 34859	34.5	23.5	4.6	7.7		
S. paradoxus	MCZ 35312	35.7	21.9	3.9	6.5		
S. paradoxus	MCZ 35311	33.8	24.0	4.2	7.2		
S. paradoxus	USNM 396963	32.3	19.5	4.0	6.0	4.2	3.7
S. paradoxus	USNM 217255	32.8	24.1	4.6	7.9	4.3	4.4
S. paradoxus	USNM 217254	33.5	23.2	4.3	7.0	4.0	4.1
S. paradoxus	USNM 172680	33.1	23.3	4.4	7.4	4.3	4.5
S. paradoxus	USNM 172745	30.8	22.7	4.5	7.6	4.7	4.2
S. paradoxus	BMNH 10.10.15.1	35.4	24.4	4.7	7.6	4.7	4.9
S. cubanus	MCZ 4810	34.9	25.1	4.0	6.8		
S. cubanus	USNM 300634	34.0	21.7	4.1	6.9	3.5	3.8
S. cubanus	USNM 49508	31.7	20.6	3.6	6.2	3.1	3.8
S. cubanus	USNM 2230/139	33.5	20.6	3.7	6.3	3.6	3.6
S. cubanus	USNM 37983	33.3	20.7	3.3	6.4	3.5	3.6
S. cubanus	FMNH 134	34.6	21.7	3.4	6.6	3.4	3.5
Setifer	AMNH 170612	21.4	15.2	2.0	4.1	2.6	2.6
Setifer	AMNH 170534	20.7	16.0	2.0	4.6	2.3	2.8
Setifer	AMNH 170533	21.5	14.0	1.8	4.4	2.1	2.7
Setifer	AMNH 100750	23.6	16.1	2.6	4.7	2.8	2.6
Setifer	AMNH 170583	20.7	14.4	2.3	4.6	2.5	2.5
Setifer[e]	AMNH 100749	26.6	19.4	2.8	6.2	2.5	2.5
Elephantulus	AMNH 85580	18.0	11.6	2.4	2.4	2.3	1.5
Elephantulus	AMNH 85581	16.0	10.9	2.1	2.3	2.2	1.5
Elephantulus	AMNH 81473	16.3	11.4	2.5	2.3	2.3	1.3
Elephantulus	AMNH 81474	16.5	11.7	2.2	2.2	2.2	1.4
Macroscelides	AMNH 167993	14.8	11.8	2.3	2.2	2.0	1.4
Macroscelides	AMNH 167994	14.8	12.3	2.4	2.3	2.1	1.5
Macroscelides	AMNH 167995	15.7	12.0	2.3	2.2	2.1	1.4

[a] All measurements are in millimeters and are displayed graphically in figure 52. See text for institutional abbreviations. Acetab indicates acetabular width and intertr indicates intertrochanteric width.

[b] Palatal width estimated.

[c] From photo.

[d] From figure.

[e] Teeth worn to stubs.

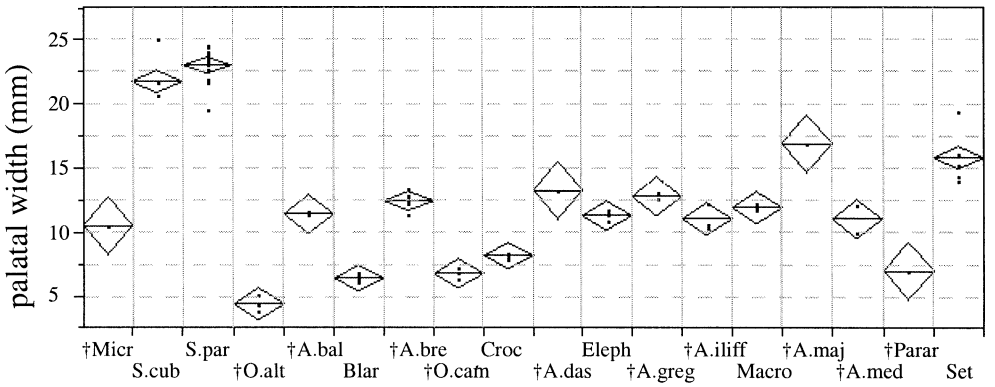

Fig. 53. Palatal width in millimeters across selected taxa. See figure 20 for taxonomic abbreviations and figure 52 for measurements taken. Dots indicate individual specimens measured. Crosses denote extinct taxa. Diamonds indicate 95% confidence intervals of the mean; nonoverlapping diamonds indicate a significant difference at alpha = 0.05, assuming normality.

ternodus sp. (Tong, 1997: fig. 11) lacks a talonid basin, and at less than 1 mm in mesiodistal length is close in size to *O. altitalonidus* and considerably smaller than any North American *Apternodus*. If this specimen really is *Apternodus*, it would be among its oldest representatives, possibly older in age than material from Badwater locality 20, Wyoming (Krishtalka and Setoguchi, 1977).

METRIC COMPARISONS

Species Diversity

Anatomical uniqueness, as expressed through combinations of discrete character states, is the prime vehicle used here to identify terminal taxa. Nevertheless, metric comparison of fossil groups to living ones comprises a useful tool in understanding species diversity, assuming that the biological unit of ''species'' has not changed qualitatively through time. Our null expectation is that morphological diversity in a single fossil species does not greatly exceed that of an ecologically similar living one (Cope, 1991 and references therein). However, this assumption must be tempered by the reality that unlike modern biological populations, fossil assemblages may sample a large span of geologic time. A single fossil locality may contain individuals separated by thousands of generations; such an interval may be accompanied by some level of metric change. Therefore, if metric variation is observed to be greater within a given fossil species than in one that is living, the hypodigm of that species may sample individuals at disparate ends of an evolving lineage (sensu Gingerich, 1976; but see Lillegraven et al., 1981). This is of course in addition to the possibility that multiple species have been conflated within a single taxon, or that males and females of the extinct species are sexually dimorphic (Plavcan, 1991).

Detailed exploration of the links between metric variation and specific integrity has been discussed elsewhere (e.g., Simpson, 1947; Simpson et al., 1960; Kimbel and Martin, 1991) and is beyond the scope of this paper. For the remainder of this section we concern ourselves only with presenting metric data for the species groups defined above and noting where variation occurs.

Measurements were taken using digital calipers to the nearest 0.1 mm and are depicted graphically in figure 52. Measurements of very small taxa (i.e., *O. altitalonidus* and the Tabernacle Butte taxon) were confirmed using digital photography and public domain NIH Image software (developed at the U.S. National Institutes of Health and available on the Internet at http://rsb.info.nih.gov/nih-image/). Raw measurements and specimen numbers are provided in table 2.

As shown in figures 53 and 54, the distribution of palatal width and approximate m2

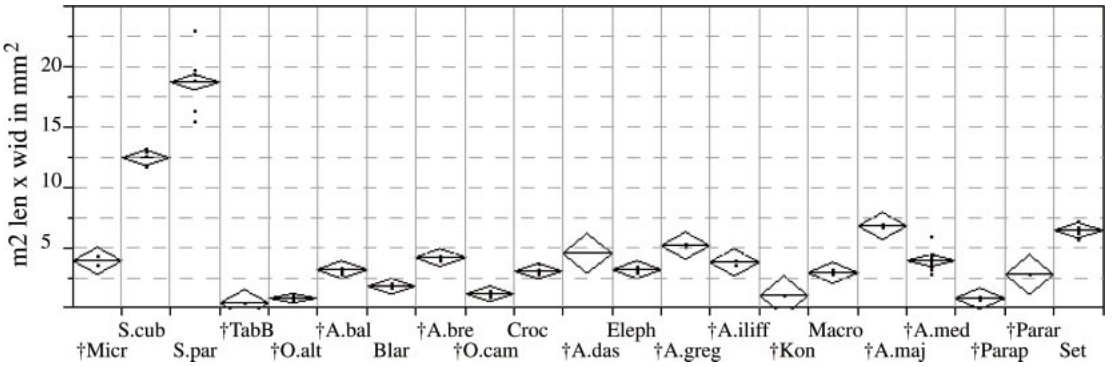

Fig. 54. Estimated m2 area (m2 length × m2 width) in square millimeters across selected taxa. See figure 20 for taxonomic abbreviations and figure 52 for measurements taken. Dots indicate individual specimens measured. Crosses denote extinct taxa. Diamonds indicate 95% confidence intervals of the mean; nonoverlapping diamonds indicate a significant difference at alpha = 0.05, assuming normality.

area (respectively) in the fossil taxa are comparable to that observed in living taxa. In fact, the most variable taxon in absolute terms for both characters is the extant *Solenodon paradoxus*. However, when the standard deviations of these characters are expressed as coefficients of variation, some fossil taxa exceed the variability seen in living ones (fig. 55). Specifically, the m2 area coefficient of variation for *A. mediaevus* (21.5), *O. cameronensis* (16.6), and *P. antiquus* (16.1) are all greater than those of any living species. The latter two taxa have samples of just five and three specimens, respectively; but *A. mediaevus* is represented by 10 individuals. Its high coefficient of variation is due primarily to the large size of CM 37455 from Canyon Ferry, Montana, included in *A. mediaevus* for anatomical reasons previously enumerated. When this specimen is eliminated from the sample, the m2 area coefficient of variation for *A. mediaevus* falls from 21.5 to 13.4, below that seen in *Solenodon paradoxus* (14.1).

In terms of palatal width, the greatest coefficients of variation are again seen among the fossils (14.9 and 13.4 for *O. altitalonidus* and *A. mediaevus*, respectively). However, these do not greatly exceed the coefficient of variation for palatal width seen in a sample of extant *Setifer setosus* (12.2). They are also based on very small samples (three individ-

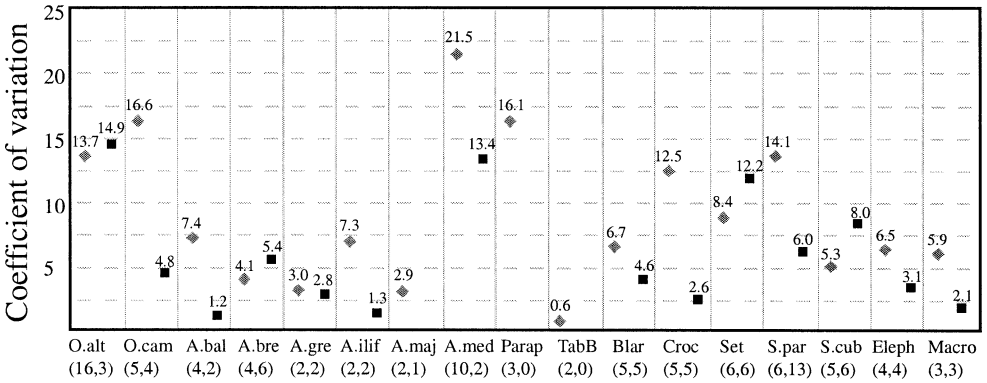

Fig. 55. Coefficients of variation ((st dev * 100) / mean) for approximate area of lower m2 (diamonds) and palatal width (squares) across examined taxa. See figure 20 for taxonomic abbreviations. Sample sizes used to generate each coefficient of variation are listed in parentheses (m2 area, palatal width) below each taxon.

TABLE 3
Diagnostic *Apternodus brevirostris* Specimens from Flagstaff Rim[a]

Specimen no.	Field notes	Stratigraphic level[a]	Material
AMNH 74949	35 ft below ash D	250	rostrum
AMNH 74951	30 ft below ash D	255	partial skull
USNM 437460	20 ft below ash D	265	rostrum
AMNH 74948	375 ft above base	375	rostrum
AMNH 76692	30 ft below ash G	405	maxilla
AMNH 74950	25 ft below ash G	410	half rostrum
AMNH 74941	20 ft below ash G	415	skull

[a] From Emry, 1973: 29.

uals for *O. altitalonidus* and two for *A. mediaevus*). Small sample sizes tend to underestimate coefficients of variation (Sokal and Braumann, 1980); however, the largest possible estimates of the coefficient of variation come from small samples (Cope, 1991). For this reason, and as recommended by Cope (1991: 233), the correction factor for calculating the coefficient of variation from small samples suggested by Sokal and Rohlf (1995: 58) was not used.

Of perhaps greater interest than the extremes are the several cases in which coefficients of variation of fossil taxa are similar to or smaller than those of modern species (fig. 55). This is the case for the m2 area coefficient of variation for *O. altitalonidus*, *A. baladontus*, *A. brevirostris*, *A. gregoryi*, *A. iliffensis*, *A. major*, and the Tabernacle Butte taxon; it also applies to the palatal width coefficient of variation for *O. cameronensis*, *A. baladontus*, *A. brevirostris*, *A. gregoryi*, and *A. iliffensis*. The recovery of more material, and the consequent increase in sample size, will test the hypothesis that these extinct species fall within the range of variation observed within ecologically similar living species.

Stratigraphic Change in *Apternodus brevirostris*

The number of *Apternodus* specimens from the stratigraphically controlled Flagstaff Rim section (Emry, 1973) is small, but permits a brief examination of morphological change through time. The only *Apternodus* species unquestionably present in this area is *A. brevirostris*, although there are several less diagnostic specimens (e.g., AMNH 74940) that may be referable to other taxa, and the nearby Harshman Quarry has yielded the type of *A. dasophylakas*. Nevertheless, there are seven measurable specimens referable to *A. brevirostris* known from several points in the section described by Emry (1973) and summarized in table 3.

Plots of M1 area and palatal width relative to stratigraphic position (fig. 56) indicate that at the highest levels of their range, specimens are smaller. More precisely, as measured by M1 area and palatal width, the largest and smallest specimens of *A. brevirostris* from Flagstaff Rim have been found at, respectively, the lowest (250 ft.) and highest (410–415 ft.) stratigraphic points in their range. The Pearson correlation coefficient (Sokal and Rohlf, 1995: 559) of M1 area to stratigraphic level is -0.74, with a probability of 0.056 (assuming normality) that the correlation is due to chance. The correlation of palatal width to stratigraphic level is -0.63, also suggestive but statistically insigificant with a *p*-value of 0.18. In both cases the sample size is small, with seven measurable specimens for M1 area and six for palatal width.

Unfortunately, there is a lack of diagnostic, measurable material in the 265 to 375 ft. interval in the Flagstaff Rim section. Moreover, USNM 437460 (found 265 ft. above the base) is slightly smaller than AMNH 74948 (found 375 ft. above the base), suggesting that size is not inversely correlated with stratigraphic height in the middle part of the section. Hence, at present we limit our conclusions to the observation that the oldest specimens of *A. brevirostris* from Flagstaff

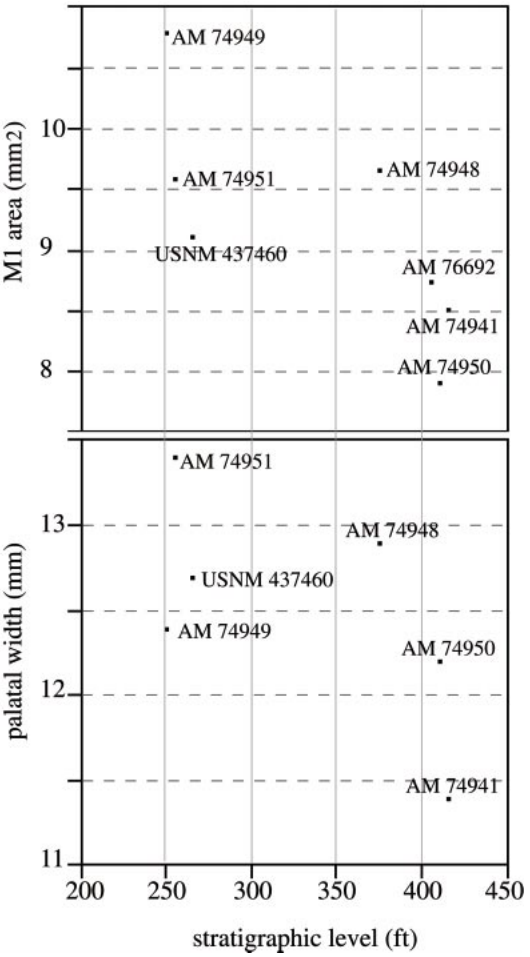

Fig. 56. Approximate M1 area (top) and palatal width (bottom) of *Apternodus brevirostris* specimens from Flagstaff Rim plotted by stratigraphic level, following Emry (1973).

Rim are slightly larger that the youngest. More fossils from the middle part of the section are necessary to infer the extent to which size change at Flagstaff Rim could be characterized as a trend, gradual or otherwise.

METHODS

Character Matrix

In order to phylogenetically analyze the terminal taxa defined above, it is necessary to have a database of heritable information. In the present study, this database is composed of 264 character states distributed in 118 morphological characters across 30 taxa. Many papers have been written on how to distill morphological information into formats appropriate for phylogenetic algorithms (e.g., Pogue and Mickevitch, 1990; Platnick et al., 1991; Lipscomb, 1992; Maddison, 1993; Simmons, 1993; Hawkins et al., 1997; Lee and Bryant, 1999; Strong and Lipscomb, 1999). As outlined by Asher (2000, 2001), we attempt to maximize the testability of primary hypotheses of homology by favoring binary characters (Pleijel, 1995), but recognize that multistate characters are better suited to deal with issues of redundancy (Strong and Lipscomb, 1999) and counterintuitive optimizations at ancestral nodes (Platnick et al., 1991). We further recognize that no single method is capable of escaping both of these pitfalls consistently (Strong and Lipscomb, 1999).

Following Lipscomb (1992), hypotheses of character order should be tested in a similar manner as hypotheses of character homology. That is, initial or ''primary'' hypotheses of order within a multistate character, as for primary homology across different characters, should be tested iteratively by the distribution of other such hypotheses. Those hypotheses of order that are optimized consistently on parsimonious cladograms, i.e., that show transformations only between adjacent states or (to use the terminology of Lipscomb, 1992) lack ''hierarchical discordance'', are considered to be robust and are retained for use in further analyses. Hypotheses of order that are not optimized consistently, i.e., that show multiple state changes within a single branch, are discarded. Multistate characters that comprise a morphocline based on the criterion of similarity (Pogue and Mickevitch, 1990; Lipscomb, 1992), upon which primary hypotheses of order are postulated, are so designated in the descriptions below.

In addition to new observations of morphological variability, the characters described below derive from the work of many other authors, including Novacek (1986: 82–89), MacPhee et al. (1988: 25–27), Frost et al. (1991: 3–15), and MacPhee (1994: 163–179). References to these papers are given below using the acronyms N86, M88, F91, and M94, respectively, preceding the character number used in that study. Citations of

other authors are also given where appropriate. Many of these characters were used by Asher (1999, 2000) and have been updated for the present data set.

For characters pertaining to tooth-position homology, we use dental formulae given by Starck (1995), supplemented by more detailed studies (e.g., Kindahl, 1959a, 1959b) where available. Due in part to their lack of functional deciduous teeth, dental homologies in soricids are unclear (Dannelid, 1998). Based on growth series of *Crocidura*, *Neomys*, and *Sorex*, Ärnbäck-Christie-Linde (1912) suggested that the anterior lower incisor in shrews was i4, and that the canine, p2, and p3 were missing in the adult dentition. This formula has not generally been followed by subsequent authors. More recently, Kindahl (1959a) argued that the dental formula for *Suncus* is 3.1.2.3/2.0.1.3 and that of *Sorex* 3.1.3.3/2.0.1.3, with the same upper (I1-I3) and anterior lower (i1) incisors as those of other placental mammals. The histological criteria upon which she based her conclusions are consistent with those of Luckett (1993), although there is some question about the identity of I3 and P2, which may actually be homologous with dI3 and dP2 in other eutherians (W. P. Luckett, personal commun.).

Resolution of soricid dental homologies is beyond the scope of this paper. For the present, we note that recent authors (e.g., Kindahl, 1959a; Shigehara, 1980) support the presence of I1-I3, C, and P4-M3 in the upper dentition, and i1 and p4-m3 in the lower. We follow these authors in using an upper dental formula of 3.1.4.3 in *Blarina* and 3.1.1.3 in *Crocidura*, and in assuming the homology of i1 and p4-m3 of shrews with those of other taxa examined in this study. Hence, characters pertaining to tooth positions between (but not including) p4 and i1 are coded as missing in shrews (i.e., nos. 75, 78–81). In the case of the fossil soricid *Domnina*, which has six upper and five lower teeth anterior to M1/m1, we assume only the homology of P3-M3/p4-m3 and I1/i1, and leave several characters pertaining to anterior premolars, canines, and posterior incisors (i.e., nos. 51, 52, 54, 55, 57, 58, 75), as well as character no. 49 (presence of functional deciduous teeth) as ''missing'' in *Domnina*. In certain cases, we have semantically avoided the problem of homology by not specifying tooth position in a given character. For example, we use presence/absence of ''antemolar diastemata'' (character no. 56) to represent the fact that regardless of tooth number, shrews (and certain other taxa) have a tightly packed row of upper teeth between P4 and I1, in contrast to the more widely spaced antemolars seen in *Didelphis*, *Echinosorex*, and other taxa.

For more general dental terminology, we follow Patterson (1956), Van Valen (1966), and Szalay (1969), as discussed in the previous section on zalambdodonty. For cranial terminology, we follow McDowell (1958), MacPhee (1981, 1994), and Novacek (1986); for postcranial terminology, we follow MacPhee (1994). Wible et al. (2001) and Asher (2001) summarize variation in the use of cranial anatomical terms.

The following characters are numbered consecutively and correspond to the matrix presented in table 4. A one-line summary of these characters is presented in table 5. This data set is available in NEXUS and NONA formats on the internet at ftp.amnh.org/pub/people/asher. Polarity is determined *a posteriori* by rooting phylogenetic trees (Farris, 1982; Nixon and Carpenter, 1993). Hence, a ''0'' character state in the following descriptions has no necessary association with primitiveness.

Tympanic Region

1. Tympanic process of basisphenoid (N86: no. 49; M88: no. 3). The basisphenoid is typically flat medial and anterior to the middle ear (e.g., *Apternodus*, state 0; fig. 11D). Alternatively, it may contribute to the anterior wall of the ossified auditory bulla (e.g., *Microgale*, state 1).

2. Piriform fenestra (M88: no. 9). This character is present when the petrosal, alisphenoid, and/or squamosal fail to ossify anterior to the promontory in the roof of the middle ear in an adult (e.g., *A. baladontus*, state 1; see fig. 11D). Other taxa have a solid tympanic roof anterior to the middle ear promontory (e.g., *Erinaceus*, state 0), or have an anteriorly extensive fenestra, extending forward to the entoglenoid process (e.g.,

TABLE 4
Character-Taxon Matrix[a]

Character number:	1	11	21	31	41	51
Taxon	|	|	|	|	|	|
Didelphis	00-1000000	0000-00000	110-112031	1010000000	0010000001	2100001000
A. mediaevus	0A00010?0	0001100011	1110011100	0111101100	0001111000	0111D02010
A. gregoryi	01000000?0	1001100011	1110011100	011111?100	00011010?0	0100101010
A. brevirostris	0A00000000	0001100011	1110011100	011110?100	00011110?0	0100111110
A. iliffensis	01000000?0	0001100001	111001110A	011110?100	00011110?0	010010111A
A. dasophylakas	01000000?0	000??00011	111001?100	?1111??100	00011110?0	0100101111
A. major	01100100?0	0101100011	111101?100	011111?100	00001010?0	0100111010
A. baladontus	01000100?0	0101100001	1110011100	0111101100	0001111000	011120F010
O. altitalonidus	021????0??	00?0?01001	??0-10???0	?10110?100	0011110001	1100111111
O. cameronensis	02101100?0	0010?01001	0-0-101010	0101101100	0001110101	1100111111
Taber. Butte	??????????	??????????	??????????	??????????	????1?????	??????????
Parapternodus	??????????	??????????	??????????	??????????	??????????	????????1?
Koniaryctes	??????????	??????????	??????????	??????????	??????????	??????????
Micropternodus	??????????	??????????	?????0????	???????10?	00210?0000	1100010100
Silvercoulee	10-?12000?	0001100?0?	1?1011?0??	?00????101	??????????	??????????
Pararyctes	10-?120?01	00?1?0??0?	??0-?0????	?00000?00?	0?10000000	??001?1100
Eoryctes	10-??21?01	00?1100?00	??10001020	?0000??10?	??1?0001??	11??????00
Nesophontes	0210100000	0001100001	0-0-101020	110010?100	0011120001	1100101100
Centetodon	02??110000	0001100?01	0-0-10101?	?110101000	0000110000	1000101110
Echinosorex	10-0010100	0001000100	120-011010	1000001001	0110010000	1000100100
Erinaceus	10-0010100	00AA010000	120-001010	1001001001	0100000000	1100100100
Microgale	1101110000	0011100001	0-0-101010	1101001100	1020020001	1100101001
Setifer	10-1000000	101111000A	100-001100	1101001100	10A0020000	0100101011
S. paradoxus	0210110000	0001100000	110-111020	1101101100	0000120100	1100111000
S. cubanus	0210100000	0001100001	0-0-111010	1101101100	0000120100	1101101010
Crocidura	0210110000	0000-00001	0-0-201100	010100?100	0011110A10	120001----
Blarina	0210110000	0000-00000	0-0-201000	010100?11-	0011000110	1100010100
Domnina	0???0000??	??00-00??1	??0-?010??	?1?100?11-	00111001?0	??0??1??00
Elephantulus	00-0121111	001A000111	0-0-000011	1000010001	0100021001	1000102010
Macroscelides	10-1121111	1010-00110	0-0-000011	1000010001	0100021001	1000112010

Crocidura, state 2; see fig. 52). These character states comprise a potentially ordered morphocline.

3. Anterior carotid foramen. In those taxa that possess a piriform fenestra, the internal carotid may enter the cranial cavity via a distinct anterior carotid foramen located medial to the piriform fenestra (e.g., *A. baladontus*; state 0; see fig. 11D). Alternatively, a distinct foramen may be absent and the artery may enter the braincase via the piriform fenestra (e.g., *Crocidura*, state 1; see fig. 52).

4. Vidian foramen. Whether or not the tympanic roof shows a distinct anterior carotid foramen for the internal carotid artery, it may be perforated anteromedially by a small vidian branch of the internal carotid (e.g., *A. baladontus*, state 0; see fig. 11D). *Setifer*, on the other hand, lacks distinct vidian foramina (state 1).

5. Caudal tympanic process of the petrosal (N86: no. 55; M88: no. 2). This outgrowth from the posterior part of the petrosal may be absent or cover only the fenestra cochleae ventrally (e.g., *A. baladontus*, state 0; see fig. 11D), or it may be larger and shield the fenestra cochleae and the entrance of the internal carotid artery as it enters the middle ear, contributing to the posterior wall of the ossified auditory bulla (e.g., *Crocidura*, state 1; see fig. 52).

6. Rostral tympanic process of petrosal (M88: no. 1). A prominent ridge may extend along the medial aspect of the petrosal, adjacent to the petrosal-basisphenoid suture (e.g., *O. cameronensis*, state 0; see fig. 40).

TABLE 4
(Continued)

Character number: Taxon	61	71	81	91	101	111
Didelphis	?001010100	1001100001	1?00010110	0H10000010	0000100100	001110A3
A. mediaevus	0201111100	1100001101	1111110110	11101111??	???010?0??	?????0?1
A. gregoryi	1211011100	1100001100	0111110110	11100011??	????????0?	?0111??1
A. brevirostris	A201011100	1100A01101	0111110110	11100111??	????10????	????????1
A. iliffensis	0211011101	1?????????	?111110110	1?10?111??	??????????	????????1
A. dasophylakas	0211011100	1100101101	0111110110	101011110?	??????????	?????0?1
A. major	1211011100	1100001101	A111110110	11101111??	???01000??	????????2
A. baladontus	0201111100	1100101100	1111A10110	11100111??	??????????	????????1
O. altitalonidus	1201011100	1021101111	0110110200	1A101021??	??????????	????????0
O. cameronensis	1201011100	1121101111	1111110200	1A101021??	??????????	????????0
Taber Butte	?201?01100	1????????11	1110110200	11???011??	??????????	????????0
Parapternodus	?201?111??	???0??????	?011010020	?D???02???	??????????	????????0
Koniaryctes	??????????	???0??????	??1?01102?	?2???1????	??????????	????????0
Micropternodus	0000010000	01?11??001	11000A1110	0110?011??	??????????	????????1
Silvercoulee	??????????	??????????	??????????	??????????	??????????	????????1
Pararyctes	1100011000	1101210100	1000110110	1E100000??	??????????	????????0
Eoryctes	1101?11100	1????????01	100?010???	??????????	??????????	????????0
Nesophontes	1001011100	1111100001	1000111110	1B100001?1	0010110101	00000A?1
Centetodon	1000011100	1011100011	1101011110	1A1000001?	?00???????	?????1?0
Echinosorex	0000010000	0011100100	0101111221	0210000102	1100110011	100001A2
Erinaceus	0000010001	03101011--	-101111021	1D10000012	0000010001	10000102
Microgale	1201010100	1111101011	1110110200	1E10000101	0000110101	10000110
Setifer	0211010000	1211100011	1111110120	1C00000011	00001A0101	10011012
S. paradoxus	0200011100	1101211000	1111000100	0G10000111	0000100101	10000003
S. cubanus	0200111100	1101211000	1111000100	0A10000111	00001A0101	10000003
Crocidura	1000010A01	1400?01???	?001111120	1311002101	1111100011	11011110
Blarina	1000010101	1400?01???	?001111120	1311002100	1111100011	11011110
Domnina	1000010001	1310?01???	?001111120	13110011??	??????????	????????0
Elephantulus	000001001-	-011100011	110-011121	0200000011	0100011-10	000A0101
Macroscelides	000001001-	-011100011	010-011---	0200000011	0100011-10	00010101

[a] Character numbers correspond to those in the text. Inapplicable entries are marked with a dash, missing data with a question mark (both are treated as missing by parsimony algorithms). Polymorphic characters are represented as follows: (01) = A, (02) = B, (03) = C, (12) = D, (13) = E, (23) = F, (012) = G, (023) = H.

In other taxa, the basicranium on either side of the petrosal-basisphenoid suture is flat (e.g., *Setifer*, state 1). In elephant shrews and palaeoryctids, the medial wall of the auditory bulla is composed of an expanded rostral process of the petrosal (state 2). These character states comprise a potentially ordered morphocline.

7. Petrosal auditory tubes. Proximal branches of the stapedial and internal carotid arteries typically traverse the middle ear without passing through elongate, ossified canals of the petrosal (e.g., *Solenodon*, state 0). In elephant shrews, one or more of these arteries is enclosed within a bony tube (state 1).

8. Tubal canal (M88: no. 4). In most examined taxa, the auditory tube exits the anterior part of the middle ear through a sulcus defined by the alisphenoid dorsally and basisphenoid medially (e.g., *Microgale*, state 0). Other taxa have a foramen completely enclosed by the alisphenoid dorsally and basisphenoid ventrally, through which passes the auditory tube (e.g., *Echinosorex*, state 1).

9. Ectotympanic expansion. Most taxa possess a simple, ring-shaped ectotympanic (e.g., *Microgale*, state 0). In others, this element is mediolaterally expanded so as to contribute significantly to at least the lateral part of the bony auditory bulla (e.g., *Elephantulus*, state 1).

TABLE 5
Summary of Characters and States[a]

Characters	Character states
1 tympanic process basisphenoid	**0** reduced **1** present
2 piriform fenestra	**0** absent **1** anterior petrosal **2** jawjoint
3 anterior carotid foramen	**0** separate **1** piriform fenestra
4 vidian foramen	**0** antmedial basisphenoid **1** absent
5 caudal tympanic process petrosal	**0** reduced **1** shields posterior bulla
6 rostral tympanic process petrosal	**0** flat **1** medial ridge **2** medial wall
7 petrosal arterial tubes	**0** absent **1** present
8 tubal canal	**0** not closed by sphenoid **1** closed by sphenoid
9 ectotympanic	**0** simple **1** expanded
10 entotympanic	**0** absent **1** present
11 EAM (external auditory meatus) angle	**0** ≥ 90 **1** < 90
12 EAM torus	**0** flat **1** present
13 alisphenoid foramen for inferior stapedial ramus	**0** absent **1** present
14 alisphenoid canal presence	**0** absent **1** present
15 alisphenoid canal position	**0** lateral sphenorb fissure **1** continuous sphenorb fissure
16 basisphenoid pit	**0** absent **1** present
17 foramen ovale size	**0** similar jugular foramen **1** larger jugular foramen
18 suboptic foramen	**0** absent **1** present
19 inferior petromastoid	**0** near glenoid **1** below glenoid
20 petromastoid position	**0** exposed posteriorly **1** exposed laterally
21 post EAM tuber presence	**0** reduced **1** prominent
22 post EAM tuber composition	**0** squamosal **1** squamosal-petromastoid **2** petromastoid
23 postlateral braincase	**0** gracile **1** lambdoid plate
24 anterior lambdoid plate	**0** straight **1** lateral flare
25 squamosal tubercle jaw distance	**0** short **1** intermediate **2** elongate
26 sagittal crest	**0** reduced **1** large
27 optic foramen-size	**0** caliber as trigeminal exit foramina **1** smaller **2** absent
28 ethmoid foramina	**0** separate sphenorb fissure **1** within sphenorb fissure
29 sinus canal opening	**0** confluent sphenorb fissure **1** in between sphenorb fissure and ethmoid foramen **2** confluent ethmoid foramen **3** absent
30 posterior sinus canal foramen	**0** present **1** absent
31 anterior sinus canal foramen	**0** present **1** absent
32 entoglenoid process	**0** no jaw support **1** jaw support
33 entoglenoid shape	**0** solid **1** posteriorly concave
34 lacrimal foramen opening	**0** open posterior **1** open lateral
35 lacrimal foramen size	**0** similar sphenopalatine foramen **1** larger
36 posterior lacrimal border	**0** separate orbit **1** flush orbit
37 orbital wing maxilla	**0** reduced **1** present
38 zygomatic arch	**0** complete **1** incomplete
39 ventral ectopterygoid	**0** narrow **1** flat
40 dual ectopterygoid	**0** no **1** yes
41 maxilla on pterygoid	**0** no **1** yes
42 postpalatine spine	**0** reduced **1** present
43 origin maxillary zygoma	**0** M1 **1** M2 **2** M3
44 size maxillary zygoma	**0** posterolateral projection **1** reduced
45 maxilla at M1-3	**0** straight **1** convex

TABLE 5
(Continued)

Characters	Character states
46 length of infraorbital canal	**0** 2× **1** 1× **2** < anterior infraorbital foramen
47 anterior infraorbital canal	**0** flat **1** anteriorly concave
48 posterior nasal foramina	**0** absent **1** present
49 calcified deciduous teeth	**0** present **1** absent
50 upper anterior dentition	**0** anterior incisor large **1** incisors similar
51 upper incisors	**0** two **1** three **2** five
52 upper antemolars (excluding incisors)	**0** five antemolars **1** four am **2** two am
53 posterior incisor crowns	**0** trenchant **1** bulbous
54 canine crown	**0** premolariform **1** bulbous
55 upper C roots	**0** one **1** two **2** three
56 antemolar diast	**0** present **1** absent
57 antemol(P2) roots	**0** one **1** two **2** three **3** four
58 P2 length	**0** similar molariform **1** smaller molariform
59 molariform P3	**0** no **1** yes
60 P3 length	**0** ≤ P4 **1** longer than P4
61 P4 parastyle	**0** weak **1** prominent
62 metacone	**0** present **1** connate w paracone **2** absent
63 protocone	**0** present **1** reduced
64 hypocone	**0** present **1** reduced
65 M1-3 size	**0** larger than antemolar **1** ≤ antemolar
66 M1-2 anterior cingulum	**0** deep **1** narrow-red
67 M1 parastyle	**0** flush **1** anterior projection
68 M2 centrobuccal cleft	**0** absent **1** present
69 upper M3 presence	**0** present **1** absent
70 upper M3 width	**0** > 70% M2 **1** reduced
71 upper M3-stylar shelf	**0** short **1** long
72 lower antemolars	**0** 8 antemolars **1** 7 am **2** 6 am **3** 5 am **4** 3 am
73 incisor cusps	**0** single **1** dual **2** triple
74 lower anterior tooth	**0** enlarged **1** gracile
75 second lower anterior incisor	**0** reduced **1** gracile **2** enlarged
76 incisors curved medially	**0** no **1** yes
77 incisor-canine crown orientation	**0** vertical **1** mesial extended
78 anterior antemolar (p2) roots	**0** two **1** one
79 antemolar (p3) anterior cusp	**0** reduced **1** present
80 antemolar (p3) posterior cusp	**0** reduced **1** present
81 antemolar (p3) cingulid	**0** present **1** weak
82 molariform p4	**0** no meta **1** yes
83 presence of talonids	**0** present **1** reduced
84 m2-3 trigonid size	**0** m2 = m3 **1** m2 > m3
85 m2 cingulid	**0** doesn't reach base **1** reaches base
86 hypoflexid basin	**0** closed **1** open
87 m2 paraconid notch	**0** present **1** absent
88 m3 talonid cusp	**0** absent **1** shorter paraconid **2** taller paraconid
89 m3 length	**0** m3 long **1** as m1-2 **2** m3 short
90 m3 paraconid	**0** distinct cusp **1** crestiform

TABLE 5
(Continued)

Characters	Character states
91 angular process	**0** broad **1** narrow
92 mental foramina	**0** p2 **1** p3 **2** p4 **3** m1
93 mandibular condyle length	**0** narrow **1** elongate
94 mandibular condyle number	**0** single **1** dual
95 coronoid shape	**0** straight **1** bowed
96 root coronoid process	**0** posterior m3 **1** overlaps m3
97 internal coronoid fossa	**0** flush **1** deep **2** pocketed
98 alveolar ridge	**0** weak **1** connects condyle
99 ventral crest on C2	**0** present **1** absent
100 verts in sacro-iliac art	**0** s1 alone **1** s1-2 **2** s1-3
101 sacral neural spines	**0** weak or not fused **1** fused
102 metacromion-shape	**0** blunt **1** elongate
103 acromion-shape	**0** blunt **1** elongate
104 deltoid ridge	**0** flat-convex **1** concave
105 medial epicondyle	**0** absent **1** present
106 olecranon fenestra	**0** absent **1** thin or present
107 distal ulna	**0** present **1** reduced
108 ulnocarpal articulation	**0** broad **1** styloid only
109 iliopectineal tubercle	**0** weak **1** prominent
110 pubic symphysis	**0** extensive **1** reduced
111 pubis length	**0** as ischium or shorter **1** longer than ischium
112 angle of pubic ramus	**0** > 15° angle **1** parallel
113 femoral head shape	**0** sphere **1** flattened
114 obturator ridge	**0** continuous with lesser trochanter **1** broken
115 femoral head greater trochanter	**0** notched **1** even
116 fusion distal tibia-fibula	**0** no **1** yes
117 calcaneal tubercle	**0** blunt **1** elongate
118 cranial size	**0** cameron **1** gregoryi **2** major **3** solenodon

[a] See text for full descriptions.

10. Entotympanic (N86: no. 49; M88: no. 7). Many mammals lack an independently ossified entotympanic contribution to the auditory bulla (e.g., *Erinaceus*, state 0; see MacPhee, 1981). Other taxa (e.g., *Macroscelides*, state 1) possess one or more ossified entotympanic elements that comprise some or all of the tympanic floor (MacPhee, 1979).

11. Ventral curvature of external auditory meatus. The type specimen of *A. gregoryi* (MCZ 17685) shows an acute, ventrally concave angle to its external auditory meatus, defined anteriorly by a sharp, anteroventrally directed entoglenoid process and posteriorly by a steeply descending petromastoid component of the lambdoid plate (state 1; see fig. 21). The external auditory meatus in other taxa (e.g., *A. illifensis*) may have a slight ventral concavity, but is subtended by an obtuse angle (state 0; fig. 27).

12. Lateral torus of external auditory meatus. In *A. major*, the ventral margin of the external auditory meatus bulges laterally, forming a ridge continuous with the lateral margin of the entoglenoid process (state 1; see fig. 32). In most other taxa, the exterior margin of the external auditory meatus does not form a torus and is flush with the rest of the posterior skull (e.g., *A. iliffensis*, state 0; see fig. 27).

13. Inferior stapedial foramen (M88: no. 4). As the inferior stapedial arterial ramus leaves the middle ear in tenrecs such as *Microgale*, it passes through a bony foramen within the alisphenoid contribution to the anterior wall of the middle ear (state 1; see Asher, 2001). *O. cameronensis* shows a similarly positioned foramen in its alisphenoid, just posterior to foramen ovale (fig. 40), dorsal to and distinct from the exit point of the

auditory tube. Other taxa show no distinct arterial foramina dorsal to the tubal canal in the alisphenoid (e.g., *Solenodon*, state 0).

Basicranium and Braincase

14. Alisphenoid canal, presence (N86: no. 34). In *A. baladontus* the alisphenoid canal consists of a foramen in the alisphenoid, just anterior and medial to foramen ovale, that leads into the cavum epiptericum, just posterior to its opening into the orbitotemporal region (state 1; see fig. 11). In *O. cameronensis*, the alisphenoid anterior to foramen ovale is solid, lacking a conduit into the cavum epiptericum (state 0; see fig. 40).

15. Alisphenoid canal, position: When present, the alisphenoid canal may have an anterior opening lateral to the sphenorbital fissure, as in *Echinosorex* (state 0; see Cartmill and MacPhee, 1980: fig. 2); or it may be ''elongate'' and anteriorly continuous with the exit foramen(ina) of the ophthalmic and/or maxillary trigeminal divisions (state 1, as in *A. baladontus* described above; see also Butler, 1988: 119).

16. Basisphenoid pit (F91: no. 30). At the dorsal and posterior margin of the nasopharynx, medial and slightly anterior to the middle ear, a marked concavity (when viewed ventrally) may occur in the basisphenoid (e.g., *Erinaceus*, state 1). Alternatively, most taxa examined here possess a flat basisphenoid continuous with the basioccipital (e.g., *Oligoryctes*, state 0; see fig. 40).

17. Size of foramen ovale. *Oligoryctes* shows an unusually large foramen ovale that is comparable in size to the entire sphenorbital fissure (state 1; see figs. 40, 45). Other taxa (e.g., *A. baladontus*; see fig. 11) show a foramen ovale that is smaller than the other exit points of the trigeminal nerve (state 0).

18. Suboptic foramen (Butler, 1956: 473). In *Elephantulus*, an opening is evident ventral to the optic foramina that passes transversely through the body of the sphenoid, ventral to the sella turcica, and connects the sphenorbital fissures on each side of the skull (state 1). In most other taxa this communication between the opposite orbitotemporal regions is not apparent in the anterior aspect of the sphenorbital fissure (e.g., *Erinaceus*, state 0).

19. External position of petromastoid (N86: no. 60). The petromastoid is the dorsal part of the petrosal and houses part of the inner ear. It may be best exposed on the posterior aspect of the skull, posterior to the nuchal crest (e.g., *Didelphis*, state 0), or it may be anterior to nuchal muscle scars and appear broadest when viewed laterally (e.g., *Oligoryctes*, state 1; fig. 40).

20. Ventral petromastoid. Some *Apternodus* species show a steeply descending process of the petromastoid that extends well ventral to the glenoid fossa and defines the external auditory meatus posteriorly (e.g., *A. major*, state 1; see fig. 32). In other taxa (e.g., *A. baladontus*; see fig. 11) the ventral margin of the petromastoid is close to the level of the jaw joint (state 0).

21. Presence of mastoid tubercle. *Setifer* shows a ventrally projecting process on the basicranium posterior to the external auditory meatus and anterior to the paroccipital process and/or occipital condyles (state 1). Other taxa (e.g., *Oligoryctes*; see fig. 40) show a rounded, gracile basicranium posterolaterally (state 0).

22. Composition of mastoid tubercle (N86: nos. 46, 58). When present, the mastoid tubercle may be composed primarily of the petromastoid (e.g., *Erinaceus*, state 2), the squamosal (e.g., *Setifer*, state 0), or have equal contributions from both elements (state 1). These character states comprise a potentially ordered morphocline.

23. Posterolateral braincase. The skull of *Apternodus* is perhaps most remarkable for its expanded, boxlike lambdoid processes composed of the squamosal anteriorly, the petromastoid medially, and the occipital posteriorly (state 1; see figs. 6, 7, 11, 15). Most other mammals show a gracile posterolateral braincase, with curved elements that are continuous with the temporal and occipital regions of the skull (e.g., *Oligoryctes*, state 0; see fig. 40).

24. Anterior lambdoid plate. Among most *Apternodus* species (e.g., *A. gregoryi*), the lambdoid plates are roughly parallel to the sagittal crest and connect with a squamosal root of the zygoma that does not extend far lateral to the jaw joint (state 0; see fig. 22). *A. major*, in contrast, shows a wide lateral flare in the anterior part of the lambdoid

plate, continuous with a squamosal zygoma that is well lateral to the entoglenoid process (state 1; fig. 32). In the current data set, this character is an autapomorphy for *A. major* and does not influence relationships among the taxa discussed below. We retain it in this character list to maximize the information content for species of *Apternodus*.

25. Squamosal length on basicranium. Soricids possess a mastoid ''tubercle'' that is an anteroposteriorly elongate extension of the squamosal on the ventrolateral margin of the basicranium (e.g., *Crocidura*, state 2; see fig. 52). This process extends from the jaw joint to the posterior margin of the middle ear and is much longer than the transverse width of the mandibular condyle. In other taxa, the posterior extent of the squamosal on the posterolateral braincase is similar in length to the transverse width of the mandibular condyle (e.g., *Oligoryctes*; state 1; see fig. 40), or shorter (e.g., *Erinaceus*, state 0). These character states comprise a potentially ordered morphocline.

26. Sagittal crest. *Apternodus* shows a pronounced, anteroposterior crest along the midline of the dorsal braincase, dividing the skull into mediolateral halves, continuous with the nuchal crest, and forking anteriorly into smaller crests posterior to the nasal bone (state 1; see fig. 15). In other taxa (e.g., *Oligoryctes*), the dorsum of the braincase is flat (state 0; fig. 40).

Orbitotemporal Region

27. Optic foramen (N86: no. 30; MacPhee 1994: 164). Several mammals possess an optic foramen that is similar in size to foramina associated with the first two divisions of the trigeminal nerve (e.g., *Elephantulus*, state 0). Most insectivorans have an optic foramen of very small caliber, a fraction of the size of trigeminal exit foramina (e.g., *Oligoryctes*, state 1; see fig. 40). *Didelphis* lacks a distinct canal for the optic nerve (state 2). These character states comprise a potentially ordered morphocline.

28. Ethmoid foramen. In *Oligoryctes*, one or more foramina within the anterior cranial fossa open bilaterally into the orbitotemporal fossa well anterior to the sphenorbital fissure (state 0; fig. 40). *Apternodus* shows an ethmoidal foramen that opens within the dorsum of the sphenorbital fissure (state 1). Ethmoidal foramina provide passage for an artery (called the ethmoidal by Gregory, 1910, and McDowell, 1958) typically continuous with the superior stapedial ramus supplying the posterior nasal region, eye, and anterior meninges (Asher, 2001).

29. Sinus canal foramen (N86: no. 38). When present, the sinus canal may open into the orbitotemporal region via a foramen confluent with the sphenorbital fissure (e.g., *Apternodus*, state 0; fig. 11), or with ethmoidal foramina (e.g., *Solenodon paradoxus*, state 2). The sinus canal may also enter the orbitotemporal region via a distinct foramen anterior to the sphenorbital fissure and posterior to the ethmoidal foramen (e.g., *Oligoryctes*, state 1; fig. 40). *Didelphis* lacks a sinus canal (state 3).

30. Posterior accessory sinus canal foramen. In most taxa, a foramen pierces the posterolateral braincase near the parietal-squamosal suture and communicates with the superior petrosal sinus and sinus canal (e.g., *Apternodus*, state 1; fig. 15). *Elephantulus* shows a solid squamosal and parietal in this region (state 0).

31. Anterior accessory sinus canal foramen. *Oligoryctes*, *Apternodus*, and shrews possess a foramen superior to the jaw joint, near the squamosal-parietal boundary, that opens into the sinus canal proximal to its anterior exit foramen into the orbitotemporal region (state 0; fig. 40). Other taxa possess a solid squamosal superior to the jaw joint (e.g., *Erinaceus*, state 1).

32. Entoglenoid jaw support (McDowell, 1958: 143–144). The flange of cranial bone supporting the mandibular condyle posteriorly may consist of the postglenoid process, located anterior to the postglenoid foramen and anterolateral to the petrosal bone (e.g., *Didelphis*, state 0). Alternatively, the postglenoid process may be reduced and the posterior glenoid fossa buttressed by the entoglenoid process, located medial to the postglenoid foramen and anterior to the petrosal (e.g., *Apternodus*, state 1; figs. 11D, 15).

33. Entoglenoid shape. *Apternodus* shows an entoglenoid process that is posteriorly concave, comprising the anterior wall of a recess in the anterior tympanic cavity, ventral

to the braincase (state 1; figs. 11D, 15). Other taxa (e.g., *Crocidura*; fig. 52) have a posteriorly flat entoglenoid process (state 0).

34. Lacrimal foramen, position (N86: no. 23). Many taxa possess a lacrimal foramen that opens along the posterior margin of the bridge of bone that forms the infraorbital canal and is directed posteriorly into the orbit, hidden from lateral view (e.g., *Didelphis*, state 0). In other taxa, this foramen opens in a lateral direction and is clearly visible in lateral view (e.g., *Apternodus*, state 1; fig. 15).

35. Lacrimal foramen, size. Most taxa show a lacrimal foramen that is smaller in size than the sphenopalatine foramen (e.g., *Erinaceus*, state 0); in other taxa it is larger (e.g., *Apternodus*, state 1; fig. 15).

36. Posterior border of lacrimal foramen. The posterior border of the lacrimal foramen is typically demarcated by a ridge of bone, separating it from the orbit (e.g., *A. brevirostris*, state 0; fig. 15). In contrast, *A. gregoryi* and *A. major* have a lacrimal foramen that is located farther from the infraorbital canal, making the posterior margin of the foramen flush with the orbit (state 1; figs. 22, 32).

37. Orbital wing of the maxilla (N86: no. 14). Most insectivorans are remarkable among mammals in possessing a broad process of the maxilla that extends dorsocaudally into the medial orbital wall, reducing the contribution of the palatine to the orbital mosaic (e.g., *A. baladontus*, state 1; fig. 13). In contrast, other mammals possess a maxilla restricted to the anteroventral margin of the orbit (e.g., *Elephantulus*, state 0).

38. Reduction of zygomatic arch (N86: no. 25). Many insectivorans have a zygomatic arch in which the jugal is vestigial or absent, leaving the arch incomplete lateral to the mandibular coronoid process (e.g., *Oligoryctes*, state 1; fig. 40). Most other mammals have a robust zygomatic process and a persistent jugal (e.g., *Didelphis*, state 0).

Rostrum

39. Ventral ectopterygoid. Some soricids, including the fossil taxon *Domnina* but not the extant *Crocidura*, show a transversely expanded, ventrally flat ectopterygoid plate on either side of the nasal choanae (state 1); these plates participate to varying degrees (considerable in *Blarina*) in a ventral, accessory jaw joint. Other taxa have ventrally narrow ectopterygoids (e.g., *Apternodus*; state 0; fig. 11).

40. Dual ectopterygoid (N86: no. 36). Most taxa possess a single pair of laminae made up primarily of the sphenoid and palatine bones which laterally border the nasal choana (e.g., *Apternodus*, state 0; fig. 11). Other taxa possess prominent ectopterygoid processes of the alisphenoid that contribute to a pair of laminae on each side of the choana, creating a large fossa for attachment of pterygoid musculature (e.g., *Erinaceus*, state 1).

41. Maxillary process on pterygoid. The maxilla posterior to the upper toothrow is not extensive in most taxa (e.g., *Erinaceus*, state 0). Tenrecs, on the other hand, show a process of the maxilla that extends well posterior to the upper toothrow along the ventral margin of each ectopterygoid lamina (state 1; McDowell, 1958: 184).

42. Postpalatine spine (N86: no. 18). The posterior margin of the palate may be smooth or have only a minor tubercle at its midpoint (e.g., *Apternodus*, state 0; fig. 7), or it may possess a large process extending caudally or caudo-dorsally at its midpoint (e.g., *Erinaceus*, state 1).

43. Origin of maxillary zygoma. Some taxa possess a maxillary root of the occasionally incomplete zygomatic arch that is relatively rostral, originating at or near the last upper premolar or the M1 (e.g., *O. cameronensis*, state 0; figs. 40, 41). It may also originate adjacent to M2 (e.g., *O. altitalonidus*, state 1; figs. 45, 46) or M3 (e.g., *Microgale*, state 2). In taxa possessing a broad maxillary zygoma (e.g., *Didelphis*), the anteriormost part of the zygoma was used to code this character. These character states comprise a potentially ordered morphocline.

44. Size of maxillary zygoma. Soricids possess a highly reduced rudiment of the maxillary root of the zygoma, barely extending lateral to the upper dentition (e.g., *Crocidura*, state 1; fig. 52). Other taxa possess a larger maxillary zygoma that extends posterolaterally (e.g., *Solenodon*, state 0).

45. Shape of maxilla supporting cheek

teeth. The bone into which the roots of the upper molar toothrow insert may be convex ventrally, such that the crown of M2 may be situated ventral to that of M1 (e.g., *Apternodus*, state 1; fig. 15). Alternatively, the maxilla may be straight in the area supporting the upper cheek teeth (e.g., *Echinosorex*, state 0).

46. Length of infraorbital canal (N86: no. 10, F91: no. 6). The infraorbital canal (transmitting the infraorbital vessels and nerve and passing dorsal to posterior cheek teeth) may be more than twice as long as its anterior exit foramen is high (e.g., *Erinaceus*, state 0), of similar size (e.g., *Echinosorex*, state 1), or shorter, composed of a simple bar of bone connecting the alveolar and facial components of the maxilla (e.g., *Elephantulus*, state 2). These character states comprise a potentially ordered morphocline.

47. Infraorbital flange. As the infraorbital canal opens on the side of the rostrum, its lateral border is typically posterior to its medial border (e.g., *Setifer*, state 0). *A. major*, in contrast, shows an anteriorly extensive lateral edge of the infraorbital canal, such that the anterior opening of the canal is concave, and its anterolateral edge reaches a point even with or anterior to its anteromedial edge (state 1; fig. 32).

48. Posterior nasal foramina. *Blarina* shows foramina opening onto the rostrum from the anterior margin of the olfactory fossa, dorsal to the cribriform plate (state 1). In other taxa (e.g., *Apternodus*; fig. 11) the frontal and nasal bones are solid in this region (state 0).

Upper Dentition

49. Deciduous teeth. Most mammals possess functional, fully calcified deciduous teeth, with a permanent dentition that erupts postnatally (e.g., *Erinaceus*, state 0). In soricids, deciduous teeth do not completely calcify or erupt; and the adult set is present from birth (Kindahl, 1959a; state 1).

50. Size of anterior upper incisor. In some taxa, the anteriormost upper incisor is longer and more robust than other anterior teeth (e.g., *Solenodon*, state 0); in other taxa, the upper incisors are similar in size (e.g., *Didelphis*, state 1).

51. Upper incisors. In therians, the number of teeth on each half of the premaxilla ranges from five (e.g., *Didelphis*, state 2) to two (e.g., *Setifer*, state 0), with intermediate states numbered accordingly. No taxon in this data set exhibits four teeth in each half of its premaxilla; therefore, this character state is omitted. These character states comprise a potentially ordered morphocline.

52. Upper antemolars, excluding incisors. The number of upper premolars and canines in each dental quadrant varies in the taxa examined from five (e.g., *Echinosorex*, state 0) to two (*Crocidura*, state 2), with intermediate states numbered accordingly. No taxon in this data set has three teeth between its incisor and molar toothrows; therefore, this character state is omitted. These character states comprise a potentially ordered morphocline.

53. Posterior incisor crowns. The last upper incisor is typically premolariform and mediolaterally compressed in appearance (e.g., *Microgale*, state 0). In contrast, *A. mediaevus* and *A. baladontus* show an enlarged I2, with similar buccolingual and anteroposterior dimensions of the base of the tooth (state 1; figs. 6, 13).

54. Upper canine crowns. As for the posteriormost upper incisor, the upper canine is typically premolariform and mediolaterally compressed (e.g., *A. brevirostris*, state 0; fig. 15). In contrast, *Solenodon cubanus* and species of *Apternodus* from Montana show squat, bulbous canines with oval or circular dimensions when viewed occlusally (state 1; figs. 6, 10, 11, 13).

55. Upper canine roots. In most taxa, the upper canine is double rooted (e.g., *Setifer*, state 1). Alternatively, it may show one (*Didelphis*, state 0) or three (*A. baladontus*, state 2; fig. 11) roots. These character states comprise a potentially ordered morphocline.

56. Upper antemolar diastemata. Some taxa show prominent interdental gaps between the upper incisors and P4 (e.g., *Echinosorex*, state 0). In others, the dentition between the posterior upper incisor and P4 is closely packed and lacks prominent diastemata (e.g., *A. brevirostris*, state 1; fig. 15).

57. Anterior premolar roots. *Echinosorex* possesses a single-rooted P2 (state 0); *Microgale* has two roots (state 1); elephant shrews

have three (state 2); and the P2 of some *A. baladontus* specimens has four (state 3). These character states comprise a potentially ordered morphocline.

58. Anterior premolar length. *Oligoryctes* and some species of *Apternodus* share a diminutive P2, similar in anteroposterior length to a single root of a molariform, more posterior premolar (state 1; figs. 15, 41). In other taxa, P2 is similar in length to P3 and/or P4 (e.g., *A. baladontus*, state 0; figs. 11, 13).

59. Molariform P3. P3 may be three-rooted with a lingually projecting protocone, similar in size to more posterior cheek teeth (e.g., *Setifer*, state 1), or smaller and close in morphology to anterior premolars (e.g., *Erinaceus*, state 0).

60. P3 length. The buccal margin of P3 may be longer (e.g., *O. cameronensis*, state 1; fig. 41) or of similar size or shorter (e.g., *A. baladontus*, state 0; fig. 13) than that of P4.

61. P4 parastyle. The mesiobuccal cusp (parastyle) of P4 in *A. gregoryi* and *A. major* projects anteriorly at a sharp angle from the anterior margin of the tooth (state 1; fig. 32), in contrast to the more anteriorly flat appearance of other taxa (e.g., *A. mediaevus*, state 0; fig. 7). Following Luckett (1993, and references therein), we code *Didelphis* as lacking a P4.

62. Metacone. Some taxa possess a prominent metacone on the posterobuccal aspect of M1 and M2 (e.g., *Echinosorex*, state 0). *Eoryctes* possesses a metacone that is closely situated to the paracone (state 1). Other taxa have a reduced or absent metacone (e.g., *Apternodus*, state 2; fig. 15). These character states comprise a potentially ordered morphocline.

63. Protocone. In some taxa, the mesiolingual cusp of the upper cheek teeth is restricted to the cingulum and is smaller than the parastylar cusp, if present at all (e.g., *A. iliffensis*, state 1; fig. 26). In other mammals, the protocone is at least as large as the anterior stylar cusp of the upper molars (e.g., *O. altitalonidus*, state 0; fig. 46).

64. Hypocone. Some taxa possess a prominent hypocone on the posterolingual aspect of M1 and M2 (e.g., *Echinosorex*, state 0). In other taxa, this cusp is reduced or absent (e.g., *Apternodus*, state 1; fig. 26).

65. Relative M1-M3 size. In most taxa, the cheek teeth comprise a larger occlusal area than the canine and anterior premolars (e.g., *A. brevirostris*, state 0; fig. 15); in others (e.g., *A. baladontus*; fig. 11), the molar occlusal area is less than that of C to P2 (state 1).

66. M1-M2 anterior cingulum. The upper M1-M2 of the Tabernacle Butte taxon shows a very deep, troughlike anterior cingulum which connects the parastylar region to the protocone (state 0). In other taxa (e.g., *Solenodon*), the mesial cingulum is weakly developed and shallow, forming a weak prominence along the anterior margin of the tooth. In the current data set, this character is an autapomorphy for the Tabernacle Butte taxon. Nevertheless, as stated previously for character no. 24 in *A. major*, we retain it to maximize information content for novel taxa discussed in this paper.

67. Parastyle on M1. On the mesiobuccal margin of M1, *Apternodus* (e.g., fig. 26) displays a large, anteriorly projecting parastyle (state 1). Other taxa show a flat mesial border to M1 with no anterior projections (e.g., *Erinaceus*, state 0).

68. Centrobuccal cleft on upper molars. The buccal margin of the upper molars (particularly M2) may be mesiodistally flat (e.g., *Echinosorex*, state 0). Alternatively, a cleft extending lingually may separate the mesial and distal stylar regions, giving the buccal margin of the tooth a V shape (e.g., *Oligoryctes*, state 1; fig. 46; MacPhee, 1987: fig. 7b).

69. M3 presence. Adults of most taxa possess M3 (e.g., *Echinosorex*, state 0); in elephant shrews it is absent (state 1).

70. M3 size. *Erinaceus*, soricids, and *Apternodus iliffensis* (fig. 30) possess a transversely shortened M3 relative to M2 (state 1). In other taxa (e.g., *Solenodon*) M3 is at least 70% of the buccolingual width of M2 (state 0).

71. M3 stylar shelf. When present, M3 may show a prominent stylar region with a distinct stylocone, mesostyle, and/or metastyle (e.g., *Oligoryctes*, state 1; fig. 46). Alternatively, this region may be reduced, and little or no occlusal surface may be present buccal to the paracone and/or metacone (e.g., *Echinosorex*, state 0).

Lower Dentition

72. Lower antemolars: The number of premolars, canines, and incisors in each mandible varies from eight (e.g., *Oligoryctes altitalonidus*) to three (e.g., *Blarina*), successively comprising character states 0–4. No taxon coded in this study shows four lower antemolars; hence, this character state is omitted. These character states comprise a potentially ordered morphocline.

73. Lower incisor cusps. *Oligoryctes* shows three distinct cusps on its posterior two lower incisors (fig. 42): one at the heel, one at the tip, and one in an intermediate position (state 2). The lower incisors of other taxa may consist of just a single cusp at the tip (e.g., *Solenodon*, state 0), or a cusp at the tip and a second at the base of the tooth (e.g., *Erinaceus*, state 1). These character states comprise a potentially ordered morphocline.

74. Lower anterior incisor. This tooth may be gracile and similar in size to (e.g., *Echinosorex*, state 1), or trenchant and larger than (e.g., *Erinaceus*, state 0), other anterior teeth.

75. Second lower incisor. This tooth may be gracile and similar in size to (e.g., *Microgale*, state 1), or trenchant and larger than (e.g., *Solenodon*, state 2), other anterior teeth. In some specimens of *Apternodus*, the second lower incisor is present but vestigial, with an alveolus confluent with that of the first lower incisor (state 0; see fig. 16 and Schlaikjer, 1934). These character states comprise a potentially ordered morphocline.

76. Medial curvature of i2. The medial aspect of i2 in *Solenodon* is concave (state 1) to facilitate this animal's poisonous bite (Nowak, 1999). Lower incisors of other taxa are usually convex (e.g., *Echinosorex*, state 0), although the medial aspect of the incisor of *Pararyctes* shows an interesting resemblance to that of *Solenodon*.

77. Incisor crown orientation. The crowns of most incisors, anterior premolars, and the canine of *Apternodus* are inclined anteriorly, such that the tooth crown meets the root at an angle (state 1; fig. 16). Other taxa (e.g., *Didelphis*) show incisor crowns that are parallel with their roots (state 0).

78. Anterior antemolar roots. Several taxa (e.g., *Solenodon*) have two roots on their anterior lower premolars, including p2 (state 0); other taxa have single-rooted anterior premolars (e.g., *A. brevirostris*, state 1; fig. 16).

79. Antemolar anterior cusp. At its anterior margin, the p3 of *Oligoryctes* shows a prominent cusp (state 1; fig. 42), absent in the antemolars of most other taxa (e.g., *A. brevirostris*, state 0; fig. 16).

80. Antemolar posterior cusp. Similarly, *Oligoryctes* shows a distinct cusp at the distal edge of its p3 (state 1; fig. 42), absent in many other taxa (e.g., *A. baladontus*, state 0; fig. 14).

81. Antemolar cingulid. *A. brevirostris* shows a prominent cingulid along the buccal margin of p3 (state 0; fig. 18); this cingulid is reduced and does not surround the buccal margin of premolars in other taxa such as *A. baladontus* (state 1; fig. 14).

82. Molariform p4. Many taxa examined show p4 with a molariform trigonid with three major cusps (paraconid, metaconid, and protoconid; e.g., *Apternodus*, state 1; fig. 18). Other taxa lack multiple trigonid cusps and have a buccolingually narrow p4 that resembles more anterior lower teeth (e.g., *Parapternodus*, state 0; see fig. 49).

83. Talonid. Lower molars of several taxa may have a talonid with a well-defined basin surrounded by ridges comprised of, or continuous with, the entoconid, hypoconid, and/or hypoconulid (e.g., *Echinosorex*, state 0). In some taxa the talonid basin is small or altogether absent (e.g., *Apternodus*, state 1; fig. 18).

84. Trigonid size. The trigonid on m2 of *O. cameronensis* is larger than that of m3 (state 1; fig. 42). Some other taxa (e.g., *O. altitalonidus*) show m2-m3 trigonids of roughly similar size (state 0; fig. 42).

85. Cingulid on m2. The lower second molar of *A. brevirostris* shows a cingulid extending from the mesial margin of the tooth to the buccal edge (state 1; Fig 18). In *Parapternodus*, this cingulid is evident only near the anterior margin of the tooth, and does not extend buccally to the tooth base (state 0; fig. 49).

86. Secondary hypoflexid basin. Among taxa with extensive hypoflexid-paracone occlusion, the paracone of the M3 may occlude with the m3 in a basin comprised of the hypoflexid bounded laterally by a cingulid (e.g., *Solenodon*, state 0). Alternatively, the

m3 hypoflexid may be buccally open (e.g., *Oligoryctes*, state 1; fig. 42).

87. Paraconid notch (Robinson and Kron, 1998). Ventral to the paraconid of the molars, several taxa show a notch that receives the distal talonid of the adjacent, anterior tooth (e.g., *A. brevirostris*, state 0; fig. 18). In a few taxa (e.g., *Koniaryctes*), this notch is absent (state 1).

88. m3 talonid cusp. *Oligoryctes altitalonidus* was named for the single cusp on its lower third molar talonid which exceeds the m3 paraconid in height (state 2; fig. 44). Talonid cusps on the m3 in other taxa (e.g., *Apternodus*) are typically shorter than the m3 paraconid (state 1; fig. 18). Some taxa (e.g., *Parapternodus*) lack a talonid cusp on m3 (state 0; fig. 49). These character states comprise a potentially ordered morphocline.

89. m3 length. When present, the m3 may be shorter (e.g., *Parapternodus*, state 2; fig. 49), equal in length (e.g., *A. brevirostris*, state 1; fig. 18), or longer (e.g., *Solenodon*, state 0) than each of the first two lower molars. These character states comprise a potentially ordered morphocline.

90. m3 paraconid. Instead of a paraconid cusp, erinaceids show on the anterior margin of m3 a crest that runs anterolingually away from the protoconid (state 1). The anteriormost cusp of most other taxa (e.g., *Solenodon*) more closely resembles the metaconid and in unworn specimens is a distinct cusp (state 0).

Dentary

91. Angular process. At the posteroventral corner of the mandible, *A. baladontus* possesses a narrow angular process that shows approximately the same width distally and at its base (state 1; fig. 12). Other taxa (e.g., *Solenodon*) have an angular process with a broader base that tapers along its length (state 0).

92. Mental foramina. Foramina for branches of the mandibular nerve and vessels appear in a number of places on the buccal side of the mammalian jaw. States observed here include ventral to m1 (e.g., *Crocidura*, state 3), p4 (e.g., *Echinosorex*, state 2), p3 (e.g., *Micropternodus*, state 1), or p2 (e.g., *A. dasophylakas*, state 0).

93. Mandibular condyle, length. Some taxa have a globular, ball-shaped mandibular condyle (e.g., *Setifer*, state 0). This contrasts with pronounced mediolateral expansion conspicuous in other taxa (e.g., *Apternodus*, state 1; fig. 14), in which the condyle is 50–100% wider transversely than m1.

94. Mandibular condyle, number. Extant soricids possess a dual craniomandibular articulation (state 1), showing two distinct articular surfaces and synovial capsules between the mandible and cranium (Fernhead et al., 1954). Other taxa show a single synovial articulation (e.g., *Erinaceus*, state 0).

95. Coronoid shape. The coronoid process of *Apternodus* is laterally convex, or bowed such that the midpoint of the coronoid reaches farther laterally than the dorsal tip (state 1; fig. 8). Other taxa show a relatively straight coronoid (e.g., *Echinosorex*, state 0), including modern soricids, which have a medially pocketed coronoid.

96. Anterior root of coronoid process. Members of the genus *Apternodus* show an anteriorly extensive coronoid process that, in lateral view, overlaps with the posterior part of the lower third molar (state 1; fig. 2). An illustration of the mandible in *A. gregoryi* in Schlaikjer (1933) misleadingly gives the impression that the anterior margin of the coronoid process is posterior to m3; however, this is not the case. In most other taxa (e.g., *Erinaceus*), the anterior root of the coronoid process is located well posterior to the m3 (state 0).

97. Internal coronoid fossa. The lingual aspect of the coronoid process of the mandible in most taxa examined is smooth and continuous with more ventral regions of the internal aspect of the posterior part of the dentary (e.g., *Erinaceus*, state 0). Extant soricids, *O. cameronensis*, *O. altitalonidus*, and *Parapternodus*, in contrast, have a lingually pocketed coronoid which increases the surface area available for jaw muscle attachments (state 2; see fig. 42). Some taxa (e.g., *Apternodus*) possess an intermediate condition in which the coronoid process has a deep internal concavity, but is not pocketed (state 1; fig. 33). These character states comprise a potentially ordered morphocline.

98. Alveolar ridge. A ridge of bone may be present on the lingual aspect of the pos-

terior dentary, running from the base of m3 to the mandibular condyle (e.g., *Apternodus*, state 1; fig. 33). In other taxa, this ridge is reduced and fails to reach the condyle (e.g., *Setifer*, state 0).

Axial Skeleton

99. Posteroventral keel on axis (F91: no. 69). The posterior aspect of the second cervical vertebral centrum may be smooth ventrally or show only a reduced tuberosity close to its midpoint (e.g., *Setifer*, state 1). The axis of other taxa shows a prominent spine projecting posteroventrally from the centrum (e.g., *A. dasophylakas*, state 0; fig. 37).

100. Number of vertebrae contributing to the sacroiliac articulation. The sacral vertebrae articulating with the ilium may include S1 alone (e.g., *Blarina*, state 0), S1-S2 (e.g., *Setifer*, state 1), or S1-S3 (e.g., *Erinaceus*, state 2). These character states comprise a potentially ordered morphocline.

101. Fusion of sacral neural spines (F91: no. 72). Most taxa show sacral spinous processes that lack consistent fusion among each other (e.g., *Microgale*, state 0). In a few taxa, these processes form a well-fused longitudinally running plate (e.g., *Echinosorex*, state 1).

Forelimb

102. Scapular metacromion shape (F91: no. 71). Most taxa possess a laterally bifid scapular spine, made up of two processes extending laterally from the scapular spine and dorsal to the scapular glenoid fossa: the acromion (directed laterally) and metacromion (directed posteriorly). Variation in this region occurs in several ways: first, the posteriorly directed metacromion may be blunt (e.g., *Erinaceus*, state 0), or elongate (e.g., *Elephantulus*, state 1).

103. Scapular spine, acromion shape (F91: no. 71). Similarly, the acromion may be blunt (e.g., *Erinaceus*, state 0) or elongate (e.g., *Blarina*, state 1).

104. Deltoid ridge. The muscular attachments for the deltoid musculature typically comprise a slightly rugose, convex bulge on the proximal half of the humerus (e.g., *A. major*, state 0; fig. 34). In soricids, however, deltoid muscle attachments form an externally concave rugosity on the proximal humerus (state 1).

105. Medial epicondyle of humerus. Most taxa possess a medially projecting epicondyle that comprises at least 25% of the distal humeral margin medial to the trochlea (e.g., *A. major*, state 1; fig. 34). Others show a reduced or absent medial epicondyle (e.g., *Erinaceus*, state 0).

106. Olecranon fenestra of humerus. Distally, the humerus may have a fenestra or a very thin lamina of bone within the olecranon fossa (e.g., *Erinaceus*, state 1); in most taxa, the olecranon process of the ulna sits in a well-ossified fossa of the humerus (e.g., *A. major*, state 0; fig. 34).

107. Distal ulna. Elephant shrews possess an ulna that tapers to an end by the radial midshaft, with no articular surface for the carpus (state 1). Other taxa possess an ulna that articulates with both the humerus and carpus (e.g., *Erinaceus*, state 0).

108. Ulnocarpal articulation. In those taxa with a distal ulna, it may have a restricted articulation with the carpus, reaching the triquetrum and pisiform only via an elongate styloid process (e.g., *Setifer*, state 1; see Kielan-Jaworowska, 1977: 72). Other taxa show a distal ulna with a broader articulation with the carpus, comparable in size to the radial articular surface (e.g., *Erinaceus*, state 0).

Hindlimb

109. Iliopectineal tubercle, presence. In *Echinosorex*, a single, prominent, ventrally projecting tuberosity is present immediately ventral to the acetabulum (state 1). Most other taxa show only a mild rugosity or a smooth surface ventral to the acetabulum (e.g., *Setifer*, state 0).

110. Pubic symphysis. Insectivorans have been characterized as having either narrow or no contact between the pubes medially (e.g., *Setifer*, state 1). Most other mammals have a craniocaudally broad pubic symphysis, similar in length to ischiopubic rami framing the obturator foramina of each os coxa (e.g., *Tupaia*, state 0). Following Allen (1910: 39), all of the specimens of *Solenodon paradoxus* observed during the course of this study show a reduced pubic symphysis, contra Leche (1907: 82).

111. Pubis length. Variation is present in the relative lengths of the pubis and ischium (Leche, 1907: 81). In some taxa, the distance from the midpoint of the acetabulum to the pubic symphysis is longer than the distance from the same point to the caudal extent of the ischium (e.g., *Echinosorex*, state 1). In other taxa, the pubis is similar in length or slightly shorter than the ischium (e.g., *Didelphis*, state 0).

112. Angle of pubic ramus. The pubis typically joins the acetabulum at an angle with the ischium and ilium of 15 degrees or greater (e.g., *Setifer*, state 0). In some taxa, the pubis is parallel to the long axis of the ilium and ischium (e.g., *Blarina*, state 1).

113. Shape of femoral head. The femoral head of most taxa is spherical (e.g., *Echinosorex*, state 0). One of the few specimens of *Apternodus* with associated postcrania (UW 13508) reveals a very distinctive proximal femur with an ovoid femoral head, slightly flattened in a dorso-ventral plane (state 1; fig. 24).

114. Obturator ridge. On the posterior aspect of the proximal femur, attachments for obturator muscles are typically defined ventrally by a ridge of bone connecting the greater and lesser trochanters (e.g., *Echinosorex*, state 0). In certain taxa (e.g., *A. gregoryi*), this ridge is weak and does not form a connection between the greater and lesser trochanters (state 1; fig. 24).

115. Greater trochanter of femur. Most taxa have a deep gap or notch between the femoral head and the greater trochanter (e.g., *Echinosorex*, state 0). *A. gregoryi*, on the other hand, has a femoral head that is essentially continuous with the superior margin of the greater trochanter (state 1; fig. 24).

116. Fusion of distal tibia and fibula. The distal tibia and fibula may be completely fused or synostosed at the ankle (e.g., *Erinaceus*, state 1). Some taxa possess a distal tibia and fibula that approximate each other but do not fuse (e.g., *Setifer*, state 0).

117. Calcaneal (peroneal) tubercle (Gregory, 1910: 250). In some taxa, the distolateral margin of the calcaneus shows a blunt rugosity (e.g., *Erinaceus*, state 0) for attachment of abductor digiti quinti and, following Gregory (1910: 250), a tarso-metatarsal ligament. In others this rugosity is elongate and similar in size to the sustentaculum tali, extending laterally and/or distally past the distal margin of the calcaneus (e.g., *Microgale*, state 1).

Other Characters

118. Cranial size. As a heritable, morphological characteristic that distinguishes many taxa considered here, cranial size is an appropriate addition to this character list. For present purposes, it is arbitrarily divided into four character states, each based on disjunctions present in the distribution of palatal widths across taxa (fig. 53). Where cranial data are lacking (i.e., for the Tabernacle Butte taxon, *Parapternodus*, and *Koniaryctes*), the dentition is used as a surrogate (fig. 54). From smallest to largest, the four states indicate similarity in size to *O. cameronensis* (state 0), *A. gregoryi* (state 1), *A. major* (state 2), and *Solenodon* (state 3). These character states comprise a potentially ordered morphocline.

Taxon Sample

We include 30 taxa in the phylogenetic analysis component of this study, including the 11 species of *Apternodus*, *Oligoryctes*, *Parapternodus*, and *Koniaryctes*, plus the unnamed Tabernacle Butte (McKenna et al., 1962) and Silver Coulee taxa (Wood, 2000) discussed above. Also sampled are *Micropternodus* (Matthew, 1903); the palaeoryctids *Pararyctes pattersoni* and *Eoryctes melanus* (Thewissen and Gingerich, 1989); the geolabidid *Centetodon* (Lillegraven et al., 1981); the Caribbean insectivorans *Nesophontes*, *Solenodon cubanus*, and *Solenodon paradoxus*; the tenrecids *Microgale cowani* and *Setifer setosus*; the erinaceids *Erinaceus europaeus* and *Echinosorex gymnura*; the soricids *Blarina*, *Crocidura olivieri*, and *Domnina*; and the macroscelideans *Elephantulus brachyrhynchus* and *Macroscelides elephantulus*. The marsupial *Didelphis* is used to root phylogenetic trees. When a trivial name is not given above, multiple species of that genus were used to code characters (e.g., *Blarina carolinensis* and *B. brevicauda*). In addition to those already listed in table 2, catalog numbers of specimens examined here are as follows: *Centetodon* (USNM 181720,

181722, 187339, 214436, 299498, 299500, MPUM 1616, UCM 38429), *Didelphis* (AMNH 28408, 28962, 29255, 70082, 145630, 146551, 148959, 210327), *Domnina* (AMNH 32647, 94257, USNM 12841), *Echinosorex* (AMNH 32640, 34698, 102781, 102782, 103736, 103851, 103883, 106066, 106067, USNM 396674, 448860), *Eoryctes* (cast of UMMP 68074), *Erinaceus* (AMNH 3770, 42561, 42563, 70613, 140469, 140470), and *Microgale* (AMNH 31245, 100717).

Analytical Protocol

NONA (Goloboff, 1993), Winclada (Nixon, 1999), and PAUP* (Swofford, 2000) were used to analyze this data set. Character entry and optimization were accomplished using Winclada and MacClade (Maddison and Maddison, 2000). We performed distinct runs on a data set that gave more weight to extreme changes in multistate characters (i.e., characters ''ordered'') that are optimized consistently with their hypothesis of order (Lipscomb, 1992), and with all character transformations requiring one step (i.e., characters ''unordered''). Searches in NONA/Winclada were heuristic using TBR branch swapping (the ''mult*max*'' option in WinClada), with at least 1000 random addition replicates and branch swapping performed on up to five trees held per replicate. Analyses in PAUP* used heuristic parsimony searches with TBR branch swapping and at least 200 random addition replicates. Branch supports (Bremer, 1988, 1994) were calculated using a NONA macro file written by Diego Pol of the American Museum of Natural History, and by using constraint trees in PAUP*. Tree lengths calculated by NONA are reported here. We configured PAUP* to collapse nodes that have zero branch lengths under any optimization (the ''amb-'' option in the ''parsimony settings'' dialog) so that it produces the same topologies as NONA.

RESULTS

Following the procedure for testing hypotheses of ordered transformations outlined by Lipscomb (1992), 15 of the 20 morphocline characters are optimized unambiguously as showing changes between adjacent states only (table 6). An analysis calculating tree lengths with these 15 multistate characters ordered produces eight trees of 374 steps, a strict consensus of which is depicted in figure 57A. This topology is similar to those produced by ordering all 20 characters, which yields four most parsimonious trees (MPTs) of 384 steps that differ from figure 57A only in showing *Micropternodus* as the sister taxon of erinaceids. With all characters unordered, the analysis produces six MPTs of 370 steps (fig. 57B). As indicated by the low branch support for many nodes, this data set is noisy. Few of the high-level clades have branch supports above 1, and the number of trees within five steps of the shortest is vast. Nevertheless, this does not change the fact that the relatively well-resolved MPTs (fig. 57) represent the least *ad hoc* explanation of the available data.

All analyses agree that the ''Apternodontidae'' as a group including taxa previously attributed to it in the literature (i.e., *Apternodus*, *Oligoryctes*, *Parapternodus*, *Koniaryctes*, *Micropternodus*, and the Tabernacle Butte and Silver Coulee taxa) is not monophyletic. Contradicting its monophyly are the positions of soricids, *Micropternodus*, and the Silver Coulee taxon. McKenna and Bell (1997) restricted the ''Apternodontidae'' to the three demonstrably zalambdodont fossil North American genera with (as of 1997) published descriptions: *Apternodus*, *Oligoryctes*, and *Parapternodus*. However, even this more restricted group is not monophyletic according to the MPTs reported here, as soricids nest within ''apternodontids'' (sensu lato) as sister taxa to *Parapternodus* and *Koniaryctes*.

The genus *Apternodus* as recognized here consists of seven species: *A. mediaevus*, *A. baladontus*, *A. brevirostris*, *A. iliffensis*, *A. dasophylakas*, *A. gregoryi*, and *A. major*, without ''*A.*'' *altitalonidus* Clark, 1937. *Apternodus* is one of the better-supported clades recovered in these analyses, the others being a Montana *Apternodus* clade (*A. mediaevus* and *A. baladontus*), soricids, extant elephant shrews, and the genus *Solenodon*. Another consistent intra-*Apternodus* clade consists of *A. gregoryi* and *A. major*, with a branch support of two across analyses (figs. 57 and 58). Within *Apternodus*, the relationships of the

TABLE 6
Ordered Multistate Characters[a]

Character (number of states)	Optimization
2. Piriform fenestra (3)	nonadjacent change from state **0** to **2** in branch leading to *Centetodon*
6. Rostral tympanic process of the petrosal (3)	adjacent changes
22. Composition of the mastoid tubercle (3)	adjacent changes
25. Extent of squamosal on ventrolateral braincase (3)	adjacent changes
27. Optic foramen size (3)	adjacent changes
43. Origin of maxillary zygoma (3)	adjacent changes
46. Length of infraorbital canal (3)	adjacent changes
51. Number of upper incisors (3)	adjacent changes
52. Number of upper antemolars (3)	adjacent changes
55. Upper canine roots (3)	adjacent changes
57. Upper P2 roots (4)	adjacent changes
62. Metacone (3)	nonadjacent change from state **2** to **0** in branch leading to parapternodontids
72. Lower antemolars (5)	nonadjacent change from state **0** to **3** in branch leading to *Erinaceus*
73. Lower incisor cusps (3)	nonadjacent change from state **0** to **2** in branch leading to oligoryctids
75. Second lower incisor (3)	adjacent changes
88. m3 talonid cusp (3)	adjacent changes
89. m3 length (3)	adjacent changes
97. Internal coronoid fossa (3)	adjacent changes
100. Sacral vertebrae (3)	adjacent changes
118. Cranial size (4)	nonadjacent changes from state **0** to **2** and **0** to **3** in branches leading to tenrecs and *Solenodon*, respectively

[a] Following Lipscomb (1992), characters are optimized on each of four ordered topologies produced by an initial analysis treating all 20 morphocline characters identified in the text as ordered. "Adjacent changes" indicates that at least one optimization exists in which all changes occur between adjacent states. "Nonadjacent change" indicates that hypothesis of order is not corroborated by congruence.

Montana and *gregoryi-major* clades to each other and to the remaining three *Apternodus* species (*brevirostris*, *iliffensis*, and *dasophylakas*) remain unresolved.

Oligoryctes, including the Tabernacle Butte taxon, is reconstructed as the sister taxon to a soricid-*Parapternodus-Koniaryctes* clade in the ordered analyses, and as unresolved in a clade including the latter group plus *Apternodus* in the unordered analysis. *Oligoryctes* consists of *O. cameronensis* as sister taxon to an *O. altitalonidus*-Tabernacle Butte taxon in both. As a clade, these three taxa enjoy slightly better support from the ordered analyses (with a branch support of two steps) than the unordered analysis (with a branch support of one step). Interestingly, according to both phylogenies illustrated in figure 57, the generic name of the Tabernacle Butte taxon should be *Oligoryctes*.

Although *Parapternodus* and *Koniaryctes* are known only from isolated mandibles and

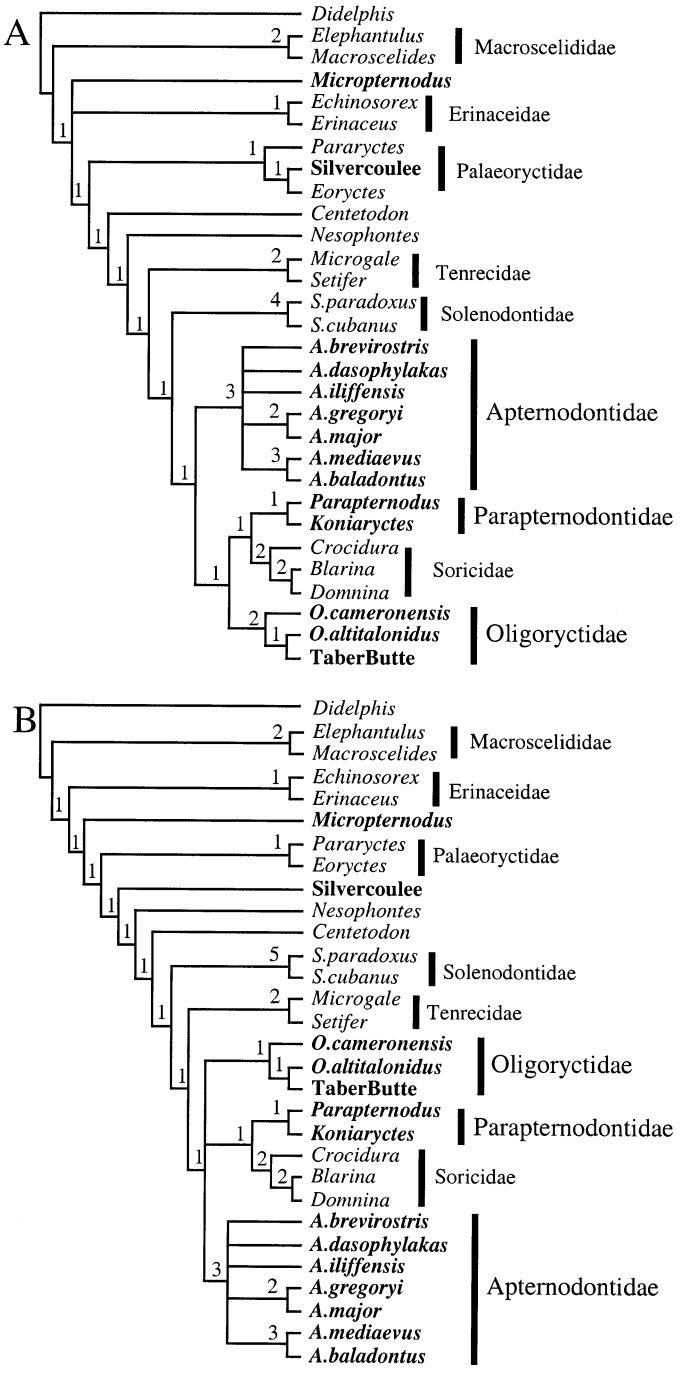

Fig. 57. Strict consensus trees from (**A**) 15-character ordered (8 MPTs, 374 steps) and (**B**) unordered (6 MPTs, 370 steps) analyses. The ordered analysis (A) gives greater weight to only those multistate characters that are optimized consistently (see text and Lipscomb, 1992). Boldface indicates taxa previously considered to comprise the Apternodontidae. Numbers adjacent to nodes indicate branch support.

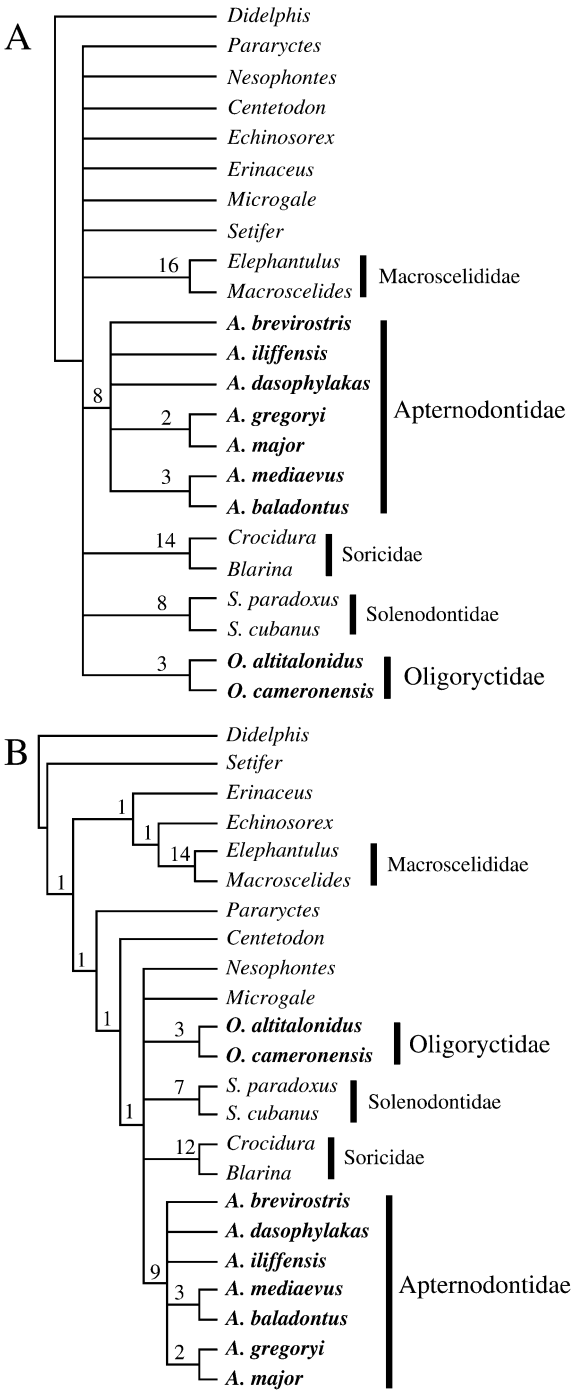

Fig. 58. Strict consensus trees from the same analyses shown in figure 57, but excluding taxa with greater than 40% missing data. (A) ordered (22 MPTs, 341 steps) and (B) unordered (10 MPTs, 338 steps). Notation as in figure 57.

teeth, and are consequently missing 82 and 92% (respectively) of the character data described above, they are reconstructed (with low branch support) as a clade with soricids as its sister group regardless of character ordering.

The extant familial taxa sampled in this study, i.e., two species of *Solenodon*, two tenrecids, two extant soricids plus *Domnina*, two erinaceids, and two macroscelidids, are reconstructed as monophyletic in all analyses. Interestingly, the extinct heterosoricine *Domnina* is reconstructed within crown Soricidae, more closely related to *Blarina* than to *Crocidura*.

According to the ordered MPTs (fig. 57A), the immediate sister taxon of the soricid-*Apternodus*-*Oligoryctes*-*Parapternodus*-*Koniaryctes* clade (hereafter referred to as the soricid-fossil zalambdodont clade) is *Solenodon*, followed by tenrecids, *Nesophontes*, and *Centetodon* as successively distant sister taxa. Subsequent sister taxa are a palaeoryctid group (consisting of the Silver Coulee taxon, *Eoryctes*, and *Pararyctes*), erinaceids, *Micropternodus*, macroscelidids, and finally the placental root as defined by *Didelphis*.

Higher-level relationships change slightly according to the unordered MPTs (fig. 57B). The positions of tenrecids and *Solenodon* switch, with tenrecids as the sister taxon to a soricid-fossil zalambdodont clade. Similarly, *Centetodon* and *Nesophontes* switch places, followed by the Silver Coulee taxon, palaeoryctids, *Micropternodus*, erinaceids, and elephant shrews. Neither the Silver Coulee taxon nor *Micropternodus* are reconstructed within palaeoryctids or erinaceids, respectively.

Six taxa are composed of over 50% missing data. *Koniaryctes* has the most (91.5%), followed by *Parapternodus* (82.2%), the Tabernacle Butte and Silver Coulee taxa (both with 76.3%), and *Micropternodus* and *Eoryctes* (both with 51.7%). *Domnina* is slightly above half complete at 40.7% missing data. Taxa with large amounts of missing data may contribute to low resolution and/or support in some analyses, but this is not always the case (Gauthier et al., 1988; Novacek, 1992). In any event, it is worth exploring the possibility that the exclusion of such taxa will affect resolution and/or support in this analysis.

When the aforementioned seven taxa are excluded from the ordered analyses, the strict consensus topology (fig. 58A) loses a great deal of resolution, only supporting the monophyly of soricids, *Solenodon*, *Oligoryctes*, elephant shrews, *Apternodus*, and Montana and Wyoming subclades of *Apternodus*. The unordered, reduced-taxon analysis is slightly more resolved (fig. 58B), showing a soricid-fossil zalambdodont clade plus *Microgale*, *Solenodon*, and *Nesophontes*, followed by *Centetodon*, *Pararyctes*, an erinaceid-macroscelidid clade, and *Setifer* as successively distant sister taxa. Both reduced-taxon analyses support an *Apternodus* clade, as well as Montana (*A. baladontus–A. mediaevus*) and Wyoming (*A. gregoryi–A. major*) subclades.

Both reduced-taxon analyses show increases in branch support at several low-level nodes, including *Apternodus*, *Solenodon*, *Oligoryctes*, soricids, and macroscelidids. Support remains low for the partially resolved soricid-fossil zalambdodont clade in the reduced-taxon, unordered analysis (which also contains *Microgale* and *Nesophontes*). This clade is completely unresolved in the reduced-taxon, ordered analysis.

DISCUSSION

The hierarchical pattern among the 30 terminal taxa produced by the anatomical data described above can be interpreted to unambiguously support six clades that appear across the four analyses just described: *Apternodus*, *Solenodon*, *Oligoryctes*, soricids, macroscelidids, and a clade within *Apternodus* composed of *A. mediaevus* and *A. baladontus*. Other clades are consistently recognized, but have weaker branch supports than the previous six: *A. gregoryi* and *A. major*, parapternodontids plus soricids, *Oligoryctes* plus the Tabernacle Butte taxon, and a soricid-fossil zalambdodont clade. A case may also be made for the placement of oligoryctids as sister taxon to parapternodontids-soricids, *Solenodon* as a sister to soricids-fossil zalambdodonts, and the Silver Coulee taxon within palaeoryctids. However, acceptance of these groups requires an *a*

priori appeal to the process of ordered character evolution.

Of the 20 characters hypothesized to comprise ordered morphoclines, 15 are optimized consistently based on examination of each of the four shortest topologies produced by an analysis in which these 20 characters are ordered (table 6). This iterative procedure based on congruence is the same as that used for testing primary homology across characters (Lipscomb, 1992), which has been justified at length elsewhere (e.g., Farris, 1983; dePinna, 1991). The topology based on the ordered data set (fig. 57A) allows for more explicit hypotheses of *Apternodus* relationships to be made. Hence, we base further discussion on the strict consensus of the ordered topologies.

Temporal Ranges of Fossil Zalambdodonts

The geological ranges of *Apternodus*, *Oligoryctes*, *Parapternodus*, and *Koniaryctes* may now be defined with greater precision than was previously possible. These ranges are summarized in table 7 and figure 59. The family Apternodontidae, because it is here limited to *Apternodus*, has a shorter range than previously estimated, with a first appearance in the early Duchesnean and a last appearance in the early Orellan. The longest-lived fossil zalambdodont is *O. altitalonidus*, with a first appearance in the early Uintan and last appearance in the late Orellan. Based on the phylogeny presented here, we hypothesize that *O. altitalonidus* and the much more temporally limited *O. cameronensis* have ghost lineages (Norell, 1992) extending back into the Bridgerian, corresponding with the range of the Tabernacle Butte taxon.

The oldest definitive soricid fossils are late Uintan in age (Krishtalka and Setoguchi, 1977; Storer, 1984), not basal Uintan as figured by Harris (1998: 135). Nessov and Gureyev (1981) argued that soricids first appeared in the late Cretaceous based on a small, edentulous dentary preserving part of the mandibular condyle and a pocketed coronoid process, the holotype for their taxon *Cretasorex*. However, both the identification and age assignment of this specimen have been questioned (McKenna and Bell, 1997: 81).

Based on the relationship hypothesized here between soricids and parapternodontids, we hypothesize that members of a stem soricid lineage extend back to the Wasatchian. If the postulated relationships among these soricids and extinct zalambdodonts is correct, then stem lineage representatives of *Apternodus* and *Oligoryctes* should also be present in the Wasatchian, again corresponding with the appearance of parapternodontids in that interval (fig. 59).

The identification of soricid, apternodontid, and oligoryctid ghost lineages in the Wasatchian is not synonymous with the belief that full-blown representatives of these groups, with anatomical complexes such as a dual jaw joint, lambdoid plates, and an enlarged foramen ovale (respectively), existed at that time. Nor are we proposing that parapternodontids comprise the actual ''ancestors'' of modern soricids (Wiley, 1981: 106–107; but see Prothero and Lazarus, 1980). Rather, the sister-taxon relationship between parapternodontids and soricids, and between the latter clade and *Oligoryctes* and *Apternodus*, leads to the hypothesis that soricids, apternodontids, and oligoryctids evolved from an unknown population related to parapternodontids during the early Eocene, as illustrated in figure 59. The recognition of such cladogenetic events has no necessary bearing on the timing of character evolution within a postulated ghost lineage (Hennig, 1965; Norell, 1992). Lambdoid plates, for example, may not have evolved until long after the first appearance of the *Apternodus* stem lineage. Such inferences require a better paleontological record (including, for example, more fossils from the Wasatchian and Bridgerian) than that currently available.

Character Optimization and Supraspecific Phylogeny

Figure 60 shows the strict consensus of the 15-character ordered analysis with unambiguous character changes illustrated graphically. Below, we highlight the more important aspects of character evolution in higher-level groups not discussed previously in the section on alpha taxonomy, as they relate to this

TABLE 7
First and Last Appearances of "Apternodontids" in North America

Taxon	First appearance	Last appearance
Apternodus	early Duchesnean (Badwater 20, Wyoming)	early Orellan (Torrington, Wyoming)
A. mediaevus	middle Chadronian (Pipestone Springs, Montana)	late Chadronian (West Easter Lily and 10N, Montana)
A. baladontus	late Duchesnean (Diamond O Ranch, Montana)	middle Chadronian (Little Pipestone Creek, Montana)
A. brevirostris[a]	middle Chadronian (Flagstaff Rim, Wyoming)	middle Chadronian (Flagstaff Rim, Wyoming)
A. gregoryi	middle-late Chadronian (Dilts Ranch, Wyoming)	early Orellan (Torrington, Wyoming)
A. iliffensis	Duchesnean (Beaver Divide, Wyoming; Red Mound, Texas)	middle Chadronian (Iliff and Fremont Butte, Colorado)
A. major	middle-late Chadronian (Dilts Ranch, Wyoming)	middle-late Chadronian (Dilts Ranch, Wyoming)
A. dasophylakas	Chadronian (Harshman Quarry, Wyoming)	Chadronian (Harshman Quarry, Wyoming)
Oligoryctes (including Tabernacle Butte taxon)	Bridgerian (Elderberry Canyon, UT; Powder Wash, UT; Tabernacle Butte, Wyoming)	late Orellan (Cook Ranch, Montana)
O. cameronensis	early Chadronian (Eureka Valley Rd., Montana)	middle Chadronian (Cameron Spring, Wyoming; Flagstaff Rim, Wyoming; Pipestone Springs, Montana)
O. altitalonidus	early Uintan (East Fork Basin, Tepee Trail Fm., Wyoming)	late Orellan (Cook Ranch Fm., Montana)
Tabernacle Butte taxon	Bridgerian (Elderberry Canyon, NV; Powder Wash, UT; Tabernacle Butte, Wyoming)	earliest Uintan (Sand Wash Basin, Colorado)
Koniaryctes	early Wasatchian (Powder River Basin, Wyoming)	early Wasatchian (Powder River Basin, Wyoming)
Parapternodus	early Wasatchian (Clark's Fork and Big Horn Basins, Wyoming)	early Wasatchian (Clark's Fork and Big Horn Basins, Wyoming)
Silver Coulee taxon	Puercan (Clark's Fork Basin, Wyoming)	Tiffanian (Clark's Fork Basin, Wyoming)

[a] Age of *A. brevirostris* type (AMNH 22466) from "Bates's Hole" of Matthew (1910) unknown, probably Chadronian.

topology. Most of these character changes apply also to the unordered analysis; exceptions are noted. It is also important to point out that most of the following characters displayed in figure 60 show homoplasy in other parts of the tree, but are nevertheless optimized as local synapomorphies for the groups indicated.

Montana *Apternodus*

A clade uniting *A. mediaevus* and *A. baladontus* has strong branch support, comparable to those of *Apternodus* itself. Several characters comprise synapomorphies for this group, as follows: a medial ridge on the petrosal comprised of the rostral tympanic process (character no. 6, also present in *A. major*), an enlarged I2 crown (character no. 53, state 1), an enlarged upper canine crown (character no. 54; state 1), three or more roots on P2 (character 57, states 2 and 3), an enlarged P2, similar in size to more molariform premolars (character no. 58; also present in *A. major* and *A. gregoryi*), a molar

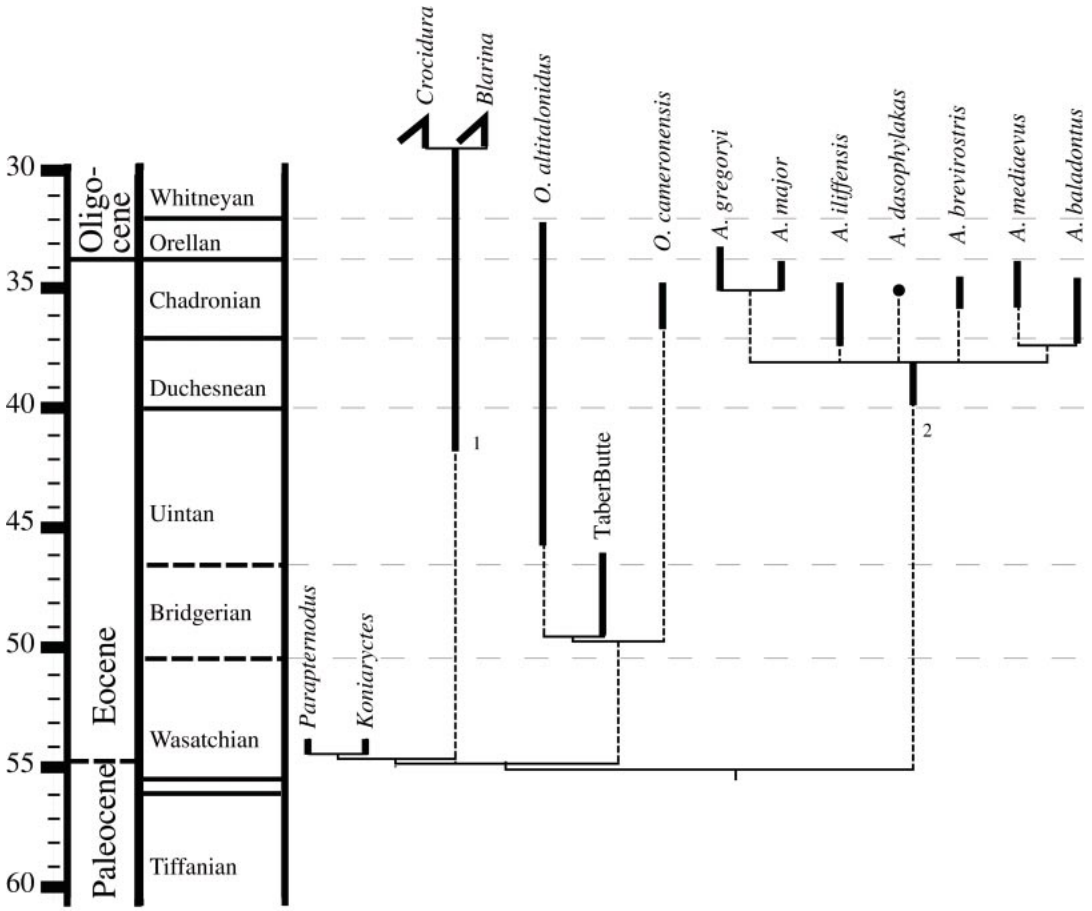

Fig. 59. Phylogeny from figure 57A plotted stratigraphically. Solid lines indicate known ranges; dotted lines indicate ''ghost lineages'' (see text and Norell, 1992). Ghost lineages for unresolved nodes within *Apternodus* are approximations only. The timescale is taken from Prothero (1998) and Prothero and Whittlesey (1998). Notes: 1, earliest definitive record of the Soricidae is late Uintan (Krishtalka and Setoguchi, 1977; Storer, 1984). 2, Earliest North American record of *Apternodus* is based on specifically indeterminate teeth from early Duchesnean deposits at Badwater 20, Wyoming.

toothrow with less occlusal surface than the combined upper C-P2 occlusal area (character no. 65, state 1), and a reduced antemolar cingulid (character no. 81, state 1).

Wyoming *Apternodus*

A. gregoryi and *A. major*, known exclusively from two localities in eastern Wyoming, form a clade to the exclusion of other *Apternodus* species. This group shares five synapomorphies: a lacrimal foramen that is posteriorly flush with the anterior orbit (character no. 36, state 1), an elongate infraorbital canal (character no. 46, state 0), an enlarged P2 (character no. 58, state 0; also present in Montana *Apternodus*), a prominent parastyle on P4 (character no. 61, state 1; polymorphic in *A. brevirostris*), and a minute i2 lacking a distinct alveolus (character no. 75, state 0; also present in *A. mediaevus* and polymorphic in *A. brevirostris*).

Oligoryctes Including the Tabernacle Butte Taxon

The association of *O. cameronensis* and *O. altitalonidus* is consistent and has a branch

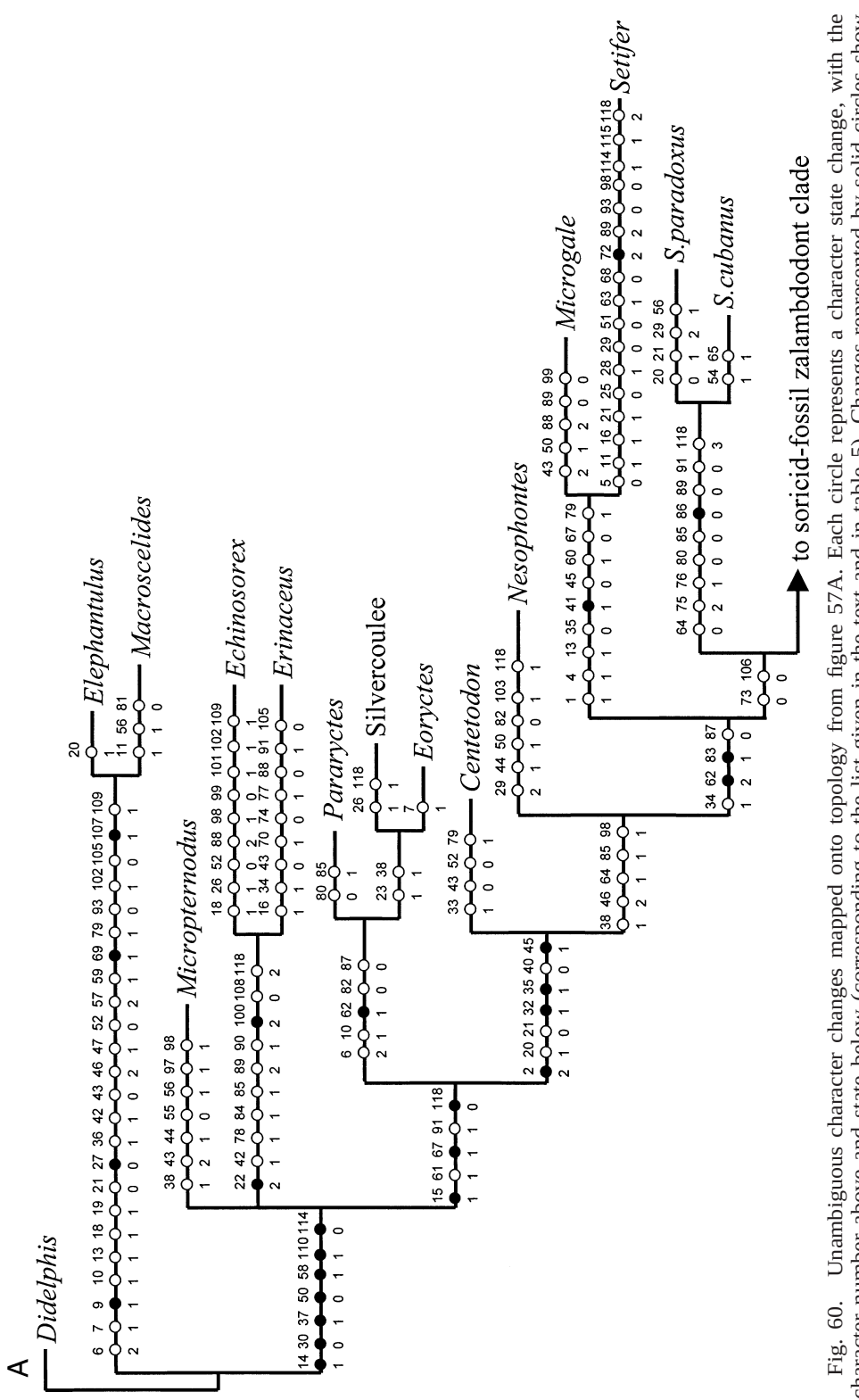

Fig. 60. Unambiguous character changes mapped onto topology from figure 57A. Each circle represents a character state change, with the character number above and state below (corresponding to the list given in the text and in table 5). Changes represented by solid circles show less homoplasy than those represented by open circles.

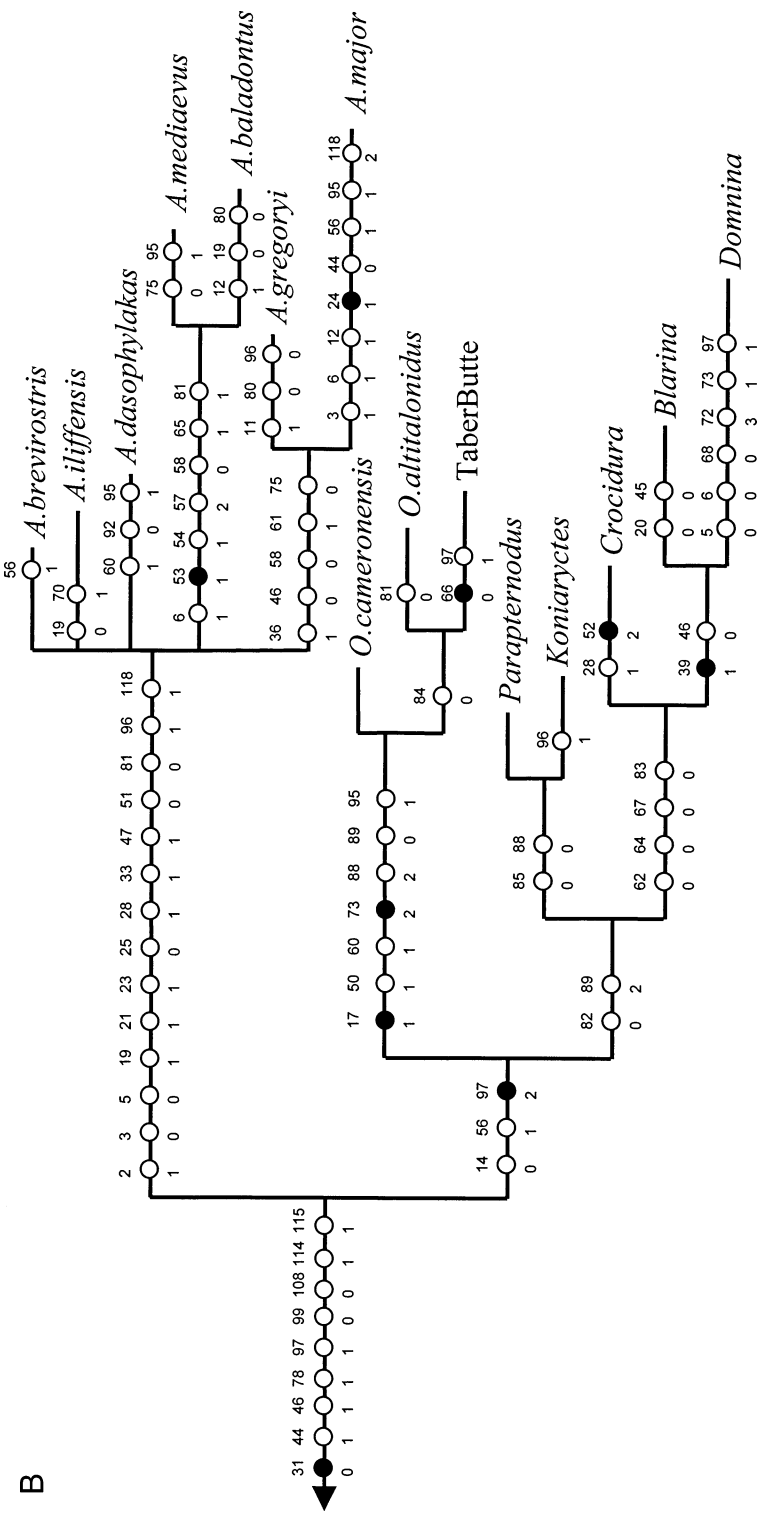

Fig. 60. Continued.

support greater than one in most analyses (figs. 57, 58). However, their relationship is complicated by the fact that when included, the Tabernacle Butte taxon forms a clade with *O. altitalonidus* to the exclusion of *O. cameronensis*. This is based in part on the similar size of the molar trigonids in *O. altitalonidus* and the Tabernacle Butte taxon (character no. 84, state 0), whereas in *O. cameronensis*, the size decrease from the trigonid of m1 to that of m3 is considerable (fig. 42). All three species share an elongate m3 (character no. 89, state 0) with a tall talonid cusp (character no. 88, state 2). The *O. altitalonidus*-Tabernacle Butte clade also owes its existence to the fact that most of the synapomorphies uniting the larger two *Oligoryctes* species are unknown in the Tabernacle Butte taxon, and are therefore optimized by parsimony algorithms as also present in the latter taxon, comprising testable predictions about the as yet unknown anatomy of this animal. These characters include an enlarged foramen ovale (character no. 17, state 1), similarly sized upper incisors (character no. 50, state 1), an elongate P3 (character no. 60, state 1), tricuspid lower incisors (character no. 73, state 2), and a laterally bowed or convex coronoid process of the mandible (character no. 95, state 1). Taxonomically, according to the MPTs represented in figure 57, the Tabernacle Butte taxon should be regarded as a species of *Oligoryctes*.

An important similarity between *O. cameronensis* and *O. altitalonidus* not shared with the Tabernacle Butte taxon is the medially pocketed coronoid process (character no. 97, state 2). In the latter taxon, the internal aspect of the coronoid fossa is deep, but not pocketed (47). However, the pocketed coronoid is optimized as primitive for *Oligoryctes* itself (60). In the ordered analyses, it appears in the stem leading to oligoryctids, parapternodontids, and soricids, and reverses to an ''internally deep'' state (character no. 97, state 1) independently in the Tabernacle Butte taxon and *Domnina*.

Parapternodontids and Soricids

As with the Tabernacle Butte taxon, the high percentage of missing data in *Parapternodus* and *Koniaryctes* greatly magnifies the impact of the few characters that are known. Synapomorphies for a parapternodontid clade consist of a reduced buccal cingulum on m2 (character no. 85; state 0) and an absent m3 talonid cusp (character no. 88, state 0). A clade of parapternodontids plus soricids is supported by two synapomorphies: a premolariform p4 (character no. 82, state 0; missing in *Koniaryctes*) and an anteroposteriorly short m3 (character no. 89, state 2). Additionally, missing characters of the skull and postcranium in parapternodontids are optimized so as to resemble character states exhibited by shrews and *Apternodus*, as discussed below.

Parapternodontids, Soricids, and *Oligoryctes*

The conclusion indicated by the ordered analyses (figs. 57A, 60) that small, extinct, North American zalambdodonts and soricids are closely related is not completely novel. Simpson (in McGrew et al., 1959) first hinted at this possibility when he suggested that an edentulous mandibular fragment of the Tabernacle Butte taxon (AMNH 55689) could be a shrew. The single character known for most taxa and optimized as a synapomorphy at this node is a pocketed coronoid process of the dentary (character no. 97, state 2; missing in *Koniaryctes*, reversed to state 1 in the Tabernacle Butte taxon and *Domnina*). Two other characters present in shrews and the larger two species of *Oligoryctes* have also been optimized as synapomorphies at this node: an absent alisphenoid canal (character no. 14, state 0) and lack of an antemolar diastema (character no. 56, state 1).

Parapternodontids, Soricids, *Oligoryctes*, and *Apternodus*

A clade uniting the preceding four groups into a fossil zalambdodont-soricid clade is supported by several craniodental and postcranial characters. These include presence of an anterior sinus canal foramen (character no. 31, state 0; unknown in *A. dasophylakas*, *O. altitalonidus*, the Tabernacle Butte taxon, parapternodontids, and *Domnina*), reduction of the maxillary process of the zygoma (character no. 44, state 1; reversed in *A. ma-*

jor, unknown in the Tabernacle Butte taxon and parapternodontids), an infraorbital canal similar in length to the width of the anterior exit foramen (character no. 46, state 1; elongate in *Blarina*, *A. major*, and *A. gregoryi*, unknown in the Tabernacle Butte taxon and parapternodontids), a single-rooted p2 (character no. 78, state 1; unknown in *A. iliffensis*, the Tabernacle Butte taxon, and parapternodontids; uncodable for soricids—see above), and a medially deep coronoid process (character no. 97, state 1; unknown in *Koniaryctes*) which in the ordered analysis is intermediate between the pocketed condition seen in *Parapternodus*, *O. cameronensis*, *O. altitalonidus*, and shrews, and the medially flat condition seen in (for example) *Setifer*.

Although postcranial remains of extinct zalambdodonts are exceedingly scarce, the fossils that are known show several interesting similarities with modern shrews, here interpreted as synapomorphies. Importantly, these postcranial characters are unknown for *Oligoryctes* and parapternodontids, but are optimized as present based on the distribution of craniodental characters and the consequent topologies of both ordered and unordered analyses depicted in figure 57. These resemblances to shrews are as follows: the axis of *A. dasophylakas* (fig. 37) has a prominent ventral keel on its centrum (character 99, state 0; also present in *Microgale* and *Echinosorex*); distal ulnae of *A. mediaevus* (fig. 10) and *A. major* (fig. 34) show a relatively broad articulation with the carpus (character no. 108, state 0; also present in erinaceids); the posterior aspect of the proximal femur in *A. gregoryi* (fig. 24) shows a noncontinuous ridge between greater and lesser trochanters (character no. 114, state 1; also present in *Didelphis*, *Setifer*, and some macroscelidids); and the femoral head and greater trochanter of *A. gregoryi* (fig. 24) are not separated by a deep notch (character no. 115, state 1; also present in *Didelphis* and *Setifer*).

Position of Tenrecids and *Solenodon*

As noted previously, the ordered analysis favors *Solenodon* as the sister taxon to a soricid-fossil zalambdodont clade, whereas the unordered analysis favors tenrecids. In favor of the latter, tenrecids and fossil zalambdodonts share a reduced hypocone (character 64, state 1; reversed in soricids, unknown in *Koniaryctes*). Tenrecids, *Apternodus*, *Oligoryctes*, and shrews also share a prominent buccal cingulid on m2 (character 85, state 1; reversed in parapternodontids, polymorphic in *A. baladontus*); and tenrecids and extant shrews share an elongate calcaneal tubercle (character 117, state 1; unknown in *Domnina* and all fossil zalambdodonts). Asher (1999) recovered a tenrecid-*Apternodus* clade under several (but not all) assumption sets regarding character ordering and weighting. These analyses used a slightly smaller morphological data set than that used here, with a single, chimaeric terminal taxon representing *Apternodus* (Asher, 1999: appendix 1), without *Oligoryctes* or other fossil zalambdodonts, but with a larger sample of tenrecid genera. Because the present data set has a much better sample of North American zalambdodonts, we believe it conveys a more accurate picture of the relationships of these fossil taxa than the study of Asher (1999). Nevertheless, future analyses that include more tenrecs and soricids, in addition to a diverse sample of extinct zalambdodonts, are clearly desirable.

At least two characters are consistent with the status of *Solenodon* as the fossil zalambdodont-soricid sister taxon. *Solenodon*, *Apternodus*, and extant soricids share a unicuspid lower incisor (character no. 73, state 0; unknown in *A. iliffensis*, parapternodontids, and the Tabernacle Butte taxon, bicuspid in *Domnina*, tricuspid in *Oligoryctes*). *S. paradoxus*, *A. major*, *A. mediaevus*, *A. brevirostris*, and extant soricids also share a solid distal humerus, lacking an olecranon fenestra (character 106, state 0; polymorphic in *S. cubanus*, missing in other fossil taxa). Another interesting similarity is the homoplastic convergence between species of *Apternodus* from Montana and *Solenodon cubanus*. In these three taxa, elements of the upper and lower anterior dentition are enlarged and bulbous (character no. 54, state 1; see figs. 6, 9, 11, 13), a condition to our knowledge not seen in any other insectivoran-grade taxon. While such ''underlying synapomorphy'' (Saether, 1979; Lockwood, 1999) does not contribute directly to

strengthening this clade, it is recognized in the ordered analysis (fig. 57A) as occurring within a fairly small group of insectivorangrade mammals, including *Solenodon*, soricids, and fossil zalambdodonts, and excluding tenrecids, *Nesophontes*, *Centetodon*, palaeoryctids, erinaceids, *Micropternodus*, and macroscelidids.

Both tenrecs and *Solenodon* share with fossil zalambdodonts two dental characters that are reversed in soricids. These are an absent metacone (character no. 62, state 2) and a reduced talonid basin (character 83, state 1). They also share the presence of a paraconid notch (character no. 87, state 0; reversed in *Koniaryctes* and soricids).

Identity of the Silver Coulee Taxon

The laterally exposed lambdoid plates of the Silver Coulee taxon (Wood et al., 2000) are similar in gross appearance to those of *Apternodus*, but the jaw joint is not. Posterior support for the mandibular condyle in YPM PU16521 is provided by a true postglenoid process, lateral to the postglenoid foramen and pars cochlearis of the petrosal (fig. 51). This contrasts to the entoglenoid process of *Apternodus* and *Oligoryctes*, which is medial to the postglenoid foramen and anterior to the promontory (e.g., figs. 11D and 40; character no. 32, state 1), and is consistent with the association of the Silver Coulee specimen with the palaeoryctids *Pararyctes* and *Eoryctes* (fig. 40A) as reconstructed in the ordered analysis (fig. 57A).

Furthermore, as noted by Thewissen and Gingerich (1989), the palaeoryctid *Eoryctes* appears also to have possessed lambdoid plates on its posterolateral braincase, although they are not as well preserved in the *Eoryctes* holotype as they are in YPM PU16521. Similar convergence in the development of boxlike muscle attachments on the posterior braincase has occurred in the erinaceid *Proterix bicuspis*, also originally believed (erroneously; see Gawne, 1968) to be related to *Apternodus* (Macdonald, 1951).

The Silver Coulee taxon is reconstructed as the sister taxon to *Eoryctes* and nested within palaeoryctids in the ordered analysis (fig. 57A), and as the sister taxon to a *Nesophontes-Centetodon*-soricid-fossil zalambdodont clade, with palaeoryctids attaching at a more basal node in the unordered analysis (fig. 57B). Characters supporting its status as closely related to *Eoryctes* include presence of lambdoid plates (character no. 23, state 1) and incomplete zygomatic arches (character no. 38, state 1); notably these character states are present in *Apternodus* as well, but are optimized as homoplastic in the two taxa based on the distribution of other characters summarized here. Supporting its status as a palaeoryctid is the rostral tympanic process of the petrosal, which contributes to the medial wall of the auditory bulla (character no. 6, state 2). Possession of a true postglenoid process supporting the jaw joint posteriorly (character no. 32, state 0) is optimized on both trees as primitive for palaeoryctids and is consistent with the placement of the Silver Coulee taxon outside of a zalambdodont-soricid-*Centetodon-Nesophontes* clade. Whether or not it is a palaeoryctid, we do not believe that the Silver Coulee taxon is closely related to *Apternodus*.

Affinities of *Micropternodus*

When all 20 multistate morphoclines identified in table 6 are treated as ordered, *Micropternodus* is reconstructed as the sister taxon to erinaceids. Two characters are optimized in support of this clade: a single-rooted P2 (character no. 57, state 0) and a short M3 stylar region (character no. 71, state 0). However, this arrangement falls apart when the five multistate characters with nonadjacent changes (table 6) are treated as unordered. Similarly, when all characters are treated as unordered, *Micropternodus* is placed between erinaceids and the remaining ingroup taxa (fig. 57B), sharing with most of the latter taxa a reduced zygomatic arch (character no. 38, state 1) and seven lower antemolars (character no. 72, state 1).

After Russell (1960) synonymized ''*Kentrogomphios*'' White (1954) with *Micropternodus* Matthew (1903), and after Stirton and Rensberger (1964) suggested that it was related to ''erinaceoids'', additional material of micropternodontids has been recovered, most notably from Asia. As illustrated by McKenna et al. (1984), *Prosarcodon lonanensis* has decidedly non-zalambdodont teeth, with

large talonid basins and distinct metacones. McKenna et al. further noted the similarity of the middle ear of *Prosarcodon* with that of *Palaeoryctes*. We agree with their implication that micropternodontids are not closely related to apternodontids, oligoryctids, or parapternodontids. More definitive conclusions about the affinities of *Micropternodus* must await an analysis that has a better sample of erinaceomorphs, palaeoryctids, and Asian micropternodontids.

SUMMARY AND CONCLUSIONS

One of the major challenges of modern paleontology is understanding how extinct biological diversity has contributed to the evolution of modern groups. Reconstructing the history of the ''Insectivora'' is particularly difficult given their perceived status as primitive among placental mammals, and the strong possibility that they do not comprise a natural, monophyletic group (Stanhope et al., 1998; Emerson et al., 1999; Murphy et al., 2001). We have attempted in the preceding pages to make sense of a relatively small assemblage of extinct insectivoran-grade mammals, previously known in the literature as the ''Apternodontidae'', and infer the extent to which they comprise a natural group unto themselves and are phylogenetically related to modern insectivoran-grade taxa.

Our analysis has several consequences. First, we propose to restrict the family Apternodontidae to the genus *Apternodus*, composed of seven species present in North America from the late middle Eocene through early Oligocene: *A. mediaevus*, *baladontus*, *brevirostris*, *iliffensis*, *dasophylakas*, *major*, and *gregoryi*. Clark's (1937) ''*A.*'' *altitalonidus* is more closely related to *Oligoryctes cameronensis* and the Tabernacle Butte taxon; as such, we formalize the combination *Oligoryctes altitalonidus*. Although it is incompletely known, the nested position of the Tabernacle Butte taxon adjacent to *O. altitalonidus*, with *O. cameronensis* as sister taxon to both, indicates that the generic designation of the Tabernacle Butte taxon should be *Oligoryctes*.

Contrary to previous conceptions of the family Apternodontidae, extinct, North American, zalambdodont placentals do not share a common ancestor to the exclusion of all other mammals. In this analysis, extant soricids are reconstructed as sister taxa to parapternodontids, a clade which is in turn closely related to *Oligoryctes* and *Apternodus*. Slightly more resolution for these taxa is achieved with the use of ordered characters, which support *Oligoryctes* as the sister taxon to a soricid-parapternodontid clade. This arrangement admittedly has weak branch support (fig. 57). Nevertheless, soricids share with one or more North American fossil zalambdodonts several characters, detailed above, including a medially pocketed coronoid process of the mandible, a premolariform p4, a mesiodistally short m3, a reduced maxillary zygoma, an absent alisphenoid canal, anterior sinus canal and posterior nasal foramina, and morphology of the proximal femur. In general, we are impressed by the similarities among *Apternodus*, *Oligoryctes*, parapternodontids, and soricids, and predict that future fossil discoveries will support the affiliation of these primarily North American fossil zalambdodonts with the Soricidae.

Another possible character linking some soricids to fossil zalambdodonts is tooth pigmentation. As detailed above, this appears to have been present in many specimens of *Apternodus*. We have opted not to include this character in our phylogenetic analyses due to the difficulty in establishing its presence consistently in fossil specimens. We would, however, encourage future researchers to examine more closely the distribution of this character in fossil zalambdodonts, shrews, and other extant taxa such as *Solenodon*.

As noted previously, McDowell (1958) argued forcefully against the association of *Apternodus* and *Oligoryctes* with any insectivoran-grade mammal, particularly shrews and *Solenodon*. In addition, McDowell was one of only a few 20th century morphologists who deemphasized the dentition in trying to infer insectivoran-grade relationships. We would agree with McDowell (1958) that dental zalambdodonty is not a shared, derived character complex of all of the placentals (notably tenrecs, golden moles, *Solenodon*, *Apternodus*, *Oligoryctes*, and parapternodontids) in which it occurs. Given the relative strength of molecular data supporting the affiliation of tenrecs and golden moles

with endemic African mammals (Stanhope et al., 1998; Murphy et al., 2001), it appears likely that these African zalambdodonts are not closely related to soricids or their North American fossil relatives.

However, as evident in the preceding pages, the material upon which McDowell based his assessment of fossil zalambdodonts is extremely limited compared to the present sample. We believe that his opinion that *Apternodus* is more closely related to creodonts than to North American insectivoran-grade placentals is incorrect. With the qualification that further tests including more extant (e.g., a greater variety of soricids) and fossil (e.g., nyctitheriids) taxa are desirable, we tentatively conclude that parapternodontids, *Apternodus*, and *Oligoryctes* were part of a radiation of insectivoran-grade placental mammals that has played an integral role in the evolution of modern soricids.

ACKNOWLEDGMENTS

We thank the following colleagues for their cooperation over many years in permitting study of specimens under their care: the late Craig C. Black, formerly of the Carnegie Museum of Natural History; William A. Clemens, Jr., of the University of California at Berkeley; Mary R. Dawson, Carnegie Museum of Natural History; John J. Flynn, William F. Simpson, and William D. Turnbull of the Field Museum of Natural History; John Alexander, Robert Evander, and the late Childs Frick, American Museum of Natural History; the late C. Lewis Gazin, formerly of the National Museum of Natural History, Smithsonian Institution; Morton Green, formerly of the South Dakota School of Mines and Technology; Philip Gingerich and Gregg Gunnell of the University of Michigan; Desui Miao and the late E. Raymond Hall of the University of Kansas; Farish Jenkins, Maria Rutzmoser, Phoebe Eckfeldt, and the late Bryan Patterson, Harvard University; the late Glenn L. Jepsen, Princeton University; Jason A. Lillegraven, Michael Cassiliano, Brian Kraatz, and Ilsa Lund of the University of Wyoming; Pamela Owen of the Texas Memorial Museum; Peter Robinson, University of Colorado Museum; the late Donald E. Savage, University of California at Berkeley; George Stanley and the late Robert W. Fields, University of Montana; Richard Stucky and Logan Ivy of the Denver Museum of Nature and Science; and Craig Wood of Providence College.

Jason A. Lillegraven (University of Wyoming), Peter Robinson (University of Colorado), Richard Stucky (Denver Museum of Nature and Science), Craig Wood (Providence College), Jonathan Bloch, Philip Gingerich, and Gregg Gunnell (University of Michigan), and the late Morris F. Skinner (American Museum of Natural History) have kindly shared unpublished data with us. We are also indebted to Pat Luckett for sharing his expertise on mammalian dental homologies, to Diego Pol for assistance using phylogeny software, and to James Orr for finding and permitting the preparation and study of the McCarty's Mountain *Apternodus* skull, now part of the collection of the Field Museum of Natural History.

We thank Meng Jin, Chester Tarka, and Lorraine Meeker for help with photography and artwork, and Jeanne Kelly and Otto Simonis for specimen preparation. Chester Tarka took the photographs shown in figures 9, 11, 43, 44, 46, 51, and the occlusal view in figure 12, and illustrated the frontispiece and figure 47. Lawrence Isham illustrated figures 38 and 39. The remaining photographs and figures were made by the senior author using equipment and software generously made available by Meng Jin. We thank Jason A. Lillegraven and an anonymous reviewer for providing insightful critiques of this manuscript.

This paper has had an extraordinarily long gestation, and many of those who have helped are now deceased. We dedicate it to their memory. In particular, we wish to remember our coauthor, colleague, and friend, the late Dr. Donald G. Kron.

REFERENCES

Allen, G.M. 1910. Mammals of the West Indies. Bulletin of the Museum of Comparative Zoology, Harvard University, 54: 175–263.

Ärnbäck-Christie-Linde, A. 1912. On the development of the teeth of the Soricidae: an ontogenetical inquiry. Annals and Magazine of Natural History 9(8): 601–624.

Asher, R.J. 1999. A morphological basis for as-

sessing the phylogeny of the ''Tenrecoidea'' (Mammalia, Lipotyphla). Cladistics 15: 231–252.

Asher, R.J. 2000. Phylogenetic history of tenrecs and other insectivoran mammals. Ph.D. dissertation, State University of New York at Stony Brook.

Asher, R.J. 2001. Cranial anatomy in tenrecid insectivorans: character evolution across competing phylogenies. American Museum Novitates 3352: 1–54.

Asher, R.J., and M.R. Sánchez-Villagra. 2000. Jurassic molars in modern mammals: 150 million years of zalambdodont teeth. Journal of Vertebrate Paleontology 20(3): 27A.

Black, C.C., and M.R. Dawson. 1966a. A review of late Eocene mammalian faunas from North America. American Journal of Science 264: 321–349.

Black, C.C., and M.R. Dawson. 1966b. Paleontology and geology of the Badwater Creek area, central Wyoming. Annals of the Carnegie Museum 38(13): 297–307.

Bown, T.M., and M.J. Kraus. 1979. Origin of the tribosphenic molar and metatherian and eutherian dental formulae. *In* J.A. Lillegraven (editor), Mesozoic mammals: the first two-thirds of mammalian history: 172–181. Berkeley: University of California Press.

Bown, T.M., and D. Schankler. 1982. A review of the Proteutheria and Insectivora of the Willwood Formation (Lower Eocene), Bighorn Basin, Wyoming. U.S. Geological Survey Bulletin 1523: 1–79.

Bremer, K. 1988. The limits of amino-acid sequence data in angiosperm phylogenetic reconstruction. Evolution 42: 795–803.

Bremer, K. 1994. Branch support and tree stability. Cladistics 10: 295–304.

Butler, P.M. 1937. Studies of the mammalian dentition—I. The teeth of *Centetes ecaudatus* and its allies. Proceedings of the Zoological Society of London 107: 103–132.

Butler, P.M. 1956. The skull of *Ictops* and the classification of the Insectivora. Proceedings of the Zoological Society of London 126: 453–481.

Butler, P.M. 1972. The problem of insectivore classification. *In* K.A. Joysey and T.R. Kemp (editors), Studies in vertebrate evolution: 253–265. Edinburgh: Oliver and Boyd.

Butler, P.M. 1985. The history of African insectivores. Acta Zoologica Fennica 173: 215–217.

Butler, P.M. 1988. Phylogeny of the insectivores. *In* M.J. Benton (editor), The phylogeny and classification of the tetrapods, Vol. 2: Mammals: 117–141. Systematics Association Special Volume 35B. Oxford: Clarendon Press.

Carpenter, J.M. 1988. Choosing among equally parsimonious cladograms. Cladistics 4: 291–296.

Cartmill, M., and R.D.E. MacPhee. 1980. Tupaiid affinities: the evidence of the carotid arteries and cranial skeleton. *In* P. Luckett (editor), Comparative biology and evolutionary relationships of tree shrews: 95–132. New York: Plenum.

Clark, J. 1937. The stratigraphy and paleontology of the Chadron Formation in the Big Badlands of South Dakota. Annals of the Carnegie Museum 25: 261–350.

Clark, J., J.R. Beerbower, and K.K. Kietzke. 1967. Oligocene sedimentation, stratigraphy, paleoecology, and paleoclimatology in the Big Badlands of South Dakota. Fieldiana Geology 5: 1–158.

Cope, D.A. 1991. Measurements of dental variation as indicators of multiple taxa in samples of sympatric *Cercopithecus* species. *In* W.H. Kimbel and L.B. Martin (editors), Species, species concepts, and primate evolution: 211–237. New York: Plenum.

Cracraft, J. 1983. Species concepts and speciation analysis. *In* R. Johnston (editor), Current Ornithology: 159–187. New York: Plenum Press.

Dannelid, E. 1998. Dental adaptations in shrews. *In* J.M. Wojcik and M. Wolsan (editors), Evolution of shrews: 157–172. Bialowieza: Polish Academy of Sciences.

dePinna, M.C.C. 1991. Concepts and tests of homology in the cladistic paradigm. Cladistics 7: 367–394.

Edinger, T. 1964. Midbrain exposure and overlap in mammals. American Zoologist 4: 5–19.

Emerson, G.L., C.W. Kilpatrick, B.E. McNiff, J. Ottenwalder, and M.W. Allard. 1999. Phylogenetic relationships of the order insectivora based on complete 12s rRNA sequences from mitochondria. Cladistics 15: 221–230.

Emry, R.J. 1973. Striatigraphy and preliminary biostratigraphy of the Flagstaff Rim area, Natrona County, Wyoming. Smithsonian Contributions to Paleobiology 18: 1–43.

Emry, R.J. 1975. Revised Tertiary stratigraphy and paleontology of the western Beaver Divide, Natrona County, Wyoming. Smithsonian Contributions to Paleobiology 25: 1–20.

Emry, R.J. 1979. Review of *Toxotherium* (Perissodactyla: Rhinocerotoidea) with new material from the Early Oligocene of Wyoming. Proceedings of the Biological Society of Washington 92(1): 28–41.

Emry, R.J. 1990. Mammals of the Bridgerian (middle Eocene) Elderberry Canyon local fauna of eastern Nevada. Geological Sociey of America Special Paper 243: 187–210.

Emry, R.J. 1992. Mammalian range zones in the Chadronian White River Formation at Flagstaff Rim, Wyoming. *In* D.R. Prothero and W.A. Berggren (editors), Eocene–Oligocene climatic and biotic evolution: 106–115. Princeton, NJ: Princeton University Press.

Emry, R.J., L.S. Russell, and P.R. Bork. 1987. The Chadronian, Orellan, and Whitneyan North American land mammal ages. *In* M.O. Woodburne (editor), Cenozoic mammals of North America: 118–152. Berkeley, University of California Press.

Farris, J.S. 1982. Outgroups and parsimony. Systematic Zoology 31: 328–334.

Farris, J.S. 1983. The logical basis of phylogenetic analysis. *In* N.I. Platnick and V.A. Funk (editors), Advances in cladistics, vol. 2: 7–36. New York: Columbia University Press.

Farris, J.S. 1989. The retention index and the rescaled consistency index. Cladistics 5: 417–419.

Fernhead, R. W., C.C.D. Shute, and A.A. Bellairs. 1954. The temporomandibular joint of shrews. Proceedings of the Zoological Society of London 125: 795–806.

Frost, D.R., W.C. Wozencraft, and R.S. Hoffman. 1991. Phylogenetic relationships of hedgehogs and gymnures (Mammalia: Insectivora: Erinaceidae). Smithsonian Contributions to Zoology 518: 1–69.

Galbreath, E.C. 1953. A contribution to the Tertiary geology and paleontology of northeastern Colorado. University of Kansas Paleontological Contributions Vertebrata 4: 1–120.

Galbreath, E.C. 1978. An apternodontid (Insectivora) from the Chadronian Oligocene of northeastern Colorado. Transactions of the Kansas Academy of Science 81: 297–302.

Galusha, T. 1975. Childs Frick and the Frick Collection of fossil mammals. Curator 18: 5–15.

Gawne, C.E. 1968. The genus *Proterix* (Insectivora, Erinaceidae) of the upper Oligocene of North America. American Museum Novitates 2315: 1–26.

Gill, T. 1883. On the classification of the insectivorous mammals. Bulletin of the Philosophical Society of Washington 5: 118–120.

Gill, T. 1884. Insectivora. *In* J.S. Kingsley (editor), The standard natural history, vol. 5, Mammals: 134–158. Boston: S.E. Cassino.

Gingerich, P.D. 1976. Paleontology and phylogeny: patterns of evolution at the species level in early Tertiary mammals. American Journal of Science 276: 1–28.

Goloboff, P. 1993. NONA version 1.9 computer program. Shareware available at www.cladistics.org.

Gould, G.C. 1995. Hedgehog phylogeny (Mammalia, Erinaceidae)—the reciprocal illumination of the quick and the dead. American Museum Novitates 3131: 1–45.

Gregory, W.K. 1910. The orders of mammals. Bulletin of the American Museum of Natural History 27: 1–524.

Gregory, W.K., and G.G. Simpson. 1926. Cretaceous mammal skulls from Mongolia. American Museum Novitates 225: 1–20.

Harris, A.H. 1998. Fossil history of shrews in North America. *In* J.M. Wojcik and M. Wolsan (editors), Evolution of shrews: 133–156. Bialowieza: Polish Academy of Sciences.

Hawkins, J.A., C.E. Hughes, and R.W. Scotland. 1997. Primary homology assessment, characters and character states. Cladistics 13: 275–283.

Hennig, W. 1965. Phylogenetic systematics. Annual Review of Entomology 10: 97–116.

Hoganson, J.W., E.C. Murphy, and N.F. Forsman. 1998. Lithostratigraphy, paleontology, and biochronology of the Chadron, Brule, and Arikaree Formations in North Dakota. Geological Society of America Special Paper 325: 185–196.

Hough, M.J. 1956. A new insectivore from the Oligocene of the Wind River Basin, Wyoming, with notes on the taxonomy of the Oligocene Tenrecoidea. Journal of Paleontology 30: 531–541.

Huxley, T.H. 1880. On the application of the laws of evolution to the arrangement of the Vertebrata and more particularly of the Mammalia. Proceedings of the Zoological Society of London 1880: 649–662.

International Commission on Zoological Nomenclature. 1999. International Code of Zoological Nomenclature, 4th ed., adopted by the International Union of Biological Sciences. London: International Trust for Zoological Nomenclature.

Kielan-Jaworowska, Z. 1968. Results of the Polish-Mongolian palaeontological expeditions. Part 1: Preliminary data on the upper Cretaceous eutherian mammals from Bayn Dzak, Gobi Desert. Palaeontologica Polonica 19: 171–191.

Kielan-Jaworowska, Z. 1977. Evolution of therian mammals in the late Cretaceous of Asia. Part 2. Postcranial skeleton in *Kennalestes* and *Asioryctes*. Palaeontologica Polonica 37: 65–83.

Kimbel, W.H., and L.B. Martin. 1991. Species, species concepts, and primate evolution. New York: Plenum.

Kindahl, M. 1959a. Some aspects of the tooth development in Soricidae. Acta Odontologica Scandanavica 17: 203–237.

Kindahl, M. 1959b. The tooth development in *Er-*

inaceus europaeus. Acta Odontologica Scandanavica 17: 467–489

Kluge, A., and J.S. Farris. 1969. Quantitative phyletics and the evolution of anurans. Systematic Zoology 18: 1–32.

Konizeski, R.L. 1961. Paleoecology of an Early Oligocene biota from Douglass Creek Basin, Montana. Geological Society of America Bulletin 72: 1633–1642.

Krishtalka, L., and T. Setoguchi. 1977. Paleontology and geology of the Badwater Creek area, central Wyoming. Part 13. The late Eocene Insectivora and Dermoptera. Annals of Carnegie Museum 46(7): 71–99.

Kron, D.G. 1978. Oligocene vertebrate paleontology of the Dilts Ranch Area, Converse County, Wyoming. M.S. thesis, University of Wyoming, Laramie.

Kuenzi W.D., and R.W. Fields. 1971. Tertiary stratigraphy, structure, and geologic history, Jefferson Basin, Montana. Geological Society of America Bulletin 82: 3373–3394.

Leche, W. 1907. Zur Entwicklungsgeschichte des Zahnsystems der Säugethiere, zugleich ein Beitrag zur Stammesgeschichte dieses Thiergruppe. II. Theil. Phylogenie. 2. Heft. Die Familien der Centetidae, Solenodontidae und Chrysochloridae. Zoologica (Stuttgart) 20(49): 1–157.

Lee, D.C., and H.N. Bryant. 1999. A reconsideration of coding inapplicable characters: assumptions and problems. Cladistics 13: 373–378.

Lillegraven, J.A., M.C. McKenna, and L. Krishtalka. 1981. Evolutionary relationships of middle Eocene and younger species of *Centetodon* (Mammalia, Insectivora, Geolabididae) with a description of the dentition of *Ankylodon* (Adapisoricidae). University of Wyoming Publications 45: 1–115.

Lipscomb, D. 1992. Parsimony, homology, and the analysis of multistate characters. Cladistics 8: 45–65.

Linnaeus (Linné), C. 1758. Systema naturae per regna tria naturae secundum classes, ordines, genera, species, cum characteribus differentiis, synonymis, locis. Vol. 1: Regnum animale. Editio decima, reformata. Stockholm, Laurentii Salvii. [Facsimilie reprinted in 1956 by the British Museum (Natural History).]

Lockwood, C.A. 1999. Homoplasy and adptation in the atelid postcranium. American Journal of Physical Anthropology 108(4): 459–482.

Love, J.D., M.C. McKenna, and M.R. Dawson. 1976. Eocene, Oligocene, and Miocene rocks and vertebrate fossils at the Emerald Lake locality, 3 miles south of Yellowstone National Park, Wyoming. United States Geological Survey Professional Paper 932A: 1–26.

Luckett, W.P. 1993. An ontogenetic assessment of dental homologies in therian mammals. *In* F.S. Szalay, M.J. Novacek, and M.C. McKenna (editors), Mammal phylogeny, vol. 1: Mesozoic differentiation, monotremes, multituberculates, and marsupials: 182–203. New York: Springer.

Macdonald, J.R. 1951. Additions to the Whitneyan fauna of South Dakota. Journal of Paleontology 25(3): 257–265.

MacPhee, R.D.E. 1979. Entotympanics, ontogeny, and primates. Folia Primatologica 31: 23–47.

MacPhee, R.D.E. 1981. Auditory regions of primates and eutherian insectivores: morphology, ontogeny, and character analysis. Contributions to Primatology 18: 1–282.

MacPhee, R.D.E. 1987. The shrew tenrecs of Madagascar: systematic revision and Holocene distribution of *Microgale* (Tenrecidae, Insectivora). American Museum Novitates 2889: 1–45.

MacPhee, R.D.E. 1994. Morphology, adaptations, and relationships of *Plesiorycteropus*, and a diagnosis of a new order of eutherian mammals. Bulletin of the American Museum of Natural History 220: 1–214.

MacPhee, R.D.E., and M.J. Novacek. 1993. Definition and relationships of Lipotyphla. *In* F.S. Szalay, M.J. Novacek, and M.C. McKenna (editors), Mammal phylogeny, vol. 2: Placentals: 13–31. New York: Springer.

MacPhee, R.D.E., M.J. Novacek, and G. Storch. 1988. Basicranial morphology of Early Tertiary erinaceomorphs and the origin of primates. American Museum Novitates 2921: 1–42.

Maddison, D.R. 1993. Missing data versus missing characters in phylogenetic analysis. Systematic Biology 42: 576–581.

Maddison D.R., and W.P. Maddison. 2000. MacClade computer program version 4.0. Sunderland, MA: Sinauer Associates.

Matthew, W.D. 1903. The fauna of the *Titanotherium* beds at Pipestone Springs, Montana. Bulletin of the American Museum of Natural History 19(6): 197–226.

Matthew, W.D. 1910. On the skull of *Apternodus* and the skeleton of a new artiodactyl. Bulletin of the American Museum of Natural History 28(5): 33–42.

Matthew, W.D. 1913. A zalambdodont insectivore from the basal Eocene. Bulletin of the American Museum of Natural History 32(17): 307–314.

McDowell, S.B., Jr. 1958. The Greater Antillean insectivores. Bulletin of the American Museum of Natural History 115(3): 113–214.

McGrew, O., J.E. Berman, M.K. Hecht, J.M. Hummel, G.G. Simpson, and A.E. Wood. 1959. The geology and paleontology of the Elk Mountain and Tabernacle Butte area, Wyoming.

Bulletin of the American Museum of Natural History 117(3): 117–176.
McKenna, M.C. 1960. The Geolabidinae: a new subfamily of early Cenozoic erinaceoid insectivores. University of California Publications in Geological Sciences 37(2): 131–164.
McKenna, M.C. 1975. Toward a phylogeny and classification of the Mammalia. *In* W.P. Luckett and F.S. Szalay (editors), Phylogeny of the primates: a multidisciplinary approach: 21–46. New York: Plenum.
McKenna, M.C. 1980. Late Cretaceous and early Tertiary vertebrate paleontological reconnaissance, Togwotee Pass area, northwestern Wyoming. *In* L.L. Jacobs (editor), Aspects of vertebrate history: 321–343. Flagstaff: Museum of Northern Arizona Press.
McKenna, M.C., and S.K. Bell. 1997. Classification of mammals above the species level. New York: Columbia University Press.
McKenna, M.C., P. Robinson, and D.W. Taylor. 1962. Notes on Eocene mammalia and mollusca from Tabernacle Butte, Wyoming. American Museum Novitates 2102: 1–33.
McKenna, M.C., X. Xue, and M. Zhou. 1984. *Prosarcodon lonanensis*, a new Paleocene micropternodontid insectivore from Asia. American Museum Novitates 2780: 1–17.
Miller, G.S. 1907. The families and genera of bats. Bulletin of the United States National Museum 57: 1–282.
Murphy, W.J., E. Eizirik, W.E. Johnson, Y.P. Zhang, O.A. Ryder, and S.J. O'Brien. 2001. Molecular phylogenetics and the origins of placental mammals. Nature 409: 614–618.
Nessov, L.A., and A.A. Gureyev. 1981. The find of a jaw of the most ancient shrew in the upper Cretaceous of the Kylzyl Kum Desert. Doklady Akademii Nauk SSSR 157(4): 1–3.
Nixon, K.C. 1999. Winclada (BETA) ver. 0.9.99m24. Ithaca, NY: Published by the author. Available at www.cladistics.org.
Nixon, K.C., and J.M. Carpenter. 1993. On outgroups. Cladistics 9: 413–426.
Nixon, K.C., and J.M. Carpenter. 1996. On simultaneous analysis. Cladistics 12: 221–241.
Nixon, K.C., and Q.D. Wheeler. 1992. Extinction and the origin of species. *In* M.J. Novacek and Q.D. Wheeler (editors), Extinction and phylogeny: 119–143. New York: Columbia University Press.
Norell, M.A. 1992. Taxic orgin and temporal diversity: the effect of phylogeny. *In* M.J. Novacek and Q.D. Wheeler (editors), Extinction and phylogeny: 89–118. New York: Columbia University Press.
Novacek, M.J. 1976a. Insectivora and Proteutheria of the later Eocene (Uintan) of San Diego County, California. Natural History Museum of Los Angeles County Contributions in Science 283: 1–52.
Novacek, M.J. 1976b. Early Tertiary vertebrate faunas, Vieja Group, Trans-Pecos Texas: Insectivora. Texas Memorial Museum Pearce-Sellards Series 23: 1–18.
Novacek, M.J. 1986. The skull of leptictid insectivorans and the higher level classification of eutherian mammals. Bulletin of the American Museum of Natural History 183: 1–111.
Nowak, R.M. 1999. Walker's mammals of the world, 6th edition. Baltimore, MD: Johns Hopkins University Press.
Osborn, H.F. 1910. The age of mammals in Europe, Asia, and North America. New York: Macmillan.
Ostrander, G. 1983. New early Oligocene (Chadronian) mammals from the Raben Ranch local fauna, northwest Nebraska. Journal of Paleontology 57: 128–139.
Ostrander, G. 1987. The early Oligocene (Chadronian) Raben Ranch local fauna, northwest Nebraska: Marsupialia, Insectivora, Dermoptera, Chiroptera, and Primates. Dakoterra 3: 92–104.
Patterson, B. 1956. Early Cretaceous mammals and the evolution of mammalian molar teeth. Fieldiana Geology 13(1): 1–105.
Patterson, B. 1962. An extinct solenodontid insectivore from Hispaniola. Breviora 165: 1–11.
Patterson, B. unpublished MS. The Oligocene insectivore *Apternodus* and the Greater Antillean insectivores.
Patterson, B., and P.O. McGrew. 1937. A soricid and two erinaceids from the White River Oligocene. Field Museum of Natural History Publications, Geological Series 6(18): 245–272.
Plavcan, J.M. 1991. Catarrhine dental variability and species recognition in the fossil record. *In* W.H. Kimbel and L.B. Martin (editors), Species, species concepts, and primate evolution: 239–263. New York: Plenum.
Platnick, N.I., C.E. Griswold, and J.A. Coddington. 1991. On missing entries in cladistic analysis. Cladistics 7: 337–343.
Pleijel, F. 1995. On character coding for phylogeny reconstruction. Cladistics 11: 309–315.
Pogue, M., and M.F. Mickevitch. 1990. Character definitions and character state delineations: the bete noir of phylogenetics. Cladistics 6: 365–369.
Prothero, D.R. 1985. Chadronian (early Oligocene) magnetostratigraphy of eastern Wyoming: implications for the Eocene-Oligocene boundary. Journal of Geology 93: 555–565.
Prothero, D.R. 1998. The chronological, climatic, and paleogeographic background to North

American mammalian evolution. *In* C.M. Janis, K.M. Scott, and L.L. Jacobs (editors), Evolution of Tertiary mammals of North America: 9–36. Cambridge: Cambridge University Press.

Prothero, D.R., and D.B. Lazarus. 1980. Planktonic microfossils and the recognition of ancestors. Systematic Zoology 28: 119–129.

Prothero, D.R., and K.E. Whittlesey. 1998. Magnetostratigraphy and biostratigraphy of the Orellan and Whitneyan land mammal ''ages'' in the White River Group. Geological Society of America Special Paper 325: 39–61.

Quinet, G.E., and X. Misonne. 1965. Les insectivores zalambdodontes de l'Oligocene inferieur. Bulletin Institut Royal des Sciences Naturelles de Belgique 41(19): 1–15.

Riel, S.J. 1963. A basal Oligocene local fauna from McCarty's Mountain, southwestern Montana. M.S. thesis, University of Montana, Missoula.

Robinson, G.D. 1963. Geology of the Three Forks Quadrangle, Montana. U.S. Geological Survey Professional Paper 370: 1–143.

Robinson, P., C.C. Black, and M.R. Dawson. 1964. Late Eocene multituberculates and other mammals from Wyoming. Science 145: 809–811.

Robinson, P., and D.G. Kron. 1998. *Koniaryctes*, a new genus of apternodontid insectivore from Lower Eocene rocks of the Powder River Basin, Wyoming. Contributions to Geology University of Wyoming 32(2): 187–190.

Robinson, P., and B.A. Williams. 1997. Species diversity, tooth size, and shape of *Haplomylus* (Condylarthra, Hyopsodontidae) from the Powder River Basin, northwestern Wyoming. Contributions to Geology University of Wyoming 31(2): 59–78.

Romer, A.S. 1966. Vertebrate paleontology. Chicago: University of Chicago Press.

Rosen, D.E. 1978. Vicariant patterns and historical explanation in biogeography. Systematic Zoology 27: 159–188.

Russell, D.A. 1960. A review of the Oligocene insectivore *Micropternodus borealis*. Journal of Paleontology 34(5): 940–949.

Saether, O.A. 1979. Underlying synapomorphies and anagenetic analysis. Zoologica Scripta 8: 305–312.

Schlaikjer, E.M. 1933. Contributions to the stratigraphy and palaeontology of the Goshen Hole area, Wyoming. I. A detailed study of the structure and relationships of a new zalambdodont insectivore from the middle Oligocene. Bulletin of the Museum of Comparative Zoology 76(1): 1–27.

Schlaikjer, E.M. 1934. A new fossil zalambdodont insectivore. American Museum Novitates 698: 1–8.

Scott, W.B., and G.L. Jepsen. 1936. The mammalian fauna of the White River Oligocene. Part 1. Insectivora and Carnivora. Transactions of the American Philosophical Society 28: 1–153.

Shigehara, N. 1980. Epiphyseal union and tooth eruption of the Ryukyu house shrew, *Suncus murinus*, in captivity. Journal of the Mammalogical Society of Japan 8(5): 151–159.

Simmons, N.B. 1993. The importance of methods: archontan phylogeny and cladistic analysis of morphological data. *In* R.D.E. MacPhee (editor), Primates and their relatives in phylogenetic perspective: 1–61. New York: Plenum.

Simpson, G.G. 1931. A new classification of mammals. Bulletin of the American Museum of Natural History 59(5): 259–293.

Simpson, G.G. 1945. The principles of classification and a classification of mammals. Bulletin of the American Museum of Natural History 85: 1–350.

Simpson, G.G. 1947. Note on the measurement of variability and on relative variability of teeth of fossil mammals. American Journal of Science 245: 522–525.

Simpson, G.G., A. Roe, and R.C. Lewontin. 1960. Quantitative zoology. New York: Harcourt, Brace.

Sloan, R.E. 1969. Cretaceous and Paleocene terrestrial communities of western North America. Proceedings of the North American Paleontological Convention Part E: 427–453.

Sprague, J.M. 1944. The hyoid region of the Insectivora. American Journal of Anatomy 74(2): 175–216.

Sokal, R.R., and C.A. Braumann. 1980. Significance tests for coefficients of variation and variability profiles. Systematic Zoology 34: 449–456.

Sokal, R.R., and F.J. Rohlf. 1995. Biometry, 3rd Ed. New York: Freeman.

Stanhope, M.J., V.G. Waddell, O. Madsen, W.W. de Jong, S.B. Hedges, G.C. Cleven, D. Kao, and M.S. Springer. 1998. Molecular evidence for multiple origins of the Insectivora and for a new order of endemic African mammals. Proceedings of the National Academy of Sciences of the United States of America 95: 9967–9972.

Starck, D. 1995. Lehrbuch der Speziellen Zoologie. Band 2: Wirbeltiere. Teile 1–2: Saeugetiere. Jena: Gustav Fischer.

Stirton, R.A., and J.M. Rensberger. 1964. Occurrence of the insectivore genus *Micropternodus* in the John Day Formation of central Oregon. Bulletin of the Southern California Academy of Sciences 63: 57–80.

Storer, J.E. 1984. Mammals of the Swift Current Creek local fauna (Eocene): Uintan, Saskatchewan. Saskatchewan Museum of Natural History Contributions 7: 1–158.

Storer, J.E. 1995. Small mammals of the Lac Pelletier Lower Fauna, Duchesnean, of Saskatchewan, Canada: insectivores and insectivore-like groups, a plagiomenid, a microsyopid, and Chiroptera. *In* W.A.S. Sargeant (editor), Vertebrate fossils and the evolution of scientific concepts: 595–615. Amsterdam: Gordon and Breach.

Storer, J.E. 1996. Eocene-Oligocene faunas of the Cypress Hills Formation, Saskatchewan. *In* D.R. Prothero and R.J. Emry (editors), The terrestrial Eocene-Oligocene transition in North America: 240–261. New York: Cambridge University Press.

Strong, E.E., and D. Lipscomb. 1999. Character coding and inapplicable data. Cladistics 13: 363–371.

Stucky, R.K., D.R. Prothero, W.G. Lohr, and J.R. Snyder. 1996. Magnetic stratigraphy, sedimentology, and mammalian faunas of the early Uintan Washakie Formation, Sand Wash Basin, northwestern Colorado. *In* D.R. Prothero and R.J. Emry (editors), The terrestrial Eocene-Oligocene transition in North America: 40–51. New York: Cambridge University Press.

Swisher, C.C. and D.R. Prothero. 1990. Single Crystal Ar/Ar dating of the Eocene–Oligocene transition in North America. Science 249: 760–762.

Swofford, D.L. 2000. PAUP*. Phylogenetic analysis using parsimony (*and Other Methods). beta version 4.0b10. Sunderland, MA: Sinauer Associates.

Szalay, F.S. 1969. Mixodectidae, Microsyopidae, and the insectivore-primate transition. Bulletin of the American Museum of Natural History 140: 193–330.

Tabrum, A.R. 1998. First record of a hypertragulid artiodactyl from the Chadronian of western Montana. Journal of Vertebrate Paleontology 18(supplement): 81A.

Tabrum, A.R., D.R. Prothero, and D. Garcia. 1996. Magnetostratigraphy and biostratigraphy of the Eocene-Oligocene transition, southwestern Montana. *In* D.R. Prothero and R.J. Emry (editors), The Terrestrial Eocene-Oligocene transition in North America: 278–311. New York: Cambridge University Press.

Tabrum, A.R., R. Nichols, and A.D. Barnosky. 2001. Tertiary paleontology of southwest Montana and adjacent Idaho. *In* C.L. Hill (editor), SVP Guidebook, Mesozoic and Cenozoic paleontology in the western plains and Rocky Mountains. Occasional Paper Museum of the Rockies 3: 93–112.

Thewissen, J.G.M., and P.D. Gingerich. 1989. Skull and endocranial cast of *Eoryctes melanus*, a new palaeoryctid (Mammalia: Insectivora) from the early Eocene of western North America. Journal of Vertebrate Paleontology 9(4): 459–470.

Tong, Y. 1997. Middle Eocene small mammals from Liguanqiao Basin of Henan Province and Yuanqu Basin of Shanxi Province, central China. Palaeontologia Sinica Whole Number 18, New Series C, no. 26: 1–256.

Tong, Y., S. Zheng, and Z. Qui. 1995. Cenozoic mammal ages of China. Vertebrata Palasiatica 33(4): 290–314.

Vandebroek, G. 1961. The comparative anatomy of the teeth of lower and nonspecialized mammals. *In* International Colloquium on the Evolution of Lower and Nonspecialized Mammals: 215–320. Brussels: Koninklijke Vlaamse Academie voor Wetenschappen.

Van Valen, L. 1966. Deltatheridia, a new order of mammals. Bulletin of the American Museum of Natural History 132: 1–126.

Walsh, S.L. 1996. Middle Eocene mammalian faunas of San Diego County, California. *In* D.R. Prothero and R.J. Emry (editors), The terrestrial Eocene-Oligocene transition in North America: 75–119. New York: Cambridge University Press.

West, R.M., and E.G. Atkins. 1970. Additional Middle Eocene (Bridgerian) mammals from Tabernacle Butte, Sublette County, Wyoming. American Museum Novitates 2404: 1–26.

Whidden, H.P., and R.J. Asher. 2001. The origin of the Greater Antillean Insectivorans. *In* C.A. Woods and F.E. Sergile (editors), West Indian biogeography: 237–250. Boca Raton, FL: CRC Press.

White, T.E. 1954. Preliminary analysis of the fossil vertebrates of the Canyon Ferry Reservoir area. Proceedings of the U.S. National Museum 103(3326): 395–438.

Wible, J.R. 1986. Transformation in the extracranial course of the internal carotid artery in mammalian phylogeny. Journal of Vertebrate Paleontology 6: 313–325.

Wible, J.R., G.W. Rougier, M.J. Novacek, and M.C. McKenna. 2001. Earliest eutherian ear region: a petrosal referred to *Prokennalestes* from the Early Cretaceous of Mongolia. American Museum Novitates 3322: 1–44.

Wiley, E.O. 1981. Phylogenetics: the theory and practice of phylogenetic systematics. New York: Wiley-Liss.

Winkler, D.A. 1983. Paleoecology of an Early Eocene mammalian fauna from paleosols in the Clarks Fork Basin, northwestern Wyoming

(U.S.A.). Palaeogeography, Palaeoclimatology, Palaeoecology 43: 261–298.

Wojcik, J.M., and M. Wolsan. 1998. Evolution of shrews. Bialowieza: Polish Academy of Sciences.

Wood, C.B., M.C. McKenna, and D. Bosko. 2000. An old specimen of a new undescribed late Paleocene *Apternodus*–like insectivore. Journal of Vertebrate Paleontology 20(supplement): 80A.